Engineering & Physical Sciences in Medicine - The Australian Biomedical Engineering Conference 2007

14 – 18 October 2007

The Fremantle Esplanade Hotel Convention Centre

Fremantle, WESTERN AUSTRALIA

Proceedings

The abstracts of the posters and oral presentations are published in the following pages. The abstracts are intended to be exactly as printed in the Conference Handbook with minor formatting changes. The conference papers have been subject to independent expert peer-review under the direction of the Conference Scientific Committee.

Prize winners

Peter Greer: best radiotherapy oral presentation prize (Sponsored by Varian Medical Systems)

Ivan Williams: best diagnostic physics oral presentation (Radcal/Health Technology Consultancy)

Michael Smith: best presentation by a young biomedical engineer (Engineers Australia)

Glenn Kennett: best paper by a member of SMBE (SMBE WA)

Jessica Hughes: best poster presentation (Dräeger Medical)

Student Prizes
Matt Carroll: John Black prize for the best oral presentation (Computerized Medical Systems, Inc)

Sian Price: Best poster presentation (Centre for Medical Radiation Physics, Uni.of Wollongong)

EPSM-ABEC 2007 contents

The abstracts have been grouped into the following sections. Abstracts within each section are in alphabetical order of the first author's surname.

PLENARY ADDRESS

TRANSLATIONAL RESEARCH, TECHNOLOGY COMMERCIALIZATION AND ENTREPRENEURSHIP

Yongmin Kim

Department of Bioengineering, University of Washington Seattle, WA, USA

Bioengineering is the fastest growing engineering discipline in the world. Numerous translational opportunities abound in and around Bioengineering, ranging from medical imaging to bioinformatics and biotechnology. While traditional engineering disciplines are trying to increase their "bio" component, basic science and clinical departments need "engineering" to solve an unmet clinical need. The University of Washington's Department of Bioengineering was set up in 1967, equally grounded in both the School of Medicine and College of Engineering. It has now 30 core faculty, 38 adjunct faculty, 139 graduate students, 117 undergraduate students and 129 staff members, including 54 postdoctoral research fellows.

Currently, there are five major areas of research and training within the Department: (1) Distributed Diagnosis and Home Healthcare (D2H2); (2) Engineered Biomaterials and Tissue Engineering; (3) Molecular Bioengineering and Nanotechnology; (4) Medical Imaging and Image-Guided Therapy; and (5) Computational and Integrative Bioengineering. Unique integration of biology, engineering, nanotechnology, information technology and medicine has been underway inside our department for a long time, continuously creating new frontiers and opportunities in research, education and technology transfer. Our annual external research funding totaled more than $26 million in 2007.

An unusual aspect of our research is our tie with industry. We have been prolific in our inventions (470), patents (240), licenses (80), and entrepreneurship. The faculty, students and staff of the Department have fostered the development of 30 start-up companies and thousands of new jobs as a spin-off of our research endeavors. Also, we have developed in the Department of Bioengineering a unique entrepreneurship/intrapreneurship educational and training program called Program on Technology Commercialization (PTC).

In this presentation, I will provide an overview on the Department of Bioengineering at the University of Washington, several entrepreneurship and technology commercialization examples, my observation and experience on the obstacles and formula of success in translational research and technology commercialization, and future directions in the 21st century.

KEYNOTE ADDRESS

EMERGING ISSUES IN CT DOSIMETRY

John M. Boone

Department of Radiology, Department of Biomedical Engineering, University of California, Davis Medical Center, Sacramento, California, USA

INTRODUCTION: The use of computed tomography in recent years has skyrocketed, with an annual increase of 15% in CT utilization seen in the United States, for example[1]. In 2006, over 70 million CT scans were performed on a population of 300 million people. This increase in CT use has heightened concern in regards to consequences of the radiation dose associated with CT. Compounding the issues of CT dosimetry is the additional concern that the standard CT dosimetry methods of the past, employing a 15 cm long PMMA phantom with a 10 cm long pencil chamber, are no longer adequate now that clinical CT scanners have x-ray beam widths of 4 cm, and some cone beam scanners (used mostly in radiation therapy systems) have beam widths of 15 cm or more.

METHODS: A number of investigators, including this author[2], have recently published on the value and utility of the computed tomography dose index (CTDI). The $CTDI_{100}$ is typically measured using a 100 mm long pencil chamber, in either a 16 cm diameter (head or paediatric phantom) or 32 cm diameter (body phantom) PMMA cylinder (15 cm in length), at both the center and the edge of the phantom. The *weighted CTDI* is computed as $CTDI_w = 0.333\ CTDI_{center} + 0.666\ CTDI_{edge}$, and to factor in helical pitch, the *volume CTDI* is computed as $CTDI_{vol} = CTDI_w$ / pitch. Finally, to include the influence of the scan length, the *dose length product* is defined as $DLP = CTDI_{vol} \times L$, where L is the length of the body part being scanned in cm. The DLP is reported on most modern CT scanner consoles.

RESULTS: There has been a widely held feeling that $CTDI_{100}$ would not be an adequate metric for current 64 slice CT scanners, which have beam widths up to 40 mm. Recent data have shown[2], however, that compared to CT scanners with a beam width of 10 mm, the difference in measurement accuracy is less than 1% when the 100 mm pencil chamber is used to measure a 40 mm CT beam. While that may be the good news, the bad news is that the $CTDI_{100}$ is not very accurate in measuring the dose of even a 10 mm wide CT beam, with errors in efficiency of up to ~35% for some geometries. The

measurement inefficiency increases as scattered radiation internal to the phantom increases, for example at the center position of the 32 cm PMMA phantom.

DISCUSSION & CONCLUSIONS: We are at a time of change in CT dosimetry, and there is a wide-spread feeling that the $CTDI_{100}$ should be replaced with a parameter which allows more accurate CT dose computation in patients. While consensus in the CT community has not yet been achieved, it is likely that the 100 mm pencil chamber will be replaced with a shorter chamber, for example 20 mm. In this scenario, instead of using a long ion chamber (100 mm) with a thin CT beam (10 mm), the short detector (~20 mm) will be placed at the centre of a long phantom and will integrate the primary and scattered radiation that reaches it during an entire helical acquisition (e.g. 300 mm in scan length). The use of the 32 cm diameter PMMA phantom for patient dosimetry has also been criticized, since its high density (ρ=1.19 g/cm^3) is not tissue equivalent and the large circular cross section is not representative of most patients. Various groups are studying the use of water-filled phantoms (ρ=1.00 g/cm^3), or the use of polyethylene (ρ=0.97 g/cm^3)phantoms. The author will describe some of the ongoing work of several CT dosimetry committees active in North America and Europe, including those in the American Association of Physicists in Medicine and the International Committee on Radiological Units and Measurement. Ideas and opinions on CT dosimetry will be solicited from scientists in this Southern Hemisphere venue.

REFERENCES:

[1]*JM Boone (2006), Radiology 241: 334-337*
[2]*JM Boone (2007), Med Phys. 34, 1364-1371*

PERFORMANCE ASSESSMENT IN DIGITAL MAMMOGRAPHY

John M. Boone

Department of Radiology, Department of Biomedical Engineering, University of California, Davis Medical Center, Sacramento, California, USA

INTRODUCTION: Digital mammography is no longer a novelty and many hospitals, screening centres, and breast imaging facilities are installing digital mammography (DM) systems. This change reflects the infrastructure realities that have evolved due to the largely digital imaging environment outside of breast imaging, coupled with the faster patient throughput and more efficient workflow (PACS) that DM provides. At UC Davis, 7 screen-film mammography systems were replaced by 5 DM systems in the past year, and with this change, the last two film processors at our institution were turned off forever.

METHODS: Acceptance testing and quality assurance methods in DM have yet to achieve full consensus in the United States, because the regulating body (the Food and Drug Administration) recognises vendor-specific guidelines for quality assurance, and these guidelines are different between DM vendors. All quality assurance methods for DM should examine the many aspects of DM performance, including spatial resolution, contrast resolution, and breast dosimetry. With DM, quantitative image quality metrics can be measured more easily than with screen film mammography, and the use of the modulation transfer function (MTF) for spatial resolution and noise power spectrum (NPS) for noise evaluation (contrast resolution) have been used routinely.

RESULTS: The author will review some of the semi-automated QC metrics that were defined and then used during the digital mammography imaging screening trial (DMIST), a large multi-institutional trial (~30 centre's) in which DM was compared to SFM. In this trial, QC was standardized across vendor platforms (where possible) and the results were retrospectively evaluated after the trial to see what parameters actually were useful[1,2]. While monitoring the technical performance of DM systems is of course prudent, a number of measured parameters were not sensitive in picking up problems with the systems, including the MTF and NPS. This result is for a two year clinical trial, and it is likely that MTF and NPS evaluation will remain important test parameters as DM systems are in use for longer time lines.

DISCUSSION & CONCLUSIONS: While the purpose of quality assurance in DM and elsewhere is to monitor the image quality and dose performance of a given piece of equipment over time, the quantitative evaluation of the MTF, NPS, and detective quantum efficiency (DQE) during the DMIST trial also provided ample data for comparing between different vendor's DM systems. These data will be reviewed and compared, as well.

REFERENCES

[1]*MJ Yaffe, et al, Med Phys. 2006 Mar;33(3):737-52.*
[2]*A Bloomquist, et al, Med Phys. 2006 Mar;33(3):719-36.*

BREAST CT FOR CANCER DETECTION AND DIAGNOSIS

John M. Boone

Department of Radiology, Department of Biomedical Engineering, University of California, Davis Medical Center, Sacramento, California, USA

INTRODUCTION: While mammography, including digital mammography, has been shown to reduce breast cancer mortality due to earlier detection, there remains in the breast imaging community the feeling that there should be a screening procedure which is better than projection mammography. Many researchers have studied a number of alternate technologies for screening, including breast MRI, PET, SPECT, ultrasound, and tomosynthesis. In our laboratory, we have developed a computed tomography (CT) system that is designed specifically for breast imaging. The breast CT scanner is currently undergoing clinical evaluation in order to better understand the role that breast CT may ultimately play in breast cancer management.

METHODS: Two prototype breast CT scanners were designed and built in the laboratory (Fig 1). The system made use of commercially available components where practical, including an x-ray source (Comet), flat panel detector (Varian 4030CB), and combination motor / bearing / encoder (Kollmorgen). All other components were designed and fabricated at UC Davis. The patient is positioned prone with the breast to be imaged hanging pendant through a hole in the table (Fig 2). The scanner hardware produces 500 projection images (cone beam views) in 16.6 seconds, while the patient holds her breath.

Figure 1. *Working components in the Albion breast CT scanner.*

Figure 2. *The patient position during scanning is shown.*

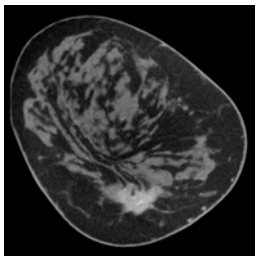

Figure 3. *A contrast-enhanced breast CT is shown.*

The reconstructed image data set currently contains from 300 to 500 CT images, each 512 x 512. Typical voxel dimensions are 0.25 x 0.25 x 0.21 mm. The x-ray technique was tuned to deliver the same radiation dose to the breast (mean glandular dose) as two-view mammography[1], using 80 kVp and between 50 and 130 mAs, depending on the diameter of the breast. To date, 130 women have been imaged in both phase I (12 women) and phase II studies (118). Contrast injection was also used in 16 of the phase II women.

RESULTS: The spatial resolution of the scanners show cut off resolution[2] on the order of 1.8 cycles / mm and the noise power spectrum shows dose-limited performance. The breast CT images (Fig 3) have excellent contrast resolution and show very good detail.

DISCUSSION & CONCLUSIONS: Initial subjective evaluation by mammographers suggests that breast CT is superior to mammography for delineation of mass lesions, while being slightly inferior in terms of microcalcification visualization[3]. An ROC study is currently being planned to further evaluation the performance of breast CT compared to mammography. Further investigation is needed to better understand the ultimate role that breast CT will play in cancer screening and diagnosis.

REFERENCES:

[1]*JM Boone, TR Nelson, KK Lindfors, JA Seibert (2001).. Radiology 221, 657-667.*
[2]*JM Boone, AL Kwan, JA Seibert, et al. (2005). Med. Phys. 32, 3767-3776.*
[3]*JM Boone, KK Lindfors (2006). Future. Oncol. 2, 351-356.*

DOSE REDUCTION STRATEGIES IN DIAGNOSTIC RADIOLOGY

Cari Borrás, D.Sc., FACR, FAAPM

Radiological Physics and Health Services Consultant, Washington DC, USA

Dose reduction should be part of a comprehensive quality assurance (QA) program. Because nowadays radiology equipment, including CT scanners, may be located not only in radiology, but in neurology, cardiology, radiation oncology and other departments, the commitment by management to adhere to radiation protection standards throughout the facility is essential. Regardless whether the decision to implement a dose reduction program is triggered from within or it is imposed by regulators, the first step is to develop a plan to evaluate risk/benefits, establish a budget and identify needed additional resources. It will be necessary to produce an inventory of all the imaging equipment, to document workloads and radiological techniques for each radiological room, and to list the staff (number of radiologists, radiological technologists, darkroom technicians, etc), evaluating their education, experience and specialized training, including radiation protection courses. Particularly important is to have a diagnostic medical physicist either as a staff member or as a consultant, and to set up a radiation protection committee if one does not exist. The implementation of the methods should be prioritized from the point of view of dose-reduction impact. Cost-benefits can be achieved by: Better utilization of capabilities already existing in

the x-ray and image processing equipment, including use of film/screens and chemicals; potential modifications to x-ray and image processing equipment; acquisition of equipment with better dose-reduction features (considerations when buying new equipment); better utilization and/or acquisition of accessories/ parts /components (i.e. organ shields); potential modifications of clinical procedures (i.e. changes in CT protocols); potential modifications of administrative procedures; creation of incentive measures to create and/or promote dose reduction awareness (i.e. increase of staff salaries), and additional dosimetry measurements. In order to set cost-effectiveness priorities, the expenses associated with each dose reduction method, including capital and operational costs, should be estimated. Approximate figures should be obtained to: pay consultant(s); hire new staff; provide continuing education to existing staff; fix deficient equipment and accessories, and buy new equipment and/or accessories. It is essential that the quality associated with each dose-reduced image and its potential impact on the diagnostic information or interventional procedure effectiveness be assessed by the imaging physicians who are to perform the dose-reduced studies prior to their adoption throughout the center. The referring physicians should be informed of appropriateness criteria and of the doses involved in each procedure they request. An effective way is to invite them to an educational workshop where they can obtain continuing education credits. Key staff and recognized professionals should present internationally-recognized referral patterns and discuss the justification of certain radiological procedures, for example whole body CT screening. A CD containing the presentations and key points made during the lectures should be .distributed to the participants and/or be available at the medical center's website. Patients also need to be informed of the dose-reduction methods being implemented at the center either through brochures especially designed for them, or through a general information section of the medical center's website. The effectiveness of the dose-reduction methods implemented should be periodically contrasted with the expected results, and adjustments made as needed.

X-RAYING HUMANS FOR SECURITY/THEFT DETECTION PURPOSES

Cari Borrás, D.Sc., FACR, FAAPM

Radiological Physics and Health Services Consultant, Washington DC, USA

The use of ionizing radiation in human imaging to prevent illegal activities is not new. The International Commission on Radiological Protection (ICRP) in 1969[1] recommended that examination of individuals "for non-medical purposes, such as "anti-crime" fluoroscopy and in customs examinations" and in 1971[2] as "a system for security screening of airline passengers" "be carried out under the supervision of a qualified medical radiologist".

Conventional x-ray systems have been used in diamond mines to radiograph workers in order to prevent them from stealing diamonds and concealing them in their body cavities. The international community failed to reach consensus on whether the practice was justified[3].

After 9/11, the need for efficient methods of detecting concealed weapons escalated, and new types of cargo and personnel scanners were developed. Today there are high-energy (from 6 to 15 MeV) x-ray imaging systems that can penetrate several inches of steel and image the contents within any cargo container. Humans hiding inside could receive doses ranging from 5 to 50 mGy depending on scanner energy. In addition, for x rays higher than 6 MV, there will also be a neutron dose component (4).

The personnel scanners can be of three types: backscatter x-ray systems (B) which use Compton backscattered x rays to create an image; transmission systems (T) which use the transmitted x-rays for the image creation, and a third type which is a combination of the other two (B,T). With backscatter systems, the x rays do not penetrate beyond the surface of the individual and are used to detect objects hidden under their clothing. At least two views are required, one anterior; the other one, posterior. With transmission systems, the x rays penetrate the whole body so objects swallowed or hidden in body cavities may be detected. Doses for six current types of cargo and personnel scanners measured with especially designed ionization chambers and electrometers resulted in personal dose equivalent, $H_p(10)$, and ambient dose equivalent, $H^*(10)$ between 0.07 μSv and 6 μSv per scan, depending on the type of system (5).

The American National Standards Institute and the Health Physics Society published a standard for backscatter systems where the effective dose limits to irradiated subjects are 0.1 μSv per scan and 250 μSv per year (6). The International Electrotechnical Commission is currently in the process of developing a comprehensive international standard, where the ambient dose equivalent, $H^*(10)$, at the reference point shall not exceed 0.3 μSv per screening procedure (that means the sum of all scans necessary to examine a person) for backscatter systems, (B), and 5 μSv for transmission systems, (T) and backscatter and transmission systems, (B,T) (7). Even complying with these standards, doses to certain types of individuals will exceed public dose limits. Examples will be shown and discussed.

REFERENCES:

[1]*International Commission on Radiological Protection, (1969). ICRP 15, paragraph 285.*
[2]*International Commission on Radiological Protection, (1971). Br. J. Radiol, 44: 814.*

[3]*Food and Agriculture Organization of the United Nations, International Atomic Energy Agency, International Labour Organisation, Nuclear Agency of the Organisation for Economic Co-operation and Development, Pan American Health Organization, World Health Organization (1996). Vienna: IAEA; (Safety series 115, paragraph II.9).*
[4]*R.J. O'Brien, D.R. Lowe, and P.W. Patton, (2007). HPS Annual Meeting Poster.*
[5]*ANSI / HPS Standard: N43.17-2002. (2002) Radiation Safety for Personnel Security Screening Systems Using X-rays.*
[6]*O. Hupe, U. Ankerhold (2006), Radiation Protection Dosimetry, 121, 4: 429-437.*
[7]*International Electrotechnical Commission (2007). Radiation protection instrumentation - X-ray systems for the screening of persons for security and the carrying of illicit items. In preparation.*

NEW ICRP/ICRU DOSIMETRY

Cari Borrás, D.Sc., FACR, FAAPM

Radiological Physics and Health Services Consultant, Washington DC, USA

In March 2007, the International Commission on Radiological Protection (ICRP), approved a new set of fundamental recommendations on radiological protection to replace the Commission's previous recommendations from 1990. The dosimetric terms to be used for radiological protection are equivalent dose, effective dose, committed dose and collective effective dose, all based on mean absorbed dose with its distributions in time and in linear energy transfer (linear collision stopping power). Their definition is the same as in the 1990 Recommendations, but some of the factors that convert absorbed dose to equivalent dose and effective dose, w_R and w_T, have changed, due to new scientific evidence. Values of w_R are unchanged for photons and alphas, but have changed for neutrons (w_R is now a continuous and not a discrete function vs energy), protons (which is now 2 instead of 5), and a value ($w_R = 2$) has been assigned to charged pions, which had not been considered before. w_T are different for the gonads (the value has decreased from 0.20 to 0.08), the breast (it has increased from 0.05 to 0.12) and the "remainder" (the treatment of which has also changed); the number of tissues has increased to 14. Since both equivalent dose and effective dose cannot be measured directly, to determine external exposure, the ICRP relies on the operational quantities, defined by the International Commission on Radiation Units and Measurements, Inc. (ICRU): ambient dose equivalent, H*(10), and directional dose equivalent, H'(0.07, Ω), for area monitoring, and personal dose equivalent, $H_p(d)$, for individual monitoring. Any statement of personal dose equivalent should include a specification of the reference depth, d, the depth below a specified point, usually where the dosimeter is worn. For the assessment of effective dose, this depth is taken as 10 mm, $H_p(10)$. For the skin dose and for the dose to the extremities, the depth is 0.07 mm, $H_p(0.07)$. The dose to the lens of the eye could be monitored with H_p (3), at a depth of 3 mm, but no such dosimeter exists in practice. Compliance with dose limits can be ascertained with the use of dosimeters if properly worn. To link the protection and operational quantities to physical quantities (such as tissue absorbed dose, air kerma free-in-air and particle fluence) that characterize the radiation field, the ICRU computed conversion coefficients. To assess internal exposure, the ICRP recommends the use of activity quantities in combination with dose coefficients based on physiological models and 4-D computations. The unit for all the ICRP and ICRU quantities listed above is the sievert (Sv). Effective dose should be used only for occupationally exposed workers and members of the public, where doses are assumed to be low, well below 100 mSv, where stochastic effects are considered. At doses above about 0.5-1 Sv, where tissue reactions (deterministic effects) may occur, the dosimetric quantity to use is the absorbed dose in the irradiated tissue modified by the radiobiological effectiveness of the radiation for the biological endpoint of concern. The unit is the gray (Gy). Effective dose should not be used for retrospective evaluation of exposed populations or to assess individual risks, as is the case in medical exposures, which are not subject to dose limitations. Exposures in radiotherapy are clearly expressed in absorbed dose to the irradiated tissue. Exposures to individual patients from medical imaging, even those at low levels, should also be expressed as absorbed doses, since both the irradiation conditions and the exposed group of patients are known.

RADIOLOGY SERVICES: MINIMUM CRITERIA FOR ACCREDITATION AND THE ROLE OF THE MEDICAL PHYSICISTS IN RADIOLOGY

Cari Borrás

Radiological Physics and Health Services Consultant, Washington DC, USA

As medical imaging increases in complexity, there is a need to ensure the quality and safety of radiology services. One such mechanism is to establish accreditation programs. Industrialized countries, such as the United States of America, have had accreditation programs for years. Their incorporation in developing countries, however, has been fraught with difficulties, mainly financial. The Pan American Health Organization (PAHO) developed a basic accreditation program for ministries of health of Latin American and Caribbean developing countries, patterned after the American College of Radiology's Accreditation Program[1]. The program could also be run by a non-governmental organization, for example, by the local radiology society. The PAHO program relies on a national "Accreditation Committee" to establish and maintain "accreditation standards". Members of such a committee should be national professionals, but foreign technical and clinical experts may be consulted before establishing the program and periodically thereafter as needed, especially when new

technologies are incorporated in the country. The accreditation process involves a peer review evaluation of: 1) Radiography, fluoroscopy, mammography and ultrasound equipment and their associated processing systems, 2) Physician and technologist staff qualifications, 3) Quality control (QC) and quality assurance (QA) programs and 4) Image quality and radiation dose (where applicable). The Radiography/Fluoroscopy Accreditation Program has three modules from which to choose: chest radiography, general radiography, and fluoroscopy. To be accredited, a medical center has to provide specific information on the facility, the equipment, the staff and the services offered, accompanied by phantom images from each imaging unit, clinical images from selected examinations and a copy of all the medical physicist's surveys. A review panel of imaging experts assesses the images. The Accreditation Committee verifies compliance with the accreditation standards and issues, on behalf of the accrediting entity, an Accreditation Certificate, which PAHO recommends be for 3-years, with the possibility of on-site surveys and film checks performed at random. Access to a medical physicist is considered essential. The functions of a medical physicist include: develop/review equipment purchase specifications; perform acceptance tests; commission radiological and processing equipment; evaluate image quality; establish diagnostic reference levels; ensure interconnectivity and interoperability of networked equipment; test and calibrate physics instruments; develop and supervise an imaging QC program; supervise the maintenance program; participate in the QA program; make patient dosimetry determinations, including in vivo measurements when appropriate; assess radiation safety levels; train the staff in imaging and protection, and participate in research projects. If the medical physicist is also the facility's radiation safety officer, his/her functions will also include: prepare the license for the regulatory authority; review the floor plans and the designation of controlled and supervised areas; perform and/or review the structural shielding calculations; order ancillary shields for staff, occasional patient relatives, survey meters and personnel dose monitors; verify compliance of equipment, radiation warning signs, door interlocks, and radiation emergency controls with IEC and ISO safety features and/or equivalent national standards; perform radiation safety surveys; establish dose constraints and operational limits; document staff and consultants' qualifications; develop and supervise a radiation safety QC program; chair the radiation safety committee; impart radiation safety training courses; maintain up-to date license-related documents, keeping up with staff changes and qualifications, and liaise with the regulatory authorities. The degree of medical physics involvement depends on the complexity of the services offered. A facility with digital equipment (computed and/or digital radiography as well as computed tomography) and/or offering interventional radiology should have at least one full-time medical physicist on the staff and as many medical physics consultants as needed.

REFERENCES:

[1]*P. Jiménez, C. Borrás, I. Fleitas (2006). Pan Am J Public Health ,20(2/3):104-112.*

HEAVY ION DOSIMETRY, TREATMENT PLANNING AND TREATMENT DELIVERY

O. Jäkel[1,2]

[1]*Department of Medical Physics in Radiation Oncology, German Cancer Research Center, Heidelberg, Germany*
[2]*Heidelberg Ion Therapy Inc., Heidelberg, Germany*

INTRODUCTION: In Heidelberg a clinical centre for radiotherapy with beam of ions and protons was established and will start clinical operation in early 2008. The application is based on a dynamic beam scanning system which requires dedicated techniques for clinical dosimetry and treatment planning.

METHODS: The active beam scanning at the Heidelberg ion beam facility relies on a set of scanning magnets to deflect a small pencil beam of particles laterally. Together with an active energy variation of the synchrotron also the position of the Bragg peak in depth can be varied and a 3D scanning procedure is realized. Moreover the first isocentric scanning gantry for ion beams was also realized in Heidelberg.

The dosimetry protocol relies on ionization chambers calibrated in absorbed dose to water in a cobalt source. Using the IAEA code of practice TRS398 as an international guideline, a chamber specific beam quality correction for the various ion types can be obtained. A number of correction factors was determined either experimentally or using Monte Carlo simulations.

For treatment planning a dedicated biological modelling of the biological effectiveness of ion beams had to be included in the routine treatment planning procedure. This enables the direct optimization of biological effective doses in the target volume in order to deliver a effective treatment.

RESULTS: The beam delivery with an active scanning system was shown to be feasible and reliable for clinical application within the German pilot project for heavy ion therapy at the heavy ion lab GSI, where more than 350 patients have been treated with this modality.

The protocol for clinical dosimetry for scanned ion beams was shown to be suitable and robust, although the overall accuracy of dose determination is not yet at the same level as for conventional radiation. This is mainly due to the complexity of the radiation field. Moreover an efficient dosimetric verification system for treatment plans delivered with the active scanning was also realized.

For the TPS, a biological modelling of the effects of high LET radiation was introduced into clinical routine. The model accurately describes the dependency of the biological effectiveness of various treatment parameters and enables the delivery of a homogeneous biological effective dose to the target volume. This is also confirmed by the excellent results of the various clinical studies performed within the pilot project.

DISCUSSION AND CONCLUSION: In total more than 250 patients have been treated with carbon ions until mid 2007 using the newly developed methods. Many new developments, however, have yet to be evaluated before the hospital based facility at the university Heidelberg can start its clinical operation in spring 2008. This especially includes new dosimetric equipment, a commercialized version of the TPS and the new isocentric scanning gantry.

MEDICAL PHYSICS RESEARCH IN GERMANY AND EUROPE

O. Jäkel[1,2]

[1]*Department of Medical Physics in Radiation Oncology, German Cancer Research Center, Heidelberg, Germany*
[2]*Heidelberg Ion Therapy Inc., Heidelberg, Germany*

The medical physics research community in Europe includes more than 6000 medical physicists from 35 countries and is currently being represented by the European Federation of Organizations for Medical Physics (EFOMP). The aims of EFOMP include the coordination of activities of National Member Organizations, dissemination of scientific information and proposing guidelines for educational programs.

In Germany, medical physics research is performed in numerous small groups at many universities and research centres, while there are only few large research centres hosting departments dedicated solely to medical physics. There are basically two of these centres. One of them is the Oncoray Center for Radiation Research in Oncology at the University of Dresden focusing on biological imaging and targeting for radiotherapy. Similarly the German Cancer Research Center hosts an institute for "Innovative Cancer Diagnostics and Therapy" including two departments for medical physics in radiology and radiation oncology. Both centres are focussed strongly on radiation physics and imaging for oncology.
On a European scale, the following centres are among the most important centres for medical physics research which are comparable to these two German centres:

- The Joint Department of Physics in the Institute of Cancer Research at the Royal Marsden Hospital in Sutton, UK
- The department of Radiation Physics and Biology of the Karolinska Institute in Stockholm, Sweden
- The Institute Curie in Paris, France, hosting a medical physics group working in conventional and proton radiotherapy
- The Division of Radiation Medicine at the Paul Scherrer Institute in Villigen, Switzerland, with its large experience in proton therapy
- The department of Medical Physics of Radiotherapy at the Netherlands Cancer Institute in Amsterdam, Netherlands

Moreover the field of Radiotherapy with Proton and Ion Beams is of increasing interest in Europe and numerous European clinical research centres are currently being established. At these clinical centres also medical physics research will play an important role in the near future.

EXPERIENCE WITH HEAVY ION THERAPY AND THE RATIONALE FOR ION BEAMS AS COMPARED TO X-RAYS OR PROTONS

O. Jäkel[1,2] and J. Debus[3,2]

[1]*Department of Medical Physics in Radiation Oncology, German Cancer Research Center, Heidelberg, Germany*
[2]*Heidelberg Ion Therapy Inc., Heidelberg, Germany*
[3]*Department of Radiation Oncology, University of Heidelberg, Heidelberg, Germany*

INTRODUCTION: In 2007, radiotherapy with ions celebrates its 50th anniversary. About 4500 patients have been treated mainly using helium and carbon ions. The interest in carbon ion therapy has increased enormously within the last decade. While there are currently 3 facilities treating patients with carbon ions (2 hospital based in Japan and a research therapy facility in Germany), there are 4 new clinical facilities scheduled to start operation between 2008/2010 (in Heidelberg and Marburg, Germany; Pavia, Italy; Gunma, Japan). Three more projects have already been approved or announced in Austria, France and Germany.

METHODS: Carbon ions offer a number of potential advantages over conventional radiation and also protons. Most important is their increased energy loss in the Bragg peak region, which gives rise to an enhanced biological effectiveness in the target vs. the surrounding healthy tissue. In vitro studies also demonstrated a reduced oxygen effect, which should allow increased efficiency in the treatment of hypoxic tumours. Moreover, heavy ions suffer less from lateral scattering than protons and induce an activation of irradiated tissues, which allows an in vivo monitoring of the applied dose in the patient by using positron emission tomography.

At the German heavy ion lab GSI (Darmstadt), a pilot project for carbon ion radiotherapy was established in 1997. Since then more than 350 patients have been treated with carbon ions within clinical studies. These includes mainly patients with tumours of the base of skull (chrodoma and chondrosarcoma), which are difficult to control with convention radiation. In these patients carbon ion therapy was delivered as primary therapy after surgical resection. Further studies include patients with tumours of the salivary glands (adenoidcystic carcinoma) and prostate cancer, where carbon ion RT is delivered as a boost to an IMRT treatment using conventional radiation.

RESULTS: The clinical results for the patients treated at GSI clearly demonstrated the effectiveness of carbon ions. The 5-year local control rates for chordoma at the base of skull are significantly higher than for conventional techniques and comparable to results from proton RT, however with very mild side effects. For a subgroup of patients, a dose escalation study demonstrated that control rates close to 100% can be reached, without increasing the treatment related morbidity.
For the adenoidcystic carcinoma it was shown in a small comparative study that introduction of a carbon ion boost can increase the 5-year local control rates from around 25% using IMRT alone, to 75% when a carbon boost is used.

DISCUSSION AND CONCLUSION: Still only very limited clinical experience with carbon ions exists. The clinical results from GSI demonstrate, however, that the treatment is very effective and very well tolerated by the majority of patients. The increased biological effectiveness of high LET radiation in salivary gland tumours was known already from neutron trials, however, at a high risk of severe side effects, which can nearly completely be excluded when carbon ions are used. There are still numerous open clinical questions, which can only be answered in larger clinical trials. A number of clinical research facilities will be needed to fully exploit the role of ion beam therapy in clinical oncology.

DISTRIBUTED DIAGNOSIS AND HOME HEALTHCARE

Yongmin Kim

Department of Bioengineering, University of Washington, Seattle, WA, U.S.A.

Distributed Diagnosis and Home Healthcare (D_2H_2) has been proposed as a new healthcare delivery framework in the 21st century. The goal of D_2H_2 is to improve quality of care and patient wellness and outcomes by transforming the delivery of healthcare from a central, hospital-based system to one that is more distributed, patient-centered and home-based. D_2H_2 has potentials to benefit patients by improving the quality and convenience of care, controlling healthcare cost, and preventing medical errors, thus leading to increased access to affordable and effective healthcare.

Technology will be the pulling force into this new era of healthcare and its delivery. Also, how to address key non-technical challenges in D_2H_2 (e.g., stakeholder's resistance and insurance reimbursement) and manage the process of unleashing technological advances will be critical to the success of this new healthcare paradigm. Moreover, the success is dependent on bridging the 'valley of death' in technologies for D_2H_2 and creating a dynamic and entrepreneurial environment and support system for translational research and closer ties and collaboration between researchers, engineers, industry, clinicians and healthcare organizations. Researchers and engineers need to develop products and services that cater to the needs of consumers by solving important unmet clinical needs. More research needs to be performed regarding enabling technologies, and more emphasis should be put onto complex systems engineering and integration strategies for current and future healthcare systems. The government should invest more resources in the forms of grants and financial support of training a new generation of researchers and engineers who are knowledgeable in complex healthcare issues, research projects, standard development and clinical applications so as to accelerate research, development and evaluation of new technologies and their deployment. Also, all the stakeholders need to increase their involvement in patient education and policy changes to equip and encourage the patient to manage their own healthcare responsibly and modify their behaviors if necessary by providing appropriate incentives and penalties. Due to the complexity and scope of D_2H_2, collaboration between researchers, engineers, and providers from many traditional disciplines will be essential in order to overcome the obstacles and realize the full potential benefits of D_2H_2.

We believe that the D_2H_2 paradigm, with all the stakeholders working together toward the common and societal good, will aid in developing a sustainable 21st-century healthcare system with the potential to improve accessibility to healthcare, increase care quality, and control healthcare costs, not only in the developed countries but also in the developing countries. This presentation will summarize the opportunities and challenges in D_2H_2.

STATE-OF-THE-ART IN PROTON THERAPY: MODERN DELIVERY TECHNIQUES AND CURRENT CHALLENGES

A..J. Lomax

Centre for Proton Radiotherapy, Paul Scherrer Institute, Switzerland

Proton therapy has been around for many years, and since the first patient was treated in 1954 in Berkeley, 50,000 patients have been treated world wide, mainly in physics research institutes. Currently, there is a wave of interest in proton therapy, with many hospitals in the USA, Europe and Asia building large scale proton therapy facilities. Interest in this technique has been ignited by the potential of proton therapy to significantly reduce the dose to normal tissues, an indisputable consequence of the fact that protons stop, where photons carry on. Traditionally, proton therapy has been delivered using passive techniques, in which conformal fields are constructed using rotating modulator wheels, scattering foils and field specific collimation and compensation. More recently, scanning methods have been developed, exploiting the fact that protons are charged particles which can be magnetically scanned, a technique which leads ultimately to the concept of intensity modulated proton therapy. The flexibility provided by this technique has been shown to bring a number of advantages over its photon equivalent, due to the possibility to modulate not only in-plane fluence, but also the Bragg peak amplitudes in depth. But is the most appreciated and advertised feature of proton therapy – that is, its well defined range - also its Achilles heal? If protons stop, they cannot be imaged on exit from the patient, and the precision of the delivered dose to the patient can only be as good as the precision of our knowledge of where the protons actually stop. Indeed, given the uncertainties inherent in the planning and delivery process, the precise range of the protons in the patient is almost certainly uncertain. So, just how robust are proton plans to changes in range, what factors can affect this, can these be detected and are there ways of adapting the therapy to deal with them? In this presentation, we will show that the robustness – or otherwise – of a plan to range uncertainties can be very dependent on the type of delivery technique used, and that in some circumstances, proton plans can be remarkably insensitive to such errors. In addition, we will show that there are ways to detect and measure range directly and that, in the presence of even very large changes in patient anatomy, adaptive techniques can be used to correct proton plans without necessarily resorting to re-planning strategies. The potential of such techniques is only just being investigated.

INTENSITY MODULATED PROTON THERAPY: THINGS WE HAVE LEARNT (AND ARE STILL LEARNING)

A..J. Lomax, F. Albertini, A. Bolsi, J. Salk, M. Steneker, T. Boehringer, A.. Coray, S. Lin, E. Pedroni, C. Ares, H.P. Rutz, B. Timmermann, G. Goitein and E. Hug

Centre for Proton Radiotherapy, Paul Scherrer Institute, Switzerland

Strictly speaking, dynamic proton therapy can only be considered to be Intensity Modulated Proton Therapy (IMPT) if the individual Bragg peaks, incident from two or more field directions, are simultaneously optimized. This generally leads to the dose distributions from the individual fields being arbitrarily complex in their form, making IMPT plans quite different in their characteristics to conventional proton treatments. By the end of 2004, 43 patients had been treated with IMPT at PSI, from which we have learnt a number of things about the nature of IMPT plans. Over all delivered IMPT plans, we have used an average of 3.3 fields per plan, and never more than 4 per plan. A systematic study comparing numbers of fields and quality of plan in 5 head and neck cases has confirmed this result, showing that little difference in target coverage or sparing of critical structures was found between 3, 5 and 9 field IMPT plans. Indeed, when estimating secondary tumour risk in these plans, there could be some advantage to using smaller numbers of beams. For instance, this may have the dual benefit of reducing the irradiated volume of normal tissue and of increasing the normal tissue dose out of the low dose, high risk area of the secondary tumor response curve. In the course of our field specific QA, the importance of the lateral distribution of secondary particles in IMPT has become evident. In the 'valleys' of the dose distributions common to IMPT fields, the lateral distribution of the secondary protons add up, leading to increased doses of 5-10% over that calculated using the primary proton fluence only. As these valleys in the distribution are often where critical structures lie, this effect needs to be investigated more thoroughly. Depending on the type of IMPT plan calculated, we have found that for range uncertainties of only 3%, systematic under- and over-dosage of the target volume can result. However, in some circumstances, IMPT has also been found to be surprisingly insensitive to errors in range. In one case, due to a significant gain in weight, changes in range were calculated as being as high as 1cm. Recalculation of the plan in the new planning CT showed that the effect of this range difference on the doses to the CTV and spinal cord were however only of the order of 1-2%. In conclusion, IMPT is a powerful method for achieving highly conformal treatments in particularly complex cases. Our experience is that this can be achieved with relatively few fields, but that special consideration probably needs to be taken of the effects of secondary particle distributions, at least with our delivery system. In addition, the effects of treatment uncertainties such as range variations are not always obvious. Therefore, tools for the analysis of the sensitivity of IMPT plans to uncertainties should be available when assessing IMPT plans.

PROFESSIONAL DEVELOPMENT OPTIONS FOR BIOMEDICAL ENGINEERS

Joel J. Nobel, MD

Founder & President Emeritus, ECRI

Biomedical engineers serve a number of critical roles in hospitals, industry, academia and government. They may also serve as independent consultants to the preceding four entities. A significant number of biomedical engineers work overseas. While this paper remarks on all of these roles it focuses much of its attention on hospital-based engineers, traces their evolution and changing roles and then gives much of its attention to the essential qualities to achieve professional excellence, the opportunities for professional advancement and specific new responsibilities.

Opportunities for professional advancement depend as much on the individual as they do on the healthcare environment, the marketplace and conventions. As in most fields, personal energy, inventiveness and the passion to innovate and excel are the key ingredients for professional success. The common requirement for professional excellence, regardless of the type of employer, is up-to-date knowledge and diligence, energy and wisdom in applying it.

STATE-OF-THE-ART IN MEDICAL IMAGE ANALYSIS

Bart ter Haar Romeny

Department of Biomedical Engineering, Eindhoven University of Technology

The human visual system is remarkably powerful in the tasks of recognition, segmentation and image retrieval. Much can be learned from recent neurophysiologic findings, such as with voltage sensitive dyes, showing neuronal firing activity over a large cortical area in experimental animals. The early stage of the visual system seems to measure mathematical derivatives in the image up to at least fourth order, has a multi-scale hierarchical structure, and has an elaborate mechanism for contextual analysis of orientations. We discuss possible physiological mechanisms for complex feature detection, for the detection of motion fields, edge preserving smoothing, and image segmentation, and image-based retrieval from PACS image databases. The methods turn out to be extremely robust, and match mathematically optimal schemes. Many illustrative examples will be discussed.

IMAGE-GUIDED NAVIGATION IN DEEP-BRAIN SURGERY

Bart ter Haar Romeny

Department of Biomedical Engineering, Eindhoven University of Technology

Parkinson patients sometimes develop sudden insults with strongly disabling tremor. It has been found that electrical stimulation of the nucleus subthalamicus can strongly reduce the insult. However, the precise targeting of this tiny nucleus in the deep brain is difficult and has high risks. The navigation can be assisted by inter-operative MRI (with a mobile MRI in the operating room), optimal path planning by evading blood vessels and ventricles in the penetration path, and by integrated interactive visualisation of the available multi-modality 3D information, such as pre-operative MRI, functional MRI and Diffusion Tensor Imaging tractography. The 3D visualization of the huge datasets is performed in real-time with modern graphics ('computer game'-) cards.

MODERN COMPUTER-AIDED DIAGNOSIS IN RADIOLOGY

Bart ter Haar Romeny

Department of Biomedical Engineering, Eindhoven University of Technology

The overwhelming production of images in modern radiology calls for computer assisted detection methods, especially in the application areas of often occurring tumours, such as breast-, colon- and chest tumours. We discuss several mechanisms in modern computer vision, for the automated detection of polyps in the colon with multi-slice CT with strongly reduced X-ray dose, for automated breast tumour detection with dynamic contrast enhanced MRI, the detection of pulmonary emboli in the lungs from multi-slice CT, and automated detection of stellate tumours in X-rays of the breast. Examples of advanced visualization techniques are discussed for the optimal presentation of the results to the clinicians.

NEW SKILLS AND TOOLS FOR THE SUCCESSFUL 21ST CENTURY CLINICAL ENGINEER

Elliot B. Sloane, Ph.D., CCE

Villanova University, USA

Clinical Engineering has evolved into a very practical and applied sub-specialty of Biomedical Engineering. At the same time, however, the Clinical Engineer's responsibilities in the healthcare enterprise now span virtually all aspects of clinical care as well as many operational efficiency and safety areas. The contemporary Clinical Engineer must necessarily develop a newly expanded range of engineering, management, and scientific skills and tools in order to succeed. In point of fact,

these skills will take most Clinical Engineers far beyond the scope that many other specialized Biomedical Engineers address. Many factors are driving these changes, including the self-contained nature of most hospitals, the modest staffing levels that can be afforded, the diffusion of healthcare technology outside the walls of the hospital, and the rapid diffusion of ICT that directly enables safer, more effective, more cost-efficient, and more wide-spread medical care. For example, because all of these factors contribute to the underlying complexity of the systems and technologies used in healthcare, Clinical Engineers need to study and embrace the new paradigm of System of Systems Engineering (SoSE) to supplement their core System Engineering skills and tools. Emerging integrated clinical decision support systems, for example, are composite systems that may depend on data and analytic resources of dozens of departmental computers to function. Such SoSE environments have novel interdependencies that may vary as each system is updated or expanded. Further, SoSE environments are characterized by "emergent properties" that, if negative, are sometimes referred to as unintended consequences. A simple example would be an integrated homecare decision support system for diabetic patients that inadvertently influenced a surprising number of patients to try to damage or fool the systems to avoid medical intervention. Another major area of skill and tool development that Clinical Engineers will be called on to support is in improving health delivery process engineering and management. This has perhaps been the territory of others to date, but the mediocre processes in most hospitals not only waste money, but they are more and more directly affecting patient health and safety. One example is bed census management, which is so poorly run in many hospitals that patients must wait a day or more for an appropriate acute care bed, or must be held be overnight in the Emergency Department – or redirected to another hospital – because the prior day's discharges were not completed as planned. In point of fact, this is also a SoSE problem, and all of the examples given above can readily be addressed with modern, readily mastered graphic-based simulation and modeling tools. Failure of Clinical Engineers to engage successfully in these areas will only contribute to declining patient care and rising expenses. As pointed out in the US by the Institute of Medicine, these are, indeed, engineering skills and tools, and they have already been widely adopted in many industries like aviation and manufacturing around the globe. The contemporary Clinical Engineer should be highly motivated and encouraged to master and use them.

CONFERENCE PAPERS

MEASURING FREQUENCY OF SPONTANEOUS SWALLOWING

Sohail Afkari[1,2]

[1]*Biomedical Engineering Dept, The Royal Melbourne Hospital, Melbourne, Australia*
[2]*Electronic Engineering Dept, La Trobe University (Bundoora), Melbourne, Australia*
Sohail.Afkari@mh.org.au

Abstract

A new multi-sensory non-invasive portable system capable of detecting spontaneous swallowing in a patient population has been developed. Swallowing signals are recorded via Electromyogram (voltage potentials generated by throat muscles), an accelerometer (laryngeal elevations) and a microphone (cervical auscultation) affixed to the neck at the coniotomy region. Simultaneous signal comparison of all three modalities provides a vastly more reliable measure of swallowing frequency by rejecting artefacts associated with speech, body movement, coughing and background intereferences. The operational accuracy of the system was validated by a hand-held manual counter on a healthy subject undertaking everyday activities. Preliminary results showed a recorded mean spontaneous swallowing frequency of 1.32 swallows/minute and a slighly higher mean voluntary swallowing frequency of 1.52 swallows/minute with the intake of 100ml of water. The device was able to detect 94.3% of dry swallows correctly, with each sensor responding differently to various noise interferences. The proposed system has potential to provide additional diagnostic information in clinical research of possible physiological problems associated with an abnormal swallowing frequency across a range of medical fields.

Key words: dsyphagia, swallowing frequency, electromyogram, cervical auscultation, laryngeal elevations

Introduction

Swallowing dysfunction (dysphagia) occurs when there is a problem with any part of the swallowing process. Dysphagia can present a debilitating and potentially dangerous set of problems that may affect not only health but also an individual's quality of life. Deglutition of liquid or food is a complex physiological procedure that requires the coordination of nerves, pharynx, oesophagus and a combination of 26 muscles found in the mouth and neck region[1]. Any irregularity or problems affecting these organs and/or muscles may have a negative impact, ranging from a mild feeling of discomfort or pain to a total incapacity to swallow altogether.

Dysphagia is commonly associated with individuals having neurological conditions such as brainstem stroke, head/neck injuries, and spinal cord damage[2]. It is also found in individuals suffering from Cerebral Palsy (CP) or Parkinson's Disease (PD) due to muscular discoordination or paralysis respectively[2-3].

Little is known about saliva production and reasons for drooling in children with CP. Literature suggests drooling in children with CP is caused by inefficient and infrequent swallowing[2]. Hence hyper-salivation (excess saliva) is *not* one of the factors responsible for drooling, suggesting a possible relationship between drooling and swallowing frequency.

Many people suffering from PD have difficulty swallowing because they lose control of their mouth and throat muscles. Dysphagia in PD patients cannot be restricted to only the oral phase: abnormalities associated with the pharyngeal stage (actual act of swallowing) are at least equally important[3]. It is suggested that various motor disorders associated with PD have considerable influence on oropharyngeal swallowing and may in fact cause hypokinesia[3] (reduced rate of spontaneous swallowing).

Gastroenterology literature suggests that gastrointestinal symptoms such as bloating, belching and flatus may relate to excessive amounts of air in the GI tract. Symptoms might not be associated with the simple accumulation of gas but may instead be related to excessive swallowing in conjunction with a motility disorder that prevents the normal passage of gas through the bowel[4]. Furthermore, excessive spontaneous swallowing may contribute to disorders such as duodenal ulcer, hiatus hernia, and irritable bowel syndrome. However, a definite link between aerophagia (excessive air swallowing) and GI symptoms is yet to be established.

Other evidence suggests that human swallowing frequency and amplitude increase substantially in stressful situations[5]. A portable recording device would be an ideal tool to study this question further in daily life.

The current gold standard method for assessment of the swallowing process is Video Fluorography Swallow Study (VFSS). VFSS is a radiological procedure allowing immediate visual inspection, detection, and localization of abnormalities and functional impairments[6]. However, VFSS is a time-consuming and a non-portable recording system lacking continual monitoring. Likewise the method cannot be used frequently due to the risk of excessive radiation exposure[6]. It may be also be rather daunting in application with child, and it lacks interactive therapy.

Other techniques include Fibreoptic Endoscopic Evaluation Study (FEES) and manometry swallowing studies. FEES provides a reliable predictor of aspiration, penetration and visualization of the pharyngeal stage of swallowing before and after, but not during, the swallow. In addition both are generally uncomfortable, poorly-tolerated

and only provide information regarding the quality of the swallowing process[7].

The use of such techniques to determine the rate of swallowing would be simply too time-consuming. Clinicians would need to count the number of recorded swallows manually, post procedure. Although the swallow detector is not a replacement for any of these techniques it may provide extra information for a more accurate diagnosis.

Non-invasive techniques are generally preferred by both patient and clinicians in any study. Studies have proposed that invasive rather than non-invasive techniques, although providing more accurate data, interfere with the swallowing rate. Irritation caused by the catheter or camera rubbing against the inside of the oesophagus may in fact increase saliva production and as a result have a direct effect on the rate of deglutition[2].

In recent years surface electromyography (SEMG), accelerometer, cervical auscultation, respiratory, electro-laryngograph and other non-invasive techniques have been used in separate swallowing studies, however, no clear best choice has as yet emerged[1].

In this paper a new, portable, non-invasive electronic device utilizing Electromyogram (voltage potentials generated by throat muscles), an accelerometer (laryngeal elevations) and a microphone (cervical auscultation) simultaneously is described.

Methodology

The different stages of swallowing and their disorders have been extensively studied using a variety of techniques. However, the rate of spontaneous swallowing and possible physiological problems associated with an abnormal swallowing frequency has rarely been investigated. Prior to any system design, the frequency and time response of swallowing needed to be investigated. Furthermore, because the system was to be portable a variety of everyday physiological and surrounding environmental signals were also researched.

Talking, coughing, laughing, carotid pulse, body movements and surrounding noises were tested for each sensor individually using the Tucker Davis Technology (TDT) physiological signal processing system. Appropriate frequency bandwidth for filtering out all possible interferences and signal amplification levels were determined, allowing for easy swallow detection.

The system can be divided into four sections; sensory, signal conditioning (amplification, filtering, threshold comparing), signal processing and display unit. A block diagram showing the main operational components of the device and their inter-relationship is presented in figure 1.

Sensory

Sensor selection for device was based on cost, practical clinical use, precision in portable applications and conclusions of reviewed relevant studies. A miniature accelerometer (ACC), three disposable surface EMG electrodes and an omnidirectional electret microphone

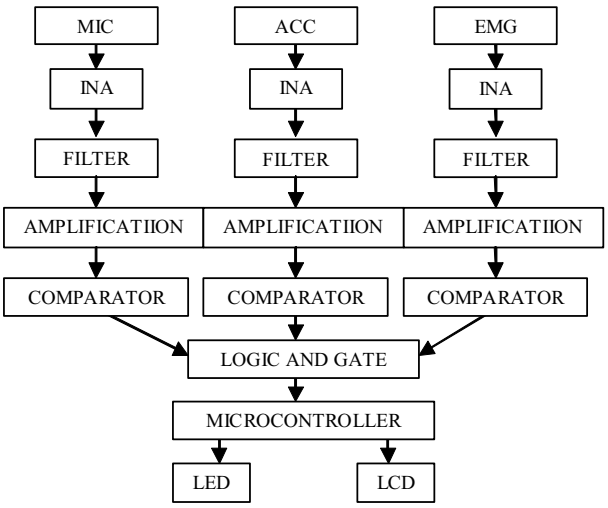

Figure 1. *Overall system block digram.*

(MIC) were placed and taped to the surface of the skin on the throat of a normal healthy subject. The accelerometer was placed at the level of the thyroid cartilage and the EMG electrodes and microphone were placed at the level of the cricopharyngeus muscles and cricoid cartilage respectively. The subject was asked to perform multiple swallows and various interferences independently, followed by a series of recordings involving swallowing and interferences together; sensor and electrode skin interference was also investigated.

The placement of sensors and electrodes is imperative for a clear signal. The placement resulted from reference to prior work[1,3,8] and own initial exploratory investigations. Placing the accelerometer at the thyroid cartilage produced the largest signal recording, particularly in males due to the Adam's Apple. The cricoid cartilage was found to be the optimal site for detection of swallowing sounds by the microphone, because the recorded signal had the greatest signal-to-noise ratio (SNR). Good electrical contact with the skin for the reference electrode in an EMG recording is crucial. The forehead was found to be the best location in terms of reducing common mode noise and providing a clear signal. However, positioning the electrode on the forehead would be both impractical and inconvenient for the patient. Other positions like the scapula and back of the neck were also tested; however, body movement corrupted the signal significantly. Hence, the most reasonable position overall was considered to be posterior to the two other recording electrodes. Figure 2 illustrates sensors and electrodes recording position.

Double-sided tape was used to secure MIC and ACC to the patient's neck, while disposal electrodes were applied by wiping the skin with isopropyl alcohol proved to be the best form of preparation for most EMG applications (the alcohol removes the dead skin and surface oils improving ion flow).

Analog signal conditioning

Each sensor signal is filtered and amplified individually. The optimal filtering bandwidth and overall

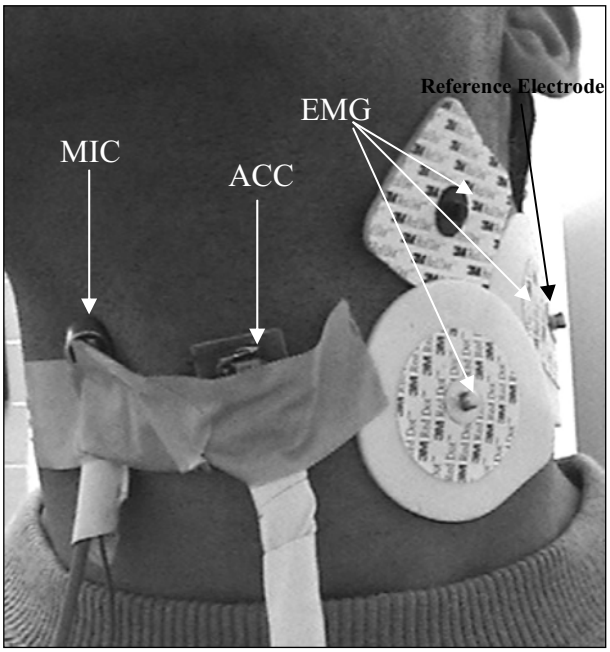

Figure 2. *Sensory placement.*

gain for each signal from each sensor was designed after extensive study of the frequency response and mean power density spectrum for a swallow and all possible interferences. Figure 3 illustrates the raw sensor signals and effects of the designed filters.

Sensor signals are amplified using a two-stage amplification process, which allows the preservation of the high common mode rejection ratio of the instrumentation amplifiers used. Furthermore, single high gain values could drive the amplifiers into saturation due to the high DC offset voltage produced by the chemical reactions between the electrodes and the skin for the EMG recording.

In order to detect only a swallow and reduce the occurrence of false positives, all three signals were compared simultaneously. The filtered signal from each sensor is individually compared to a reference voltage to produce a sensor pulse. These three sensor pulses are inturn applied to a triple input logic AND GATE, producing a single swallow pulse.

Digital signal processing

The generated swallow pulse from the logic AND gate is fed to a microcontroller which drives a LED and a LCD screen, flashing and displaying the swallow count on every detected swallow respectively.

Interference

The two main sources of interference even after filtering, giving way to inaccurate detection, was found to be talking and body movements in particular head movements.

Talking

The EMG and microphone filters attenuated the talking signal in comparison to a swallow allowing for easy detection. However, it was found that talking recorded by the accelerometer had some frequency components in the

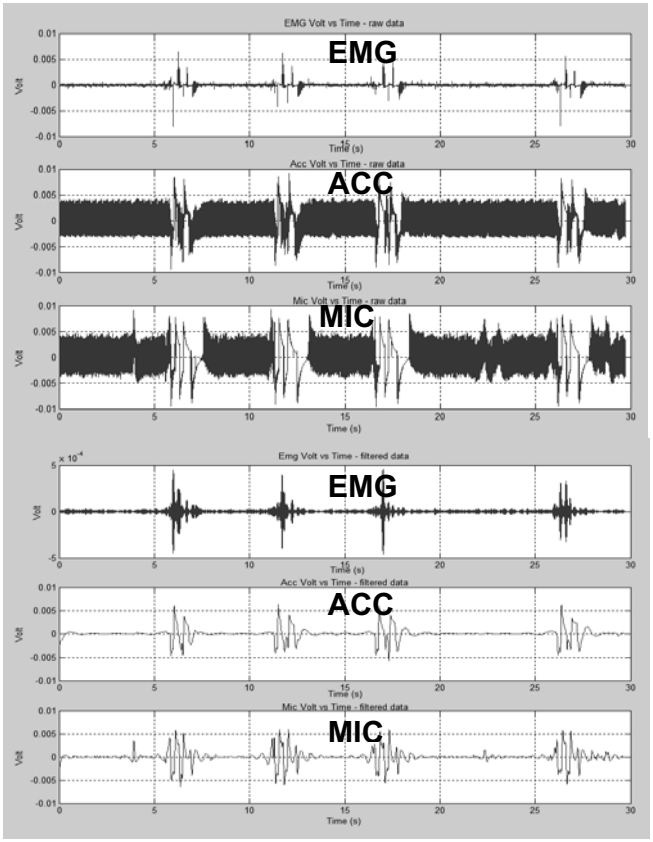

Figure 3. *Raw swallow signal (top) and filtered swallow signal g*

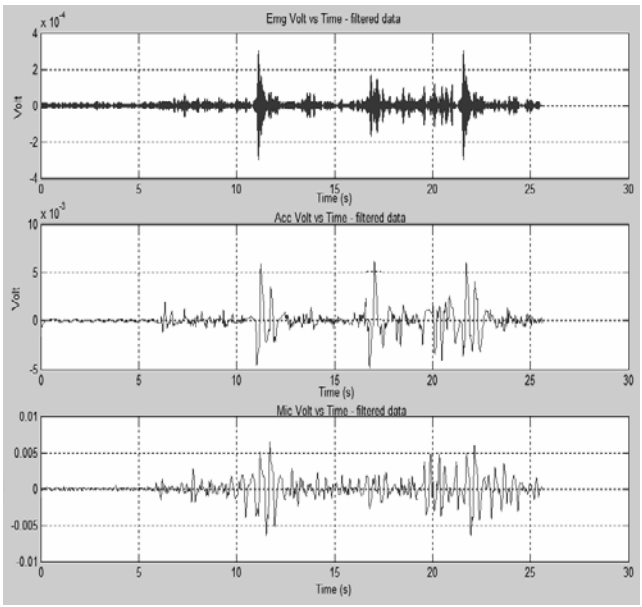

Figure 4. *Time domain representation - swallowing and talking after filtering.*

same bandwidth as the designed filter (figure 5): this would potentially produce false positives.

Body movements

In contrast, frequency components associated with head/neck movements were found to fall in the EMG's and microphone's filter bandwidths. This accounts for

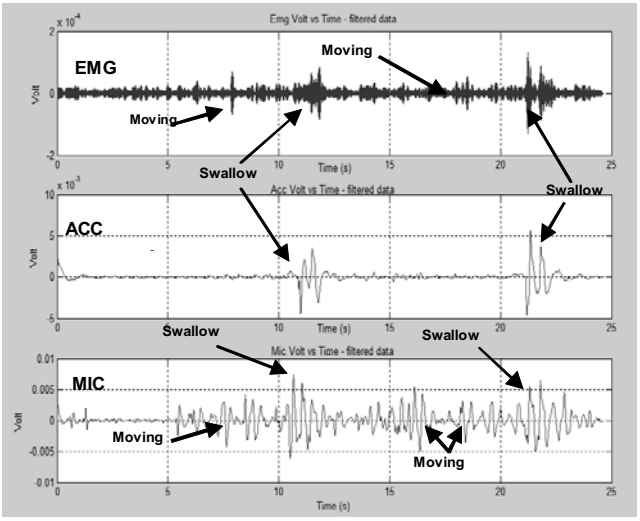

Figure 5. *Time domain representation - swallowing and body movements after filtering.*

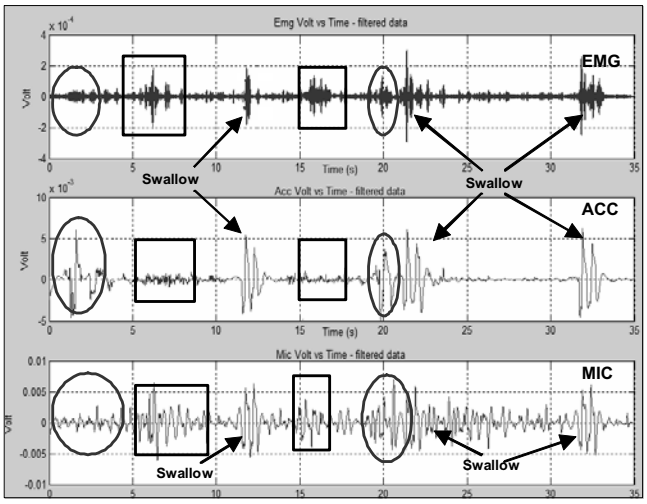

Figure 6. *Time domain representation - talking, body movement and swallows after filtering (Talking illustrated in ovals and body movements in rectangles).*

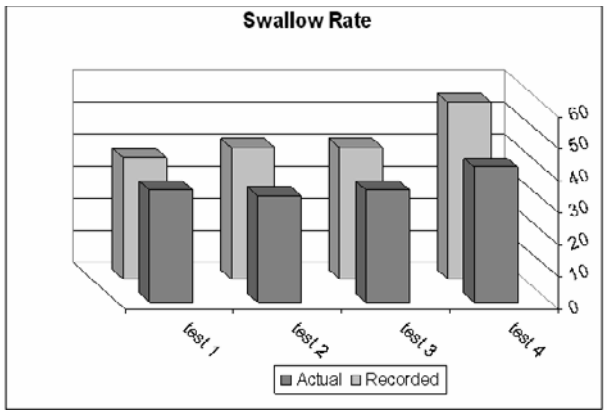

Figure 7. *Device accuracy (Detected Vs actual swallow).*

head/neck movement not being removed from the signal for the EMG and slightly attenuated in the microphone as shown in figure 6. Again this would likely produce false positives. However, the accelerometer filter completely removed any artefacts associated with movement.

Swallow detection

To reduce the occurrence of false positives due to taking and body movement the three signals were compared simultaneously. Figure 7 demonstrate the effects of talking and body movement in comparison to swallows for each sensor. The EMG and microphone filtered signals can be corrupted by head movements, however, the accelerometer cannot. Therefore the output of the AND GATE will remain low and no swallow will be counted. In contrast, the accelerometer signal may become corrupted by talking but the EMG will not, and again no swallow will be registered. Thus, a swallow is considered to occur if and only if all three sensor pulses are high concurrently. Although this will not stop the occurrence of all false positives, it was found to significantly reduce them.

Results

A healthy subject with no prior swallowing abnormalities undertook four thirty minute tests with 24 hour intervals between each test. With the device connected the subject was asked to perform various activities. Three out of the four were dry swallows (spontaneous) and the other a wet swallow with the intake of 100mls of water; the subject was asked to drink the 100ml of water as fast as possible. A hand-held counter was manually incremented for every actual swallow. The total number of swallows recorded by the system was compared to the hand-held manual counter at five minute intervals.

Under dry swallowing conditions the system recorded a spontaneous swallowing frequency of 1.32 swallows per min with an error of 5.67%. With the consumption of 100ml of water the voluntary swallowing frequency increased to 1.52 swallows per min with an error of 7.25%.

During the first test the subject was asked to sit still; during the second test the subject undertook general talking, walking and calm moments of limbs and head. During the third test the subject was asked to yell and shake both head and limbs. Test One produced the smallest error (3%), while Test Three had the highest (8%).

Conclusion and future work

A non-invasive and portable system capable of detecting swallows was successfully developed. Preliminary testing on a healthy subject showed promising results as to the accuracy of the designed system. Using three different methods of recording: EMG, accelerometer and microphone, an accurate swallow rate was acquired. The detection of false positives was reduced, in contrasted to other similar studies, comparing all three sensor signals simultaneously.

The design of such a system paves the way for future clinical research studies into possible physiological problems associated with an abnormal swallowing frequency across a wide range of medical fields.

The present development stage of the device includes

undergoing further testing in a clinical study in parallel to a manometry study in a patient population. The study protocols are to test and validate the limitations and reliability of the overall system as well as the usefulness and significance of each sensor individually. The detected swallows will be compared to the true number of swallows that occurred during the manometry study across varying parameters, such as gender, age, neck circumference and swallowing depth, which determine whether the swallow is detected or not.

Acknowledgments

The authors thankfully acknowledge the support received from Paul Junor (Electronic Engineering Dept, La Trobe University), Assoc Professor Geoff Hebbard (Gastroenterology, Royal Melbourne Hospital), Libby Ferguson (Speech Pathology) and Assoc Professor Dinah Reddihough (Developmental Medicine) at The Royal Children's Hospital. In addition the continued support of the Biomedical Engineering department at the Royal Melbourne Hospital.

References

1. Firmin, H., Reilly, S. and Fourcin, A., *Non-invasive monitoring of reflexive swallowing*, Department of Phonetics and Linguistics, Speech Hearing and Language: work in progress, Vol.10, 1997.
2. Senner, J.E., Logemann, J. and Zecker, S., *Drooling, saliva production, and swallowing in cerebral palsy,* Developmental Medicine and Child Neurology, Vol. 46; Issue 12, pages: 801-806, 2004.
3. Ertekin, C., Tarlaci, S., Aydogdu, I., Kiylioglu, N., Yuceyar, N., Turman, B., Secil, Y. and Esmeli, F., *Electrophysiological evaluation of pharyngeal phase of swallowing in patients with Parkinson's disease,* Movement Disorders, Vol. 17, Issue 5, Pages: 942 – 949, Apr 2002.
4. Bredenoord, A., Weusten, B., Timmer, R. and Smout, A., *air swallowing, belching, and reflux in patients with gastroesophageal reflux disease*, American Journal of Gastroenterology, Vol. 101 Pages: 1721–1726, 2006.
5. Ritz ,T. and Thöns, M., *Affective modulation of swallowing rate*, *unpleasantness or arousal*; Journal of Psychosomatic Research, Vol. 61, Issue 6, Pages: 829-833, Dec 2006.
6. Perlman, A., He, X., Barkmeier, J. and Van Leer, E., *bolus location associated with videofluoroscopic and respirodeglutometric events*, Journal of Speech, Language, Hear & Respiratory, Vol. 48, Pages: 21–33, 2005.
7. Lim, S., Lieu, P., Phua, S., Seshadri, R., Venketasubramanian, N., Lee, S. and Choo, P., *accuracy of bedside clinical methods compared with fiberoptic endoscopic examination of swallowing (FEES) in determining the risk of aspiration in acute stroke patients*; Dysphagia, Vol. 16, Issue 1, Pages: 1–6, 2001.
8. Takahashi, K., Groher, M. and Michi, K., *Methodology for Detecting Swallowing Sounds, Dysphagia*; Vol. 9, Issue 1, Pages: 54-62, 1994.

ELECTRICALLY-EVOKED CONTROL OF THE SWINGING LEG AFTER SPINAL CORD INJURY: OPEN-LOOP OR MOTION SENSOR-ASSISTED CONTROL?

G.P. Braz[1,2], M. Russold[1], R.M. Smith[2] and G.M. Davis[1,2]

[1]*Rehabilitation Research Centre, The University of Sydney, Australia*
[2]*Discipline of Exercise and Sport Science, The University of Sydney, Australia*
gbra6016@usyd.edu.au

Abstract

In paraplegics, gait can be restored by means of functional electrical stimulation (FES). Because the electrophysiological responses of the lower limbs to the neuromuscular stimulus are not completely deterministic, several stimulation strategies have been reported in an attempt to refine stepping motion. In open-loop (OL) systems, the electrical stimulation sequences applied over the leg muscles are often tuned for each patient in order to improve the quality of gait. Our aim was to contrast this traditional technique against variable stimulation sequences based on motion sensors (MS) data feedback. Both strategies were tested over 240 stepping trials in three complete paraplegics. In comparison to OL, which used a customised stimulation sequence for each subject, the same MS strategy was as functional for all three subjects. Despite MS producing a lower variability on step lengths, the toe clearances had a similar pattern of variability regardless of the strategy applied. Although the novel MS showed promising results, the reliability of OL was also demonstrated. Therefore, we still recommend the use of OL mainly due to its faster donning and doffing, since this is a matter of importance for the user acceptance of any rehabilitation systems.

Key words: Functional Electrical Stimulation (FES); Control; Gait Rehabilitation; Motion Sensors.

Introduction

For paraplegics, the re-establishment of upright mobility by means of functional electrical stimulation (FES) is a well-established topic in the research community. The basis of FES-evoked gait relies on two major components: the maintenance of knee extension of the stance leg and the quality of the swinging leg motion. Although the first has a significant importance in terms of safety, it is the manner in which the leg swings forward that will determine the regularity of the step lengths and therefore the quality of overall locomotion.

The control of FES-evoked stepping can be made with the stimulation of hip flexors and hamstrings to promote toe clearance with knee flexion; and subsequent stimulation of quadriceps engendering knee extension prior to heel-strike[1].

Table 1. *Stimulation frequencies, pulse widths and intensities applied for each subject. During the experiments the quadriceps stimulation amplitude of the stance leg was increased by 20mA to sustain knee extension in the event of fatigue-driven knee buckle.*

	Quadriceps	Gluteus	CPN		
			-	Right	Left
S1	33Hz-150μs-80mA	33Hz-150μs-65mA	50Hz-400μs	70 mA	85 mA
S2	33Hz-150μs-80mA	33Hz-150μs-65mA	100Hz-400μs	155 mA	180 mA
S3	33Hz-150μs-70mA	33Hz-150μs-50mA	50Hz-400μs	45 mA	45 mA

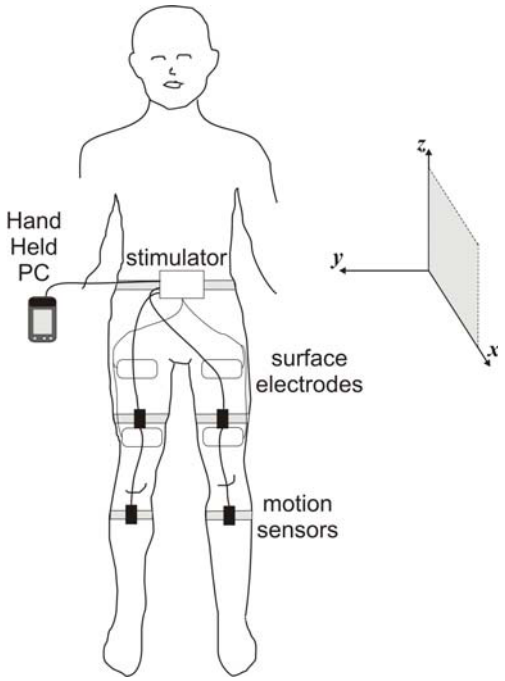

Figure 1. *The surface FES System composed of a stimulator, motion sensor packs and a hand-held PC. During the experiments, the hand-held PC was controlled by an operator with the sensors providing absolute angles from the sagittal plane (xz-plane of the diagram).*

In recent years, the predominant stimulation practice to evoke stepping has used surface stimulation on: (i) common peroneal nerve (CPN) in the popliteal fossa to elicit withdrawal reflex; (ii) quadriceps to extend the knee during the swing phase and (iii) gluteus for hip stabilization [2,3].

Some complications with this technique have been carefully documented. They are mostly related to the intra and inter-subject variability of latency, i.e. the delay for the initiation of the withdrawal reflex from the stimulus onset and variability in hip flexion[4]. Also, the decrease in hip flexion responses over a certain number of reflex stimuli (habituation) has been shown to reach levels of complete attenuation[5].

The need for more appropriate stimulation strategies has been emphasized[4], especially those applying mechanisms to modulate flexion reflex excitability[6]. Many of these studies have an electrophysiological focus to overcome the decline in flexion reflex responses by applying a low frequency/long pulse width stimulus (dishabituating stimulus)[7,8]. Results from these studies have shown that although habituation could be attenuated, hip flexion was still variable.

In an attempt to refine not only hip flexion motion but also knee angular velocities during stepping, open-loop FES-systems using customised stimulation sequences are often used[9]. This measure, however, requires the presence of a FES-gait specialist to fine-tune the stimulation sequences, thus limiting this practice to the research environment.

Accordingly, we proposed a novel control strategy where the stimulation sequences were automatically adapted based on the feedback of four compact motion sensors. The kinematics of stepping resulting from this strategy and from customised open-loop sequences were contrasted over multiple stepping trials and their respective advantages for the clinical field were examined.

Material and Methods

System overview

The electrical stimulator used in this experimental study was the ExoStim (formerly Neopraxis Pty. Ltd., Lane Cove, Australia). It consisted of an 8-channel surface stimulator designed to apply biphasic pulses (charge-balanced with inter-pulse phase delay of 1/*f*) within a range of 20-100Hz, at a pulse width of 150-400μs and amplitude of 0-180mA (pulse peak, constant current)[10].

Four compact motion sensors, containing one rate gyroscope and two 2-D accelerometers each were strapped to the thighs and shanks of the subjects and provided absolute angular data in the sagittal plane. This sensor configuration allowed data collection of angular displacements of the thigh and shank segments in relation to the direction of gravity. Consequently, knee angles were defined as the angle between thigh and shank and hip angles as the angle between the trunk and the thigh. A previous study performed at our laboratory verified the accuracy of these sensors in multiple able-bodied sit-to-stand and walking cycles[11]. The dimension of each sensor pack was 63 x 35 x 10 mm and data were sampled at 10Hz.

A hand-held PC (Cassiopeia EG-800STG, Casio Inc., Japan) running a C++ embedded software controlled the stimulator and sensors (Figure 1).

Study participants

The subjects of this study were three complete paraplegics (S1: T4; S2: T8-9; S3: T4), all experienced FES users with at least 32 weeks of training.

Stimulation parameters

The stimulation parameters used for each subject are described in Table 1. During stepping, CPN, quadriceps and

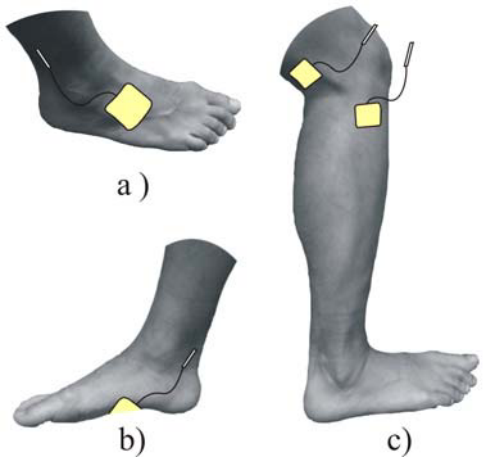

Figure 2. *Electrode placements in the foot region of the extensor digitorum brevis muscle (a) and medial plantar arch (b) for S2 and in the region of the knee popliteal fossa (a) for S1 and S3.*

gluteus were stimulated. The subject's stance leg was straightened via stimulation of quadriceps and gluteus.

Electrode placement

Stimulation was delivered by Empi gel-backed self-adhesive surface electrodes. Quadriceps and gluteus electrodes were placed over the bellies of these muscle groups (SE6000 7 x 13cm oval electrodes). CPN stimulation was applied with 5 x 5cm square electrodes (SE5000) in the knee region of the popliteal fossa for S1 and S3 (Figure 2c). For this site, S2's reflex responses were ineffective, however a good response ocurred when stimulating the CPN afferent nerve fibres in the foot region of the extensor digitorum brevis muscle and medial plantar arch (Figure 2a and 2b). Electrode placement was measured during the first day of testing, and kept consistent during other days of testings to ensure that muscle fibre recruitment and reflex-responses were comparable.

Control strategies

Open-Loop (OL) stimulation sequences

The optimal stimulation sequences for stepping were determined for each subject in 2-4 sessions with the support of the Vienna FES System (Ottobock Healthcare GmbH, Austria)[12]. These sequences were then duplicated for experimental deployment with the ExoStim. A graphical representation of the stimulation sequences is shown in Figure 3. Due to the weight transfer prior to the steps, the stimulation on the stance leg was increased by 20mA to enable a greater 1-leg support during swing phase (shown as QST's thickened line in Figure 3).

Motion Sensor (MS) driven stimulation sequences

Our motion sensor-oriented stepping was structured as a finite state controller with deterministic rules controlling the stimulation channels. After the command to trigger a step was initiated, the stimulation of the quadriceps and glutei muscles was switched off and the CPN stimulation was activated, thus engendering toe-off. With the thigh swinging upwards and the knee flexing, when both knee and thigh excursion angles reached 30° and 25° respectively, CPN stimulation was switched off. The quadriceps stimulation was then ramped back up within 300ms followed by the stimulation of glutei (Figure 4). During this swing phase the quadriceps stimulation of the stance leg had an increment of 20mA as in the open-loop approach.

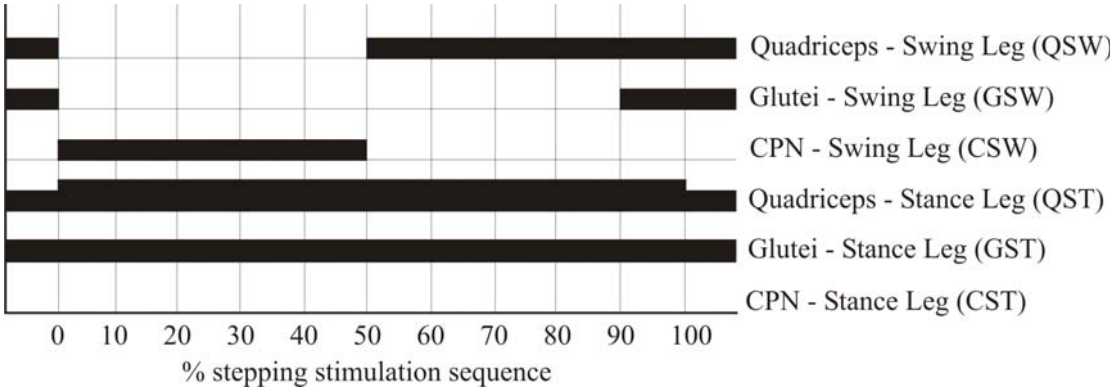

Figure 3. *Typical activation patterns for the open-loop stimulation sequences during stepping. From the double support phase, the weight is transferred to the stance leg prior to the initiation of a step. After the stepping command is triggered, the stimulation amplitude in the QST is increased by 20mA and toe-off commences with the CSW activation and QSW-GSW deactivation. Approximately in the middle of the stepping cycle, the QSW is switched on extending the knee and bringing the foot forward prior to heel-strike. Finally, GSW is activated to enhance hip stabilization. The illustrated timings were different for each of our three subjects accordingly to the best stepping responses obtained over approximately 3 experimental sessions.*

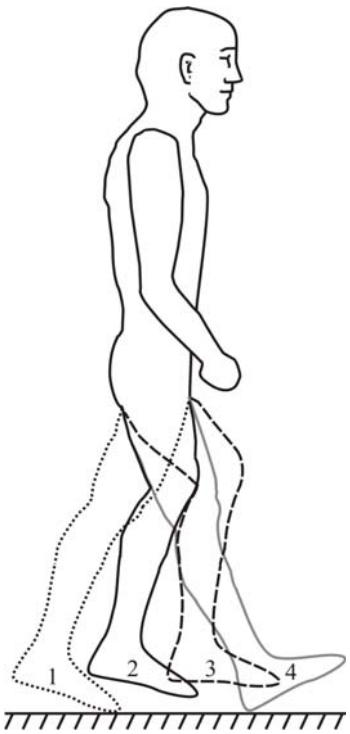

Figure 4. *Phases of the leg swing controlled by MS: 1) toe-off: CPN activation; 2) When $\theta_{THIGH} \geq 25°$ and $\theta_{KNEE} \geq 30°$ from toe-off position: CPN deactivation/quadriceps activation; 3) swing through: quadriceps stimulation ramping up for 300ms followed by glutei activation; 4) heel-strike.*

Table 2. *Retro-reflective marker setting used to define the body segments.*

Defined body segment	Marker placement
Trunk	C7 Sternum T10
Left/Right Thigh	Greater trochanter Anterior mid-thigh Lateral epicondyle
Left/Right Shank	Medial epicondyle Anterior mid-shank Lateral malleolus
Left/Right Foot	Head of 1st metatarsal Head of 5th metatarsal Medial malleolus

Experimental set-up

Experiments were undertaken in a biomechanics laboratory using the Expert Vision Advanced™ (EVa) motion analysis system (Motion Analysis Corp., CA, USA). It consisted of eight cameras (Eagle) that captured video data at 100Hz. Retro-reflective markers were attached to the study participants to define the body segments (Table 2).

As a safety procedure all subjects used a harness system to prevent falling in case of severe knee buckle and wore malleable ankle guards to protect their ankles from harmful inversion/eversion. To minimise the load on the stance leg, subjects used an elbow frame during the experiments. This allowed the subjects to step forward with their stance leg and torso leaning slightly forward, in a position similar to those that most subjects step when using a rolling frame.

Testing protocol

Each subject performed multiple stepping trials within 4 testing days. One strategy was tested per day: 2 days of OL and 2 days of MS, applied in a counter-balanced order (OL, MS, OL, MS). The protocol for one day of testing consisted of: (i) 2 sets of 5 consecutive steps with the left leg and (ii) 2 sets of 5 consecutive steps with the right leg. A resting interval of 5 minutes was carried out between each set of 5 steps, which were alternated between right and left leg accounting for stance leg's quadriceps fatigue. Prior to the initiation of a step, the swing leg's toe was positioned approximately in line with the stance leg's heel (Figure 5). After a step was performed, the swing leg was manually repositioned before another step with the same leg was initiated. At least one day of rest was given between testing days. Accordingly, this protocol collected a total of 40 steps per subject's leg, 20 for each strategy.

Data analysis

The collected data was analysed with KinTrak 6.2 (Human Performance Laboratory, University of Calgary, Alberta, Canada). Hip flexion was a variable of interest in our analysis since it has already been used in a substantial

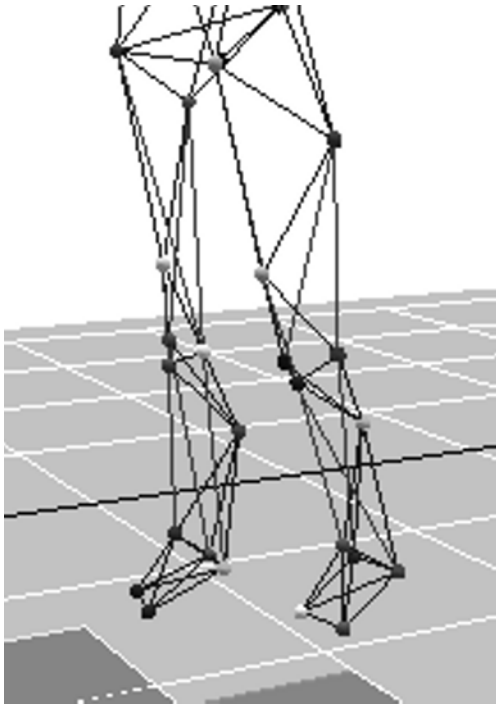

Figure 5. *Marker set from the motion analysis system, indicating the alignment between stance and swing leg prior to the initiation of a step.*

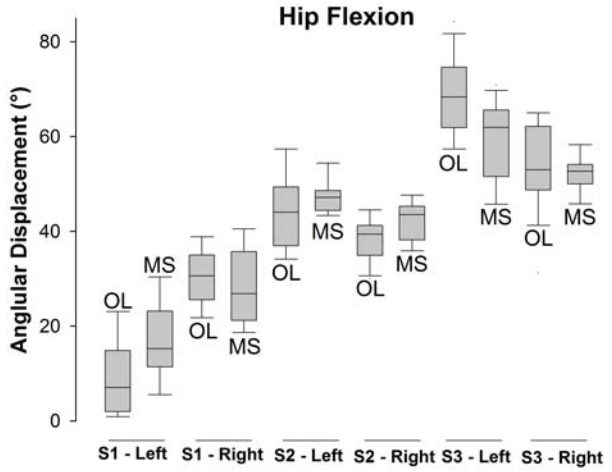

Figure 6. *Range of hip flexion obtained during OL and MS. For S1's left leg, MS slightly improved the poor hip flexion obtained during OL. On the other hand, MS also attenuated S3's high hip excursion. For S2, the hip flexion for both OL and MS were in a similar range.*

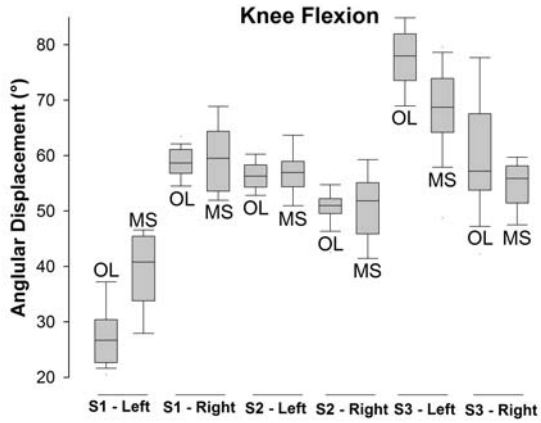

Figure 7. *Range of knee flexion obtained during OL and MS. Similarly to the hip flexion outcomes, despite S2 having comparable values between OL and MS, MS slightly improved S1's small knee flexion on his left leg and at the same time decreased S3's extremely high knee flexion.*

number of FES stepping studies[4,5,7,8]. In addition, we considered knee flexion, toe clearances and step lengths to be of relevance, especially as the last two have an important relationship to overground locomotion.

Results

Interestingly, the hip flexion patterns varied within different ranges amongst our subjects (Figure 6). S1 showed a small hip flexion in his left leg during OL, but not during MS. S2 had similar results for both strategies while S3 demonstrated large hip flexions during OL. This was reduced when MS was used.

Similar results were found for knee flexion (Figure 7). Again, MS increased knee flexion in the left leg of S1 and reduced the knee flexion of S3. S2 showed very similar results for MS and OL. The variability (i.e. the difference between the maximum and minimum values observed) was visibly smaller during OL in S1, S2 and for the left leg of S3.

In all subjects MS showed a trend towards "limiting" toe clearances, thus avoiding outliers with very high or very low clearances (Figure 8). However OL's variability in toe clearances was in most cases also within a small 5cm range. The narrow range of toe clearances in both OL and MS indicated that habituation did not occur during our protocol of 5 consecutive steps within the same leg.

Step length variation was less using MS than with OL for subjects S2 and S3 (Figure 9). Although a greater variability was observed for S1, this subject had a particularly good symmetry on the range of step lengths between right and left leg for MS.

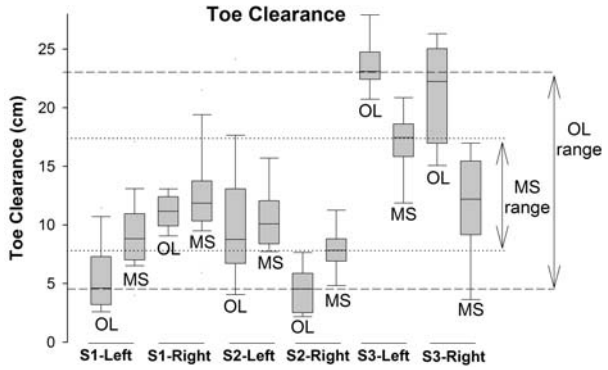

Figure 8. *Toe clearances for OL and MS. In most cases the variation of toe clearance displayed within the 25th and 75th percentile intervals (box area) was within a range of 5cm for both MS and OL, which was a positive outcome. Considering the range between the maximal and the minimal median values for MS (dotted lines) and OL (dashed lines), MS had a markedly lower variability.*

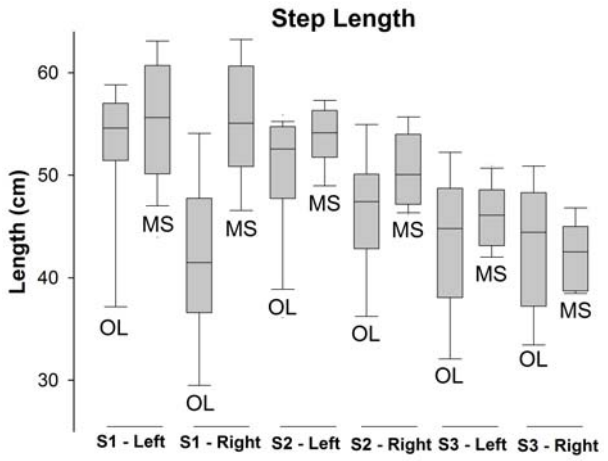

Figure 9. *Step lengths for OL and MS. This data indicated that although MS had a lower variability for S2 and S3, its variability was still considerable for S1. However, for this subject in particular, the step length differences between right and left leg were significantly lower when compared to OL.*

Discussion

In order to provide a more clinically practical closed-loop strategy our MS strategy with a simplified setup of four miniaturised motion sensors was deployed in three paraplegic subjects. To better understand the stepping kinematics, data from the MS strategy were contrasted to the data of open-loop stimulation sequences.

Surprisingly, our results revealed that greater hip and knee excursions have not necessarily engendered greater step lengths or toe clearances. As shown in our data, greater hip flexions were also likely to be associated with greater knee flexions. These larger knee flexions were probably the reason why step lengths were limited, as the combination of a big hip and knee flexion were more likely to result on a step on the spot rather than forward. This is an important point because the literature often cites large hip flexions as a good outcome in FES stepping[4,5].

Our data indicated that the variability of hip and knee flexion was more likely to be associated with the individual responses of each leg to the stimulation rather than to the strategy that was applied. In principle, MS was designed to limit extensive thigh angular excursion, and consequently toe clearance. However, even after deactivating CPN stimulation (once the angular criterion was met), the thigh still continued to swing upwards. Subject S3 was a good example as his toe clearances were excessively high for both MS and OL. During our 3 days of pre-tests tuning his OL sequences, we observed two distinct stepping responses: one "quasi-unresponsive" with very short step lengths and low clearances when CPN stimulation was below 45mA (50Hz, 400μs); and another more functional, but with high clearances, when CPN stimulation was equal to or higher than 45mA (50Hz, 400μs). Steps with lower frequencies and pulse-widths were unresponsive. MS was probably a better strategy for this subject because its angular criterion reduced the overall range of toe clearances compared to OL. The middle 50% of toe clearances were also less spread for MS. This subject's toe clearances could probably be further decreased by using smaller values for the MS angular criterion; however, this was not applied in our study as we aimed to demonstrate the feasibility of the same angular criterion for all three subjects.

It was interesting to note that the values of hip and knee flexion in S2 still resulted in insufficient toe clearances when compared to S1 and S3. This may have because S2's CPN stimulation was through the sole of the foot, which was more likely to produce a "passive" plantarflexion rather than an "active" dorsiflexion for this subject. This could have been related to the lack of tibialis anterior contraction due to the stimulation of the sole.

One suggestion that we have for future studies is the use of knee angular velocities (ω_{knee}) as a feedback variable controlling the stepping motion. This was not done on our study due to limitations in the sensor's sampling frequency of our system. Since ω_{knee} is linearly associated with joint power (JP = angular velocity x angular moments), the minimization of ω_{knee} could reduce the mechanical energy of the swinging leg, thus minimising the possibility a joint injury[13]. Although the control of ω_{knee} during CPN-evoke reflexes might not be feasible, a smoother activation of the quadriceps during the knee extension phase might be useful to refine the end of the leg swing motion.

Conclusions

Overall, our results demonstrated that the control of leg swing by means of FES has limitations that are closely related to the variability in the responses of the nerves and muscles to the stimulation. Our MS strategy tried to counteract the effects of latency on the flexion responses of paralysed legs and the results were translated into more repeatable step lengths in relation to OL.

Although MS provided interesting results, the cost-benefit of using motion sensors were still questionable, since the OL also provided good and functional outcomes with a much simpler setup. The understanding that an easier setup is a key factor for the clinical acceptance of any assistive system is not only fundamental, but crucial to benefit more individuals in need of special technologies.

Acknowledgements

This research was supported by the National Health and Medical Research Council project grant #302013, the NSW Office of Science and Medical Research and CAPES, Brazilian Government.

References

1. Franken, H. M., Veltink, P. H., Baardman, G., Redmeyer, R. A., and Boom, H. B. *Cycle-to-cycle control of swing phase of paraplegic gait induced by surface electrical stimulation*. Med Biol Eng Comput, *33:* 440-51, 1995.
2. Popovic, D., Radulovic, M., Schwirtlich, L., and Jaukovic, N. *Automatic vs hand-controlled walking of paraplegics*. Med Eng Phys, *25:* 63-73, 2003.
3. Chaplin, E. *Functional neuromuscular stimulation for mobility in people with spinal cord injuries. The Parastep I System*. J Spinal Cord Med, *19:* 99-105, 1996.
4. Granat, M. H., Heller, B. W., Nicol, D. J., Baxendale, R. H., and Andrews, B. J. *Improving limb flexion in FES gait using the flexion withdrawal response for the spinal cord injured person*. J Biomed Eng, *15:* 51-6, 1993.
5. Nicol, D. J., Granat, M. H., Baxendale, R. H., and Tuson, S. J. M. *Evidence for a human spinal stepping generator*. Brain Res, *684:* 230-2, 1995.
6. Knikou, M., and Conway, B. A. *Effects of electrically induced muscle contraction on flexion reflex in human spinal cord injury*. Spinal Cord, *43:* 640-8, 2005.
7. Granat, M. H., Nicol, D. J., Baxendale, R. H., and Andrews, B. J. *Dishabituation of the flexion reflex in spinal cord-injured man and its application in the restoration of gait*. Brain Res, *559:* 344-6, 1991.
8. Nicol, D. J., Granat, M. H., Tuson, S. J., and Baxendale, R. H. *Variability of the dishabituation of flexion reflexes for FES assisted gait in spinal injured man*. Med Eng Phys, *20:* 182-7, 1998.
9. Bijak, M., Rakos, M., Hofer, C., Mayr, W., Strohhofer, M., Raschka, D., and Kern, H. *Stimulation parameter optimization for FES supported standing up and walking in SCI patients*. Artif Organs, *29:* 220-3, 2005.

10. Simcox, S., Davis, G., Barriskill, A., Middleton, J., Bruinsma, I., Duncan, M., and Smith, R. *A portable, 8-channel transcutaneous stimulator for paraplegic muscle training and mobility - A technical note*. J Rehabil Res Dev, *41:* 41-51, 2004.
11. Simcox, S., Parker, S., Davis, G. M., and Smith, R. *Performance of orientation sensors for use with a FES mobility system*. J Biomech, *38:* 1185-90, 2005.
12. Bijak, M., Mayr, W., Rakos, M., Hofer, C., Lanmuller, H., Rafolt, D., Reichel, M., Sauermann, S., Schmutterer, C., Unger, E., Russold, M., and Kern, H. *The Vienna functional electrical stimulation system for restoration of walking functions in spastic paraplegia.* Artif Organs, *26:* 224-7, 2002.
13. Dolan, M. J., Andrews, B. J., and Veltink, P. H. *Switching curve controller for FES-assisted standing up and sitting down*. IEEE Trans Rehabil Eng, *6:* 167-71, 1998.

MECHANICAL DESIGN AND DRIVING MECHANISM OF AN ISOKINETIC FUNCTIONAL ELECTRICAL STIMULATION-BASED LEG STEPPING TRAINER

N.A. Hamzaid[1], C. Fornusek[1], A. Ruys[2], G.M. Davis[1]

[1]*Rehabilitation Research Centre, Discipline of Exercise and Sport Science, The University of Sydney, Sydney, Australia*
[2]*School of Aerospace, Mechanical and Mechatronic Engineering, The University of Sydney, Sydney, Australia*

nham0064@mail.usyd.edu.au

Abstract

The mechanical design of a constant velocity (isokinetic) leg stepping trainer driven by functional electrical stimulation-evoked muscle contractions was the focus of this paper. The system was conceived for training the leg muscles of neurologically-impaired patients. A commercially available slider crank mechanism for elliptical stepping exercise was adapted to a motorized isokinetic driving mechanism. The exercise system permits constant-velocity pedalling at cadences of 1-60 rev·min^{-1}. The variable-velocity feature allows low pedalling forces for individuals with very weak leg muscles, yet provides resistance to higher pedalling effort in stronger patients. In the future, the system will be integrated with a computer-controlled neuromuscular stimulator and a feedback control unit to monitor training responses of spinal cord-injured, stroke and head injury patients.

Key words: elliptical stepping, isokinetic exercise machine, neurologically impaired users.

Introduction

Individuals with neurological impairments may need technological innovations to maintain physical fitness, especially if their lower body is paralysed or paretic due to their neurological condition[1]. Functional electrical stimulation (FES) has been frequently used to evoke muscle contractions and promote exercise training in this population of patients. The most common exercise modality employing this technique is FES-evoked cycling[1,2].

FES-cycling is achieved by applying low-amplitude pulses of electrical current to stimulate and recruit leg muscles in a pre-determined sequence. Left and right legs are stimulated periodically with similar patterns, with a half revolution phase offset for the right and left legs, respectively. Users usually are seated in the semi-recumbent posture to support their body weight, and their legs are extended forwards[3]. Upright FES-evoked cycling, whereby the individual is seated on a bicycle saddle is less preferred, since neurological patients may have insufficient strength or poor thoracolumbar muscle control to balance themselves. In contrast, during semi-recumbent seated cycling, individuals pedal with their legs slightly flexed at leg extension and their feet are usually affixed to the cycle pedals to provide greater knee joint stability[4].

Physiologically, the cyclic movement of the legs, being the limbs with the largest muscle mass, act as a pumping mechanism that assists arterial circulation and venous return of blood through the paralysed legs back to the heart. FES-evoked cycling at high cadence (40-60 rev·min^{-1}) promotes cardiorespiratory fitness, whilst cycling at lower cadences (10-30 rev·min^{-1}) promotes the development of muscle strength and endurance[1,5].

The significant features of FES-evoked exercise have been previously reviewed by Fornusek[6]. Since 1982, FES exercise systems have either used large electronically-braked flywheels to maintain cycling momentum or employed motor assistance to resist dynamic leg muscle contractions. A motor-assisted pedalling device was first described by Eichhorn et al[7], that allowed pedalling even at low muscle forces or for those with poor tolerance to neuromuscular stimulation. In 1997, Fornusek[8] developed the first prototype of an isokinetic FES leg exercise system, which allowed pedalling movements in neurological patients even when there was insufficient muscle force to cycle at higher pedalling cadences. This isokinetic exercise method was implemented in the current study[9].

Design concept and objectives

The purpose of the present investigation was to describe the mechanical design and some biomechanical features of a modified FES cycle – the isokinetic FES leg stepping trainer (iFES-LST).

The functional gains from FES-evoked exercise for neurologically-impaired patients, apart from improved physical fitness, would be their ability to stand and walk following leg strengthening. We considered that stepping

exercise might be more relevant than cycling when the primary focus of such exercise was improved gait. Possessing kinematic properties similar to walking, a leg stepping exercise trainer might deliver potentially greater benefits for people with neurological disabilities. Having body weight supported in a chair would be ideal for chronically-injured people, while strengthening activities could be achieved simultaneously with better range of motion that would resemble walking.

Hamzaid and colleagues[10,11] compared voluntary cycling to elliptical stepping exercise in a cohort of able-bodied subjects, and suggested that stepping activated the quadriceps muscles for a longer duration and at a higher intensity than cycling. The authors reasoned that this was due to the linear component of the movement. Their study also revealed marked differences in hip, knee and ankle extension angles between the two exercise modalities. Leg movements on an elliptical stepping trainer produced less hip and knee angle excursions, while the ankle angle excursion was greater. The leg movements in elliptical stepping mimicked those observed during natural gait. Furthermore, the foot movement pattern during elliptical stepping resembled the foot movement of walking[12].

Another significant feature of the iFES-LST system was its isokinetic (constant velocity) operation. Isokinetic exercise has been proven safe for the joints of patients and is an effective form of strength training[5]. Our key design goal for the iFES-LST was to develop an exercise system that could offer safe and intense training, with additional benefits that were relevant to gait re-training.

Methods

The exercise system under development was an isokinetically-driven elliptical leg stepping trainer. It comprised a mechanical system that facilitated elliptical stepping motion and a constant-velocity driving mechanism. This system will be used as the mechanical foundation of an isokinetic functional electrical stimulation leg stepping trainer (iFES-LST).

Mechanical design of iFES-LST

A mechanical system comprising a slider-crank mechanism was used to produce horizontal linear component of the elliptical stepping pattern. A fixed extension at the end of the slider provided the vertical component. Combination of these components resulted in an elliptical movement pattern (Figure 1) whereby the foot will be placed to emulate walking.

When an elliptical pattern is produced repeatedly, the motion has a tendency to stop at each horizontal excursion before continuing in the opposite direction. These horizontal ends are also known as “dead spots”. Smooth movement is achieved through the attachment of flywheels, weighted cranks and linkages, as well as spring attachments at the end of each slider. The spring components provide energy absorption and release to propel the slider horizontally without production or accumulation of external energy. The

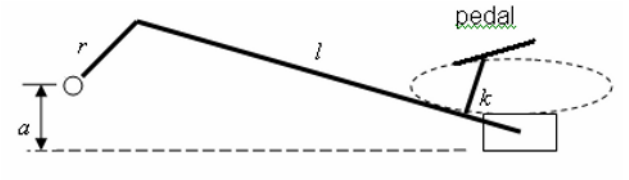

Figure 1. *The left side of the exerciser with technical representation of slider-crank mechanism. The subject’s left foot is placed securely on the pedal while the seat is above the rotating crank. Pedal rotation produces an elliptical movement. A horizontal component provided by the slider and vertical component provided by the extension link, k. The primary crank, r, rotates around pivot point, carrying the rigid connecting link, l, that is connected to the slider component. The dimensions r, l, and offset, a, allows the kinematic properties of the system be predicted from equations by Davidson[11].*

flywheel component provides momentum for propulsion as the pedalling motion continues, thus smoothens the overall motion. These features help prevent the natural occurrence of “dead spots” at the end of horizontal path to ensure smooth and continuous motion[13].

To estimate leg forces, the acceleration of the pedal can be predicted using equations developed for slider crank mechanisms by Davidson[14]. The slider acceleration (see equation 1) relates the dimensions of the rotating crank *r*, connecting link *l* and offset between crank rotation point and slider platform *a* (Figure 1). The prediction is valid as long as the rotation velocity is assumed to be constant, the mechanism is rigid and the connecting link is long enough (see equation 2).

$$\left(\frac{r}{l}+\frac{a}{l}\right)<0.3 \tag{1}$$

$$\ddot{x}=-\frac{r\omega^2\omega_\theta^{\,2}}{\omega_\theta^{\,2}-1}\cos\theta-\frac{ra}{l}\left(\frac{\omega^2\omega_\theta^{\,2}}{1-\omega_\theta^{\,2}}\right)\sin\theta-\frac{r^2}{l}\left(\frac{\omega^2\omega_\theta^{\,2}}{\omega_\theta^{\,2}-4}\right)\cos2\theta \tag{2}$$

A commercial elliptical stepping trainer that satisfied these design criteria (BioStep Semi Recumbent Elliptical, Biodex Medical System Inc. USA)[13] was the mechanical foundation used in the development of the iFES-LST, but any similar device would have been acceptable.

Feedback controlled isokinetic component

The ability of the iFES-LST to control the movement speed meant the exercise parameters could be precisely controlled and monitored. To ensure isokinetic (constant velocity) operation, the driving mechanism was a crucial component of the system. The ideal driving mechanism would enable precise speed control even at very low cadence or very high torque.

The driving mechanism selected was an AC servo motor. The motor (Brushless AC Servo motor, Baldor Electronic Co., Australia) with its driver (Digital Single Axis Brushless AC Servo Controller, Baldor Electronic Co., Australia) was able to withstand precise constant velocity operation over a wide range of speed (0 – 2500 rev·min^{-1}) and wide range of power outputs.

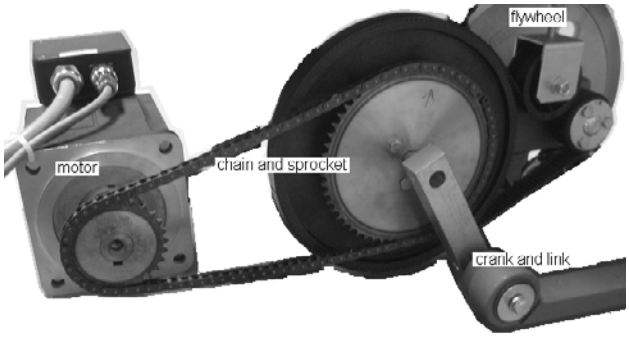

Figure 2. *The chain and sprocket installation on the right side of the back of the exercise system. The motor connected via a chain and sprockets for direct power transmission. The crank is connected to flywheel on the left side of the elliptical stepper (as in Figure 3).*

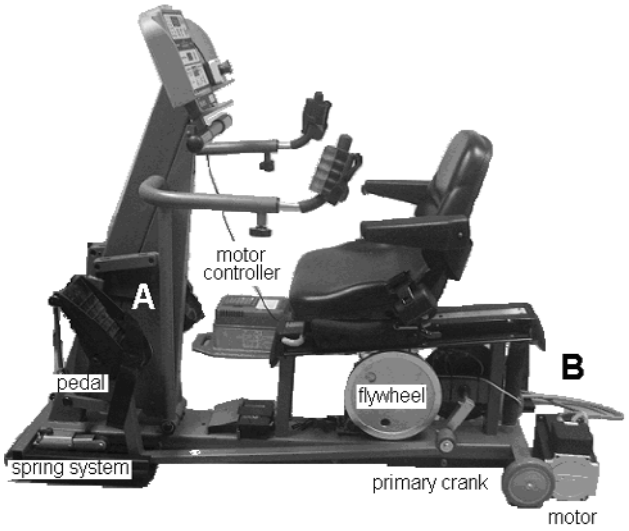

Figure 3. *Prototype iFES-LST system. This figure shows the elliptical stepper, A, and driving mechanism, B. Linkages on the crank are rigid metal bars, which are connected to the pedal. The pedal is equipped with strap to hold the foot in place. The mechanical design is a modified commercial system (BioStep, Biodex Medical Systems Inc. USA).*

The motor was connected to the primary crank of the slider-crank mechanism in the commercial exercise machine, via a chain and sprockets (Figure 2). This allowed direct power transfer from motor to crank.

The intention of the project was to develop an exercise system that when patients are unable to produce sufficient leg power to commence stepping, the servo motor could initiate the elliptical movement. Later, when the muscles eventually experienced fatigue and could no longer produce sufficient power to sustain the exercise, the motor would maintain the leg movements, and thus the driving speed. Additionally, the brushless feature of the AC servo motor enabled greater cycling velocity and force, and was able to maintain isokinetic exercise at higher power outputs. Once the initial momentum of stepping is overcome, the stepping velocity could be kept constant throughout the cycle.

Results

The leg exercise component of iFES-LST with elliptical stepping trainer attached with an isokinetic driving mechanism (Figure 3). Leg exercise is initiated by switching on the power supply on the motor controller and keying in a preset velocity. The motor speed should be twice the desired pedalling cadence (the motor to crank sprocket ratio is 1:2).

The motor responses, such as voltage and current properties, are displayed on a motor controller display screen. This display shows the changing motor current corresponding to fluctuations in driving torque in order to keep the rotational speed constant. The rotating crank carries the slider link as load. Therefore the rotational force (i.e torque) changes with respect to the position of the crank throughout the cycle. The current changes are approximately sinusoidal due to the linkage bars rotating around the crank. In a future deployment, the current changes can be used to calculate the motor power required to drive the slider linkages by multiplying current and cadence.

Discussion and conclusion

The use of a constant velocity motor to isokinetically drive the BioStep elliptical stepping training system is an important component of the iFES-LST system. Using a computer and an analogue-to-digital data acquisition card, motor performance, such as power and torque can be monitored, while the desired exercise cadence can be programmed via software designed for the system. An encoder will be attached on the primary crank to read the crank angular position throughout a single cycle. The instantaneous crank angle will be input to a FES stimulator system to recruit appropriate leg muscle contractions based on the position of the leg. With an integrated FES sub-system and careful selection of appropriate muscle groups, the system can provide safe and intense muscle strength training for patients with spinal cord injury, hemiplegic stroke or traumatic head injury**.** The block diagram of iFES-LST is illustrated in Figure 4.

The ability of an isokinetic FES leg stepping trainer to provide the essential benefits of pre-gait training creates a potentially more advanced version of currently available FES cycling exercise systems. While the driving mechanism concept may be somewhat similar to that developed by Fornusek[6], the mechanical setup of the proposed iFES-LST system will allow movements which more closely resemble walking.

The current implementation of the iFES-LST can be employed under two paradigms of rehabilitation – ‘conscious effort free’ exercise and ‘hybrid’ exercise. Conscious effort free exercise involves FES-evoked dynamic muscle contractions under feedback-control to maintain the stepping cadence. Hybrid exercise involves integrating upper body effort to drive the leg stepper, and thereby maintain the pedalling cadence and exercise

intensity. Such exercise allows the patient to be as physically active as possible, by involving muscle mass both above and below their spinal cord lesion or as similarly affected by hemiparetic stroke[15]. Passively driven movements of the arms can be advantageous as passive limb movements maintain the 'conscious effort free' exercise paradigm while increasing whole body activity.

In addition, handle bars that are reciprocal to leg stepping create the prospect of inter-limb coordination to train whole body movements. This may be useful as it facilitates neural coupling of the upper and lower limb muscles[16]. In addition, people with incomplete paraplegia or hemiparetic stroke may benefit from such coordination training to potentially regain some functional ability[17,18]. It was a particular feature of the commercial BioStep system that led to its selection as our leg step training platform.

In conclusion, this paper described the design and development of an isokinetically-driven elliptical leg stepping trainer as a foundation of a prototype iFES-LST. An isokinetic driving mechanism was connected directly to the primary crank of a slider-crank mechanism. The system was driven at a preset speed, aiding low pedalling forces while resisting high pedalling forces. This functional system will be the foundation of a FES based exercise machine, to be used by individuals with neurological disabilities.

Acknowledgement

The authors acknowledge Dr David Rye, Mr Ray Patton, Mr Peter Spooner, Mr Mick Jurd, Mr Paul DeHon and Ms Ilhee Kim for their contribution to the mechanical developments throughout this project. The primary author received funding from a JPA Malaysian Government Scholarship. This project was funded by a Program Grant from the NSW Office for Science and Medical Research.

References

1. Hamzaid, N.A. and Davis G.M. *Health and Fitness Benefits of Functional Electrical Stimulation-Evoked Leg Exercise on Leg-Paralyzed Individuals*, ISSC Proceedings, p29-30, 2006.
2. Hamzaid, N. and Davis, G.M. *Exercise Technology after Spinal Cord Injury: Functional Electrical Stimulation Leg Cycling*, IFBME Proceedings, p681-683, 2006.
3. Rasmussen, J., Christensen, S.T., Gfohler, M., Damsgaard, M. and Angeli, T. *Design optimization of a pedaling mechanism for paraplegics*, Struct Multidisc Optim; 26:132-138. 2004.
4. Van Soest, A.J., Gfohler, M. and Richard, Casius, L.J. *Consequences of Ankle Joint Fixation on FES Cycling Power Output: A Simulation Study*, Med Sci Sports Exerc; 37:797-806. 2005.
5. Fornusek C and Davis GM. *Maximizing muscle force via low-cadence functional electrical stimulation cycling*, J Rehabil Med 36:232-7. 2004.
6. Fornusek, C. *Development of Isokinetic Functional Electrical Stimulation Leg Cycling Ergometer*, unpublished PhD thesis, Sydney: The University of Sydney. 2004.
7. Eichhorn, K.F., Schubert, W. and David, E. *Maintenance, Training and Functional Use of Denervated Muscles*, Journal of Biomedical Engineering; 6:205-211, 1984.
8. Fornusek, C. *Modification of a Motorized Exercycle to behave as an Isokinetic Ergometer*, unpublished Masters Thesis, Sydney: University of New South Wales, 1997.
9. Hamzaid, N.A., Fornusek, C., Ruys, A.J. and Davis, G.M. *Conceptual Design of an Isokinetic Functional Electrical Stimulation (FES) Leg Stepping Trainer for Individuals with Neurological Disability*, IFBME Proceedings, p662-664, 2006.
10. Hamzaid, N.A., Davis, G.M. and Smith, R.M. *Leg Muscle Activation in Isokinetic Cycling versus Elliptical Stepping*, AAESS Proceedings, p169, 2006.
11. Hamzaid, N., Davis, G.M. and Smith, R.M. *Isokinetic cycling versus elliptical stepping: A kinematic and electromyography analysis*, ICMMB Proceedings, p514-515, 2006.
12. Hamzaid, N.A., Davis, G.M. and Smith, R. *Elliptical Stepping and Cycling: Leg Joint Angles and Range of Motion*, unpublished findings, 2006.
13. Martin MR, Behan EB, Bisesti R and Gronachan DB; *Semi Recumbent Exerciser*, United States, patent US 2004/0259692 A1, Dec 23 2004.
14. Davidson, J.K. *Analysis and Synthesis of a Slider-Crank Mechanism with a Flexibly-Attached Slider*, Journal of Mechanisms; 5:239-247, 1970.
15. Franklin, B.A. *Semi recumbent elliptical*. BioStep News; 1-4, 2006, http://www.biodex.com/rehab/cycles/pdf/biostep_news.pdf
16. Ferris, D.P., Huang, H.J. and Kao, P.C. *Moving the arms to activate the legs*, Exerc Sport Sci Rev; 34:113-20. 2006.
17. Huang, H.J. and Ferris, D.P. *Neural coupling between upper and lower limbs during recumbent stepping*, Journal of Applied Physiology; 97:1299-1308. 2004.
18. Kao, .PC. and Ferris, D.P. *The effect of movement frequency on interlimb coupling during recumbent stepping*, Motor Control; 9:144-163. 2005.

SCATTERED NEUTRON DOSE EQUIVALENT FROM AN ACTIVE SCANNING PROTON BEAM DELIVERY SYSTEM

Draik Hecksel[1], George A. Sandison[1], Jonathan B. Farr[2] and Andrew C. Edwards[3]

[1]*School of Health Sciences, Purdue University, West Lafayette, Indiana, USA*
[2]*Midwest Proton Radiotherapy Institute (MPRI), Bloomington, Indiana, USA*
[3]*Indiana University Cyclotron Facility (IUCF), Bloomington, Indiana, USA*

sandison@purdue.edu

Abstract

A study of neutron production from a novel active scanning proton beam delivery system at the Midwest Proton Radiotherapy Institute (MPRI) has been performed. The neutron dose equivalent was determined using a neutron rem (roentgen equivalent in man) detector which has an upper energy limit of 10 MeV. Measurement were taken at 0, 45, and 90 degrees from the proton beam central axis and for various proton beam energies (127-208 MeV) and scanned field sizes (25-144 cm^2). The maximum neutron dose observed was 0.43 mSv / (proton treatment Gy) at 90 degrees from the beam axis for a beam energy of 208.4 MeV and a scanned field size of 144 cm^2. It is still possible to further mitigate this secondary neutron dose during treatment by optimizing parameters within the treatment nozzle and using shielding.

Key words scattered neutrons, proton radiotherapy, active scanning proton beam delivery system

Introduction

Proton therapy beams generate unwanted neutron radiation by inelastic scattering with atomic nuclei in the beam line and within the patient. The production of neutrons from proton beams increases with proton energy and atomic number of the absorbing materials.[1] Therefore, any atomic number differences in materials comprising the proton beam line will alter the production rate of neutrons and their energy spectrum. It is possible that neutrons produced from 200 MeV proton therapy beams will have an energy spectrum ranging from thermal up to the original proton energy. However, it is difficult to detect high energy neutrons due to their small interaction cross sections. Many fast neutron detectors therefore moderate the high energy neutrons and rely on a thermal neutron detector such as a BF_3 proportional counter or LiI scintillator surrounded by moderating material.

Several studies evaluating dose equivalent from secondary neutrons in proton therapy beam lines observed large differences in their results as summarized in Table 1.[2-10] These different results may be due to corresponding differences in beam line components, room and beam line shielding, proton beam treatment energy, and room layout. Passive scattering proton beam delivery systems were modeled or used in the studies listed in Table 1 except for the work performed at the Paul Scherrer Institute in Sweden[3,5]. Many of these studies were restricted to Monte Carlo computer simulations while those studies including physical measurements typically employed a simple water phantom. A notable exception is the work of Roy and Sandison[4] and Mesolaras et. al.[9] who used an anthropomorphic phantom to simulate a treatment of a pregnant woman and then assessed the scattered neutron dose equivalent to a point representative of her fetus.

For a typical proton treatment (<70 Gy), the anticipated secondary neutron dose to the patient is relatively low with a correspondingly low risk of severe complications or radiation treatment induced cancer within the adult patient's lifetime. However, for pediatric patients, this risk is higher and is potentially a significant concern for the fetus when its mother is undergoing treatment[11]. The purpose of this study was to measure the scattered neutron dose equivalent to the patient following proton beam therapy delivered by a novel active scanning system. It is anticipated that the scanning system will produce a lower neutron dose equivalent than passive scattering systems due to the absence of high atomic number scattering foils in the beam line.

Materials and methods

Beam delivery system

MPRI treatment room number two – active scanning

MPRI treatment room two houses an active beam scanning proton beam delivery system (Figure 1) that rotates on a gantry. This system employs a magnet to linearly scan the proton beam across the treatment field then offsetting and reversing the scan to ultimately define a square pattern that borders three centimeters beyond the field setting. A series of carbon plates move in and out of the beam line and they function to degrade the beam's energy and form the spread out Bragg peak (SOBP). Two ion chambers positioned in the beam line to monitor the dose delivered to the patient. A treatment field snout defines the maximum field size diameter available for treatment and holds the individually-designed patient aperture and compensator. The active scanning system nozzle can accommodate any one of the 10, 20, or 30 cm snouts, which also define the corresponding maximum field size diameter. A patient specific collimator aperture defines the final shape of the treatment field to match that of the anatomical target from the beam's eye view. Finally, a patient specific compensator shapes the proton dose distribution to the distal edge of the target volume while accounting for tissue density changes along the beam path and any changes in the patient skin surface contour upon which the beam is incident.

Methods

A neutron detector model NRD(neutron radiation detector) with an E600 survey meter (Thermo Fisher Scientific Incorporated, Waltham, MA USA) was used to measure neutron dose equivalent. This detector consists of a 9" polyethylene moderating sphere surrounding a BF_3 proportional counter and is sensitive to neutrons in the energy range from thermal through 10 MeV.[12] The energy response function of the detector follows the fluence to dose conversion function which allows the survey meter to determine the dose from each energy bin and integrates to provide the total dose equivalent measurement. The error for the detector is reported to be 10% by Thermo Fisher

Table 1. *Summary of previous studies involving neutron dose from proton therapy.*

Authors	Beam Line System	Beam Energy Studied (MeV)	Secondary Radiation Dose or Neutron Dose Equivalent per Treatment Gray	Method of Measurement
Binns and Hough (1997)	National Accelerator Center (South Africa)-Passive Scattering System	200	33-80 mSv/Gy	Tissue Equivalent Proportional Counter
Agosteo et. al (1998)	Centre Antoine-Lacassagne in France-Passive Scattering System	65	1.45 x 10^{-6} to 1.302 x 10^{-4} Gy per therapy Gy	Monte Carlo simulation (neutrons and photons)
	National Accelerator Center (South Africa)-Passive Scattering System	200	.0708 -12.6 mGy/treatment Gy	Monte Carlo simulation (neutrons and photons)
	Paul Scherrer Institute (Switzerland)-Spot Scanning System	200	1.5-5 mGy/treatment Gy	Monte Carlo simulation (neutrons and photons)
Roy and Sandison (2000)	MPRI – Passive Scattering system	197.86	.1-.26 mSv/Gy	Bubble Detectors
Schneider (2002)	Paul Scherrer Institute (Switzerland)-Spot Scanning System	200	2-4 mSv/treatment Gy	Bonner Sphere and Etch Detectors
Yan (2002)	Harvard Cyclotron Laboratory- Passive Scattering System	160	1-15 mSv/Gy	Bonner Sphere
Polf and Newhauser (2005)	Harvard Cyclotron Laboratory- Passive Scattering System	158	4-15 mSv/Gy	Bonner Sphere and Monte Carlo simulation
Jiang (2005)	Northeast Proton Therapy Center – Passive Scattering System	162.1-178.9	26 mSv for paranasal plan 162 mSv for lung plan	Monte Carlo Simulation
Mesolaras et. al. (2005)	MPRI – Passive Scattering system	78-157	.071 - .292 mSv/Gy	Bubble Detectors
Zheng et. al. (2007)	MD Anderson Cancer Center – Passive Scattering System	250	.5-20 mSv/Gy	Monte Carlo Simulation

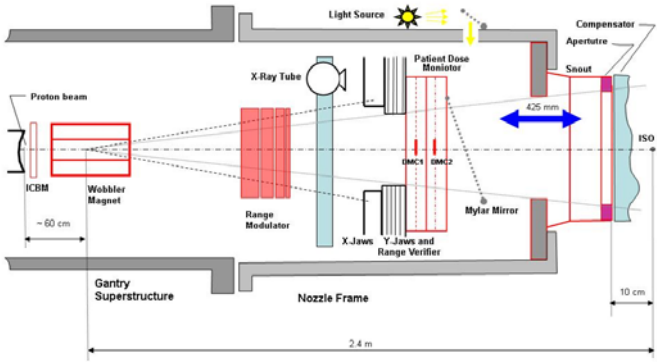

Figure 1. *Diagram of the active scanning proton therapy treatment nozzle at MPRI.*

Scientific Inc., and this error is incorporated into the statistical uncertainty of the data shown in appropriate figures of this article.

Proton beams of maximum energy 208.4 MeV were delivered to an anthropomorphic Phantom Patient™ (Phantom Laboratory Inc., Salem, NY) to simulate a single treatment field aimed laterally at the prostate. These energy protons allowed for maximum neutron production and an expected upper limit on neutron dose equivalent during treatment at the MPRI. The detector was then placed at angles of 0, 45, and 90 degrees to the beam line. In this experiment, 0 degrees is defined in the beam line down stream of the patient. At 0 degrees the detector was placed at distances of 23, 53, and 84 cm. At 45 degrees, the detector was placed at distances of 94, 124, and 155 cm, while at 90 degrees it was placed at distances of 97, 127, and 157 cm. The distances and angles were measured from the point where the central axis of the proton beam was incident on the patient. These distances and angles were chosen to avoid coincidence with the robotic arm attached to the patient bed that supported the phantom. The detector

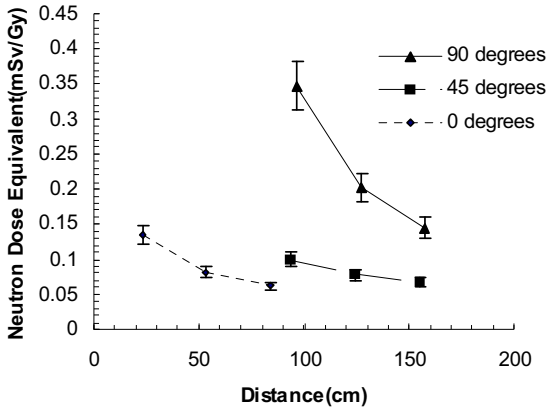

Figure 2. *Neutron survey results from active scanning proton beam delivery system.*

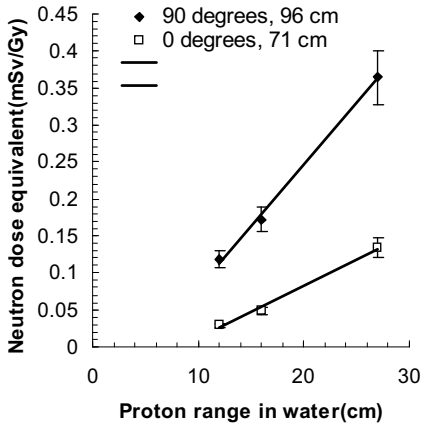

Figure 3. *Measurements were taken at 0 degrees 71 cm and 90 degrees 96 cm from the beam axis while the proton beam range in water was varied.*

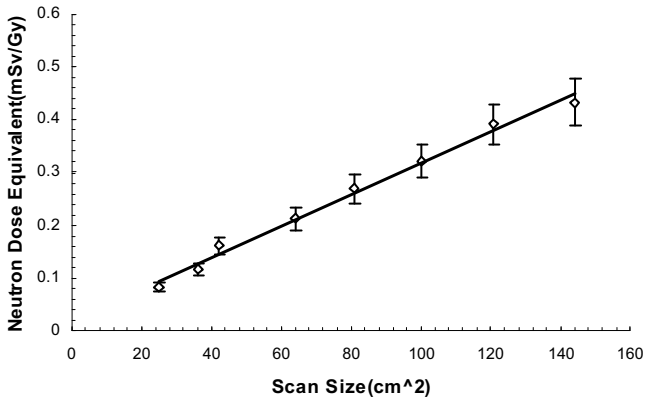

Figure 4. *Measurements were taken at 90 degrees and 96 cm from the beam axis while the scan size was varied.*

was placed at points meant to represent the position of a patient during treatment. The neutron dose was normalized to the treatment dose delivered to give scattered neutron dose equivalent in units of mSv/proton treatment Gy.

Results

A proton beam energy of 208.4 MeV corresponds to a beam penetration range in water of 27 cm. A 10cm SOBP, 10 cm aperture, 10 cm air gap, and a 2 nA beam intensity were used as the standard treatment delivery conditions for the experiment. The middle of the detector was placed at the height of the treatment snout which was 138.4 cm from the room floor. Further experiments varied the proton energy and scan field size.

Angle and distance

Figure 2 shows the variation in scattered neutron dose equivalent with both angle and distance. For the angles studied, the highest neutron dose equivalent occurred at 90 degrees. At angles of 0 and 45 degrees the patient phantom absorbed neutrons which caused an observable decrease in neutron dose equivalent beyond the patient compared to the 90 degree results. Studies performed by Yan[6], Zheng[10], and Polf and Newhauser[7] showed a higher dose at 90 degrees than either 0 or 45 degrees for distances of 50 cm or less from the proton beam central axis. However, their results revealed a higher dose at 45 degrees for distances of 100 cm or more. These differences in trends may be explained by the use of different phantoms for each study. The simulation by Zheng et. al.[10] did not use a phantom to simulate the patient, and the simulation by Polf and Newhauser[7] used a Lucite phantom 26 cm in length. Yan et. al.[6] did not make measurements beyond 50 cm. It is possible that the use of the phantom patient™ in the present study absorbed a fraction of the neutrons that otherwise might have been able to penetrate the detector or reach the simulation point in experiments performed for those previous studies.

Energy variation

Figure 3 shows variation in neutron dose equivalent with proton beam energy at 0 and 90 degrees. The detector was 97 cm from the incident beam at 90 degrees and 71 cm at 0 degrees. An apparent linear behavior exists between proton beam energy and scattered neutron dose equivalent over this energy range. This linear behavior for the scanning system is similar to the trend observed by Mesolaras et al[9] for a passive scattering beam delivery system. Extrapolation suggests that the proton beam energy for a measurable scattered neutron dose equivalent occurs at about 89 MeV (5.26 cm in water) for 90 degrees and 107 MeV (8.41 cm in water) for 0 degrees. This difference is most likely due to patient absorption of the lower energy neutrons in the phantom patient™ at 0 degrees.

Scan size

Figure 4 describes a linear relationship between the measured neutron dose equivalent and scanned field size used. In order to maintain flatness and symmetry, the proton treatment beam is over scanned across the opening of the snout. This over scanning causes significant neutron production in the snout collimator close to the patient. As the field scan size decreases, the neutron dose equivalent decreases in a linear fashion.

Discussion

Results indicate that the scattered neutron dose equivalent from the novel active scanning proton beam delivery system is low compared to results previously published in the literature for passive scattering beam delivery systems (Table 1) with the exception of the measurements by Roy and Sandison and Mesolaras et al. However, it is possible to further lower the scattered neutron dose equivalent from the MPRI beam line by including more beam line shielding and reducing the extent of over scanning of the collimation system if it is possible to still maintain acceptable field flatness and symmetry. It may also be possible to collimate the proton beam further up stream of the patient to take advantage of inverse square law dose reduction from the sources of the neutron production in the beam line.

The detector was placed at representative points corresponding to the position of the patient during treatment. While the phantom and robotic arm prevented measurements closer to the proton beam central axis, the distances at each angle represent a point that would be the distal edge of the patient during treatment. An approximation of the scattered neutron dose at 20 cm from the central beam axis is 1 mSv/Gy based on an exponential fit to the data at 90 degrees. This calculation was performed to estimate a scattered neutron dose equivalent at distance comparable to those in other studies.

The main limitation of this study was the restricted energy range sensitivity of the neutron REM detector. When treating with 208.4 MeV protons, a significant number of neutrons having energies above 10 MeV is expected. Unfortunately their contribution to the scattered neutron dose equivalent cannot be recorded by the REM detector. In a recent study performed by Zheng et. al[10], the neutron spectrum from 250 MeV protons incident on a passive scattering delivery system was determined using Monte Carlo simulations. They found that neutrons above 10 MeV contributed half to two thirds of the total neutron dose to a patient during proton therapy. Higher energy neutrons are expected to contribute more dose at 0 degrees since they are likely to have scattered less and so maintain high energy compared to those detected large angles such as 90 degrees and maintain high energy. By applying Zheng's estimation that half the neutron dose is above 10 MeV at 90 degrees and two thirds is above at 0 degrees, the maximum dose measured at 0 and 90 degrees is estimated to be 0.39 and 0.86 mSv/Gy respectively. This is merely a rough approximation as the lower proton beam energy and different beam delivery system could alter the dose contribution of neutrons above 10 MeV.

Future work will concentrate on the neutron energy spectrum. It will be measured in air and tissue using a Bonner sphere system and will be calculated using Monte Carlo simulation. This should provide a more exact correction for the measurements presented in this experiment.

Conclusions

The observed scattered neutron dose equivalent at the patient skin during treatment reaches a peak at 90 degrees from the central beam line axis and decreases with distance from the beam line. The neutron dose equivalent also increases with proton beam energy and scanned field size. The dose equivalent at the surface of the skin is low when compared to results published using passive scattering beam delivery systems and depending upon the prescribed dose, may fall below the 50 mSv annual dose equivalent limit for the skin recommended by the ICRP[13]. Further reduction of the neutron dose equivalent is possible by increased beam line shielding or reduced over scanning of the snout. Results may be artificially low due to the limited sensitivity range of the detector leading to the exclusion of scattered neutron dose equivalent from neutrons of energy greater than 10 MeV. However, it is anticipated that the results quoted in this paper will be correct within a factor of three and hence suitable for radiation protection purposes.

References

1. Tesch, K., *A simple estimation of the lateral shielding for proton accelerators in the energy range 50 to 1000 MeV*, Rad. Prot. Dosim. 11, 165-172(1985).
2. Binns, P. J. and Hough, J.H., *Secondary dose exposures during 200 MeV proton therapy*, Radiat. Prot. Dosim. 70, 441-444 (1997).
3. Agosteo, S., *Secondary neutron and photon dose in proton therapy*, Radiother. Oncol. 48, 293-305 (1998).
4. Roy, S. C. and Sandison, G. A., *Scattered neutron dose equivalent to a fetus from proton therapy of the mother*, Radiat. Phys. Chem. 71, 997-998 (2004).
5. Schneider, U. *et al.*, *Secondary neutron dose during proton therapy using spot scanning*, Int. J. Radiat. Oncol., Biol., Phys. 53, 244-251 (2002).
6. Yan, X., Titt, U., Koehler, A. M. and Newhauser, W. D., *Measurement of neutron dose equivalent to proton therapy patients outside of the proton radiation field*, Nucl. Instrum. Methods Phys. Res. A 476, 429-434 (2002)
7. Polf, J. C. and Newhauser, W. D., *Calculation of neutron dose equivalent exposure from range-modulated proton therapy beams*, Phys. Med. Biol. 50, 3859-3873 (2005).
8. Jiang, H. *et al.*, *Simulation of organ-specific patient effective dose due to secondary neutrons in proton radiation treatment*, Phys. Med. Boil. 50, 4337-4353 (2005).
9. Mesoloras *et al.*, *Neutron scattered dose equivalent to a fetus from proton radiotherapy of the mother*, Med. Phys. 33, 2479-2490 (2006).
10. Zheng *et. al.*, *Monte Carlo simulations of stray neutron radiation exposures in proton therapy,* J. Nucl. Mater. 361, 289-297 (2007).
11. Stovall, M. *et al*., *Fetal dose from radiotherapy with photon beams: Report of AAPM radiation therapy committee task group No. 36*, Med. Phys. 22, 63-82(1995).
12. Thermo Electron Corporation. E600/NRD Product Specifications. Santa Fe, NM. USA
13. ICRP. *1990 Recommendations of the International Commission on Radiological Protection.* ICRP Publication 60 (Oxford: Pergamon Press), (1991).

ADDRESSING RELATIVE MOTION OF TUMORS AND NORMAL TISSUE DURING DYNAMIC MLC TRACKING DELIVERY

Ryan McMahon[1], Lech Papiez[2] and George Sandison[1]

[1]*Purdue University, West Lafayette, IN, USA*
[2]*University of Texas Southwestern Medical Center, Dallas, TX, USA*
Lech.Papiez@UTSouthwestern.edu

Abstract

A general methodology for addressing relative motion of targets and normal tissue for dynamic-MLC (DMLC) tracking is discussed. The basic idea is to exploit the extra degrees of freedom that tissue motion introduces into DMLC delivery. This principle is illustrated through the use of a simple example which uses a moving rigid target whose projection in the beam's eye view intersects a stationary critical organ. DMLC delivery which tracks the target motion is simulated, and it is shown that the choice of leaf motion and the time of the onset of delivery can have a large impact on the exposure of the critical organ. Depending on the choice of these parameters, the integral MU delivered to the critical organ ranged from -75% to +250% relative to the delivery planned for static geometry. These results indicate that deliveries using DMLC tracking should accommodate any normal tissue that is moving with respect to the tumor. This should be done to (1) avoid deliveries which result in large over-exposures of critical organs, and (2) to seek out deliveries that result in critical organ exposures that are lower than what is possible with any static geometry (4D therapy).

Introduction

It is well established that if the delivery of intensity modulated radiation therapy (IMRT) ignores tissue motion altogether, artifacts can be created in the entire dose distribution[1] (in both the target *and* normal tissue). These artifacts can be reduced by accommodating target motion while ignoring any relative motion of normal-tissue ('tracking' the target), but this may still result in unwanted artifacts in the normal-tissue dose. Motion of critical organs relative to the tumor volume has been observed[2], which means the current formulation of MLC tracking[3-8] (which ignores this effect) is only a first order solution to the problem of tissue motion. The goal of this study is to accommodate *both* target and normal-tissue motion in IMRT delivery using dynamic-MLC (DMLC).

We will exploit the fact that, when using an MLC to deliver IMRT, there is an interplay effect between the leaf motion and tissue motion. The primary results of this paper show that leaf motion can be chosen such that this interplay effect leads to increased sparing of critical organs without compromising the dose delivered to the target. We also demonstrate the idea that tissue motion provides an extra degree of freedom for delivery, which suggests that plans optimized for a dynamic geometry can potentially result in dose distributions which are superior to anything achievable by using static geometry. Thus, a secondary goal of this study is to show that *taking advantage of tissue motion*, rather than minimizing its effects, should be the true motivation for 4D radiation therapy.

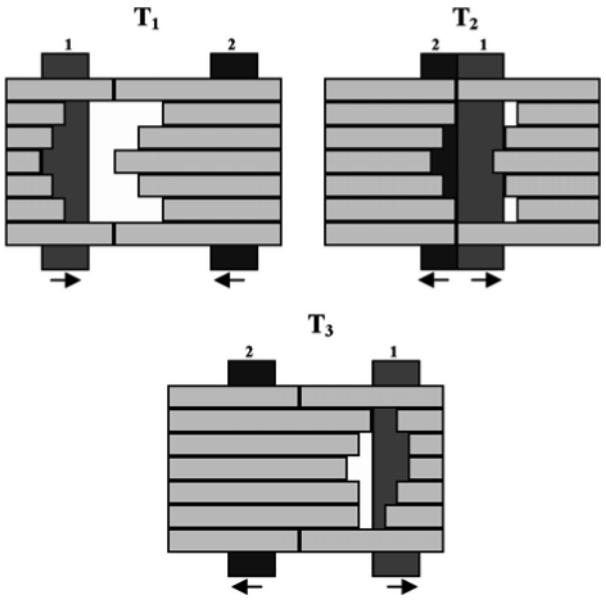

Figure 1. *Schematic showing how the starting time of delivery (relative to tissue motion) can result in different interplay effects. Shown are three snapshots (T1, T2, T3) of a DMLC delivery. OAR 1 represents a delivery which is started when the OAR is moving opposite to leaf motion, and OAR 2 represents a delivery which is started when the OAR is moving in the same direction as the leaves. As shown, the OAR 2 stays in the open field for a longer period of time, meaning it will likely receive a larger dose. Shown here is the case when the OAR is moving, but this is analogous to the situation in which a target moves over a stationary OAR.*

Methods

The principle of 4D-IMRT with DMLC can be traced back to the interplay that occurs between tissue motion and MLC leaf motion. This interplay effect and its effect on irradiation of moving organs at risk are shown schematically in Figure 1. Three snapshots of a DMLC delivery are shown. There is a critical organ that is moving with respect to the target (along the axis of leaf travel in this case). OAR 1 and 2 represent deliveries for two different phases of tissue motion at the onset of delivery. In the case of OAR 1, delivery is started when the OAR is moving in the same direction as the leaves. Due to this correlation, the organ follows the open field and is exposed at T_1, T_2 and T_3 (i.e. the organ is likely overexposed). In the

case of OAR 2, delivery is started when the OAR is moving in a direction opposite to leaf motion. This causes the organ to quickly pass through the open field at T_2 and avoid the open field at all other times.

The goal of 4D-IMRT with DMLC is to exploit this interplay effect and choose deliveries for which irradiation of critical organs is minimized (OAR 2 in Figure 1). For this study, we demonstrate this with a simplified example which uses the following assumptions:

(1) The target is a rigid body which only translates along the direction of leaf travel.
(2) The target exhibits regular sinusoidal motion

$$x_{tar}(t) = A \cdot (1 - \cos(\omega t + \theta)) \quad (1)$$

(3) There is a stationary critical organ near the target which is unavoidably exposed for the beam under consideration.

The first step is to identify all the free parameters associated with both target motion and leaf motion. Since we have assumed regular periodic target motion, the free parameter associated with it is the phase at the onset of delivery (θ). For leaf motion, we will choose our free parameters to be the maximum admissible leaf velocity (v_{Max}) at each point in the target. For the standard DMLC sliding window technique, one leaf (of each opposing pair) is chosen to move at this maximum leaf velocity over each point in the target. The velocity of the remaining leaf is then uniquely determined by[3]:

$$v_{Lead}(m) = \frac{[v_{Foll}(m + I(x)) - v_{Tar}(m + I(x))]}{1 - I'(x) \cdot [v_{Foll}(m + I(x)) - v_{Tar}(m + I(x))]} + v_{Tar}(m) \quad (2)$$

Where v_{Tar} is the target's velocity along the direction of leaf travel. x is a position in the target frame of reference. m denotes the time measured in monitor units (if m is the time the leading leaf reaches x, then the following leaf reaches the same point at $I(x)$ MU later). $I(x)$ is the intensity to be delivered over point x, and $I'(x)$ is its gradient along the axis of leaf travel.

All other quantities (A, ω, $I(x)$) are assumed to be constants given for any particular delivery. Our task is then to choose θ and $v_{Max}(x)$ to minimize the exposure of the critical organ which is moving with respect to the target.

Here we have primarily investigated the θ-dependence of the organ exposure, but we also made a limited investigation of how v_{Max} can be exploited. Only a single leaf pair was analyzed, and the θ-dependence was analyzed by calculating the intensity delivered over the OAR for 360 evenly spaced phases on $[0,2\pi]$. For this preliminary investigation, the dependence on v_{Max} was studied by simple trial and error. An underlying assumption of this approach is that a reduction in intensity delivered over the OAR will translate into a reduction in absorbed dose (no attempt was made to calculate dose distributions). The target-tracking DMLC deliveries were simulated using software developed in Mathematica 5.2 (Wolfram Research). These simulations used an idealized MLC (no leakage, transmission, or scatter included).

Results

The following are the results of an investigation into the effects of DMLC delivery parameters (θ, v_{Max}) on the intensity delivered over a critical organ moving relative to the target.

Figure 2 shows the modeled geometry used in this investigation as well as the motion of the target. Figure 3 shows the intensity maps to be delivered to the target and to the organ at risk. The organ at risk is assumed to be stationary in this example, while the target is a rigid body translating along the direction of MLC leafs according to the formula $A(1 - \cos(\omega t + \theta))$, where A = 1 cm and ω = 0.96 radians/s. Trajectories of points with y coordinates equal to 1, 2, 3 and 4 cm are displayed in Figure 2b. The phase angle θ was assumed to be a user-specified parameter. The consequences of this choice are summarized in the results below.

Figure 4 shows DMLC leaf trajectories for four different cases of delivery. The intensity profile that each leaf pair delivers is identical (see Figure 3), so these plots only show the trajectories of a single leaf pair. Figure 4a shows the intended delivery for the static geometry used for planning. As Figures 4b-d show, using DMLC to track the target motion results in deliveries that are substantially different (with respect to relative position of target and organ) than what was intended. It is important to note that each of the four deliveries shown in Figure 4 results in the delivery of the planned intensity map *over the target*. A more in depth analysis of the intensity delivered over the organ is shown in Figures 5-7 and Table 1.

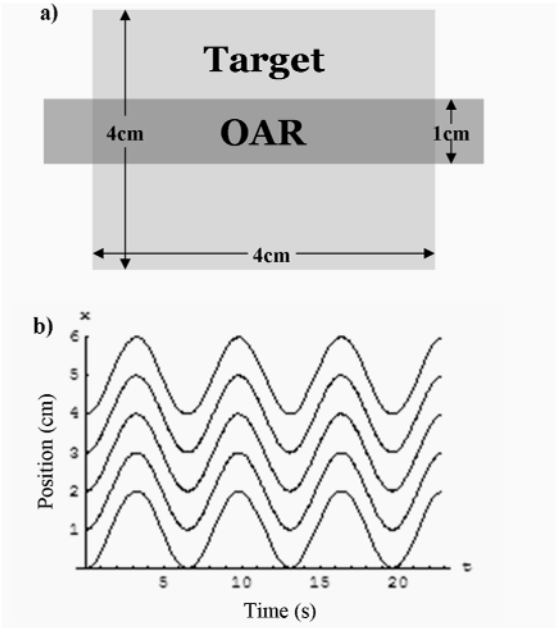

Figure 2. *This figure shows (a) The modeled geometry (rigid moving target, stationary OAR) used for this investigation. (b) Trajectories of target points with y-coordinates equal to 1, 2, 3, 4 cm. It is assumed that treatment planning was done for the case of static geometry shown in a), for which the intensity delivered over the OAR corresponds to the central 1cm of the target's intensity map.*

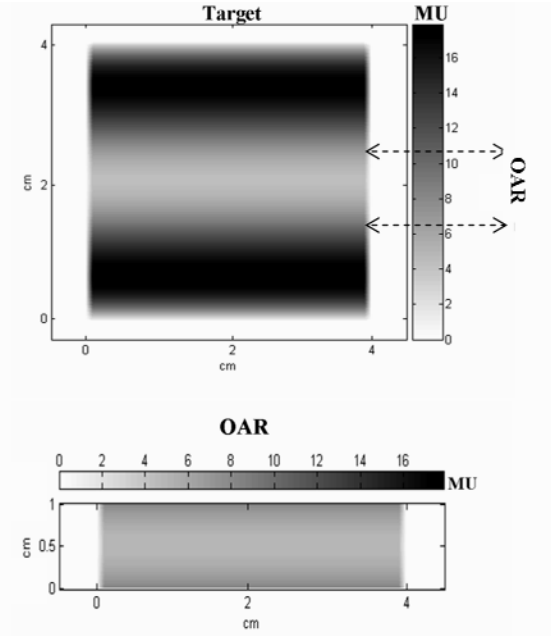

Figure 3. *This figure shows the intensity maps to be delivered over the target (top) and OAR (bottom). It is assumed that treatment planning was done for the case of static geometry shown in a), for which the intensity delivered over the OAR corresponds to the central 1cm of the target's intensity map.*

Figure 5 shows the actual intensity delivered over the OAR for the three cases of delivery, one for the case of static geometry and two defined by two different choices of the phase of the target motion at the onset of delivery. Figure 5b shows that, with a proper choice of starting phase (in this case $\theta = 3.65$), it is possible to reduce the intensity delivered over the OAR relative to the intensity deliverable for the case of static body geometry. However, Figure 5c shows that the opposite situation, in which the OAR is greatly overexposed, can also occur when a disadvantageous choice of starting phase is used (in this case $\theta = 1.00$).

Figure 6 shows a plot of the integral MU calculated at 360 uniformly spaced phases on $[0, 2\pi]$. This demonstrates that, for this particular geometry and target/OAR motion, situations in which the OAR would be potentially overexposed in multiple fractions relative to delivery for static body geometry are more prevalent. The average (assuming uniform allocation of initial phases) of the distribution of the integral intensity delivered to the OAR is 42.10 MU-cm^2, which is a 75.7% increase relative to the static geometry case (23.96 MU-cm^2). Note that the actual optimum appears to be near $\theta = 4.0$. We have chosen to use $\theta = 3.65$ in the examples to highlight the effect of including v_{Max} as an additional parameter ($\theta = 4.0$ may be optimal when only phase is considered, but not when both phase and leaf velocity are free parameters). The numerical difference in the integral MU delivered over the OAR for $\theta = 3.65$ and $\theta = 4.0$ is less than 3%.

Cases shown in Figure 5 used MLC leaf trajectories which minimized the delivery - time ('delivery - time optimal') when particular starting phases of the target motion were chosen for the onset of delivery. However, if

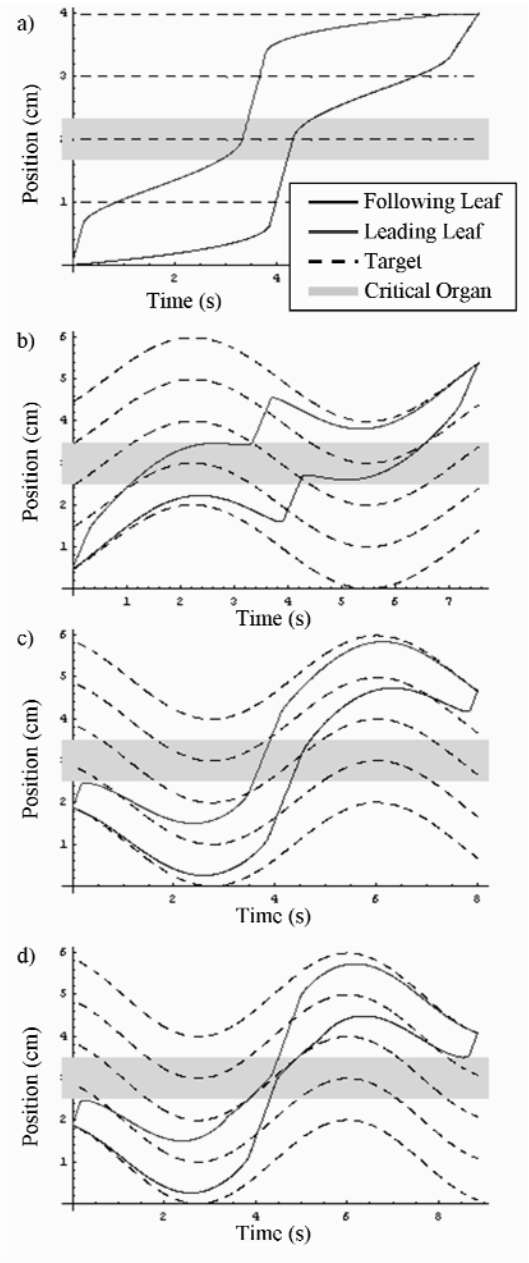

Figure 4. *Graphs show leaf, organ, and target trajectories for DMLC delivery for the case of (a) static geometry used for planning, (b) adverse choice of starting phase ($\theta = 1.0$), (c) advantageous choice of starting phase ($\theta = 3.65$) with leaf velocities chosen to minimize delivery time, and (d) advantageous choice of starting phase ($\theta = 3.65$) with leaf velocities chosen to reduce exposure of organ ('delivery time suboptimal').*

the "delivery time optimal" criteria is relaxed, multiple DMLC leaf trajectories are possible that offer delivery of the same, predetermined intensity to the target while at the same time allowing a reduction of the intensity delivered over an OAR moving relative to the target. Figure 7c (corresponding to trajectories in Figure 4d) presents one such example. For this delivery, a favourable phase ($\theta = 3.65$) was first chosen. Rather than choose leaf velocities to minimize the total delivery time, the leaves were slowed down at the time the OAR was passing through the open field (but their slowdown was matched so that delivery of

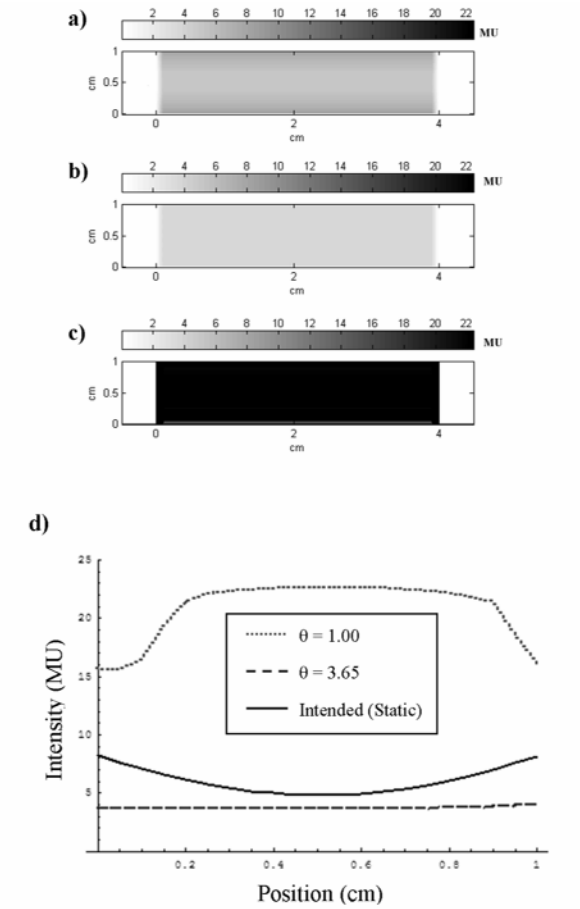

Figure 5. *Graphs show intensities delivered over the OAR for cases of leaf motion displayed in Figure 4a-c. This shows the effect of starting phase on the exposure of the organ. (a) shows full 2D profile of intensity delivered to OAR for stationary geometry, (b) shows full 2D profile of intensity delivered to OAR for moving target when favorable choice of starting phase (θ = 3.65) is utilized and (c) shows full 2D profile of intensity delivered to OAR for moving target when adverse choice of starting phase (θ = 1.00) is utilized. (d) displays cross-sectional profiles (along direction of MLC leaf travel) of intensity delivered over OAR for each of these cases.*

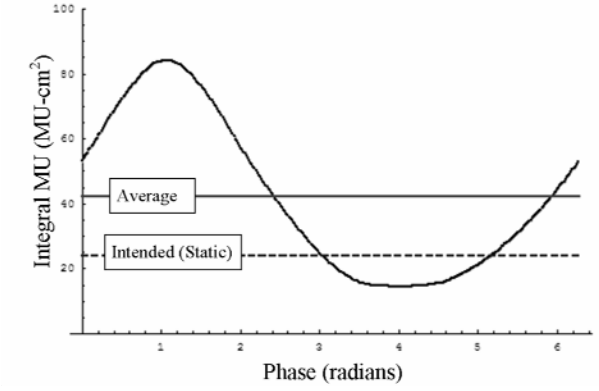

Figure 6. *Distribution of the integral MU delivered to OAR as a function of the phase of target motion at onset of delivery. The average of this distribution (solid red) and the intended value (i.e. for stationary geometry) (dashed blue) are also shown for comparison.*

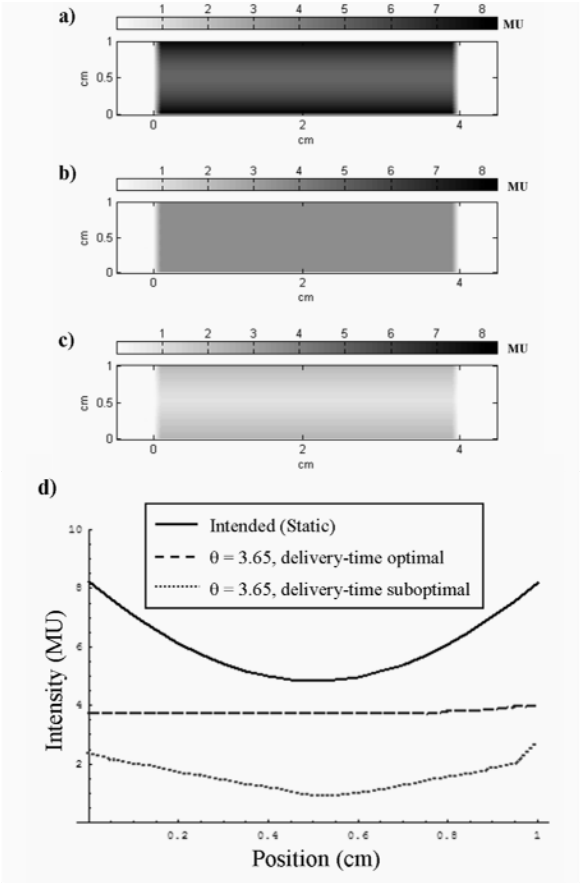

Figure 7. *Graphs represent intensities delivered over OAR for cases of leaf motion shown in Figure 4a,c,d. This demonstrates the effect of choosing leaf velocities to minimize organ exposure rather than delivery time. (a) shows full 2D profile of intensity delivered to OAR for stationary geometry, (b) shows full 2D profile of intensity delivered to OAR for moving target when favorable choice of starting phase (θ = 3.65) is utilized and leaf velocities are chosen to minimize delivery time. (c) shows full 2D profile of intensity delivered to OAR for moving target when favorable choice of starting phase (θ = 3.65) is utilized and when 'delivery-time suboptimal' leaf trajectories are utilized with the goal of minimizing the intensity delivered to the OAR. (d) displays cross-sectional profile (along direction of MLC leaf travel) of intensity delivered over OAR for cases a-c.*

cumulative intensity to each point of the target was not affected). The reduction in leaf gap resulting from this leaf motion adjustment over the OAR meant that the amount of time each OAR point was exposed was reduced. Thus, as shown in Figure 7c, the intensity profile delivered over the OAR is further improved from what was attained with a favorable choice of phase and delivery-time optimal leaf trajectories. The cumulative (integrated) intensity delivered to OAR by the DMLC strategy shown in Figure 4d has been reduced by 74.6% relative to delivery planned for static body geometry and by 59.2% relative to the DMLC delivery of intensity based on the favorable choice of initial phase (θ = 3.65) of target motion for the start of delivery.

Table 1 summarizes the integral MU delivered to the critical organ for each of the cases examined (static geometry, θ = 1.00 delivery-time optimal, θ = 3.65 delivery-time optimal, θ = 3.65 delivery-time suboptimal).

Table 1. *Comparison of the integral MU delivered to the OAR for each of the cases presented in Figure 3. For delivery-time suboptimal case, the leaf velocities were chosen to reduce the exposure of the organ, rather than minimize the delivery time.*

Leaf Trajectories	Integral MU (MU-cm^2)	% Difference (from static)
Intended (Static geometry)	23.96	0
Adverse phase correlation 'Delivery-time optimal' (θ = 1.00)	83.97	+250.5
Favorable Phase Correlation 'Delivery-time optimal' (θ = 3.65)	14.95	-37.6
Favorable Phase Correlation 'Delivery-time suboptimal' (θ = 3.65)	6.095	-74.6

The integral MU ranged from -74.6% (reduction) to +250% (increase) relative to the planned delivery (static geometry).

Discussion

The general methodology for extending 3D beamlet-based inverse planning to 4D (i.e. including motion as a degree of freedom) has been outlined and tested[9,10], but it generally leads to treatment plans which are undeliverable with current technology. In this study, we have demonstrated the principles of a 4D-IMRT system that takes advantage of tissue motion while producing treatment plans that can be delivered with already widespread DMLC technology.

Due to the interplay that occurs between tissue motion and leaf motion, delivering IMRT over a moving target with an MLC can result in severe under- or over-dosages. It is difficult to predict these effects, but any delivery that uses the same leaf trajectories and tissue motion will result in the same artifacts. The fact that fractionation tends to wash out these effects has been well established[11]. However, these arguments have primarily relied upon the case when target exhibits regular periodic motion and the phase of this motion at the onset of delivery is a uniform random variable (i.e. there is no bias towards choosing one phase over another). Under this assumption, the delivered dose in any voxel converges (over the course of several fractions) towards the convolution of the intended dose distribution with the probability density function of the voxel's motion. This means that while the interplay effects may wash out, the underlying effects of the tissue motion of course do not.

Most of the concern with these interplay effects has been raised with respect to delivering IMRT with an MLC over a moving *target volume*. However, there is now substantial interest in tracking moving targets with MLCs[3-8] (using leaf motion to make the beam follow the target). For this situation, the interplay effects in the target volume are minimized, but they will be present in any tissue that is moving with respect to the target volume. For example, when tracking a tumor that is moving along a stationary spinal cord, the interplay effects will show up in the dose delivered to the cord. If we again assume that all free parameters are uniform random variables, then the interplay effects will begin to wash out over the course of several fractions. However, it is reasonable to assume that if the technology to track moving targets with DMLC exists, then it is also possible to deliberately choose these parameters (i.e. choose the starting phase of delivery). We have shown that if this done, it may be possible to systematically bias the interplay effect and choose deliveries that result in minimal toxicity of critical organs. It should be noted that this effect is amplified by short delivery times. In the example shown here, delivery required less than two breathing periods.

We have also demonstrated a phenomenon that should be one of the primary motivations for four-dimensional radiation therapy: *Tissue motion can be used as an advantage in the delivery of radiation therapy*. Although this was an idealized example, Figures 5 and 7 both show that a favorable choice of starting phase (regardless of the choice of leaf velocities) resulted in an intensity delivered over the organ that was lower (at every point) than what was possible for the static geometry used for planning. While the magnitude of this decrease is expected to be smaller for more clinically realistic deliveries, the principle remains the same. Again, generally speaking, the effect is more prominent for fields requiring shorter delivery times (i.e. high dose rates or low-MU fields).

In this study, it was assumed that the tissue motion was periodic and remained unchanged from planning to delivery. While this may be a fair assumption for patients that are able to comply with breath-coaching, it will clearly be violated for others. Thus, in any optimization scheme, it would be beneficial to search for deliveries that (1) keep normal tissue toxicity low and (2) are robust with respect to uncertainty in the tissue motion.

The simple example used could be viewed as a lung tumor moving over a stationary spinal cord. Admittedly, one would expect that mutual displacement in the opposite direction (tumor moving along the cord) would be encountered more frequently. There also may be other OARs to consider. In such cases, the goal of delivery may not be as clear as it was here when the biological response of healthy tissue is taken into consideration, although the underlying concept remains the same. In the example shown, we have avoided any ambiguity (as to what is meant by 'improving' delivery) by providing an example where the intensity delivered over an OAR can be reduced at every point (relative to delivery planned for static geometry). The fundamental idea is that DMLC tracking allows us, in a limited fashion, to shape the dose distribution to healthy tissue while delivering a planned dose to a moving target volume.

Conclusion

Since critical organs may be moving with respect to a target, accounting for only the target motion is not sufficient. When tracking the target motion (with DMLC

for example), situations in which this relative motion results in significant over-exposure of critical organs must be avoided. More advanced 4D deliveries should aim at using motion as another degree of freedom available for sparing critical organs. Temporally optimized DMLC tracking is a promising tool to investigate in this context.

References

1. Webb, S., *Motion effects in (intensity modulated) radiation therapy: a review*, Phys. Med. Biol. 51: R403-R425, 2006.
2. Weiss, E., Wijesooriya, K., Vaughn, S. and Keall, P., *Tumor and normal tissue motion in the thorax during respiration: analysis of volumetric and positional variations using 4DCT*., Int. J. Radiat. Oncol. Biol. Phys. 67: 296-307, 2007.
3. Papiez, L., *DMLC leaf-pair optimal control of IMRT delivery for a moving rigid target*, Med. Phys. 31: 2742-2754, 2004.
4. Papiez, L. and Rangaraj, D., *DMLC leaf-pair optimal control for mobile, deforming targets*, Med. Phys. 32: 275-285, 2005.
5. Papiez, L., Rangaraj, D. and Keall, P.J., *Real-time DMLC IMRT delivery for mobile and deforming targets*, Med. Phys. 32: 3037-3049, 2005.
6. Keall, P.J., Kini, V.R., Vedam., S.S. and Mohan, R., *Motion adaptive x-ray therapy: A feasibility study*, Phys. Med. Biol. 46: 1-10, 2001.
7. Webb, S., *The effect on IMRT conformality of elastic tissue movement and a practical suggestion for movement compensation via the modified dynamic multileaf collimator (dMLC) technique*, Phys. Med. Biol. 50: 1163-1190, 2005.
8. McQuaid, D. and Webb, S., *IMRT delivery to a moving target by dynamic MLC tracking: delivery for targets moving in two dimensions in the beam's eye view*, Phys. Med. Biol. 51: 4819-4839, 2006.
9. Trovimov, A., Rietzel, E., Lu, H.M., Martin, B., Jiang, S., Chen, G.T. and Bortfeld, T., *Temporo-spatial IMRT optimization: concepts, implementation and initial results*, Phys. Med. Biol. 50: 2779-2798, 2005.
10. Jiang, S., *Tracking tumor with dynamic MLC: Be SMART,* Proc. 14th Conf on the Use of Computers in Radiation Therapy (Seoul, Korea, May 2004) p47.
11. Bortfeld, T., Jiang, S.B. and Rietzel, E., *Effects of motion on the total dose distribution*, Semin. Radiat. Oncol. 14: 41-51, 2004.

CORRELATED POINCARÉ INDICES FOR MEASURING HEART RATE VARIABILITY

Anne-Louise Smith[1,2], Karen J. Reynolds[2] and Harry Owen[3]

[1] *Flinders Biomedical Engineering, Flinders Medical Centre, Adelaide, Australia*
[2] *School of Informatics & Engineering, Flinders University, Adelaide, Australia*
[3] *School of Medicine, Flinders University, Adelaide, Australia*
anne-louise.smith@fmc.sa.gov.au

Abstract

Poincaré indices are usually applied to HRV to summarise long data sets collected over 24 hrs. Many applications of HRV are interested in dynamic, short term changes (<1min). This study uses Poincaré indices published through the 1990's to the present, to determine which of them are correlated over the short term (25 beats). Dynamic changes were observed in 12 subjects pre-operatively receiving fentanyl and midazolam sedation with ECG collected for 5 mins before and 5 mins after fentanyl administration. Poincaré indices with a strong correlation ($r>0.85$) between the indices for each of the 12 subjects ($p<0.001$) (particularly with the common measures SDNN, RMSSD, pNN50 and meanRR) were identified. These indices will not be used for further investigation of dynamic effects of fentanyl and midazolam, two sedative drugs used in anaesthesia and intensive care. Indices that proved less suitable for short term analysis (eg. presence of outliers, inability to produce a valid index with smaller number of beats) were also identified. A shortlist of Poincaré indices that do not correlate strongly with commonly used measures may prove interesting in determining dynamic characteristics of the effect of sedative drugs on autonomic nervous system activity.

Key words Poincaré plot, heart rate variability, HRV, fentanyl, sedative

Introduction

Poincaré plot is the common name used for a scatter plot to analyse heart rate variability (HRV) where the time between R-waves on an ECG, the R-R interval (RRI) is plotted against the succeeding RRI. A typical plot can be seen in Fig 1. Traditionally, Poincaré plots are made with data collected over 24hrs[1-6] or 12 hrs[7]. Shorter time periods have also been used more recently: 5-20mins[8-13], and <2mins[14,15].

Many indices have been developed to characterise the nonperiodic behaviour of HRV displayed in Poincaré plots, particularly with 24hr data, and these have been compared

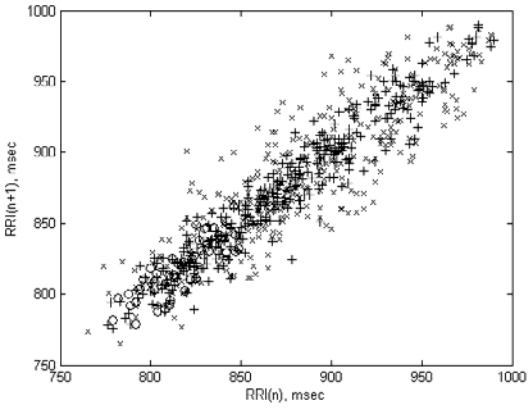

Figure 1. *Typical Poincaré plot (subject 3) for 10 mins of R-R intervals. Legend: x=baseline, o=fentanyl administration, +=post-fentanyl.*

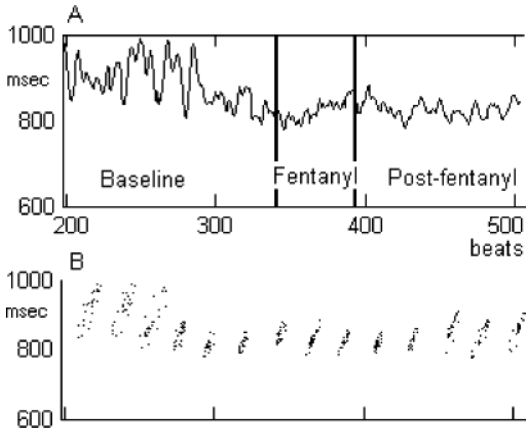

Figure 2. *A. Portion of typical data set (subject 3). B. Poincaré plots for each subset of 25 RRI.*

with known markers for autonomic nervous system activity: time-domain, and spectral power indices.

The time-domain indices are well described and extensively used as markers of autonomic system activity[16]. SDNN, the standard deviation of the RRI, reflects all cyclic components responsible for variability, the variance being mathematically equal to total power of spectral analysis. RMSSD, the square root of the mean squared differences of successive RRI, is a purely vagal index. pNN50, the proportion of intervals greater then 50 ms, is used as a reliable marker of vagal activity[17]. Furthermore, the RRI itself is an index of sympathovagal balance[18,19].

This study will compare these common measures of HRV with the published Poincaré indices. Indices which do not correlate strongly with commonly used measures may be useful in investigating dynamic and short-lived changes to HRV, such as those that occur during exercise[20] and fentanyl and midazolam sedation.

This study uses the dynamic effect of fentanyl on HRV to assess these indices. Fentanyl is a well-known depressor of the respiratory system, heart rate, and HRV power. Fentanyl was used because of its lipophilic nature; it enters the brain rapidly after intravenous injection. Contradictory results have been reported regarding the effect of fentanyl to cause a shift to increased parasympathetic dominance[21-24]. This study will determine indices that may be useful in further analysis of the effect of sedative drugs on autonomic nervous system activity.

Methods

Indices

A survey of published methods of Poincaré analysis with literature from the 1990's to the present day (Table 1)[25] found 48 indices applicable for short period HRV analysis. Indices not used were those using patterns, 3D, and density indices[1,2,6].

In addition to the surveyed Poincaré indices, three statistical time-domain indices (SDNN, RMSSD and pNN50), and an index of sympathovagal balance (mean RR interval[18], meanRR) were used to analyse the same data set: 12 subjects undergoing fentanyl and midazolam sedation.

Table 1. *Summary of Poincaré indices surveyed.*

Author	Index	Description
Ashkenkazy [33]	*A.mag|sd| *A.sgn(sd)	Magnitude and sign of differences
Contreras[34] Lagged plots	*SDsd8 *SDsd10	Lag of 8 beats Lag of 10 beats
Copie [3]	C.Area *C.pNN30	(pi.L.W)/4
D'Addio [5]	D.PLW	% length at Wmax
Ewing[35]	*E.pNN6.25	Percentage successive difference >1/16
Goldberger [18,19]	*meanRR *G.RMS	Sympathovagal balance Deviation of RRI from straight line
Griffin [36]	*p50	Median data point
Guzik[37] Assymetry	*Gz.acc *Gz,dec	Accelerations Decelerations
Hirose [38]	*Hi.SD/SDsd	Ratio SDNN to SDsd
Huikuri [4] Ellipse	nSD1 nSD2 H.D1 H.D2	Normalised SD Distances from mean to avg max diff & max diff
Kamen [9,10] Histogram variances	K.SD1 K.SD2 *K.NRR *K.Nsd	Width of RR histogram Width of delta RR Normality of RR and differences
Lewkowicz [39] Multipoles	*skew.RR *skew.sd *kurt.RR *kurt.sd	Skewness Kurtosis
Marciano [1] Radii of inertia	M.A M.B M.G	Max radius Min radius Gradient RR (avg)
Moraes [6] 3D	P2 P3	Max longitudinal & transverse ranges
Otzenberger [12] Pearson	rRR	Interbeat autocorrelation
Raetz [8] Quadrants	Qa-d *Qchi2	Distribution of sequences
Schechtman [7] Dispersion	W10 W90	Width at 10% Width at 90%
Toichi [11]	L T *log(L*T) L/T CV	4* SD longitudinal & transverse axis Coefficient of variation
Tulppo [30]	T.SD1 T.SD2 T.SD1/SD2 T.SDsd	Ellipse rotated +/- 45deg in polar coordinates, then SD along axis

Table 2. *Summary of patient data.*

	F n=10 Mean (SD)	M n=2 Mean (SD)	Total n=12 Mean (SD)
Age	40.5 (14.3)	36.0 (25.5)	39.8 (15.1)
Weight	75.6 (12.3)	93.0 (5.7)	78.4 (13.2)

Subjects

Ethics approval for the study was given by Flinders Medical Centre Ethics Committee. Consenting subjects were recruited if they were scheduled for minor surgical procedures, aged between 18 and 80 years, weight 40-120 kg, with a low frequency of ventricular arrhythmias (<10 premature complexes/hr), no recent history of cardiac-rate controlling drugs, and no clinical signs of peripheral neuropathy. They were studied in the ten minutes before anaesthesia was induced. Before testing they had been supine for at least 15mins, however, they were not all relaxed. As could be expected before surgery, they were often anxious. Baseline ECG, SpO2 and spirometry was recorded (Datex-Ohmeda AS/3 Anaesthetic monitor with S/5 Collect) for 5 minutes then a standard dose of midazolam (2.5 milligram) was given, followed by a randomly selected bolus of fentanyl (50, 75, 100 or 150 microgram). A further 5 minutes was then recorded. Oxygen was administered by facemask throughout.

Data collection

The analog ECG, lead II (Hewlett Packard 78353B, CA, USA) was digitised at 1000 Hz with 12 bits resolution (NI 6035E DAQ, National Instruments Corp, TX, USA) and stored (LabVIEW, National Instruments Corp, TX, USA) for off-line analysis.

Analysis of the data was performed using custom software developed for this study on a PC using MatLab (The MathWorks Inc., Natick, MA, USA). The ECG R-waves were identified by whichever of two methods produced the least artifacts: simple threshold or mean of backward differences[26]. Artifacts were automatically identified if the RRI was more than 30% from the mean RRI and then visually verified and corrected to the actual ECG R-wave peak. The few remaining artifacts were visually identified and manually corrected.

Data analysis

The indices were measured over data sets of 25 beats. This window size was selected as a trade-off between a small window size that captures dynamic changes, and the ability to generate meaningful indices from the number of beats. This provided at least 26 observations for each subject (some data sets were longer than 10 minutes).

The linear relationship strength between variables was determined by measuring Pearson correlation coefficients between the common indices and the Poincaré indices, and also between the Poincaré indices. For a correlation coefficient to be meaningful there are some conditions that must be met[27]: a) the relationship is linear, b) no outliers, c) no subgroups, and d) one of the variables has a normal distribution. Visual analysis of the index values confirmed linear relationship and no subgroups. Normal distribution of the main indices was assessed with Shapiro-Wilks test. Outliers were recorded for analysis. The criteria for a strong correlation was an average coefficient $r>0.85$ (explained variance of 72%) and $p<0.001$ for each of the 12 subjects.

Results

Summary of the patient data is shown in Table 2. Female subjects predominated in the scheduled operating lists available for this study.

The Shapiro-Wilks test showed the main indices were normally distributed for most subjects. Normal distribution was rejected in only a few subjects for each of the main indices: SDNN 1, RMSSD 2, meanRR 3, rRR 2. The test for pNN50 could not be calculated due to the low number of counts in some subjects.

Strong correlations with an average coefficient $r>0.85$ (explained variance of 72%) and $p<0.001$ for each of the 12 subjects with total variance (SDNN) and vagal activity (RMSSD, pNN50), and sympathovagal balance (meanRR), were seen in 18 of the 48 published indices(Table 3). In the (Table 3) column headed Subjects $p<0.001$, an asterisk indicates all 12 subjects had $p<0.001$. Where a number is written it indicates the number of subjects who had $p<0.001$. However for the mean correlation coefficients given, all subjects at least had a $p<0.05$.

One other index was observed to have multiple strong correlations: rRR, the correlation of each RR interval with the subsequent RR interval. This was strongly correlated with 3 other indices (Table 3).

Table 3 also includes four less-strongly correlated indices: C.Area, E.pNN6.25, M.A & M.B. These indices failed to meet the criteria of $r>0.85$ and $p<0.001$ for each of the 12 subjects. These indices also had the highest counts of outliers.

The surveyed Poincaré indices that were not strongly correlated with SDNN, RMSSD, meanRR or rRR are listed in Table 4.

Discussion

Technical problems

Some index calculations proved difficult to determine with smaller window length, and some required changes to the published method (previously published[25]).

Correlation

The criteria for a strong correlation were set high for this small sample of subjects undergoing limited dynamic change in heart rate variability. Using $r>0.85$ explained 72% of the variance in the sample. Requiring a $p<0.001$ for all 12 subjects reduced the likelihood of chance correlation.

The number of outliers varied between indices: the highest (12) in Table 4 is only 2.2% of data points. Useful indices would be expected to have fewer outliers.

Table 3. *Pearson correlation coefficients, mean of 12 subjects, for well correlated (r>0.75) indices.*

Index	Corr with[a]	r [b] (avg 12)	Subjects p<0.001[c]	Outliers
A.mag|sd|	R	0.97	*	3
C.Area	R	0.77[d]	11‡	8
CV	S	0.98	*	2
E.pNN6.25	P	0.88 [d]	10	6
G.RMS	M	1.00	*	1
Hi.SD1/SD2	C	0.89	*	6
K.SD1	S	1.00	*	2
K.SD2	R	1.00	*	4
L	S	0.98	*	2
L/T	C	0.91	*	4
log(L*T)	S	0.92	*	5
M.A	S	0.76 [d]	10‡	5
M.B	R	0.85 [d]	11‡	9
nSD1	S	0.94	*	2
nSD2	R	0.98	*	4
P2	S	0.94	*	1
P3	R	0.92	*	7
p50	M	0.99	*	1
SDsd10	R	0.89	*	1
SDsd8	R	0.88	*	4
T	R	1.00	*	4
T.SD1	S	0.98	*	2
T.SD1/SD2	C	0.91	*	4
T.SD2	R	1.00	*	4
T.SDsd	R	1.00	*	4

[a] C=rRR, M=meanRR=G.RR, P=pNN50, R=RMSSD, S=SDNN
[b] n = 26, number of 25 beat observations
[c] *all subjects p<0.001, ‡all subjects p<0.05
[d] correlation not considered strong by criteria

Table 4. *Shortlist of indices for very short periods (25 beats): common measures and uncorrelated indices.*

Index	Outliers	Correlated with
SDNN	2	See Table 3
RMSSD	4	See Table 3
meanRR	1	See Table 3
rRR	1	See Table 3
A.sgn(sd)	0	Qb, Qc (r=0.78)
K.NRR	11	
K.Nsd	8	
Qchi2	10	
W10	3	
W90	6	
Qa	3	
Qd	3	
D.PLW	0	
H.D1	3	H.D2 (r=0.86)
M.G	8	
skew.RR	2	
skew.sd	6	
kurt.RR	12	kurt.sd (r=0.97)
Gz.acc	0	Gz.dec (r=-0.92)

Agreement

Strong correlations with vagal markers predominate as found by Hayano et al[28]. Vagal effects on the sinus node occur faster than sympathetically mediated effects[4], causing instantaneous changes in RRI that are easily measured over short windows. This is demonstrated by the number of indices strongly correlated with RMSSD.

This study finds correlations in agreement with published studies for: E.pNN6.25, K.sd1, K.sd2, L, T, M.A[1], nSD1 & nSD2[4], P2 & P3[6], T.SDsd, T.SD1 & T.SD2[29,30].

The index rRR was known not be equivalent to SDNN or RMSSD; Otzenberger[12] claiming it revealed a different characteristic of dynamic behaviour.

In this study the set of pNN50, pNN30 and pNN6.25 showed no correlation with RMSSD. This was due to the absence of intervals greater than 50 msec in many of the 25 beat windows.

Some unexpected strong correlations were found with:
RMSSD: A.mag|sd|, C.Area[3], M.B (not M.G[1]), SDsd8 & SDsd10 (not sympathetic)
SDNN: CV[11], log(L*T) & S (not vagal activity[11])
meanRR: G.RMS (not RMSSD), p50
rRR: Hi.SD1/SD2, L/T (not sympathetic activity[11]), T.SD1/SD2[12].

Advantages

Poincaré plot indices were chosen because the data has no requirement for normal distribution as with summary statistics, no requirement for stationarity[30], minimum data set (e.g., the low frequency peak needs 2 mins[16]) or special processing that spectral analysis requires, and is more resistant to the influence of ectopic beats and other arrhythmias[9]. Measures of chaotic behaviour have been found to be reliable on samples as short as 500 beats[31], however the application of these indices on shorter 25 beat samples has not been investigated.

The commonly used time domain indices are recognised by Carrasco[32] as simple-to-calculate surrogates for many indices that are difficult to measure (including frequency domain variables).While SDNN reflects total power of variation, and RMSSD reflects vagal tone, there are no indices for measuring sympathetic tone. Indexes that do not correlate strongly with SDNN or RMSSD may prove useful in determining dynamic characteristics of cardiac nervous system activity.

Limitations

Throughout this study, all subjects received oxygen using a facemask to ensure adequate oxygenation after fentanyl administration. The application of a facemask does affect the HRV, but this effect should be consistent over the 10 mins of the study.

This study uses only a limited range of HRV over a short time (10 mins) to assess correlations of the indices. This is in agreement with the proposed application: further assessment of the dynamic effect of fentanyl on HRV.

Conclusion

The use of Poincaré indices over shorter time periods may require different methods for calculating for the indices due to the smaller sample sizes, but even small windows of only 25 RR intervals can still hold useful information.

This study using subjects undergoing fentanyl and midazolam sedation has shown that many published Poincaré indices are strongly correlated over short periods with commonly used indices SDNN, RMSSD, meanRR and rRR. Strongly correlated indices can be set aside and not used in further analysis of the fentanyl effect.

Further investigation of the Poincaré indices that do not correlate strongly with commonly used indices may prove interesting in determining dynamic characteristics of the effect of sedative drugs on autonomic nervous system activity.

References

1. Marciano, F., Migaux, M.L., Acanfora, D., Furgi, G. and Rengo, F., *Quantification of Poincare maps for the evaluation of heart rate variability,* Comput Cardiol, 21:577-580, 1994.
2. Hnatkova, K., Copie, X., Staunton, A. and Malik, M., *Numeric processing of Lorenz plots of R-R intervals from long-term ECGs. Comparison with time-domain measures of heart rate variability for risk stratification after myocardial infarction,* J Electrocardiol, 28 Suppl:74-80, 1995.
3. Copie, X., Le Heuzey, J.Y., Iliou, M.C., Khouri, R., Lavergne, T., Pousset, F. and Guize, L., *Correlation between time-domain measures of heart rate variability and scatterplots in postinfarction patients,* Pacing Clin Electrophysiol, 19:342-7, 1996.
4. Huikuri, H.V., Seppanen, T., Koistinen, M.J., Airaksinen, J., Ikaheimo, M.J., Castellanos, A. and Myerburg, R.J., *Abnormalities in beat-to-beat dynamics of heart rate before the spontaneous onset of life-threatening ventricular tachyarrhythmias in patients with prior myocardial infarction,* Circulation, 93:1836-44, 1996.
5. D'Addio, G., Acanfora, D., Pinna, G.D., Maestri, R., Furgi, G., Picone, C. and Rengo, F., *Reproducibility of short- and long-term poincare plot parameters compared with frequency-domain HRV indexes in congestive heart failure,* Comput Cardiol, 25:381-384, 1998.
6. Moraes, R.S., Ferlin, E.L., Polanczyk, C.A., Rohde, L.E., Zaslavski, L., Gross, J.L. and Ribeiro, J.P., *Three-dimensional return map: a new tool for quantification of heart rate variability,* Auton Neurosci, 83:90-9, 2000.
7. Schechtman, V.L., Harper, R.K. and Harper, R.M., *Development of heart rate dynamics during sleep-waking states in normal infants,* Pediatr Res, 34:618-23, 1993.
8. Raetz, S.L., Richard, C.A., Garfinkel, A. and Harper, R.M., *Dynamic characteristics of cardiac R-R intervals during sleep and waking states,* Sleep, 14:526-33, 1991.
9. Kamen, P.W. and Tonkin, A.M., *Application of the Poincare plot to heart rate variability: a new measure of functional status in heart failure,* Aust N Z J Med, 25:18-26, 1995.
10. Kamen, P.W., Krum, H. and Tonkin, A.M., *Poincare plot of heart rate variability allows quantitative display of parasympathetic nervous activity in humans,* Clin Sci (Lond), 91:201-8, 1996.
11. Toichi, M., Sugiura, T., Murai, T. and Sengoku, A., *A new method of assessing cardiac autonomic function and its comparison with spectral analysis and coefficient of variation of R-R interval,* J Auton Nerv Syst, 62:79-84, 1997.
12. Otzenberger, H., Gronfier, C., Simon, C., Charloux, A., Ehrhart, J., Piquard, F. and Brandenberger, G., *Dynamic heart rate variability: a tool for exploring sympathovagal balance continuously during sleep in men,* Am J Physiol, 275:H946-50, 1998.
13. Carrasco, S., Gonzalez, R., Gaitan, M.J. and Yanez, O., *Reproducibility of heart rate variability from short-term recordings during five manoeuvres in normal subjects,* J Med Eng Technol, 27:241-248, 2003.
14. Bergfeldt, L. and Haga, Y., *Power spectral and Poincare plot characteristics in sinus node dysfunction,* J Appl Physiol, 94:2217-24, 2003.
15. Boardman, A., Schlindwein, F.S., Thakor, N.V., Kimura, T. and Geocadin, R.G., *Detection of asphyxia using heart rate variability,* Med Biol Eng Comput, 40:618-24, 2002.
16. Task Force of European Society of Cardiology, *Heart rate variability. Standards of measurement, physiological interpretation, and clinical use. Task Force of the European Society of Cardiology and the North American Society of Pacing and Electrophysiology,* Eur Heart J, 17:354-381, 1996.
17. Bigger, J.T., Jr., Albrecht, P., Steinman, R.C., Rolnitzky, L.M., Fleiss, J.L. and Cohen, R.J., *Comparison of time- and frequency domain-based measures of cardiac parasympathetic activity in Holter recordings after myocardial infarction,* Am J Cardiol, 64:536-8, 1989.
18. Goldberger, J.J., *Sympathovagal balance: how should we measure it?,* Am J Physiol, 276:H1273-80, 1999.
19. Goldberger, J.J., Le, F.K., Lahiri, M., Kannankeril, P.J., Ng, J. and Kadish, A.H., *Assessment of parasympathetic reactivation after exercise,* Am J Physiol Heart Circ Physiol, 290:H2446-52, 2006.
20. Hautala, A.J., Makikallio, T.H., Seppanen, T., Huikuri, H.V. and Tulppo, M.P., *Short-term correlation properties of R-R interval dynamics at different exercise intensity levels,* Clin Physiol Funct Imaging, 23:215-23, 2003.
21. Reitan, J.A., Stengert, K.B., Wymore, M.L. and Martucci, R.W., *Central vagal control of fentanyl-induced bradycardia during halothane anesthesia,* Anesth Analg, 57:31-6, 1978.
22. Kohno, K., Koh, J., Kosaka, Y., *Effect of fentanyl on heart rate variability during mechanical ventilation,* Journal of Anesthesia, V11:270-276, 1997.
23. Michaloudis, D., Kochiadakis, G., Georgopoulou, G., Fraidakis, O., Chlouverakis, G., Petrou, A. and Pollard, B.J., *The influence of premedication on heart rate variability,* Anaesthesia, 53:446-53, 1998.
24. Galletly, D.C., Westenberg, A.M., Robinson, B.J. and Corfiatis, T., *Effect of halothane, isoflurane and fentanyl on spectral components of heart rate variability,* Br J Anaesth, 72:177-80, 1994.
25. Smith, A.L. and Reynolds, K., *Survey of Poincare indices for measuring heart rate variability,* Australasian Physical & Engineering Sciences in Medicine, 29:97-101, 2006.
26. Suppappola, S. and Sun, Y., *A comparison of three QRS detection algorithms using the AHA ECG database,* IEEE Eng Med Biol Soc, 13:586-587, 1991.
27. Petrie, A. and Sabin, C., *Medical statistics at a glance*, 2nd edn. Blackwell, Oxford, Pages, 2005.
28. Hayano, J., Sakakibara, Y., Yamada, A., Yamada, M., Mukai, S., Fujinami, T., Yokoyama, K., Watanabe, Y. and Takata, K., *Accuracy of assessment of cardiac vagal tone by heart rate variability in normal subjects,* Am J Cardiol, 67:199-204, 1991.

29. Penttila, J., Helminen, A., Jartti, T., Kuusela, T., Huikuri, H.V., Tulppo, M.P., Coffeng, R. and Scheinin, H., *Time domain, geometrical and frequency domain analysis of cardiac vagal outflow: effects of various respiratory patterns,* Clin Physiol, 21:365-376, 2001.
30. Tulppo, M.P., Makikallio, T.H., Takala, T.E., Seppanen, T. and Huikuri, H.V., *Quantitative beat-to-beat analysis of heart rate dynamics during exercise,* Am J Physiol, 271:H244-52, 1996.
31. Seker, R., Saliu, S., Birand, A. and Kudaiberdieva, G., *Validity Test for a Set of Nonlinear Measures for Short Data Length with Reference to Short-Term Heart Rate Variability Signal,* Journal of Systems Integration, V10:41-53, 2000.
32. Carrasco S, Gaitan MJ, Gonzalez R, Yanez O, *Correlation among Poincare plot indexes and time and frequency domain measures of heart rate variability,* J Med Eng Technol, 25:240-8, 2001.
33. Ashkenazy, Y., Ivanov, P.C., Havlin, S., Peng, C.K., Goldberger, A.L. and Stanley, H.E., *Magnitude and sign correlations in heartbeat fluctuations,* Phys Rev Lett, 86:1900-3, 2001.
34. Contreras, P., Canetti, R. and Migliaro, E.R., *Correlations between frequency-domain HRV indices and lagged Poincare plot width in healthy and diabetic subjects,* Physiological Measurement, 28:85-94, 2007.
35. Ewing, D.J., Neilson, J.M. and Travis, P., *New method for assessing cardiac parasympathetic activity using 24 hour electrocardiograms,* Br Heart J, 52:396-402, 1984.
36. Griffin, M.P. and Moorman, J.R., *Toward the early diagnosis of neonatal sepsis and sepsis-like illness using novel heart rate analysis,* Pediatrics, 107:97-104, 2001.
37. Guzik, P., Piskorski, J., Krauze, T., Wykretowicz, A. and Wysocki, H., *Heart rate asymmetry by Poincare plots of RR intervals,* Biomedizinische Technik, 51:272-5, 2006.
38. Hirose, M., Imai, H., Ohmori, M., Matsumoto, Y., Amaya, F., Hosokawa, T. and Tanaka, Y., *Heart rate variability during chemical thoracic sympathectomy,* Anesthesiology, 89:666-70, 1998.
39. Lewkowicz, M., Levitan, J., Puzanov, N., Shnerb, N. and Saermark, K., *Description of complex time series by multipoles,* Physica A: Statistical Mechanics and its Applications, 311:260-274, 2002.

CORRELATION BETWEEN PARAMETERS DESCRIBING TUMOUR MOTION AND ITS LOCATION IN THE LUNGS

Huanmei Wu[1], George Sandison[2], Li Zhao[2], Qingya Zhao[2], Hiroki Shirato[3] and Steve Jiang[4]

[1]*Purdue School of Engineering and Technology, IUPUI, Indianapolis, IN, USA*
[2]*School of Health Sciences, Purdue University, West Lafayette, IN, USA*
[3]*Hokkaido University School of Medicine, Sapporo, Japan*
[4]*University of California, San Diego (UCSD) School of Medicine, La Jolla, CA*
hw9@iupui.edu

Abstract

Characterizing respiratory-induced tumour motion is an important step in the effective image-guided radiation treatment of moving tumours, especially for tumours in the lung and lower abdomen. This study characterized tumour motion based on a piecewise linear model representing tumour motion at defined stages of the breathing cycle. Lung tumour locations were categorized based on broncho-pulmonary segments. Association rules between tumour motion characteristics and their locations in the lung were discovered and parameterized through statistical analysis. Results show there is a correlation between tumour motion characteristics and tumour location in the lungs. Generally, tumours with small motion (amplitude < 10mm) are observed most frequently in the apex region of lung or when attached to a fixed structure, such as the chest wall or aorta. Tumours with relatively large motion (amplitude > 20mm) are located close to the diaphragm or mid-level periphery of the lungs close to the chest wall.

Key words tumour locations, respiratory motion, correlations

Introduction

The goal of radiation therapy is to ensure precise and accurate delivery of a curative radiation dose to a tumour while limiting the exposure of surrounding healthy tissues and critical structures to radiation and so avoid serious treatment complications[1]. Radiation therapy for localized cancers of the lung is common and often applied in daily fractions over a few weeks. Intra-fraction tumour motion is often induced by the patient's respiration and it is this motion that poses a major challenge for precise radiation treatment delivery, especially when the amplitude of tumour motion is greater than a centimeter[1-3]. Understanding and characterizing the natural tumour motion behavior in various locations is of some importance to precision radiation treatment delivery. Once understood and characterized, prediction of this tumour motion behavior will facilitate advanced real-time treatment of patients under free breathing conditions.

It is known that tumours of the lung, kidney, liver or prostate have distinctive respiratory-induced motion properties[4]. The objective of this work is to identify the correlation between respiratory-induced tumour motion characteristics and its location in the lungs. Establishing reliable correlations between the motion characteristics and tumour location will enable refinement of the predictive

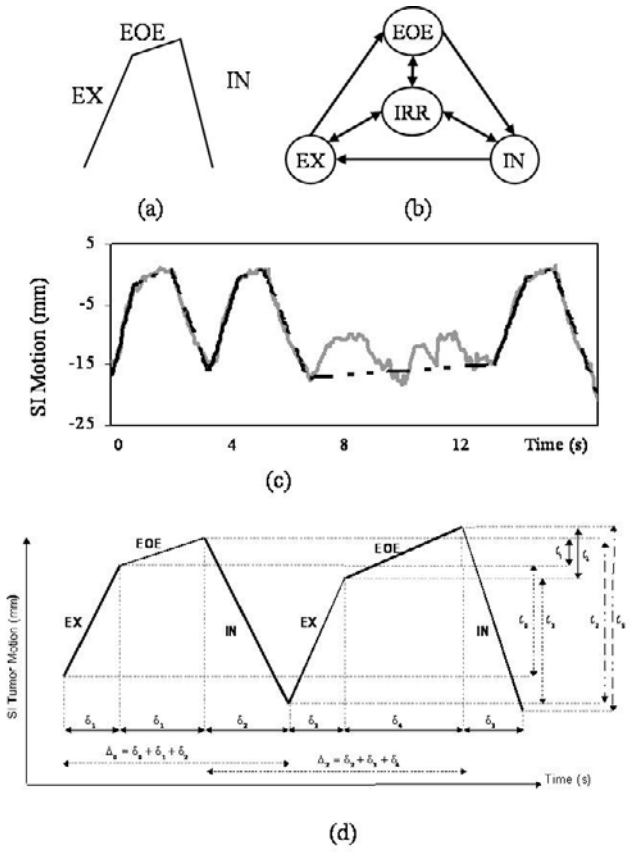

Figure 1. *Tumour motion modeling and statistical analysis: (a) regular motion and the corresponding line segments, (b) finite state model (FSM) for respiratory motion, (c) irregular motion and the corresponding line segments, and (d) illustration of duration and travel distance of the superior-inferior tumour motion. The* ***state duration*** *is labeled as δ_i, where δ_0 and δ_3 are for EX state durations, δ_1 and δ_4 for EOE, and δ_2 and δ_5 for IN. The* ***cycle duration*** *is the sum of three adjacent state durations. For example, Δ_0 is a cycle duration beginning with an EX state while Δ_2 is a cycle duration beginning with an IN state. The* ***state travel distance*** *is labeled as l_i, where l_0 and l_3 are EX travel distances, l_1 and l_4 for EOE, and l_2 and l_5 for IN. The* ***cycle travel distance*** *(which is not shown in the figure) is the sum of three adjacent state travel distances. For example, the cycle distance beginning with an EX state can be $l_0 + l_1 + l_2$ or $l_3 + l_4 + l_5$ while the cycle distance beginning with IN state can be $l_1 + l_2 + l_3$.*

power of recently developed models for respiratory-induced tumour motion, such as the recently developed finite state model[5-6].

Materials and methods

Materials

A retrospective study was performed on lung tumour motion data for patients previously treated using the real-time tumour-tracking (RTRT) system available at Hokkaido University[7]. In this RTRT system, a 2mm or 1.5mm diameter gold marker is inserted into or near the lung tumour using image guided implantation. The system can detect the actual marker position at a rate of 30Hz using two X-ray imaging systems. Lung tumour motion data of 42 patients treated between 2001 and 2002 were analyzed.

Introduction to the finite state model

Our previous research introduced a finite state model based on the understanding of natural breathing actions[5]. In this model, a normal breathing cycle is decomposed into three states: inhale (IN), exhale (EX), and end of exhale (EOE), Figure 1a. A fourth state is also introduced to handle irregular breathing (IRR). IRR state includes any abnormal tumour motion, such as the motion when a patient coughed. Each state is represented by a single line segment. The transition from one state to another is automatically guided by a finite state model (FSM). The example provided in Figure 1 is for one-dimensional motion in the superior-inferior direction. This real-time algorithm has been applied successfully in the analysis of tumour motion for 42 lung cancer patients. This model is the base of the mathematical characterization of tumour motion patterns in our study.

Statistical analysis

Tumour motion analysis based on the FSM allows grouping of patients with similar tumour motion characteristics into subsets and facilitates better modeling and predictive accuracy of the tumour's motion in real time[6-7]. Statistical analysis was performed on each of the defined motion characteristics. Some of these characteristics illustrated in Figure 1d, including state travel distance (such as l_0 for EX state), cycle travel distance (such as $l_0 + l_1 + l_2$), state duration (such as δ_0 for EX state), and cycle duration (such as $\delta_0 + \delta_1 + \delta_2$). The aggregates (including the minimum, maximum, average, range and standard deviation) and histogram of these properties were quantified[12].

Correlating tumour motion with location in the lungs

Tumours were clustered based on the associations between their motion characteristics and their location. Figure 2a is a schematic of the location of 36 tumours selected from the database of 42 patients. (In the database, the positions of some tumours were not recorded.) The regions of the lung described in Figure 2 follow the prescription provided by the web site "Get Body Smart by ConceptCreators, Inc"[8]. Patient's left and right lungs are each categorized into 10 regions (S1 through S10). Indicated in the figure is an annotation describing whether the tumour was free or attached to another structure, and if it was located in the anterior or posterior half of the lung. The regions S1 through S10 correspond to recognized broncho-pulmonary segments which have been previously used to describe tumour location[9-11].

Translation of the available data on patient tumour location and adhesion status was required since the original patient data defined geometrical information based on; the primary site of the tumour, the broncho-pulmonary segment, the cranio-caudal location (upper, middle or lower), the ventro-dorsal location (anterior, middle or posterior), tumour adhesion to the heart, aorta, chest wall or

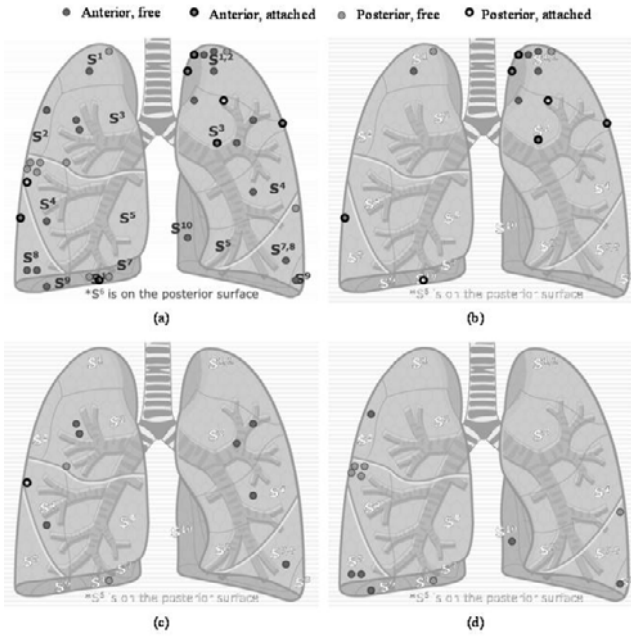

Figure 2. *The correlation of average cycle travel distance with tumour location in the lungs. (a) Tumour locations based on broncho-pulmonary segments, where* ***Attached*** *means a tumour is attached to one or more of: the chest wall, the vertebra, the aorta or aortic arch and* ***Free*** *means the tumour dose not attached to any of these structures. (b) tumour locations whose cycle travel distance is less than 10mm; (c) tumour locations whose cycle travel distance is between 10mm and 20mm, and (d) tumour locations whose cycle travel distance is more than 20mm.*

if it was free of attachment. Other information included the distance from the heart or chest wall.

Results

The duration and travel distance of a breathing state or a breathing cycle was computed for each of the tumours (the comprehensive results are summarized in Wu *et al*, 2007[12]). The histograms of the average state and cycle travel distance and duration are illustrated in Figure 3a-b. It can be seen that tumour motion characteristics are highly patient specific.

The correlations between tumour motion characteristics and tumour locations are analyzed. Figure 3c provides an example of the correlation between cycle travel distance and lung segments. Based on the significance of the cycle travel distance, four patient clusters were identified. Then, tumours in each of these clusters were mapped back onto the lung anatomy as shown in Figures 2b-d, where Figure 2b is for the locations of tumours in cluster C1, Figure 2c is for C2 and Figure 2d is for the combination of C3 and C4.

Discussion and conclusions

Figures 2 and 3 illustrate the correlations between tumour location and cycle travel distance. For superior-inferior motion, tumours with less motion (cycle travel distance<10mm) are either in left lung segment S1+2 and right S1 or are attached to fixed structures. Tumours with medium motion (10mm<cycle travel distance<20mm) are typically free and centrally located (S3 or S4) or close to the diaphragm (S7, S8 or S10). Tumours with large motion (cycle travel distance>20mm) are free and close to the lung periphery including the diaphragm.

Similar analysis has been performed for IN, EX and EOE travel distances and duration. The results of the IN and EX travel distance correlation with tumour locations are similar to the overall cycle travel distance. The EOE travel distance had no strong correlation with tumour location (The EOE state has little travel distance in comparison to the IN and EX states.). Further analysis showed that there is not a strong correlation between the tumour motion duration parameters and the tumour location.

Knowledge of the tumour travel distance correlation with lung location that is described in this article will help to refine predictive models of tumour motion behavior critical to real-time treatment[5-6]. Future work will concentrate on correlating the inter- and intra-fractional changes of tumour characteristics with tumour locations.

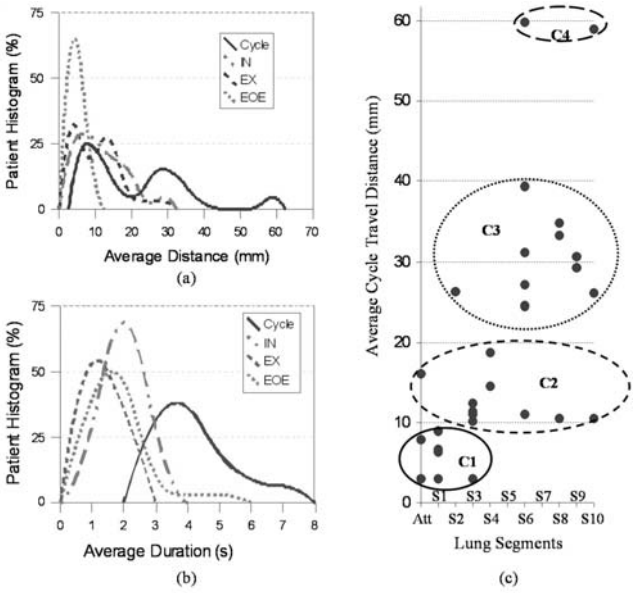

Figure 3. S*tatistical analysis results: (1) a histogram of a specific tumour's average state and cycle travel distance, (b) the histogram of the tumour's average state and cycle duration, and (c) the correlation between the tumour's average cycle travel distance and the broncho-pulmonary segment, where C1 through C4 are groups of tumours based on the average cycle travel distance. The average cycle travel distance in C1 is less than 10mm, in C2 is between 10mm and 20mm, in C3 between 20mm and 40mm, and in C4 is more than 55mm. The x-coordinate shows that broncho-pulmonary segments, where* ***Att*** *(stands for attached) indicates a tumour is attached to one or more structures e.g: the chest wall, a vertebra, the aorta or the aortic arch. (S1 included right lung segment 1 and left lung segments 1 and 2. S2 only included the right segment 2. S3 to S10 included both the right and left segments, respectively.)*

Reference

1. Keall, P. J., Kini, V. R., Vedam, S. S. and Mohan, R., *Motion adaptive x-ray therapy: a feasibility study,* Phys. Med. Biol., 46(1) 1-10, 2001.
2. Bortfeld, T., et al., *Effects of intra-fraction motion on IMRT dose delivery: statistical analysis and simulation.* Phys Med Biol, 47(13): p. 2203-20, 2002.
3. Jiang, S.B., C. Pope, K.M. Al Jarrah, J.H. Kung, T. Bortfeld, and G.T. Chen, *An experimental investigation on intra-fractional organ motion effects in lung IMRT treatments.* Phys Med Biol, 48(12): p. 1773-84, 2003.
4. Keall, et al, *The Management of Respiratory Motion in Radiation Oncology*, Handout for AAPM, Continuing Education Session, 2005.
5. Wu, H., G.C. Sharp, B. Salzberg, D. Kaeli, H. Shirato, and S.B. Jiang, *A finite state model for respiratory motion analysis in image guided radiation therapy.* Phys Med Biol, 49(23): p. 5357-72, 2004.
6. Wu, H., Salzberg, B., Sharp, G.C., Jiang, S.B., Shirato, H., and Kaeli, D., *Subsequence matching on structured time series data*. Proceeding of the ACM SIGMOD, 682-693, 2005.
7. Sharp, G.C., S.B. Jiang, S. Shimizu, and H. Shirato, *Prediction of respiratory tumour motion for real-time image-guided radiotherapy*. Phys Med Biol, 49(3): 425-40, 2004.
8. Shirato et al, *Four-dimensional treatment planning and fluoroscopic real-time tumor tracking radiotherapy for moving tumor.* IJROBP, 48(2): p. 435-42, 2000.
9. http://www.getbodysmart.com/ap/respiratorysystem/lungs/segments/tutorial.html
10. Sealy, W, Connally, S. and Dalton, M., *Naming the bronchopulmonary segments and the development of pulmonary surgery.* Ann Thorac Surg, 55 (1): 184-8, 1993.
11. Tompsett, D. H., *The Bronchopulmonary Segments,* Med Hist, 9(2): 177–181, 1965.
12. Wu, H., Sharp, G., Zhao, Q., Shirato, H., and Jiang, B J., *Statistical analysis and correlation discovery of tumor respiratory motion*, Phys Med Biol, 52(16), 4761-4774, 2007.

JTIENT-SPECIFIC MARGINS FOR PROTON THERAPY OF LUNG

Li Zhao[1], G A Sandison [1], J. B. Farr[2], Wen-Chien Hsi[3], Huanmei Wu[4] and X. Allen Li[5]

[1]*School of Health Sciences, Purdue University, West Lafayette, IN, USA*
[2]*Midwest Proton Radiotherapy Institute, Bloomington, IN, USA*
[3]*University of Florida Proton Therapy Institute, Jacksonville, FL, USA*
[4]*Indiana University Purdue University Indianapolis, Indianapolis, IN, USA*
[5]*Department of Radiation Oncology, Medical College of Wisconsin, Milwaukee, WI, USA*

Sandison@purdue.edu

Abstract

Lung cancer treatment presents a greater treatment planning and treatment delivery challenge in proton beam therapy compared to conventional photon therapy due to the proton beam's energy deposition sensitivity to the breathing-induced dynamic tissue density variations along the beam path. Four-dimensional computed tomography (4D-CT) has been defined as the explicit inclusion of temporal changes of tumor and normal organ mobility into an image series. It allows more accurate delineation of lung cancer target volumes by suppression of any breathing motion artifacts present in the CT images. It also allows analysis of the tumor's 3D spatial movement within a breathing phase cycle. The motivation for this study was to investigate dosimetric errors caused by lung tumor motion in order to find an optimal method of design for patient compensators and apertures for a passive scattering beam delivery system and treatment of the patient under free breathing conditions. In this study, the maximum intensity projection (MIP) method was compared to patient-specific internal margin designs based on a single breathing phase at the end-of inhale (EOI) or middle-of-exhale (MOE). It was found that MIP method provides superior tumor dose distribution compared to patient-specific internal margin designs derived from 4D-CT.

Keywords 4D-CT, proton therapy, lung tumor, maximum intensity projection

Introduction

Proton beam radiation therapy offers some distinct advantages compared to photon therapy since the proton beam's enhanced dose deposition region known as the Bragg peak may be exploited for the irradiation of a tumor and the rapid fall-off in dose just beyond the Bragg Peak may provide increased sparing of normal tissue from damage. A few studies have reported a possible benefit of proton therapy in the treatment of lung cancer [1-3]. However the proton beam's range is well-defined by the composite electron density of tissue along its path and compared to photon treatment this makes proton beam treatment more sensitive to lung motion during breathing and the dynamic change in lung density.

The conventional method to address organ motion and setup errors is to expand the treatment volumes. Using ICRU 62[4] nomenclature, an internal margin (IM) is added for the variation in position and/or shape and size of the clinical target volume (CTV), as seen during simulations, to define the internal target volume (ITV). Geometric misses of the target may occur if the tumor motion is greater than expected on the basis of the simulator or there may be some unnecessary irradiation of the surrounding normal tissue if the tumor motion is smaller than expected.

In common clinical technique, fluoroscopy is acquired during simulation to aid in estimation of the internal margin. Free-breathing CT or breath-hold CT scans are

used in the planning. The free-breathing CT studies may erroneously indicate the position and volume of the critical structure and, thus, may lead to faulty planning. The reproducibility of the tumor motion plays a significant role on the use of the breath-hold method. Recently, four-dimensional computer tomography (4D-CT) [5-7] provides both spatial and temporal information on tumor and normal organ mobility. This can lead to more precise patient specific internal margin estimation. 4D treatment planning has some advantages over existing methods [8-9]. However, without automation tools, it introduces another level of complexity in the treatment planning process [10]. Therefore, using a single CT from 4D-CT with patient-specific margin to account for tumor motion would expedite the process. The other method is to use the maximum intensity projection CT [11] to obtain the tumor-motion-encompassing target volume. In this paper, we investigate a dosimetric comparison of the above two approaches for proton therapy in the treatment of lung cancer.

Materials and methods

4D-CT acquisition

A multislice CT scanner (LightSpeed, GE) was used to acquire 4D-CT images tagged to the patient breathing cycle by use of a Real-Time Position Management system (RPM) (Varian Medical Systems, Inc.). Patient image acquisition occurred under free-breathing conditions. The CT scanner was operated in axial cine mode with multiple scans performed at each couch position for a duration equal to or longer than the breathing cycle. Each image was then sorted into one of ten respiratory phase bins using a commercially available 4D simulation package (Advantage, GE). These ten phase bins were selected to be evenly spaced in time over the respiratory cycle. Motion phases were reported in percentage values, e.g. 0% corresponded to phase1, 40% to phase5 and 90% corresponded to phase10.

Treatment plans

Two discrete phases, an end-of-inhale (EOI) CT scan and a middle-of-exhale (MOE) CT scan were selected as "representative" CT scans. The centroid of the gross tumor volume (GTV), which is independent of the tumor density, was used to assess the extent of tumor movement by means of the magnitude of its displacement in all three directions: Right-left (RL), superior-inferior (SI), and anterior-posterior (AP). The peak to peak amplitude of 3D movement was found to be 1.60cm in the SI direction, 0.21cm in the AP direction and 0.25cm in the RL direction. The amplitude in the SI direction was much larger than in the AP direction and RL direction. Treatment planning was implemented on a Computerized Medical Systems (CMS) XiO treatment planning system. The Midwest Proton Radiotherapy Institute's (MPRI, Bloomington, IN) passive scattering beam delivery system and its commissioning data were used in this study. Beam shaping devices, patient aperture and compensator were used to sculpt the proton dose distribution to the tumor volume, both laterally and distally. GTVs were semi-automatically delineated on all 10 phases of the 4D-CT scan using standard window and level setting. A uniform margin of 7mm was added around the GTVs to take into account undetected microscopic spread. Only respiratory motion was considered in this study, other sources of error were assumed to be the same when comparing the different treatment plans. In our study, 3mm smearing of the compensator was used to account for a setup error of 3mm. The CT uncertainty was 1% and beam range uncertainty was 1mm. The prescribed dose to the clinical target volume (CTV) was 72Gy. A 3-field treatment beam arrangement was used to reduce radiation dose to the lungs, heart and spinal cord.

The ITVs were generated by adding the internal margins (IMs) to the CTVs symmetrically (Figure 2): 1.5cm in the SI direction, 0.2cm in the AP direction and 0.2cm in the RL direction. For Plan ITV_{MOE}, the CTV was contoured on the middle-of-exhale (MOE) phase of the 4D-CT data instead of the end-of-inhale (EOI) used in Plan ITV_{EOI}. The expansion margins and the beam design were the same as Plan ITV_{EOI}. By taking account of the set up uncertainty plus the 90-50% penumbra, the margin between the aperture edge and the edge of ITV was a uniform 1cm. For Plan $ICTV_{MIP}$, the internal gross tumor volume (IGTV) was contoured on the maximum intensity projection (MIP) images. MIP images were generated by reassigning each pixel's CT number to the maximum CT number the pixel encountered during any of the 10 phases in each slice position. The internal clinical target volume (ICTV) was generated by uniform 7mm expansion of the IGTV. The ICTV is comparable to the ITVs used in the other two methods. No internal margin was used for MIP method. The apertures and range compensators were separately optimized on the basis of the ITV_{EOI}, ITV_{MOE} and $ICTV_{MIP}$.

We would like to emphasize the following. The internal margins we used are approximately the total range of displacement. Based on ICRU Report 62, if a respiratory management device is not used, the entire range of motion should be considered when establishing the internal margin. Here, we try to describe a scenario that there was no respiratory management device used in the beam delivery process, such as gating or tracking. If the average position of the tumor is preknown, using the amplitude instead of the full range of the motion as the IMs would reduce the ITVs and thereafter reduce the normal tissue complication. But, it requires the tumor motion characteristic to be analyzed through the breathing cycle in advance. In other words, the tumors in different phases need to be outlined. This is exactly what we want to avoid at the beginning by using a single CT from 4D-CT. Although MOE CT image shows the approximate average tumor position, we treated it as nothing more than another single phase CT from 4D-CT. The EOI CT and MOE CT might have similar characteristic to the breath-hold CT scans, but this subject is out of scope. Also, symmetric margins are used. We believe there is a lack of evidence to support that asymmetric margins are superior to symmetric margins. If the respiratory pattern is not sufficiently reproducible, the asymmetric margin might induce higher dose error during the course of the treatment. Again, pre-knowledge of the tumor motion pattern is required when an asymmetric

Table 1. *Volume definition and treatment beam setup.*

	GTV	CTV	ITV	Beam setup
Plan ITV_{EOI}	GTV_{EOI}	GTV_{EOI}+7mm	GTV_{EOI}+7mm+IM	Setup error : 3mm compensator smearing CT uncertainty: 1% Range uncertainty: 0.1cm.
Plan ITV_{MOE}	GTV_{MOE}	GTV_{MOE}+7mm	GTV_{MOE}+7mm+IM	
Plan $ICTV_{MIP}$	IGTV	IGTV+7mm		

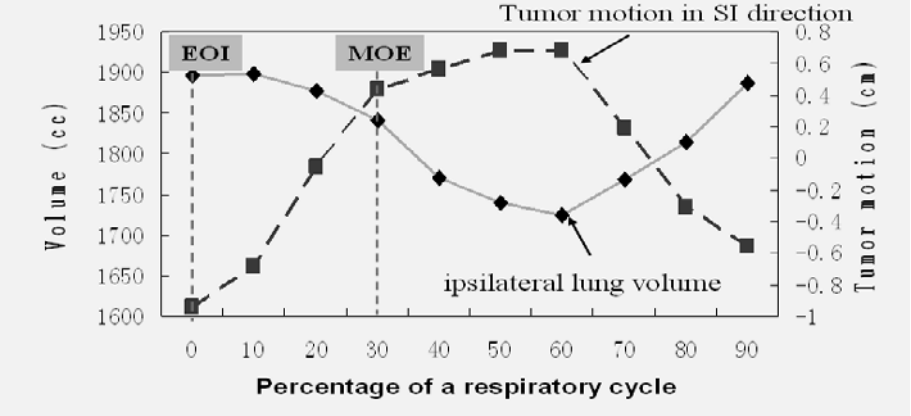

Figure 1. *The changes of ipsilateral lung volumes and the tumor motion in SI direction. Solid line denotes the volume changes of the ipsilateral lung. Dashed line denotes the SI direction tumor movement, 0% represents phase 1, 10% represents phase 2, and so forth.*

margin is applied, which is not what we want to include in this study. Because we decided to use the centroid of the gross tumor volume displacement to estimate the patient-specific margin, the tumors have been outlined in ten phases. However, the internal margin estimation is not limited to this method. Fluoroscopy still can be used to monitor the diaphragm motion as a surrogate to estimate tumor motion.

Table 1 lists the volume definition and treatment plans setup in the three plans. Treatment plans generated from these three designs were mapped back onto each respiratory phase CT image to recalculate the planned dose distribution. The resultant dose distributions were evaluated phase by phase for the three different plan designs on the basis of tumor coverage and normal tissue sparing.

Results

The changes of ipsilateral lung volumes and the displacement of the centroid f the GTV in the SI direction are shown in Figure 1. Lung volume changed by 10% through the respiratory cycle. Lung volumes at different breathing phases were substantially different from each other based on the 4D-CT information.

Besides the tumor displacement, tumor deformation was also noted. Figure 2 shows the GTV, CTV, ITV, IGTV, ICTV contours of three different plans in one coronal plane. Dose–volume histograms (DVH) for each constituent breathing phase and each plan are provided in Figure 3 for the CTVs and ipsilateral lung excluding CTV. In terms of the target coverage, severe underdosage occurred in certain respiratory phases for Plan ITV_{EOI} and slight underdosage occurred in three respiratory phases for Plan ITV_{MOE}. In contrast, the maximum intensity image method ensures the tumor coverage through the entire respiratory cycle. The mean normal lung dose was maintained at the same level for all three plans, and is below the tolerance limit value of 24Gy [11]. There is negligible dose to either the spinal cord or the heart, so they are not recorded in this article. Table 2 lists the average, minimum and maximum value of mean normal lung doses (MLD) from all 10 respiratory phases for each of the three treatment plans. The average, minimum and standard deviation of the percentage of prescribed dose covering 99% of the CTV are listed in Table 3.

Conclusions

Respiration-induced tumor motion is an important issue for proton therapy and careful planning to account for tumor motion is required. Designing a treatment plan for a passive scattering beam delivery system utilizing patient compensators and apertures that are based on maximum intensity image sets provide superior and consistent tumor coverage under condition of patient free breathing. Normal

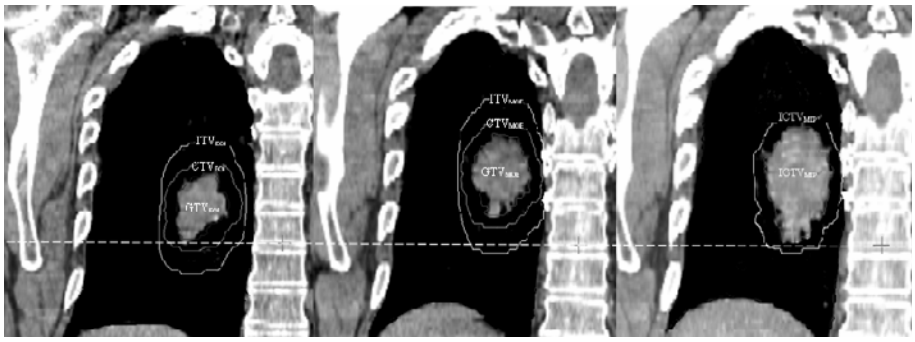

Figure 2. *Target volume delineation on the different plans. A) GTV, CTV and ITV on the EOI phase. B) GTV, CTV and ITV on the MOE phase. C) IGTV and ICTV on the MIP image. The dashed line indicts the tumor displacement. The difference between the left and middle panels of Figure 2 is due to the tumor displacement and tumor deformation.*

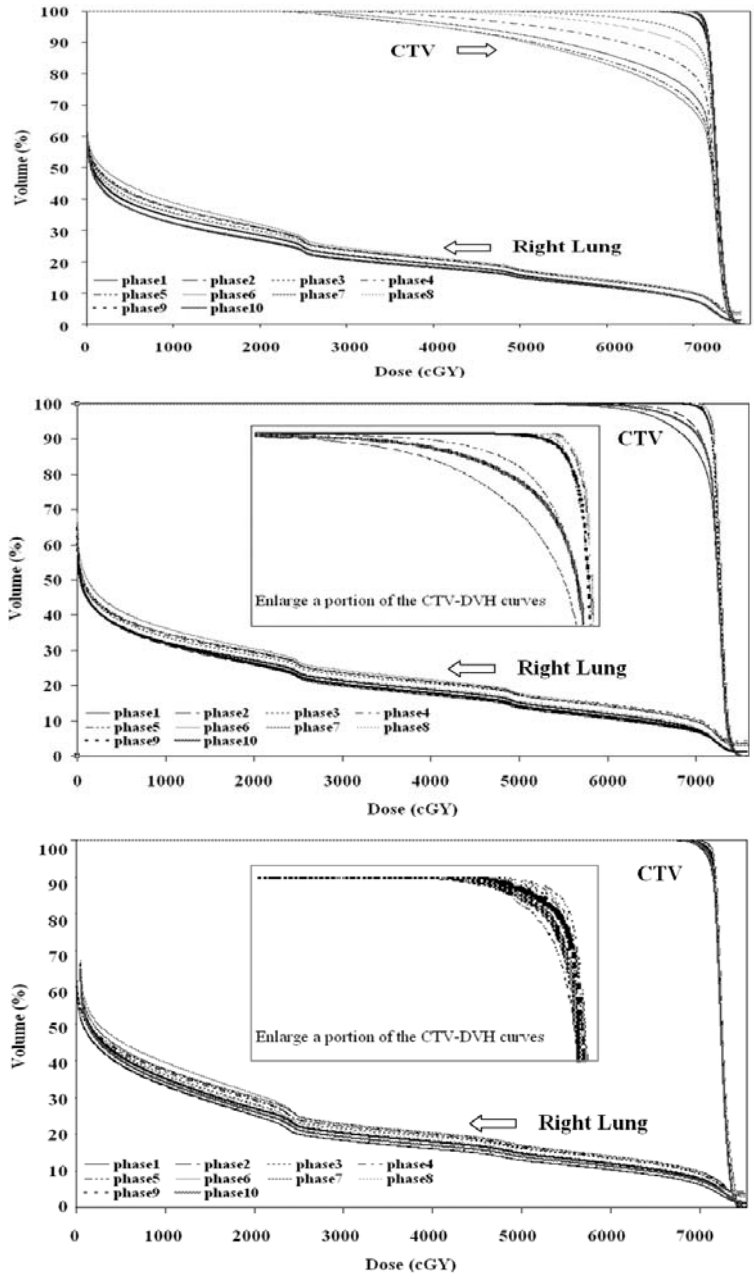

Figure 3. *DVHs for the target and right lung dose in Plan ITV_{EOI} (A), Plan ITV_{MOE} (B), and Plan $ICTV_{MIP}$ (C).*

Table 2. *Comparison of mean lung dose (MLD).*

	AVG	MIN	MAX
Plan ITV_{EOI}	15.20Gy	14.40Gy	16.20Gy
Plan ITV_{MOE}	14.70Gy	13.80Gy	15.70Gy
Plan $ICTV_{MIP}$	14.60Gy	13.50Gy	15.60Gy

Table 3. *Percentage of prescribed dose covering 99% of the CTV.*

	AVG	MIN	SD
Plan ITV_{EOI}	71.00%	37.60%	18.9
Plan ITV_{MOE}	94.70%	83.50%	4.0
Plan $ICTV_{MIP}$	97.40%	96.40%	0.5

lung tissue doses remain within tolerance limits and are comparable regardless of whether plan design is based on ITVs at the end-of-inhale or middle-of-exhale or based on MIP images derived from 4D-CT. We advocate the maximum intensity projection (MIP) treatment planning strategy for proton therapy of lung tumors when the proton beam delivery system is of the passive scattering type.

Acknowledgement

We wish to thank Dr. Paul Keall for his kind support of this work and Dr. Michael F. Moyers for his valuable advice at an early stage of the project. Ms Li Zhao was supported by Purdue Research Foundation fellowship from Purdue University for this study.

References

1. Bush, D.A., Slater, J.D., Bonnet, R., Cheek, G.A. (FCCP)., Dunbar, R.D., Moyers, M. and Slater, J.M., *Proton-beam radiotherapy for early-stage lung cancer,* Chest. 116 1313-1319, 1999.
2. Shioyama, Y., Tokuuye, K., Okumura, T., Kagei, K., Sugahara, S., Ohara, K., Akine, Y., Ishikawa, S., Satoh, H., Sekizawa, K., *Clinical evaluation of proton radiotherapy for non-small-cell lung cancer* , Int J Radiat Oncol Biol Phys. 56 7-13, 2003.
3. Bjelkengren, G. and Glimelius, B., *The potential of proton beam radiation therapy in lung cancer (including mesothelioma)*, Acta Oncol. 44 881-883, 2005.
4. Vedam, S.S., Keall, P. J., Kini, V. R., Mostafavi, H., Shukla, H. P. and. Mohan, R., *Acquiring a four-dimensional computed tomography data set using an external respiratory signal*, Phys. Med. Biol. 48 45–62 , 2003.
5. Keall, P.J., Starkschall, G., Shukla, H., Forster, K. M., Ortiz, V., Stevens, C.W., Vedam, S.S., George, R., Guerrero, T. and Mohan, R., *Acquiring 4D thoracic CT scans using a multislice helical method*, Phys. Med. Biol. 49 2053–2067, 2004.
6. Pan, T., Lee, T.Y., Rietzel, E. and Chen, G.T., *4D-CT imaging of a volume influenced by respiratory motion on multi-slice CT*, Med. Phys. 31 333–340, 2004.
7. ICRU Report 62, *Prescribing, Recording and Reporting Photon Beam Therapy (*Supplement to ICRU Report 50), 1999.
8. Rietzel, E., Chen, G.T., Choi, N.C. and Willet, C.G., *Four-dimensional image-based treatment planning: Target volume segmentation and dose calculation in the presence of respiratory motion.* Int J Radiat Oncol Biol Phys. 61 1535-1550, 2005.
9. Keall, P.J., Mageras, G.S., Balter, J.M., *et al, The management of respiratory motion in radiation oncology report of AAPM Task Group 76.* Med Phys. 33 3874-3900, 2006.
10. Wolthaus, J.W., Schneider, C., Sonke, J.J., van Herk, M., Belderbos, J.S., Rossi, M.M., Lebesque, J.V. and Damen, E.M., *Mid-ventilation CT scan construction from four-dimensional respiration-correlated CT scans for radiotherapy planning of lung cancer patients* ,Int. J. Radiat. Oncol. Biol. Phys. 65 1560-1571, 2006.
11. Underberg, R.W., Lagerwaard, F.J., Slotman, B.J., Cuijpers, J. P. and Senan, S.,*Use of maximum intensity projections (MIP) for target volume generation in 4DCT scans for lung cancer* Int. J. Radiat. Oncol. Biol. Phys. 63 253-260, 2005.
12. Marnitz, S. et al, *Intraindividual comparison of conventional three-dimensional radiotherapy and intensity modulated radiotherapy in the therapy of locally advanced non-small cell lung cancer a planning study* Strahlenther. Onkol. 178 651–8, 2002.

RADIOTHERAPY TALKS

DOSE INVESTIGATION OF THE MAMMOSITE APPLICATOR USING MONTE CARLO METHOD

S.Bensaleh[1, 2, 3], E. Bezak[2, 3] and M. Borg[4]

[1]*Renewable Energy and Water Desalination Research Centre, Liby*
[2]*Department of Medical Physics, Royal Adelaide Hospital, Adelaide, Australia*
[z]*School of Chemistry & Physics, University of Adelaide, Adelaide, Australia*
[4]*Department of Radiation Oncology, Royal Adelaide Hospital, Adelaide, Australia*

INTRODUCTION: Brachytherapy technique for treatment of early stage breast cancer following lumpectomy uses the MammoSite applicator (MSA; Proxima Therapeutics, Marlborough, MA, USA), delivering 34 Gy in 10 fractions (3.4 Gy/fraction twice daily) at 1 cm from the balloon surface with minimum of 6 hours between fractions on the same day (Edmundson *et al.* 2002). There are several sources of uncertainties in MammoSite brachytherapy and their effect needs to be investigated. For example, the brachytherapy planning system does not account for the inhomogeneities in the dose calculation. There also could be variations in balloon shape, size, contrast densities and air cavities. This is important when the balloon is in close proximity to the normal tissues such as the lung and the heart. The purpose of this study is to set up Monte Carlo EGS4 code to simulate MammoSite treatment uncertainties. During this process the following was investigated: (1) the effect of different voxel sizes on variation in dose distribution, (2) import of Computed Tomography (CT) images obtained following the balloon placement of an actual patient to the EGS4 code to assess the dose to normal tissues.

METHODS: The ^{192}Ir source was approximated as an isotropical parallelepiped source. The previously published γ-ray energy spectrum for ^{192}Ir source was used in simulations (Borg *et al.* 1999). A water phantom of 10 x 10 x 10 cm^3 was set up. The source was positioned in the middle of the phantom. Dose distributions in the phantom were computed for voxel sizes ranging from 1 x 1 x 1 to 5 x 5 x 5 mm^3. Three dimensional CT patient data were extracted from Pinnacle^3 TPS and imported to the EGS4 code. The brachytherapy source was positioned in the middle of the balloon and the densities of anatomical structures and balloon contrast were defined according to CT numbers. Calculation has been completed successfully using imported patient CT data.

RESULTS & DISCUSSION: Based on this investigation, the results have showed that 1.5 mm^3 is the suitable voxel size as reducing the voxel any further will increase calculation time without improving accuracy of dose distribution as shown in figure 1.

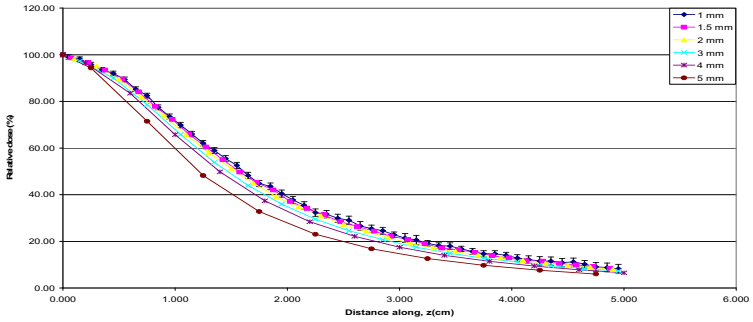

Figure 1. *Dose fall off along the source axis for different voxel sizes.*

CONCLUSIONS: Our preliminary results of importing CT images to EGS4 suggest that this code may be used to assess accurately dose distribution for MammoSite brachytherapy. In the future, we will modify several parameters in the EGS4 code to assess the effect of individual uncertainties on dose distributions.

REFERENCES:

[1]*Borg J and Rogers D W (1999). "Spectra and air-kerma strength for encapsulated 192Ir sources." Med Phys 26(11): 2441-4.*
[2]*Edmundson G K, Vicini F A, et al. (2002). "Dosimetric characteristics of the MammoSite RTS, a new breast brachytherapy applicator." Int J Radiat Oncol Biol Phys 52(4): 1132-9.*

AN ECONOMICAL AND RELIABLE METHOD FOR AUTOMATED QUANTITATIVE ANALYSIS OF *IN VITRO* CELL COLONIES

J. Bewes[1,2], N. Suchowerska[1,2], M. Zhang[2], E. Claridge[2] and D. McKenzie[1]

[1]*School of Physics, University of Sydney, Australia*
[2]*Department of Radiation Oncology, Royal Prince Alfred Hospital, Camperdown, Australia*

INTRODUCTION: Clonogenic assays are widely used in cancer research to investigate the effect of radiation, mutagens, carcinogens and chemotherapeutic agents on cellular proliferation. Manual counting of colonies is the standard procedure in evaluating clonogenic survival, however this is a lengthy task and subject to inter-experimenter bias. Automated colony-counters eliminate subjectivity across experimenters and have the potential to significantly increase the speed of the counting process.

Automated solutions to colony counting are commercially available, but have limited flexibility and are expensive, with prices beginning at US$30000. To make studies using clonogenic assays more accessible, we have developed a low-cost, robust and accurate method of automatic colony counting and analysis.

METHODS: Prior to scanning, stained flasks were filled with talcum powder to improve image contrast and reduce reflection artefacts. Scanning was performed using a typical office scanner set at a resolution of 200 dots per inch. Three flask types and three cell lines of varying morphology, cell size and plating density were examined for validation purposes.

Software capable of analysing scanned images of flasks and Petri dishes was developed. Identification of viable colonies was achieved through the use of the Hough algorithm and basic image-processing techniques. To distinguish between viable and non-viable colonies, the user was required to input a minimum colony size.

RESULTS: The accuracy of the software was tested by comparing the colony count using the automatic system with traditional manual count. Colony counts generated by the program demonstrated good correlation with manual counts ($r \sim 0.95$). Additional parameters returned by the program included average colony area, nearest neighbour distance and spatial distribution.

DISCUSSION & CONCLUSIONS: The software provides clonogenic assay analysis comparable in accuracy to commercially available automated systems, but at a fraction of the cost. The minimalist assumptions concerning colony form allow the software to successfully analyse a wide range of cell and flask types. Furthermore, the ability of the software to generate spatial and qualitative information describing the detected colonies provides the user with more in-depth tools for analysis.

FERROUS-XYLENOL ORANGE GELS: REPRODUCIBILITY, ACCURACY, STABILITY AND TIME DEPENDENCE FOR 3D OPTICAL CT SCANNING

M. Bhat[1,2]

[1]*Department of Physics and Engineering, Adelaide Radiotherapy Centre, Adelaide South Australia, Australia*
[2]*School of Chemistry and Physics, University of Adelaide, South Australia*

INTRODUCTION: Fricke gel is a non-toxic, cheap, and easy to prepare dosimeter for full three-dimensional radiation dosimetry using an optical tomographic method[1]. It has been reported that preparation method, concentration of gel constituents, storage condition affects its response to radiation. Aim of this report is to determine the dose response characteristics of ferrous-xylenol orange-gelatin with preparation method, concentration of gel constituents and storage conditions.

METHODS: Gel samples were prepared by mixing stock solutions of Bezoic acid, sulphuric acid (Merck) and xylenol orange (Aldrich) into 25 mM sulphuric acid and a 40°C solution of gelatin (4% by mass 300 bloom, porcine, Sigma). To this mixture 0.1 mM ferrous ammonium sulphate (Aldrich) is added and stirred well to obtain final gel. Concentrations were varied slightly in other batches and their response to radiation was studied. Freshly prepared gel was poured in cuvettes and immediately placed in dark at 4°C refrigerator for 24 hours for optical attenuation measurement. Irradiation of gel in 1 cm cuvettes was done in a 6 MV Varian linear accelerator with dose ranging from 0.5Gy to 6 Gy. Optical density was measured in a Varian Carry 300 UV-Vis spectrometer at 543 nm wave length. Time dependence characteristics and effect of changing the sulphuric acid concentration from 25mM to 50 mM were also tested. Measurements were made to characterise the gel dosimeter in terms of reproducibility, accuracy, diffusion rate and sensitivity to radiation dose.

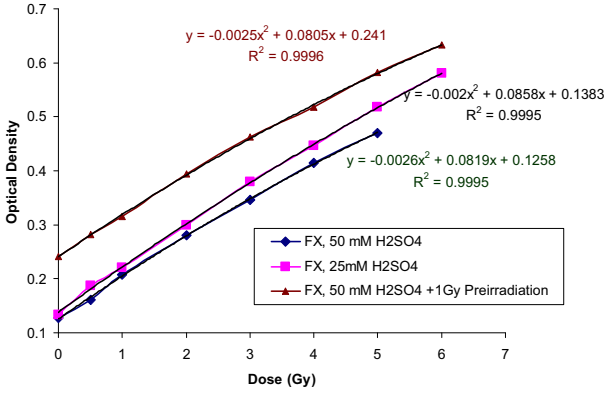

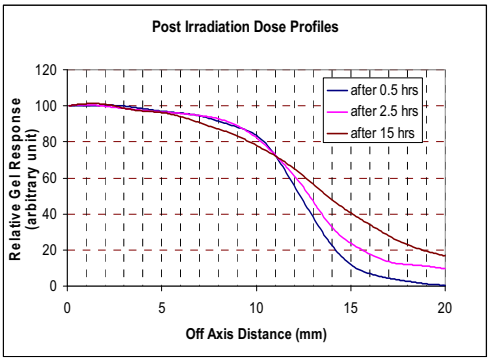

RESULTS: The rate of change of optical density was 4×10^{-4}/hr for an FXG gel stored in dark at 4°C. Sensitivity of gel FXG gel with 25 mM sulphuric acid was 0.085 OD/Gy and with 50 mM it was 0.080 OD/Gy. The change in optical density of gel with radiation dose had a general shape of second order polynomial. The post irradiation measurement showed that the full width half maximum (FWHM) of dose profile increased by 1 mm and 4 mm after 2.5 and 15 hours respectively when compared to 0.5 hrs post irradiation measurement.

DISCUSSION & CONCLUSIONS: The dose response curve of the gel dosimeter is not strictly a straight line but follows a second order polynomial shape. Applying this nonlinear response curve in optical density measurements will improve 3D dose map accuracy. Diffusion of Fe^3 is a known problem in Fricke gel dosimetry. But the measurement made within 30 minutes of irradiation will have negligible effect of Fe^3 ion diffusion.

REFERENCES:

[1] *T. van Doorn, M. Bhat, T. P. Rutten, T. Tran, and A. Costanzo, (2005) Austral Eng Phys Bio Med 28, 76-85.*

OPTIMIZED RADIOTHERAPY DOSIMETRY WITH RADIOCHROMIC FILM

Martin J Butson[1,2,3], Tsang Cheung[1] and Peter K. N. Yu[1]

[1] *City University of Hong Kong , Dept. of Physics and Materials Science, Kowloon Tong, Hong Kong*
[2] *Illawarra Cancer Care Centre, Department of Medical Physics, Crown St, Wollongong, Australia*
[3] *Centre for Medical Radiation Physics, University of Wollongong, Wollongong, Australia*

INTRODUCTION: Gafchromic EBT film has created a new wave of excitement in radiotherapy radiation dosimetry due to its optimized characteristics specifically suited for high energy x –ray dosimetry.

METHODS: Dosimetry qualities such as energy dependence, dose response, scanner properties and 2 dimensional dosimetry have been studied.

RESULTS: Qualities such as low energy dependence, high spatial resolution and ease of use and handling make it close to ideal for radiation dosimetry. This paper highlights some commonly encountered dosimetric characteristics and problems associated with EBT Gafchromic film radiation dosimetry and examines ways to improve your dosimetry accuracy. Some clinical useful measurements and results are also reports such as surface dose and low energy isodose verification.

DISCUSSION AND CONCLUSION: EBT Gafchromic film has made a significant mark in radiation dosimetry for radiotherapy applications with many characteristics close to ideally suited for such applications. As the film is now relatively cheap, accurate film dosimetry can be performed without the need of a processor or strict light conditions. The film can also be used in solid or water phantoms.

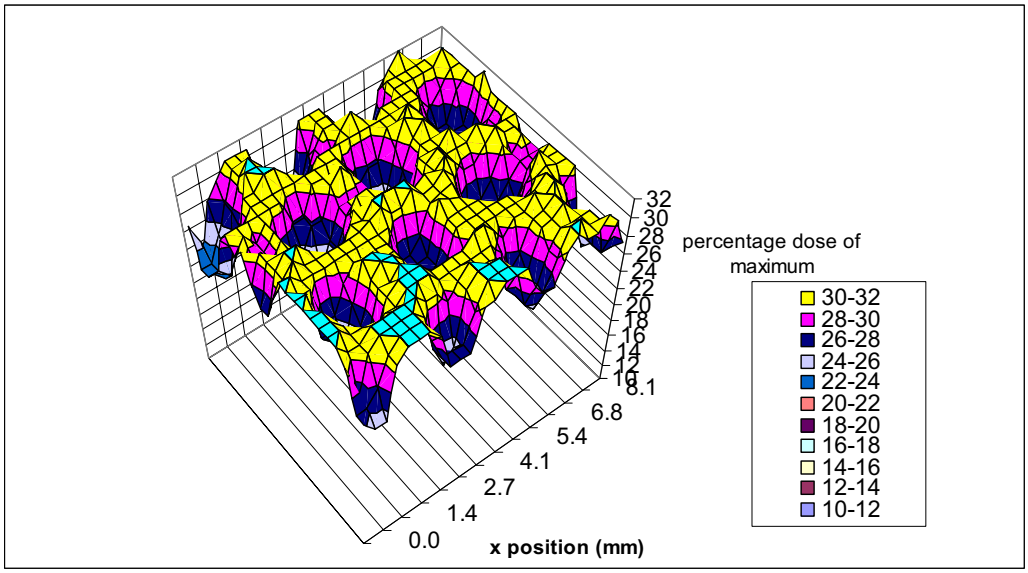

COMMISSIONING IMRT PHANTOMS: A STREAMLINED APPROACH

A. Chapman[1], R. Gupta[1] and P. Metcalfe[2]

[1] *St George Cancer Care Centre, St George Hospital, Kogarah, Australia*
[2] *Centre for Medical Radiation Physics, University of Wollongong, Australia*

INTRODUCTION: Intensity Modulated Radiation Therapy (IMRT) is a proven technique for providing conformal dose to targets while sparing normal tissue. The St George Cancer Care Centre (STGCCC) plans to implement IMRT in the near future, intending to concentrate on providing prostate treatments. In anticipation of this a dedicated IMRT plan-check phantom was purchased (CIRS Model 002H9K).
Initial work has previously been done at the Illawarra Cancer Care Centre (ICCC) on the use of a basic cubic phantom made up of RMI Solid Water slabs for dosimetric verification of IMRT[1]. Since then a more elegant IMRT phantom (I'mRT Phantom, Scanditronix-Wellhofer GmBH) has been adopted at ICCC[2].

METHODS: Using experience gained at ICCC and current work at STGCCC a generic commissioning process was developed that may be applied to any phantom and chamber intended for use in IMRT plan checking.
The procedure is an adaptation of testing for a standard phantom that takes into account the special features of an IMRT treatment; the most notable of these is that IMRT may involve much smaller field sizes and lower dose deliveries per segment than a conventional treatment. Testing includes:

- Verifying the physical aspects of the phantom characteristics.
- Scanning the phantom as a 'patient' into the planning system for use in all future plans.
- Establishing linearity of response to:
- Field size, down to very small field sizes (0.5 cm x 0.5 cm).
- Dose, down to very small doses delivered (1 monitor unit).
- Establishing a calibration standard, where a known dose may be delivered to the phantom in order to calibrate the chamber response for use in relative dose measurements.
- Checking the chamber response against a variety of simple plans.
- Checking the chamber response against a variety of complex plans, as the phantom is intended to be used.
- Establishing a straightforward protocol for using the phantom for future IMRT plan checking.

RESULTS: The CIRS phantom was calibrated against known dose measurements in water. Dose checks were evaluated against manual planning data and computerised planning calculations.

DISCUSSION & CONCLUSIONS: A successful IMRT phantom commissioning process has been developed and recommendations will be reported.

REFERENCES:
[1]*A. Chapman (2005) Dosimetric Verification of IMRT, MSc Thesis, University of Wollongong.*
[2]*M. Currie, M. Williams and P. Metcalfe (2007) IMRT QA at the ICCC, EPSM-Abstract 2007.*

LINEAR ACCELERATOR QUALITY ASSURANCE WITH AN a-Si EPID

L.Clews[1,2] and P.B.Greer[1,3]

[1]*Department of Radiation Oncology, Calvary Mater Newcastle, Newcastle, Australia*
[2]*School of Applied Sciences, RMIT University, Melbourne, Australia*
[3]*School of Mathematics and Physical Sciences, University of Newcastle, Australia*

INTRODUCTION: This work investigates the use of amorphous silicon electronic portal imaging devices (EPIDs) for regular dosimetric quality assurance of linear accelerator beams.

METHODS: An EPID-based quality assurance procedure has been developed that acquires images for all monthly dosimetric and mechanical quality assurance tests through the accelerator record and verify system. These data include EPID dose response, beam profile constancy, enhanced dynamic wedge profile[1], pixel sensitivity matrix (PSM) stability[2], asymmetric jaw matchlines, radiation/light field coincidence, and dynamic MLC positioning. Data acquisition requires approximately 15 minutes. Software modules were developed to assess the dosimetric EPID results. Data was acquired using this procedure for both 6 and 18 MV beams for two accelerators over a 15 month time interval. Data has also recently started being collected on two new accelerators that will allow monitoring of long term stability of the PSM. The long-term stability of the EPID central axis pixel location, collimator positioning and relative beam profile response has been investigated.

RESULTS: The central axis pixel location was determined to sub-pixel accuracy using the jaw positions found by linearly interpolating EPID measured penumbra for 2 images acquired at 180 degrees. This method was shown to be independent of field size and yielded CAX position results that varied by 0.5% over a 15 month period. Highly accurate recordings of jaw positions were then determined with the EPID allowing precise knowledge of the variation and errors in jaw positioning. The variation in the measured field size of a 20x20 cm^2 field over a 15 month period was a maximum 0.1% standard deviation for both 6MV and 18MV. The deviations in flatness and symmetry of both energies had maximums of 0.7% and 1.0% standard deviations, respectively.

CONCLUSIONS: Due to the reproducibility of the EPID measurements and the rapid setup and data acquisition time, the device is highly suited to regular linear accelerator quality assurance measurements. Pixel sensitivity corrections that allow

direct measurement of beam profile are currently being developed as an alternative method for EPID QA measurement. All monthly dosimetric QA measurements are now performed at our centre with a-Si EPIDs on four linacs.

REFERENCES:
[1]*Greer PB and Barnes M, Investigation of an amorphous silicon EPID for measurement and quality assurance of enhanced dynamic wedge, Phys. Med. Biol., 52:1075-1087, 2007.*
[2]*Greer PB, Correction of pixel sensitivity variation and off-axis response for amorphous silicon EPID dosimetry. Med. Phys., 32:3558-3568, 2005.*

CALCULATING THREE DIMENSIONAL DOSE DISTRIBUTIONS FOR SUPERFICIAL PHOTON TREATMENTS

B. Currie

Medical Physics, Wellington Blood & Cancer Centre, Wellington Hospital, Wellington, New Zealand
Physics & Astronomy Department, University of Canterbury, Christchurch, New Zealand

INTRODUCTION: Providing accurate and appropriate dosimetric information for clinicians to base treatment decisions upon is one of the important roles of radiation oncology medical physicists. The availability and quality of dosimetric information for patients undergoing treatment on superficial x-ray machines can be improved to the point where 3 dimensional dose distributions can be made available for comparison and optimisation purposes. There are a number of issues surrounding the introduction of this information into superficial photon treatments; including but not limited to the availability of computer facilities and CT or MRI scanners for superficial treatment planning purposes. This paper focuses on the fundamental issue of actual dose determination utilising the Monte Carlo method.

METHODS: The simulation of a Comet MXR-161 x-ray tube on a Pantak Therapax SXT150 was done under the EGSnrc system of codes[1]. Specifically BEAMnrc was used to construct a virtual x-ray tube and generate a computer file detailing the energy, direction and type of particles exiting the front face of the x-ray tube for millions of particles. From this file DOSXYZnrc was used to generate dose distributions in both water phantoms and phantoms representative of patient treatments. The water phantom simulations were compared against PTW MP3 water phantom scans using a PTW Pinpoint chamber. The Washington University in St. Louis MATLAB application CERR (Computational Environment for Radiotherapy Research) was used to analyse the Monte Carlo generated dose distributions on CT based DICOM-RT plans exported from the Varian Eclipse treatment planning system.

RESULTS:.A series of profiles and depth dose curves were generated for 80kV and 100kV Pantak Therapax SXT150 beams for applicator sizes of 1, 3 and 5 cm. These compared favourably against empirically determined profiles and depth dose curves from the PTW MP3 water phantom scans; this is based upon Björk *et al*.[2] who give a stipulation of ±2mm in high dose gradient regions and ±2% in low dose gradient areas. From this it was assumed that the simulation represented the photon beam well and was then used to generate dose distributions in three clinical cases: ear, lateral nose and medial canthus. Each of these sites was chosen for comparison with and without bolus and/or lead shielding present in the field.

DISCUSSION & CONCLUSIONS: The ability to be able to visualise 3 dimensional dose distributions for superficial photon treatments provides the ability to compare and optimise superficial treatment plans. This can also be extended to allow a comparison between any radiotherapy modality provided that sufficient information is available to be able to simulate the output of the device. This has been done by the author for 6 and 9 MeV electron beams from a Varian Clinac 2100C linear accelerator. The qualitative features of the dose distributions will be compared.

REFERENCES:
[1]*Kawrakow, I. and Rogers, D. W. O. (2003), The EGSnrc Code System: Monte Carlo Simulation of Electron and Photon Transport, NRCC Report PIRS-701 (Available on-line via: http://www.irs.inms.nrc.ca/inms/irs/EGSnrc/EGSnrc.html)*
[2]*Björk et al. (2002) influence of initial electron beam characteristics on Monte Carlo calculated absorbed dose distributions for linear accelerator electron beams. Phys. Med. Biol., 47:4019-4041*

IMRT QA AT THE ILLAWARRA CANCER CARE CENTRE

M. Currie[1], M. Williams[1] and P. Metcalfe[2]

[1]*Illawarra Cancer Care Centre, Wollongong Hospital, Wollongong, Australia*
[2]*Centre for Medical Radiation Physics, University of Wollongong, Wollongong, Australia*

INTRODUCTION: Intensity Modulated Radiation Therapy (IMRT) has the potential to conform dose to complex target structures as well as sparing normal tissue. The complexity of the technique requires additional verification steps to ensure that the treatments are planned, transferred and delivered correctly. IMRT was introduced at the Illawarra Cancer Care Centre (ICCC) in 2002. Since that time over 70 head-and-neck cases have been treated. An overview of the current IMRT QA program at the ICCC and a summary of QA results for the last 5 years will be presented.

METHODS: All treatment plans at the ICCC are checked by physics staff. IMRT plans have additional checks of ROIs, an on-screen plan review and phantom based dosimetry checks. The IMRT plan, generated on the Pinnacle RTPS (Philips Radiation Oncology Systems, Milpitas, CA), is reproduced on a phantom CT dataset (I'mRT Phantom, Scanditronix-Wellhofer GmBH) and delivered on a Varian 21EX linear accelerator (Varian Medical Systems, Palo Alto, CA). A point dose is measured with a 0.13 cc ionisation chamber and an axial 2D dose distribution measured with film. An independent monitor unit check is performed with RadCalc (Lifeline Software Inc.).

RESULTS: For all IMRT plans, the average percentage difference between the predicted and measured dose per plan was 0.2% with a standard deviation of 1.7%. Of the 32 plans checked with RadCalc, the average percentage difference between RadCalc and Pinnacle per plan was 1.1% with a standard deviation of 1.1%.

DISCUSSION & CONCLUSIONS: RadCalc was found to be accurate enough for routine use in IMRT treatment plan QA, however verification of the delivered dose still has to be performed to confirm that the plan has been transferred and delivered correctly.

RADIOBIOLOGICAL MODEL COMPARISON OF 3D CONFORMAL RADIOTHERAPY AND IMRT PLANS FOR THE TREATMENT OF PROSTATE CANCER

P. K. Deb[1] and A. Fielding[1]

[1]*School of Physical and Chemical Sciences, Queensland University of Technology, Australia*

INTRODUCTION: The main aim of radiotherapy is to deliver a dose of radiation that is high enough to destroy the tumour cells while at the same time minimising the damage to normal healthy tissues. Clinically, this has been achieved by assigning a prescription dose to the tumour volume and a set of dose constraints on critical structures. Once an optimal treatment plan has been achieved the dosimetry is assessed using the physical parameters of dose and volume. There has recently been an interest in using radiobiological parameters to evaluate and predict the outcome of a treatment plan in terms of both a tumour control probability (TCP) and a normal tissue complication probability (NTCP). In this study, a radiobiological model has been used to compare a three dimensional conformal radiotherapy treatment (3D-CRT) and an intensity modulated radiotherapy (IMRT) of the prostate. There has been some debate in the literature about the value of α/β ratio that should be used to model the response of a prostate tumour to radiation. We investigate the sensitivity of the model to the α/β ratio used for the prostate and also the sensitivity of the model to inter-observer variability at the planning stage.

METHODS: Two 3D-CRT treatment plans (one with 4 fields, another with 5 fields) and an IMRT treatment plan were developed for a case of prostate cancer. Pinnacle[3] Planning (Pinnacle v7.6c, Philips Medical Systems, USA) systems were used to plan and evaluate the radiobiological probabilities. Initially both 3D-CRT and IMRT were planned for 2 Gy per fraction to a total dose of 60 Gy to prostate. The prescription dose was gradually increased to investigate the sensitivity of NTCP and TCP to dose escalation. The biological responses were calculated using the Källman S-model [1]. The complication free tumour control probability (P+) is generated from the combined NTCP and TCP response values [2]. Several choices of α/β were investigated for prostate tumour [3].

RESULTS: Table 1 lists the salient biological responses for the three different treatment plans.

ROI	Organ/ Tumour	TCP			NTCP			P+		
		3D-CRT 4Fields	3D-CRT 5Fields	IMRT 5Fields	3D-CRT 4Fields	3D-CRT 5Fields	IMRT 5Fields	3D-CRT 4Fields	3D-CRT 5Fields	IMRT 5Fields
Prostate	Prostate	0.867	0.871	0.883				0.837	0.846	0.86
Rectum	Rectum				0.03	0.024	0.022			
Bladder	Bladder				0	0	0			
RtF/Head	Femur				0	0	0			
LtF/Head	Femur				0	0	0			
Composites					0.03	0.024	0.022			

Table 1. *Biological responses for the different treatment plans.*

The biological responses above are for a total prescription dose of 60 Gy (in 2 Gy fractions) to the prostate. When the dose is increased, both the TCP and NTCP increased gradually as expected.

DISCUSSION & CONCLUSIONS: P+ was higher for the IMRT plans than for the 3D-CRT plans. It supports the hypothesis that accurately delivered IMRT for prostate carcinoma reduces the complication rate among the organs at risks while increasing the tumour control probability compared to standardized 3D-CRT.

REFERENCES:

[1]*P. Källman, A. Ågren, and A. Brahme, (1992) Int. J. Radiat. Oncol., Biol., Phys. 62:249-262.*
[2]*A. K. Ågren, A. Brahme, and I. Turesson, (1990) Int. J. Radiat. Oncol., Biol., Phys. 19:1077-1085.*
[3]*J. Fowler, R. Chappell, and M. Ritter, (2001) Int. J. Radiat. Oncol., Biol., Phys. 50:1021-1031.*

MC MODELING OF STEREOTACTIC RADIOTHERAPY SYSTEM FOR SMALL LUNG TUMORS

H.M. Deloar[1], E Kunieda[2], Y Oku[2], T Kawase[2], J Griffin[1] and D McKay[1]

[1]*Medical Physics and Bioengineering Department, Christchurch Hospital, New Zealand*
[2]*Department of Radiology, Keio University, Tokyo, Japan*

INTRODUCTION: A stereotactic radiotherapy (SRT) system for small lung tumors uses different cylindrical collimators depending in the size of the tumor. One important criteria of SRT is that the dose distribution conforms to the target shape and falls-off rapidly outside the target volume. The choice of energy may be important for small lung tumours as it is likely the dose distribution will vary with energy due to differences in lateral electronic disequilibrium.

METHODS: In this study using Monte Carlo methods [1-2], we have modelled 4 different cylindrical collimators, 5mm, 10mm, 20mm and 30mm, at 3 energies, 6, 10 and 18 MV, to investigate the dependency of dose distributions on energy for small lung tumours. The model was validated using measured profile and PDD data for a standard 10cm × 10cm field at 6, 10 and 18 MV. The stereotactic collimators were validated using only 6MV PDD and profiles data.

RESULTS: Simulated data of profiles and PDD for a standard 10cm × 10cm field, at a range of energies were well matched to the experimental data showing that the standard treatment head of the Varian linear accelerator had been accurately modelled. The simulated PDDs and profiles for stereotactic field at 6MV, obtained by adapting this model for the stereotactic collimators, were also in good agreement with the measured data.

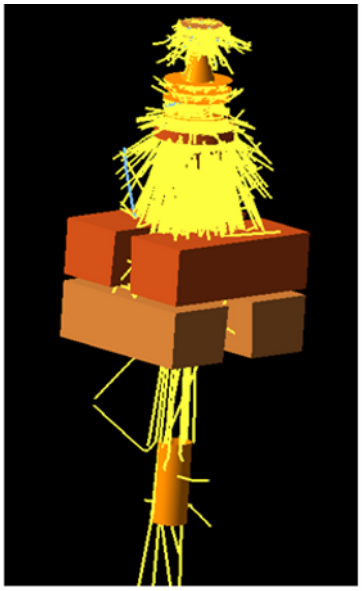

Figure: Display of 6MV MC linac with a stereotactic collimator

DISCUSSION & CONCLUSIONS: Monte Carlo modelling of beams used in stereotactic radiotherapy agreed well with measured data. Ongoing work will use the Monte Carlo data to investigate the effect of energy on lateral electronic disequilibrium and dose conformity for small lung tumours.

ACKNOWLEDGEMENT: This work would not have been possible without the cooperation of Varian Oncology Systems in providing details of head design of the linear accelerator.

REFERENCES:

[1]*D. W. O. Rogers, B. A. Faddegon, G. X. Ding, C.-M. Ma, J. Wei, and T. R. Mackie. BEAM: A Monte Carlo code to simulate radiotherapy treatment units.* Med. Phys., *22:503 - 524, 1995.*
[2]*Nelson WR, Hirayama H, and Rogers DWO. 1985 The EGS4 Code System, Report SLAC-265, Stanford Linear Accel. Center, Stanford, California.*

EVOLUTION AND ADVANCEMENT OF TEAP IN NSW

L. Duggan[1,2]

[1]*Calvary Mater Newcastle, Newcastle, Australia*
[2]*School of Mathematical & Physical Sciences, University of Newcastle, Australia*

OVERVIEW: The implementation of a structured, competency based Teaching, Education and Accreditation Program (TEAP) in Radiation Oncology Medical Physics commenced in 2003 in New Zealand, followed by the public sector in NSW (2004), Victoria, SA and ACT, and the private sector in QLD and SA. From 1st January 2006 all new Trainees must enrol in TEAP. In 2007, the Department of Health and Aging (DHA) has provided funding to ACPSEM for 2.5 full time equivalent (FTE) positions to manage TEAP on a national level (i.e. a Developer, Coordinator and Administrator).

In 2007, the number of NSW TEAP Trainee positions increased to 36.5FTE (24.5FTE supernumerary and 12 permanent positions). To maintain a commitment to TEAP, Trainees in permanent positions are either on one year renewable contacts and/or the requirement is included in their Conditions of Employment.

Due to the numbers of NSW Trainees, the enthusiasm of TEAP participants and the significant financial support from DHA and NSW Health, NSW has continued to play a pivotal role in the evolution and advancement of TEAP. The NSW-Health funded Clinical Placement Coordinator (CPC) provides an independent and anonymous feedback loop for TEAP participants and has the unique perspective of overseeing the TEAP infrastructure across 10 Radiation Oncology Treatment Centres.

Funding provided by NSW Health continues to support training infrastructure development, including the development of training material, an annual workshop for Clinical Supervisors, facilitation of Training Days, attendance of Trainees at the Basic Sciences of Oncology course and external competency tests.

Recently there has been a change in focus in training documentation in NSW.

- Logbooks have evolved from a chronological record of training/clinical activities to the concept of recording activities under individual competencies for validating the competency assessment process. Workbooks are still in use.
- Portfolio reports are now being reviewed externally. The 2007 TEAP Supervisors' workshop identified the need for a criterion referenced assessment structure for portfolio reports to ensure the expectations are understood by the Trainee and Supervisor, and the assessment structure is transparent and robust. Portfolios will be the focus of the 2008 TEAP workshop.
- Competency checklists based on the TEAP Knowledge and Competencies Document are still being utilised however it has been proposed to transfer to the RCA Clinical Training Guide (financially supported by the IAEA) as it provides suggestions for methods of training and a criterion referenced assessment matrix, flexible to be utilised by developing and developed countries alike. A working party will be compiling a proposal to the ACPSEM Professional Standards Board and Radiation Oncology Accreditation Panel. A criteria for competency assessment was developed at the 2006 TEAP Supervisors' workshop.
- Annual training plans are evolving from a general overview of training activities to include a detailed timeline for addressing competencies and assessment deadlines to ensure progress.
- As Trainees prepare for and commence their examination process, there is a need for external practical and oral assessment.
- Nuclear Medicine and Radiology rotations requirements are being met by self study utilising external resource material, opportunistic day visits and Radiation Oncology-based activities.

CONCLUSIONS: TEAP is evolving based on the needs and feedback of TEAP participants, the desire for more transparent and robust competency assessment methods, and limitations of the available manpower of other Medical Physics Specialities. The advancement of TEAP will be driven by an external review of TEAP, collaboration with the IAEA and the National TEAP "managers" who will provide a vital feedback loop and networking infrastructure for TEAP participants and Coordinators across Australasia.

AUSTRALASIAN BRACHYTHERAPY DOSIMETRY AUDIT

L. Duggan[1,2], A. Haworth[3,4], M. Ebert[5,6], G. Duchesne[3], D. Joseph[5], J. Bucci[7] and T. Kron [3,4]

[1]*Calvary Mater Newcastle, Newcastle, Australia*
[2]*School of Mathematical & Physical Sciences, University of Newcastle, Australia*
[3]*Dept. Physical Sciences, Peter MacCallum Cancer Centre, Melbourne, Australia*
[4]*School of Applied Sciences, RMIT University, Melbourne, Australia*
[5]*Dept. Radiation Oncology, Sir Charles Gairdner Hospital, Perth, Australia*
[6]*School of Physics, University of Western Australia, Australia*
[7]*St George Cancer Care Centre, Kogarah, Australia*

INTRODUCTION: Brachytherapy is a versatile modality for treating cancer patients. Due to the source location and inverse square law, it delivers higher doses of radiation, more accurately, limiting dose to critical structures and treats sites previously inaccessible. However, in the absence of a computerised record and verify system and, if appropriate quality assurance is not in place, this technology may do more harm than good. In particular, there is in increasing risk with the implementation of image guided brachytherapy where the treatment is planned and delivered in one theatre session. International studies[1,2] have demonstrated that a well organised audit process can identify geometric and dosimetric errors that may significantly impact on clinical outcomes. Based on experience gathered in level I, II and III dosimetric audits for external beam radiotherapy and increased likelihood and impact of a deviation from the intended treatment, it appears now necessary to develop also a national brachytherapy audit to verify accuracy of treatment delivery.

METHODS: The audit process will involve a two step process. A Level I dosimetry audit, using a standard thimble chamber calibrated with a unique Ir-192 primary standard, will verify absolute source calibration. A level III dosimetry audit is then proposed that will verify the entire treatment planning/treatment delivery chain. TLDs will be placed throughout the target volume and organs at risk (OAR) of an anthropomorphic prostate phantom and treatment planned and delivered for a range of techniques and equipment available in Australasian prostate brachytherapy services.

RESULTS: The NSW Cancer Institute recently sponsored a workshop to discuss the need for a national centre for clinical dosimetry. The workshop was attended by representatives from public and private hospitals, professional organisations, government bodies and standards laboratories as well as a consumer representative. There was unanimous support for the concept of a national dosimetry audit service and it was noted that brachytherapy was an area of most urgent attention due to the handling of radioactive material and the relatively higher likelihood for accidents. A small working group is developing a formal proposal that will seek appropriate funding. It is therefore timely for the ACPSEM to consider supporting this concept that will address the need for a brachytherapy audit.

Industry partners and local hospitals are supporting the Level I audit by providing equipment and finance for the calibration factor. St George Hospital and Calvary Mater Newcastle are collaborating to determine the most appropriate detector to use

in the Level III audit, comparing such factors as reproducibility, resilience, energy response and dose response.

DISCUSSION & CONCLUSIONS: International studies have demonstrated that geometric and dosimetric audits can identify errors that can impact on clinical outcomes. Australasia has not yet had the opportunity to participate in a brachytherapy audit and until this happens we are unable to verify that all centres that have introduced complex treatment techniques are able to provide high quality, accurate brachytherapy treatments.

REFERENCES:

[1]*Roue A, Ferreira I, van Dam J et al The EQUAL-ESTRO audit on geometric reconstruction techniques in brachytherapy Radiother Oncol 78(1);78-83 2006*

[2]*Roue A, Venselaar J, Ferreira I et al. Development of a TLD mailed system for remote dosimetry audit for 192 Ir HDR and PDR sources. In press*

PROGRESS ON SUPPORT FOR COLLECTION AND ANALYSIS OF ELECTRONIC TREATMENT PLANNING DATA IN RADIOTHERAPY CLINICAL TRIALS

M.A. Ebert[1,2], A. Haworth[3,4], B. Hooton[1], R. Kearvell[1], R. Coleman[1], N. Spry[1], S. Bydder[1] and D. Joseph[1]

[1]*Department of Radiation Oncology, Sir Charles Gairdner Hospital, Australia*
[2]*School of Physics, University of Western Australia, Australia*
[3]*Department of Physical Sciences, Peter MacCallum Cancer Centre, Australia*
[4]*School of Applied Sciences, Royal Melbourne Institute of Technology, Australia*

INTRODUCTION: In radiotherapy, trials frequently involve treatment approaches and protocols of considerable technical complexity. It has been recognised that increases in this complexity are placing extra demands upon quality-assurance (QA) requirements for trials, and have increased the number of correlates that can be examined relating treatment technique to clinical outcome. A lack of QA of complex 3D treatment planning data during a trial will lead to concealment of the correlations being investigated. SWAN has been developed to address this issue for Australasian trials. Progress on the development, application and validation of the system is described.

METHODS & RESULTS: SWAN has been used for QA of all patient planning data for the TROG 03.04 'RADAR' trial since 2003. Other then the display of axial, coronal and sagital image reconstructions with isodoses and structures displayed, SWAN can display and independently calculate DVH information and perform a large number of tasks related to ensuring data matches trial protocol requirements. Data import has been validated for all treatment planning systems in common use in Australasia.

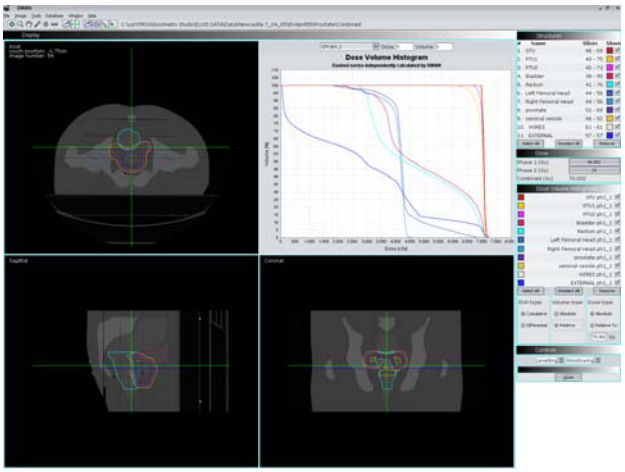

Figure 1. *Principal functions of SWAN – display of image reconstructions, structures and DVHs.*

SWAN is now being used in 5 trials or pre-trial assessments, and will now be more widely used throughout Australasia following a development agreement reached with the Trans-Tasman Radiation Oncology Group (TROG). Linked database and data filtering capabilities make it possible to automate the data collection and QA processes for specific trials. Processes are underway to enhance the capabilities of the software including 3D reconstruction and viewing including beams-eye view, and the ability to use the system over a web-based portal for remote data review.

DISCUSSION & CONCLUSIONS: By using systems such as SWAN, we will be able to increase the accuracy and hence power of clinical trials in discerning those characteristics of treatment plans that directly affect patient outcome. Collection of data in a query-able will allow rapid post-trial analysis of treatment planning data including the derivation of dose-volume response indices which will permit the prompt translation of trial results to clinical practice.

ACCELERATOR OUTPUT IN AUSTRALASIA – COMPARISON WITH OTHER INTERNATIONAL LEVEL I STUDIES

M.A. Ebert[1,2], S. Howlett[3], K. Harrison[3], D. Cornes[4], J. Denham[3] and C. Hamilton[5]

[1]*Department of Radiation Oncology, Sir Charles Gairdner Hospital, Australia*
[2]*School of Physics, University of Western Australia, Australia*
[3]*Department of Radiation Oncology, Newcastle Mater Hospital, Australia*
[4]*Trans-Tasman Radiation Oncology Group, Newcastle Mater Hospital, Australia*
[5]*Department of Clinical Oncology, Princess Royal Hospital, Hull, East Yorkshire, UK*

INTRODUCTION: This paper describes the process and results of a survey of linear accelerator outputs as part of an Australasian Level III Dosimetry Intercomparison. This survey provided an independent measure of accelerator output under reference conditions. Such studies are important for ensuring accurate and consistent dose delivery, and have been undertaken multiple times by collaborative international groups.

METHODS: The Level I measurements performed in this study formed part of a larger intercomparison of dose delivery in an anthropomorphic phantom treated according to TROG rectal and prostate radiotherapy trial protocols. Absolute dose output was measured in a water tank using a Wellhöfer Scanditronix CC13 chamber connected to a Dose1 electrometer. This equipment was transported by study-team members to all participating centres. Measurements were made according to the IAEA TRS-398 absolute dose-to-water protocol [1]. Demographic information on each centre was available for correlation with output measurements.

RESULTS: Output was measured for 35 beams at 27 centres. The mean ratio of measured to locally-determined dose was 1.001 ± 0.010 (1 standard deviation) with a range from 0.981 to 1.024. No correlation could be found between output ratio and accelerator type or local absolute dose calibration protocol. The small-volume chamber used satisfied most requirements for the study though showed some variation in sensitivity via repeated intercomparison with a chamber calibrated at a standards laboratory.

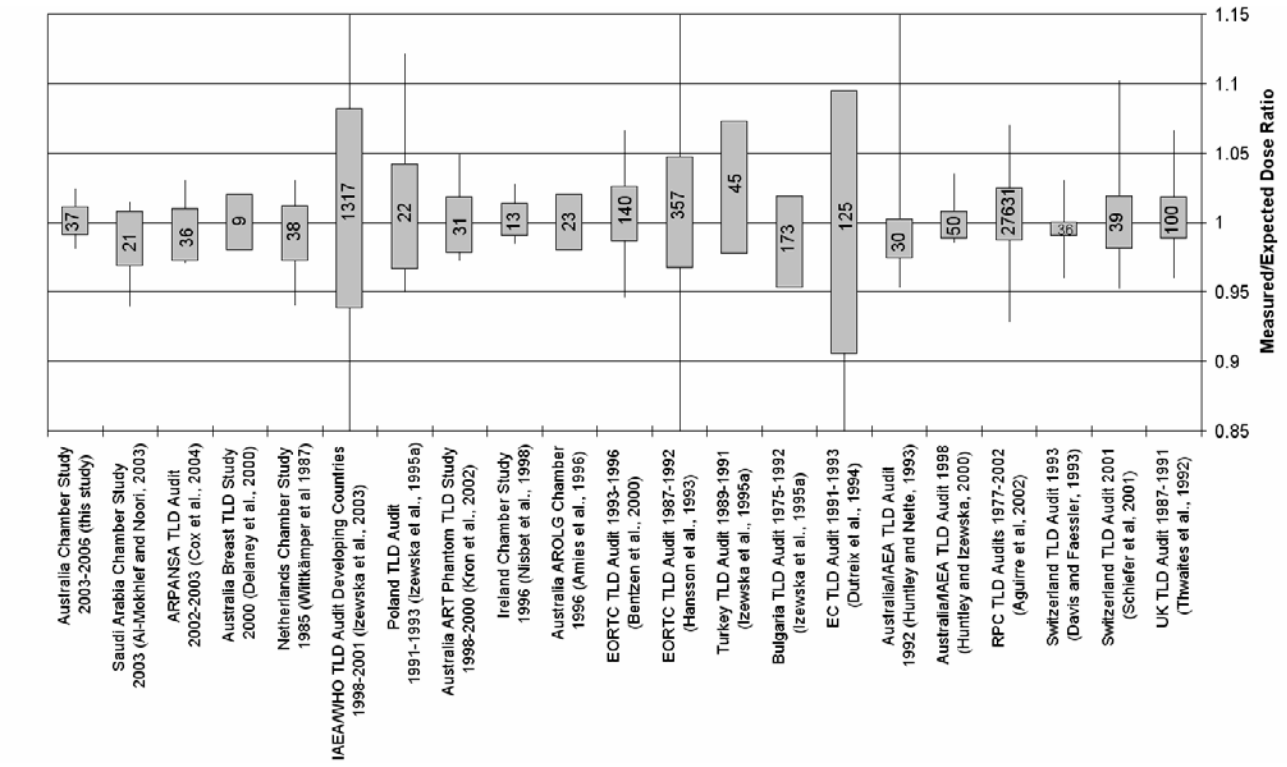

Figure 1. *Results of international Level I studies since 1987.*

DISCUSSION & CONCLUSIONS: As seen from Fig. 1, this study compares very favourable with other international Level I studies undertaken in the last 20 years. This was assisted by use of the small-volume chamber rather then TLD. This study has helped define a process and establish a benchmark for ongoing Level I studies as part of the services of a National Dosimetry Centre.

REFERENCES:

[1]*IAEA (2000) International Atomic Energy Agency, Report TRS 398, Vienna.*

IMAGE GUIDED RADIOTHERAPY (IGRT) WITH ELEKTA SYNERGY

Wasantha Fernando, Nikki Shelton, Catherine Irvine, Guilin Liu, Karl Roozen and Kym Rykers

Radiation Oncology Centre, Austin Health, Victoria, Australia

INTRODUCTION: The new generation of an Elekta linear accelerator, "Elekta Synergy" was installed and commissioned recently at the Radiation Oncology Centre of Austin Health. The accelerator is equipped with integrated imaging functionality that consists of kilovoltage X-ray volume imaging (XVI) and megavoltage X-ray 2D imaging (iViewGT). The imaging features, particularly the XVI, which is in the form of cone beam CT, provides IGRT capabilities with improved soft-tissue delineation for precise patient treatment positioning.

The XVI system consists of a kV X-ray source and an amorphous silicon detector panel mounted opposite each other, across the drum of the digital accelerator. During image acquisition, the x-rays produced are projected as planar images onto the detector panel. The acquired images are then stored and reconstructed to a volume image, which is subsequently used for image registration by comparison with reference scans (planning CT scans). Patient positioning adjustments are applied based on the results of the registration.

METHODS: Mechanical stability, 3-D imaging system checks, and the image registration accuracy checks were carried out for the XVI system in the commissioning phase. One of the important mechanical stability checks, called flexmap calibration, which ensures the positions of kV and MV isocentres are coincident, was carried out by imaging a high-density ball-bearing phantom at the isocentre. The calibration procedure is repeated monthly and a new flex map calibration file is created if results are found to be outside the specifications. In addition to this calibration, mechanical stability constancy is carried out daily with the Quasar, Penta-Guide phantom. The image registration accuracy was evaluated by scanning the Rando phantom at different known locations and comparing with the translational movements determined using the different alignment options within the software. The 3D imaging system checks were carried out with the Catphan phantom CTP503. The checks included low contrast visibility, vertical/ horizontal/sagittal scaling, spatial resolution and uniformity. To ensure the image quality is persistent, the tests are repeated monthly. Finally the dose measurements were performed in the GE phantoms with a CT chamber for different scanning pre-sets.

RESULTS: The mechanical stability checks of the XVI showed no major variation in medium-term mechanical integrity. Improved image quality, in particular for soft-tissue delineation, is highly useful in the process of alignment and registration, and as a result image registration accuracy of about 1mm could be achieved. The 3D imaging system checks showed that the image quality is well within the specifications. The measured nominal dose for standard head and neck scans, and pelvis scans are approximately 1 and 15 mGy respectively.

DISCUSSION & CONCLUSIONS: The XVI system available with the Elekta Synergy linear accelerator is a useful tool for precise patient positioning. It is efficient for on-line corrections and can also be used for off-line analysis of patient shifts.

COMBINING MILD HYPERTHERMIA AND IONIZING RADIATION; PRELIMINARY RESULTS OF THE CELL-KILLING EFFECT ON RODENT LEUKAEMIA CELLS

L. C. A. Flewellen[1], J. Meyer[2], M. Bird[3] and L. Reinisch[4]

[1,2,4]*Department of Physics and Astronomy, University of Canterbury, Christchurch, New Zealand*
[3]*Oncology Service, Christchurch Hospital, Christchurch, New Zealand*

INTRODUCTION: Total body irradiation (TBI) applied to patients with leukaemia prior to a bone-marrow transplant can result in significant adverse effects such as radiation pneumonitis in the lungs [1]. Such side effects are likely to be minimised by reducing the overall radiation dose while maintaining the same cell-killing effects in combination with other means. One possible approach to accomplish this is to combine ionizing radiation with mild hyperthermia. Only limited data are available in the literature for this combined approach regarding leukaemia. In this study, basic *in vitro* experiments are undertaken to investigate whether leukaemic cells become more radiosensitive when subjected to mild hyperthermia.

METHODS: P388 leukaemia mouse lymphoid cells were grown *in vitro,* dispensed in plate-wells and placed in an incubator. Cell-survival curves for hyperthermia were obtained by varying the temperature in the incubator and measuring the cell-kill over a period of days. The curves were corrected for natural cell-kill in an unexposed control group. As the cells were grown at the University of Canterbury and needed to be transported to Christchurch Hospital biohazard safety containers to house the cells during transport were constructed. The possibility of keeping the temperature of the cells constant at 37 degrees Celsius during transportation was investigated. Preliminary experiments were carried out to calculate the build-up material needed for our final experimental set-up. The cells were then irradiated with x-rays for a range of doses, and the cell-survival curve for ionizing radiation alone was obtained. When combining hyperthermia with radiation the maximum cell-kill occurs when both treatments are delivered simultaneously [2]. As this was not possible with our experimental set-up, the cells were returned immediately to the University of Canterbury after irradiation at Christchurch

Hospital and underwent hyperthermia there. The cells that survived were characterized by their ability to continue to metabolise dye and were counted using a spectrophotometer. Cell-survival curves were generated and compared to cell-kill by both hyperthermia and radiation alone.

RESULTS: A cost effective transportation protocol was constructed to be biohazard safe. To maintain the cells at a constant temperature of 37 degrees Celsius a large thermal mass of water surrounded the biohazard safe containers throughout transportation. The cell-survival curves resulting from this research are currently being analysed and will be presented during the conference. Ministry of Agriculture and Forestry approval for this project is underway.

DISCUSSION & CONCLUSIONS: The basic *in vitro* experiments undertaken in this study are an initial step toward developing an understanding of heat as a radiosensitizer for leukaemia cells. The effects of the combined modality technique on response to tissue are much more complex than the *in vitro* system we investigated. This is due to important physiological changes produced by hyperthermia when applied *in vivo* [3]. Thus, further work that observes the effects of total body irradiation combined with whole body hyperthermia is required.

REFERENCES:

[1]*T E Wheldon, (1997) The British Journal of Radiology, 70: 1204-07.*
[2]*J R Stewart, F A Gibbs Jr, (1984) Cancer, 54: 2823-30.*
[3]*H D Suit, M Shwayder, (1974) Cancer, 34: 122-29.*

TIN FOIL MODIFIED ELECTRON BEAMS

S. Geoghegan[1], P. Rampant[1], G. Auzac[1], W. Arancini[2] and J. Heywood[2]

[1]*Medical Engineering and Physics, Royal Perth Hospital, Perth, Australia*
[2]*Perth Radiation Oncology, 24 Salvado Road, Wembley, Perth, Australia*

INTRODUCTION: In external beam radiotherapy it is possible to use bolus made from high atomic number materials when it is important to ensure that a therapeutic dose is delivered to the skin surface and it is impractical or more difficult to use conventional tissue equivalent bolus because the thickness of the tissue equivalent bolus makes a conformal delivery of a skin dose problematic. Examples of high atomic number bolus used for these purposes include metal mesh and metal foils. Although the physics of radiation transport in these materials is known from data tables based on the many basic experiments performed on radiation transport in matter it is not common that these types of bolus are used in the clinic even when the theoretical advantage over conventional bolus is large. Of particular interest is metallic bolus because it potentially provides a useful therapeutic modality when dealing with complex superficial geometries, such as the nose, where it is important to be able to conform the bolus to the underlying shape and thereby, due to the fact that the bolus is very thin and effectively acts like a very thin scatter source, enables the delivery of a highly conformal dose to the relatively complex underlying superficial target volumes.

METHODS: Since 2001 tin foil bolus for electron beams has been successfully used at Perth Radiation Oncology (PRO) and Royal Perth Hospital (RPH) to treat superficial cancers with Elekta Precise linear accelerators. This modality was introduced to treat superficial cancers of the nose where the alternative surgical intervention results in a poor cosmetic outcome. The tin foil modified electron beams were measured in phantoms of various types (water, slab and anthropomorphic) and the relevant data transferred into the Pinnacle^3 treatment planning system (TPS). It is possible to directly use the measured data in the Pinnacle^3 TPS without modification which was confirmed by independent dosimetric verification using ion chambers, diodes and radiochromic film. A subset of these data was also confirmed using Monte Carlo simulation (BeamNRC). Several planning studies were undertaken to determine the practicality of using tin foil modified electrons for superficial cancers which demonstrated the superiority of this technique when compared with the conventional tissue equivalent bolus techniques used until then at PRO and RPH. These data were then used to plan treatments, using the Pinnacle^3 TPS, for superficial cancers (BCC, SCC, Merkel cell carcinoma, etc.) and in vivo dosimetry measured using radiochromic film and TLDs.

RESULTS: Compared with conventional tissue equivalent bolus techniques, tin foil bolus electrons enables a much more conformal dose to be delivered to superficial cancers of the nose avoiding normal tissue structures, such as a the septum, and provides a superior cosmetic outcome to surgery. The technique used to plan a treatment on a nose is dependent on the patient because the shape of the nose varies quite considerably between individuals and some experience is required to ensure appropriate dose coverage. The dose delivered to the surface of the nose is that which is prescribed which is superior to the conventional tissue equivalent bolus techniques that were previously used at RPH and PRO where the dose to the surface of the nose was found to be less than prescribed. Some courage is required because the skin reaction is strong which is indicative of the prescribed dose being delivered (confirmed by in vivo dosimetry). Five year follow up of patients show very good cosmetic outcomes, no adverse reactions and excellent control.

DISCUSSION & CONCLUSIONS: The introduction of tin foil modified electron beams to a radiation oncology practice using the Pinnacle^3 TPS with Elekta Precise linear accelerators will provide better target volume coverage of complex superficial structures than using conventional tissue equivalent bolus. There is a large amount of medical physics work

required to implement this modality and it is possible that other treatment planning systems, other models of linear accelerators and other metals used in the foil could provide similar results.

A FLUENCE-CONVOLUTION MODEL FOR PREDICTION OF AMORPHOUS SILICON EPID IMRT IMAGES

P.B. Greer[12], P.Cadman[3] and K.Bzdusek[4]

[1]*Department of Radiation Oncology, Calvary Mater Newcastle, Newcastle, Australia*
[2]*School of Physical and Mathematical Sciences, University of Newcastle, Australia*
[3]*Dept. of Medical Physics, Saskatchewan Cancer Foundation, Saskatoon, Canada*
[4]*Phillips Medical Systems, Madison, Wisconsin, USA*

INTRODUCTION: The aim of this work is to develop a convolution method to predict amorphous silicon EPID images for verification of IMRT using the incident fluence model of the Pinnacle planning system.

METHODS: Energy fluence maps were extracted from the Pinnacle RTP system. An EPID dose-deposition kernel was developed based on the triple exponential model of Kirkby et al.[1] that incorporates both scatter and optical glare. The kernel was further optimized to match measured EPID response to MLC field sizes to within 2%. A further correction factor $OF_c(FS)$ was derived to correct convolution results for jaw defined field sizes (FS) to measured EPID data. The EPID prediction model is based on the Pinnacle system dose calculation model:

$$D_{epid}(x,y)=MU.T(x,y)*K(x,y).C_F,OF_c(FS) \quad (1)$$

$$T(x,y)=F(x,y)[\ \mu_{open}(x,y)F_{op} + (1-F_{op})\ \mu_{tr}(x,y)] \quad (2)$$

Where T(x,y) is the TERMA which is calculated from the incident fluence F(x,y). To account for the EPID energy-dependent response, the fraction of open (F_{op}) and MLC transmitted fluence are determined for each EPID pixel location from the dynamic MLC file. Separate interaction coefficients are applied to these to give the primary dose deposited in the EPID[2]. This is convolved with K(x,y) a radially symmetric dose-deposition kernel. C_F is a dose conversion factor. EPID images were acquired and converted to dose with a measured calibration factor and compared to calculations for various test and IMRT fields.

RESULTS: Figure 1 shows a comparison of an EPID image of a clinical IMRT field compared to the convolution model.

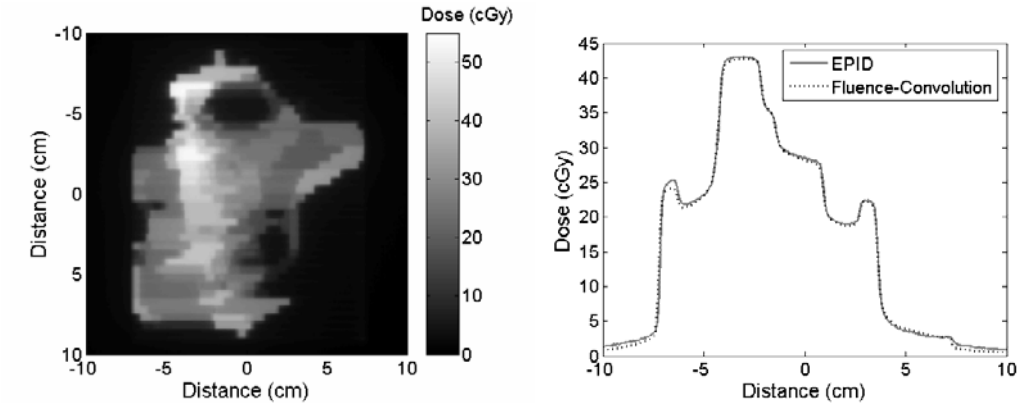

Figure 1. *EPID dose for IMRT field and dose profiles of model compared to EPID.*

DISCUSSION & CONCLUSIONS: The model accurately predicts EPID dose images for IMRT, incorporating tongue-and-groove modelling and energy-dependent EPID response.

REFERENCES:

[1]*C.Kirkby and R.Sloboda (2005), Med. Phys., 32:1115-27.*
[2]*W.Li, J.V.Siebers and J.A.Moore (2006), Med. Phys., 33: 4469-80.*

MONTE CARLO SIMULATION AND EXPERIMENTAL VERIFICATION OF RADIOTHERAPY ELECTRON BEAMS

J. Griffin[1,2] and H. M. Deloar[1]

[1]*Christchurch Hospital, Christchurch, New Zealand*
[2]*University of Canterbury, Christchurch, New Zealand*

INTRODUCTION: Based on fundamental physics and statistics, the Monte Carlo technique is generally accepted as the most accurate method for modelling radiation therapy treatments. A Monte Carlo simulation system has been installed, and

models of linear accelerators in the more commonly used electron beam modes have been built and commissioned.
A novel technique for radiation dosimetry is also being investigated. Combining the advantages of both water tank and solid phantom dosimetry, a hollow, thin walled shell or mask is filled with water and then raised above the natural water surface to produce a volume of water with the desired irregular shape.

METHODS: The selection of EGS/BEAM Monte Carlo software, and the process of modelling electron beam linacs, will be covered briefly. Linac models were built from information supplied by the manufacturer (Varian), supplemented with measurements of components from a decommissioned linac. The initial electron beam energies were adjusted to obtain matches between the simulations and measured commissioning data from another linac.
Patient immobilisation masks have been mounted in a Scanditronix water tank to produce water phantoms with irregular shapes. A diode array radiation detector system has been designed, built and tested for use with the water phantom system. The construction and performance of this system will be discussed.

RESULTS: A test was run comparing the EGS/BEAM Monte Carlo system, the diode array and water tank, and a conventional CMS Xio treatment planning system. This test confirmed that Monte Carlo and conventional electron pencil-beam algorithms predict significantly different dose distributions for an irregularly shaped object irradiated with megavoltage electron beams. The experimental results, although limited, were consistent with the Monte Carlo results.
Areas identified for further work and improvement are: the software for processing data from the diode array, and some characteristics of the Monte Carlo simulations, in particular the electron energy spectra and depth dose curves near phantom surfaces.

ACKNOWLEDGEMENTS: This work was done as a MSc project at Canterbury University. I want to acknowledge the support and help of my supervisors: Graham Sorell, Deloar Hossain, Lou Reinisch, Mat Hasler, and Steve Morgan.

INVESTIGATION OF AN OBJECTIVE COMPARISON OF MEASURED AND CALCULATED PROFILES USING DOSE AND DISTANCE TO AGREEMENT

J. Hatton[1], T. Tehovnik[1] and P. Greer[1,2]

[1]*Radiation Oncology Department, Calvary Mater Newcastle, Newcastle, Australia*
[2]*School of Mathematical and Physical Sciences, University of Newcastle, Australia*

INTRODUCTION: When commissioning a linear accelerator or treatment planning system (TPS), an analytical assessment using an objective, quantitative method is required for comparison of measured and calculated profiles. The gamma index[1] compares, for each point, the combined difference in both dose and distance to agreement (DTA). For a point that may be out of tolerance on dose (e.g. in steep penumbra gradient) but acceptable on DTA, the gamma includes an assessment of the dose discrepancy. The resulting high gamma index value may indicate a local failure in agreement. For clinical use, it is acceptable for either dose or DTA to be within the preset limits, given by the minimum value of gamma for either dose or DTA. The aim of this work is to investigate the contribution of both dose and DTA differences to a final gamma agreement value, to assess the validity of using the Gamma function for TPS beam profile comparison.

METHOD: The gamma function was rewritten, using Matlab, to separately determine the dose and DTA gamma for calculated and measured profiles. This "gamma minimum" assigns the gamma value using the minimum difference for dose or DTA, to represent clinical requirements. These results were compared to the conventional gamma calculation.

RESULTS: The example shown in the graph (Fig 1) shows calculated and measured profiles at 6 MV under a "lung" inhomogeneity, using agreement criteria of 2% of maximum dose and 2 mm. Table 1 shows the numerical results for comparison of the gamma function and the gamma minimum values.

	Gamma index (Low)	Gamma minimum
% points with gamma index value <1.0	92.2	90.4

Table 1. *Calculated gamma values.*

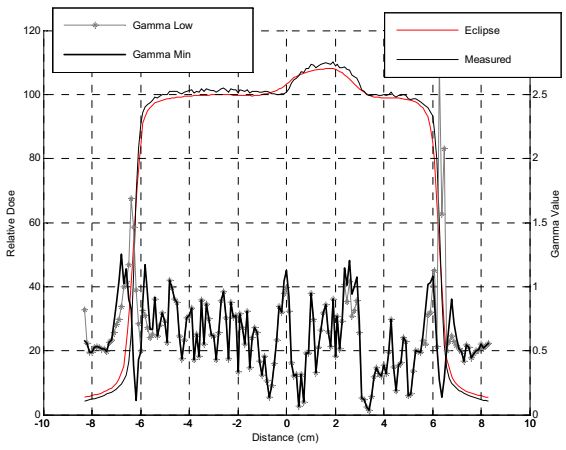

Figure 1. *6MV profiles under lung inhomogeneity.*

DISCUSSION & CONCLUSION: In steep penumbra regions the gamma function gives local failures due to the large dose discrepancy when DTA is within acceptable limits. Results for other regions of the comparison are similar. The gamma function is not suitable for comparison of beam profiles for TPS systems and the minimum gamma of dose and DTA applied separately should be used.

REFERENCE

[1]*Low D et al, 1998, A technique for the quantitative evaluation of dose distributions, Med Phys, 25(5), 656-661.*

IMAGE QUALITY RESPONSE OF ELECTRONIC PORTAL IMAGING DEVICE AT CLINICAL MONITOR UNIT SETTINGS

J. Hatton[1], G. Godwin[2], C. Steen[2] and T. Crabtree[2]

[1]*Medical Physics, Radiation Oncology Department, Calvary Mater Newcastle, Newcastle, Australia*
[2]*Medical Physics Department, The Townsville Hospital, Townsville, Australia*

INTRODUCTION: Amorphous silicon (a-Si) electronic portal imaging devices (EPIDs) are used for positioning verification of clinical treatment fields, immediately prior to irradiation. Typical exposures for pre-treatment verification images use 3 to 8 monitor units (MU) per field. Actual MU are chosen to optimise image quality and to minimise additional patient dose, as these exposures may not be included in the treatment prescription. Elekta recommend calibration of iViewGT a-Si panel using 100 monitor units. Many quality assurance images are acquired using 100 MU. The aim of this work was to investigate the image quality of the amorphous silicon detector, using the different MU values used for clinical images and for calibration.

METHODS: Images were acquired for maximum field size of 26cm sq at isocentre, using MU settings from 1 to 100MU. Profiles through the centre of the panel were normalised at the central axis. The panel was then re-calibrated following the manufacturer's recommended method and the flood field images were repeated. The behaviour of this panel was compared with other panels in similar installations from the same manufacturer. PIPSpro phantom images were acquired for image quality assessment.

RESULTS: Firstly it was established that the EPID response across the panel became stable for MU settings greater than 30 MU. Smaller MU settings show a marked reduction in image response in the central section. After re-calibration, the profiles showed a similar response.

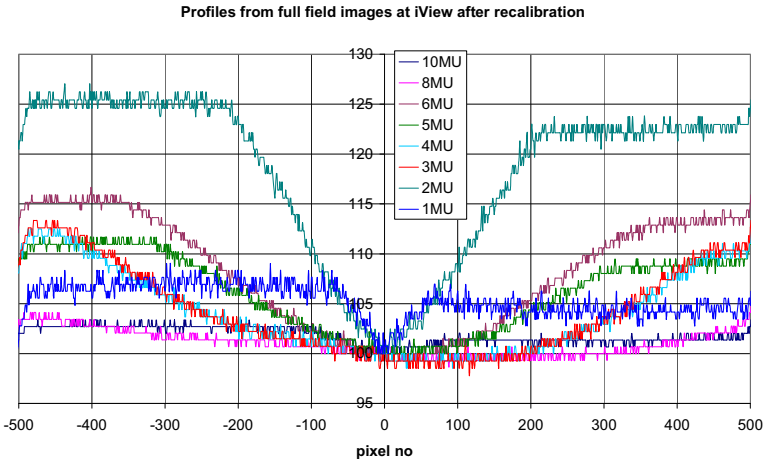

Figure 1. *Profiles from full field images after panel re-calibration.*

DISCUSSION & CONCLUSIONS: The change in large field profile, with MU setting, was significantly greater than was expected. There are significant implications for clinical images at the lower MU settings, and for using the system for IMRT verification. Routine quality assurance tests are being analysed to establish optimal MU settings for panel calibration to reflect routine clinical usage. Further investigation is required to establish a method of correcting for these flood field image quality variations.

CLINCAL ACCURACY – STUDIES TO SUPPORT EFFECTIVE INTRODUCTION OF IMRT IN AUSTRALASIA

A. Haworth[1,2]

[1]*Peter MacCallum Cancer Centre, Melbourne, Australia*
[2]*RMIT University, Melbourne, Australia*

INTRODUCTION: IMRT techniques are part of routine clinical practice in a number of centres in Australasia. Multi-centre clinical trials are therefore now required to justify the introduction these techniques by comparing their efficacy with standard forms of planning and treatment delivery. Furthermore, clinical trials of the future will need to accommodate IMRT techniques for their results to be clinically relevant. The success of any clinical trial requires adequate attention to quality assurance so that errors in treatment delivery and inhomogeneities in treatment planning and delivery do not mask the results of the study.

METHODS: International trials groups such as those supported by the National Cancer Institute (NCI) and the European ESTRO group have developed IMRT quality assurance programs that include site credentialing through facility questionnaires and phantom studies. Both trials groups have attempted to develop generic IMRT credentialing programs, with the opportunity to develop trial specific QA programs when a significant part of the trial question includes the IMRT technique. The ESTRO IMRT QA group (the QUASIMODO project) developed a phantom similar to that used by the NCI group, containing a horseshoe-shaped PTV surrounding a cylindrical OAR and tested their criteria for evaluation of acceptability of planned versus delivered dose of 4% relative to prescribed dose (RPD) and 3mm distance to agreement (DTA) in a feasibility study (4) that was also used to validate their methodology.

RESULTS: Although the first attempt at developing a generic NCI benchmarking exercise that is clinically relevant and with unambiguous instructions prompted some debate in the literature (1-3), the study was able to detect significant errors (greater than 7% RPD or 4mm DTA) in 30% of institutions. Recently, the NCI has further developed its guidelines for IMRT in clinical trials to include intra-thoracic tumours, with recommendations to apply appropriate corrections for tissue heterogeneity and target motion. These guidelines include 14 recommendations, including documenting procedures for correct and reproducible positioning of the patient and target volumes. The ESTRO QUASIMODO feasibility project also successfully determined differences in planned versus delivered IMRT dose distributions but also stressed the value of using a central service to prepare and develop films and perform the data analysis to ensure reliability and validity in reporting inconstancies and errors.

DISCUSSION & CONCLUSIONS: International clinical trials groups have demonstrated that, whilst phantom studies may be effective in detecting systematic errors between planning and treatment delivery, such as incorrect modeling of MLC round leaf ends, they do not provide a complete picture of all uncertainties in patient treatments such as uncertainties in contouring clinical targets and organs at risk, and also daily patient set-up uncertainties (for example due to organ motion), all of which must be take into consideration in a complete IMRT QA program. International clinical trial groups have demonstrated some the difficulties in developing a clinically relevant IMRT credentialing program including the need to verify the feasibility of the project and its evaluation criteria before implementing on a broad scale. With such valuable information at hand, it is now time for Australasia to develop a similar program to support our clinical trials which in turn will determine the appropriate use of this relatively new and complex technique.

REFERECES:

M.J Engler, M.J. Rivard (2003) Int. J. Radiat. Biol Phys 57:S260.
J.R. Palta, J.A. Deye et al (2004) Int. J. Radiat. Biol Phys 59:1257-1259.
M.J Engler, M.J. Rivard (2004) Int. J. Radiat. Biol Phys 59:1259-1261.
S. Gillis, C De Wagter et al (2005) Radiother Oncol 76:340-353.

DEVELOPMENT OF A QUALITY ASSURANCE PROGRAM FOR CLINICAL TRIALS – THE RAVES DRY RUN

A. Haworth[1,2], K. Wiltshire[3], M. Pearse[4], S. Williams[1], D. Joseph[5], D Willis[1], C. Sproston[1], A Thompson[1] and A. Kneebone[6]

[1]*Peter MacCallum Cancer Centre, Melbourne, Australia*
[2]*RMIT University, Melbourne, Australia*
[3]*Royal North Shore Hospital, Sydney, Australia*
[4]*Auckland Hospital, Auckland, NZ*
[5]*Sir Charles Gairdner Hospital, Perth, Australia*
[6]*Liverpool Hospital, Sydney, Australia*

INTRODUCTION: The ultimate aim of any multi-centre clinical trial is to determine the optimal treatment technique for a select group of patients. Clinical trials may start with a feasibility study and eventually progress to a randomised phase III study. Regardless of the phase group, the clinical trial requires all centres to comply with the trial protocol instructions to deliver meaningful results that can answer the study question and be translated into general clinical use. A good clinical trial will provide unambiguous guidelines for treatment delivery that are practical and safe. The physicist has the opportunity to assist with clinical trial design to meet these objectives and an example of such involvement is described.

METHODS: RAVES, a randomised clinical trial comparing adjuvant versus early salvage radiotherapy in post-prostatectomy patients is set to open late 2007. Guidelines for delineation of the CTV and PTV were developed by a working group following a consensus workshop held in 2006. These guidelines have been incorporated into the RAVES protocol along with recommendations for treatment planning and quality assurance in treatment delivery. To test the

feasibility of the contouring guidelines and measure the variability in interpretation, a credentialing program has been developed that requires participating centres to contour a unique CT data set. A sub study of the trial will aim to provide clinical evidence for the recommended CTV-PTV margins.

RESULTS: The first attempt at following the contouring guidelines demonstrated a significant variation in contouring that, in some cases, lead to volumes that could not be treated without violating the rectal dose constraints. These guidelines, particularly with regard to target volume delineation have since been modified resulting in reduced variation in contouring practice. With a greater understanding of the variability in contouring practices and practical measurement of treatment delivery accuracy, recommendations for CTV-PTV margins can be provided.

DISCUSSION & CONCLUSIONS: Previous clinical trials have demonstrated a good quality assurance program can improve the quality of treatment delivery in participating centres and with 3D treatment plan review software, trial compliance can be improved which in turn has been shown to be a predictor of clinical outcome. The RAVES study provides an example of the framework for the development of a quality assurance program in a clinical trial that may be used in the development of similar trials, in particular those that incorporate new technology or require high standards of treatment delivery.

CLINICAL IMPLEMENTATION OF AN ADAPTIVE RADIOTHERAPY TECHNIQUE FOR POST-PROSTATECTOMY PATIENTS (PPP) USING CONE BEAM CT

A. Haworth[1,2], T. Kron[1,2], P. Roxby[1], A. Paneghel[3], A. Phillips[3], A. Rolfo[3], M. Laferlita[3], S. Soteriou[3] and F. Foroudi[4]

[1]*Dept. Physical Sciences, Peter MacCallum Cancer Centre, Melbourne, Australia*
[2]*RMIT University, Melbourne, Australia*
[3]*Radiation Therapy Services, Peter MacCallum Cancer Centre, Melbourne, Australia*
[4]*Division of Radiation Oncology, Peter MacCallum Cancer Centre, Melbourne, Australia*

INTRODUCTION: Accuracy of treatment delivery in the post-prostatectomy patient (PPP) has previously been difficult to quantify as treatment set-up verification is commonly based on bony anatomy that has been shown to be a poor surrogate for target volume accuracy in the intact prostate group. Movement of the target volume in the PPP is not well documented though significant changes in rectal volume and position have been well demonstrated in the prostate series. An in-house developed adaptive technique allows appropriate treatment margins to be applied to the individual patient to maximise target volume coverage and minimise dose to OAR.

METHODS: All patients were planned using a 3D conformal technique according to draft Australian consensus guidelines. A kV cone beam CT (CBCT) image was acquired daily during the first week of treatment. This was immediately followed by orthogonal kV imaging using the Varian on-board imaging device (OBI) and then patient treatment. At the end of the first week of treatment, CBCT images were transferred to the Eclipse treatment planning computer. Target coverage by the 95% isodose and rectal DVHs were calculated for all images and for the "average" target and rectum position. Data from the OBI was used to determine a systematic deviation in patient position based on bony anatomy. Using the revised position of the average target volume and rectum, the patient was re-planned if defined constraints were not met.

RESULTS: The rectum was well visualised on CBCT though considerable intra-observer variability was demonstrated in contouring the PTV. As a result of this and changes in daily position of the PTV, coverage of the 95% isodose decreased by up to 18%. At the level of the isocentre, the distance between the anterior rectal wall and the anterior pubic symphysis was found to vary by up to 20mm but this did not directly relate to changes in the rectal DVH. Deviations were seen on a daily basis using CBCT however the averages were sufficiently close to conventional planning volumes so that replanning was generally not necessary when using standard treatment planning margins.

DISCUSSION & CONCLUSIONS: CBCT and an adaptive radiotherapy technique may be useful if aiming to reduce treatment planning margins in the PPP. Data from this project may be used to determine appropriate margins for non-adaptive radiotherapy techniques which may provide reliable data to correlate dosimetry parameters with clinical outcomes in the PPP.

COLLISION AVOIDANCE IN STEREOTACTIC RADIOTHERAPY

M. A. Haynes[1] and A. Merchant[2]

[1]*William Buckland Radiotherapy Centre, The Alfred Hospital, Melbourne, Australia*
[2]*Royal Melbourne Institute of Technology (RMIT), Department of Applied Physics, Melbourne, Australia*

INTRODUCTION: Linac based stereotactic radiosurgery and therapy (SRS/SRT) treatments involve the delivery of multiple beams of radiation through several degrees of freedom in gantry, couch and collimator rotation and couch lateral, longitudinal and vertical movements. The multiple degrees of freedom in the linac introduces the possibility of collisions with the patient or with the couch during the treatment. Commercial planning software generally incorporates a

system for collision avoidance, but it is generally not machine specific and guards only against the apparent collisions of the gantry and couch.

Our current clinical arrangement for SRS/SRT treatments at the William Buckland Radiotherapy Centre incorporates a Varian 600C Linac equipped with a BrainLab micromultileaf collimator. On this system it is envisaged to implement a specific collision avoidance system to address possible collision conditions resulting from patient planning, set-up and physics QA. The system will incorporate a software application that is available to the treatment planner that will access SRS/SRT patient treatment data after the plan is completed to warn the planner of possible collision incidences. At this stage of the treatment, a modification to the plan to avoid these situations is a relatively straightforward process. It is also of interest to incorporate a real-time system into the software and have the software running on the treatment computer to simultaneously access real-time data on gantry, couch and collimator positions and warn of possible impending collisions.

METHODS: The objective is to determine whether a collision would occur for a particular combination of gantry angle, couch angle, collimator angle and lesion isocentre coordinates. Collision detection is analytically determined by representing a surface on the gantry and couch as a plane in three dimensional space and determining where the surfaces intersect [1]. The gantry surface is modelled as a rectangle representing the MLC cover and the couch surface is modelled as a rectangle representing the couch bracket. The user interface will be developed in consultation with all departments associated with the treatment of stereotactic radiosurgery. This approach was undertaken so that an appropriate, user friendly interface would be produced for all users associated with treatment delivery. A further requirement is for the system to integrate with the planning process and planning and treatment computers.

RESULTS: The outcomes from a survey given to the stereotactic radiotherapy staff will be presented along with the final design for the user interface. The survey involved answering a series of questions on the information to be displayed and interpreting a series of images representing possible designs for the user interface. The final algorithm was tested on data acquired from previously treated patients and the results will be presented.

DISCUSSION & CONCLUSIONS: A collision avoidance algorithm has been implemented and tested in-situ using data from near misses in stereotactic radiosurgery. A survey of staff involved has identified an optimal solution for presenting collision avoidance information.

REFERENCES:

[1] *C. Hua, J. Chang et al, (2004) Med Phys, 31 (7):2128-2134.*

IMPROVING IMRT PLANNING FOR MESOTHELIOMA WITH CMS MONACO

C.Irvine[1], M.Grace[2], S.Marshall[3], K.Rykers[1], W.Fernando[1], N.Shelton[1], J.McNamara[1], B.Sloman[3], M.Lawlor[1], E.Zupan[1] and M.Feigen[1]

[1]Radiation Oncology Centre, Heidelberg Repatriation Hospital, Melbourne, Australia
[2]CMS Alphatech, Sydney, Australia
[3]CMS inc., St. Louis, Mo, USA

INTRODUCTION: Mesothelioma is an aggressive malignancy with a high mortality rate. Standard treatment modalities fail in most patients and innovative solutions are being explored. The potential to improve the high local failure rates after radical surgery is being addressed using IMRT to target large treatment volumes in the involved hemithorax and along the diaphragm, while delivering tolerable doses of radiation to the contralateral lung, liver, heart, spinal cord and kidneys[1].

Two Melbourne hospitals have recently joined the MARS (Mesothelioma and Radical Surgery) trial, a UK-based phase III trial designed to establish whether there is any benefit in terms of survival and/or quality of life from the major operation of extrapleural pneumonectomy (EPP) as part of multimodality treatment. All eligible patients will be given induction chemotherapy, and then randomized to EPP (removal of the entire ipsilateral lung, pleura, diaphragm, and pericardium) followed by hemithoracic radiotherapy, or no-EPP.

For patients not undergoing EPP, the less morbid operation of pleurectomy/decortication may be performed. This involves the removal of the pleura, leaving the lung in situ. For these patients, radiotherapy treatment planning is extremely challenging, as the treatment volume surrounds the ipsilateral lung and the risk of radiation pneumonitis is very high. To avoid this complication, the dose to the ipsilateral and contralateral lungs must be minimized. The advent of IMRT has helped, but to date, we have not been able to produce acceptable treatment plans with CMS XiO without compromising the target volume.

The advanced prescription and optimisation features of CMS Monaco, as well as the use of Monte Carlo calculation algorithms have the potential to improve IMRT planning for such cases, and to produce treatment plans with sufficient target coverage, but lower ipsilateral lung doses.

METHODS: A planning study was carried out on a single mesothelioma patient, with “typical” treatment volumes, post-pleurectomy/decortication. The aim was to deliver 50Gy and 60Gy to the PTV and boost PTV respectively, whilst keeping doses to organs at risk within published tolerances. The case was planned on both XiO (v4.3.1) and Monaco (1.0) with

multiple iterations, in order to optimise the planned distribution. The best plans achieved with both XiO and Monaco were compared in terms of dose-volume histogram (DVH) data, dose distribution and the required number of segments.

RESULTS: The Monaco plan provided improved and acceptable target coverage over the XiO plan, whilst reducing the dose to the ipsilateral lung. DVH data for all other organs at risk were similar and acceptable for both plans. The number of segments required by Monaco was also lower, which leads to shorter treatment times.

DISCUSSION & CONCLUSIONS: With further iterations and refinement of the entered prescription, it is likely that Monaco will be able to generate an IMRT plan which shows further improvement to the data presented herein. This could greatly improve local control for mesothelioma patients who have not undergone EPP, leading to increased long-term survival rates.

REFERENCES:

[1]*Ahamad A, Stevens CW, Smythe WR, et al, (2003). Promising early local control of malignant pleural mesothelioma following postoperative intensity-modulated radiotherapy (IMRT) to the chest. Cancer J 9:476-484*

THE AMORPHOUS SILICON ELECTRONIC PORTAL IMAGING DEVICE AS A GAUGE FOR PATIENT THICKNESS: EXPERIMENT VS. SIMULATION

T. Kairn[1], D. Cassidy[2], A. Fielding[1] and P. Sandford[1,3]

[1]*School of Physical and Chemical Sciences, Queensland University of Technology, Brisbane, Australia*
[2]*Cancer Care Services, Royal Brisbane & Women's Hospital, Brisbane, Australia*
[3]*Now at Princess Alexandra Hospital, Brisbane, Australia*

INTRODUCTION: There has recently been an increasing interest in the use of amorphous silicon electronic portal imaging devices (a-Si EPIDs) to verify the delivery of the correct radiation dose during a radiotherapy treatment. In this work, through a combination of experimental measurement and Monte Carlo (MC) simulation, we investigate the validity of calibrating the EPID to generate a patient thickness image and potentially using this as a surrogate for delivered dose.

METHODS: The response of the a-Si EPID is calibrated by innovatively adapting a technique previously applied to scanning liquid ion chamber EPIDs. The calibrated EPID is then used to measure the radiological thickness of planar, stepped and anthropomorphic phantoms subjected to various photon-beam fields. Through adaptation and application of EGSnrc/BEAMnrc codes, a full MC simulation model of the entire linac-phantom-detector system is developed. This model is used to both validate the thickness measurement technique and to calculate an expected thickness image for comparison with the experimentally measured image.

RESULTS: The simulations and experiments produce profiles in calibration coefficients, intensity ratios and radiological thicknesses that are directly, quantitatively comparable to each other and are in very good accord. We find that the agreement between our MC and experimental calibration results is strong enough that calibration of the EPID as a thickness gauge can reliably be achieved using simulations alone.

The EPID is shown to be capable of both accurately measuring the thickness of a given planar solid-water phantom, and reliably identifying a 2mm change to that thickness. For non-water-equivalent phantoms, MC results show an approximately linear relationship between measured thickness and material density. This result is related to experimental measurements of more-complex anthropomorphic phantoms, and thus predictions about their composition are made.

DISCUSSION & CONCLUSIONS: Thickness measured in radiological terms, using an EPID image, is shown to depend upon the delivered dose, and the composition and physical thickness of the attenuating medium. Consequently, radiological thickness could be used to verify a patient's treatment at each fraction, monitoring any problems with delivery and/or changes in patient setup or anatomy.

MONTE CARLO SIMULATION OF RADIOTHERAPY TREATMENT BEAM GENERATION: POTENTIALITIES AND LIMITATIONS

T. Kairn[1], A. Fielding[1] and S. Crowe[1]

[1]*School of Physical and Chemical Sciences, Queensland University of Technology, Brisbane, Australia*

INTRODUCTION: With the increasing recognition of Monte Carlo (MC) techniques as capable of reliably simulating radiotherapy beam transmission and dose deposition has come a growth of interest in the problems of commissioning MC systems to reliably model actual clinical or experimental systems.

METHODS: Our commissioning of linear accelerators modelled using BEAM firstly applies the well-known general methodology of simulating a set of clinical beam data in a water phantom and refining the parameters (energy, radial width) that model the initial electron beam on the target to achieve suitable replication of measured dosimetric data. We examine

the applicability of this technique to fields of various sizes with different nominal energies. We suggest a minimum set of simulations which must be completed to guarantee that the model is adequately reliable.

Additionally, we broaden this study to examine the individual components that make up the linear accelerator and explore the accuracy and detail with which they need to be modelled, as well as whether they each need to be included at all, with a view to minimising the time-cost of running MC simulations. We identify the sensitivity of the beam shape and intensity made to jaws and MLC design, as well as the effects of flattening filter and monitor chamber design. To investigate this we: remove the backscatter plate from the virtual accelerator's monitor chamber and examine its effect on backscatter and output; model the jaws with more/less complex end shapes and examine their effects on the penumbra of the beam; build the model MLC using alternative BEAM modules and identify limitations on the use of 'MLCE'; include and exclude flattening filter support-structures from our model and examine their effect on machine output; and build the virtual flattening filter out of alternative materials (including air) and examine its effect on dose and fluence profiles.

RESULTS: These virtual experiments lead to observations such as that: the inclusion of a backscatter plate and flattening filter support-plate does not affect the shape of the beam within the field, but does broaden the penumbra of the beam; modifying the shape of the upper (backup) jaw ends similarly effects the penumbra; the replacement of the BEAM component module 'MLCE' with 'MLCQ' is necessary for the secondary collimation of an Elekta machine to be modeled correctly; broadening the initial electron beam target inset does not change the flatness of the beam; narrowing the flattening filter can affect the flatness of the beam; changing the position of the flattening filter affects beam's flatness, but also affects its dimensions; and increasing the density of the flattening filter can result in profiles which are in good agreement with experimental data, but demands the use of a fictitious material.

DISCUSSION & CONCLUSIONS: We produce a model linear accelerator which accurately models the output of a radiotherapy treatment machine by permitting the individual components of that model to vary from the manufacturer's specifications. We therefore contend that in using the BEAM Monte Carlo simulation method to model a radiotherapy treatment, it is the phase space file that's important, not the geometry or construction of the machine that produced it.

CLINICAL TRIALS WITH IMRT

Kron T.[1,2]

[1]*Peter MacCallum Cancer Centre, Melbourne, Australia*
[2]*RMIT University, Melbourne, Australia*

There is an increasing awareness in society that evidence should inform clinical decision making and allocation of resources. Clinical trials are an important method to generate clinical evidence and radiation oncology has a proud history of conducting these trials. However, more than 10 years after the first IMRT treatments there are still only a few randomized multicentre clinical trials addressing the use of IMRT in a prospective fashion. This is due to a multitude of issues - the large variety of approaches and significant differences in equipment being one of them. A very important argument against clinical trials involving IMRT is also the lack of equipoise: how can we justify randomizing patients to different arms if the IMRT plan looks better than the conventional one? This argument does not take into consideration that IMRT dose distributions are inherently different (eg different margin design), may take longer to deliver, and could result in larger leakage radiation. The presentation will explore areas where this may lead to a genuine equipoise in treatment arms calling for a prospective randomized trial.

Another method of learning about IMRT in clinical trials is stratification for IMRT if different methods of delivery are allowed. Several current prostate cancer trials conducted by RTOG allow this. Finally, single arm clinical trials (phase I/II) lend themselves to include technical endpoints such as feasibility, safety and resource implications. In the Australian context this offers an excellent method to introduce IMRT in different clinical scenarios in a controlled way and provide administrators at the same time with essential information for planning and resource allocation.

A PROPOSAL FOR AN AUSTRALIAN CENTRE FOR CLINICAL DOSIMETRY

T. Kron[1], A. Haworth[2] and L. Smith[3]

[1,2]*Peter MacCallum Cancer Centre, Melbourne, Australia*
[3]*William Buckland Radiotherapy Centre, Melbourne, Australia*

INTRODUCTION: Radiation Oncology is an essential part of cancer management. It relies on accurate delivery of radiation dose to patients. As radiotherapy techniques become increasingly complex it is essential to verify that radiation is given to patients in an accurate, reproducible and safe fashion in all radiotherapy facilities. This can be ensured through dosimetric intercomparisons that test that all radiotherapy facilities operate to the same quality standards. Such intercomaprisons involve independent validation of radiation dose measurement, calculation and delivery. They are also essential quality processes for multicentre clinical trials that provide the best method for enhancing clinical knowledge and evidence based practice.

METHODS: A workshop was held on December 12, 2006 in Sydney to discuss the establishment of a National Centre for Clinical Dosimetry (Sydney, December) with particular emphasis on

- Organisation of dosimetric intercomparisons for radiation oncology facilities in Australia
- Provision of quality assurance for clinical trials
- Establishment of dosimetric quality assurance for brachytherapy

A small working party was established to develop a detailed proposal for an Australian Centre for Clinical Dosimetry (ACCD).

RESULTS: After consultation with stakeholders including Cancer Australia, ACHS, RORIC and the federal government, two proposals were submitted to the Department of Health and Aging on behalf of the radiotherapy tripartite and the Transtasman Radiation Oncology Group (TROG). The proposal for establishment of the ACCD as a quality initiative has as objectives to:

- establish the centre and its services. These will include dosimetric intercomparisons ranging from level I (verification of calibration) to III (verification of the complete treatment chain using an anthropomorphic phantom),
- determine needs, uptake and acceptance of the services within the Australian radiotherapy community,
- develop tools for web based electronic data collection and feed back to users
- establish a database for dosimetry in radiotherapy, and
- confirm costs of the service and resource requirements for participating radiotherapy facilities in order to establish an on-going, sustainable clinical dosimetry service for Australia – this may include the investigation of different funding models.

The ACCD proposal is accompanied by a project description outlining the development of an intercomparison tool for brachytherapy. The scope of this project would make it fit within the Research Component of the recent Better Access to Radiation Oncology budget measure.

DISCUSSION & CONCLUSIONS: The proposed Australian Centre for Clinical Dosimetry will be a unique resource for Australian radiotherapy departments. The concept is modeled on the successful Radiological Physics Center (RPC) in Houston. As such, the support of clinical trials will be one of the major components of its work. Challenges for the future will be to determine a sustainable financial model and inclusion of brachytherapy in the dosimetric services.

ACKNOWLEDGEMENT:
The financial support of the NSW Cancer Institute for conducting the NDC workshop is gratefully acknowledged.

SUITABILITY OF THE MOSKIN DETECTOR FOR SKIN DOSIMETRY

I. Kwan[1], D. Wilkinson[1], M. Butson[2], D. Cutajar[1], M. Lerch[1] and A. Rosenfeld[1]

[1]Centre for Medical Radiation Physics, Univ. of Wollongong, Wollongong, Australia
[2]Illawarra Cancer Care Centre, Wollongong, Australia

INTRODUCTION: The rising popularity of MOSFET detectors for use in clinical radiation dosimetry is due to their small size, high spatial resolution, and ability to offer real-time dose information. Current MOSFET detectors, however, have their limitations. Few reports have shown that today's MOSFET-based dosimeters are suitable for measuring the dose at 0.07 mm, the depth of the basal cell layer, as recommended by the ICRP (1992). The epoxy encapsulation used in most MOSFET detectors have issues related to the thickness of the encapsulation, and poor manufacturing (and response) reproducibility amongst individual detectors of the same design. The new MOSkin detector, developed by the Centre for Medical Radiation Physics, is engineered to address these issues by utilizing a thin, reproducible film over-layer rather than an epoxy bulb.

METHOD: Six MOSkin detectors were individually placed on the surface of a solid water phantom and irradiated by a Varian 2100EX linear accelerator using a 6 MV x-ray beam of 10x10 cm field size. The surface dose was normalised to the response at 15 mm depth (d_{max}). The normalised dose, or "percentage depth dose " (PDD), was compared to RadFET and Attix chamber results. An Attix chamber is a parallel plate detector proven to be a reliable surface dosimeter when compared to extrapolated chamber results; while the RadFET is a commercially available MOSFET detector that utilises an epoxy bulb.

The response of six individual MOSkin detectors were compared to examine the manufacturing reproducibility of the film overlayer. As Scalchi noted, a reproducible build-up layer was critical in creating a reproducible response between detectors of the same design [1].

RESULTS: At 0° incidence, the mean PDD of the six MOSkin detectors was 18.3±0.7%. In comparison, the RadFET and Attix chamber have a PDD of 35.8% and 16%, respectively. PDD results among the six individual MOSkin detectors were 17.2%, 17.9%, 18.0%, 18.0%, 18.2%, and 20.4%.

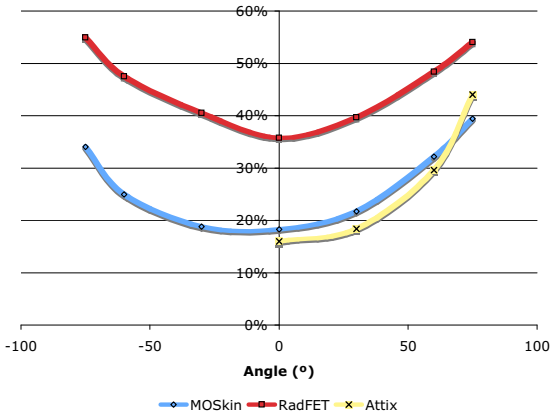

Figure 1. *Percentage depth dose (PDD) comparison between the MOSKin, RadFET, and Attix Chamber at irradiation angles from 0 – 75°.*

DISCUSSION & CONCLUSIONS: When placed on the surface of a solid water phantom, the response of the MOSkin is quite similar to the response of the Attix chamber, while the RadFET response was much greater, indicating its inability to adequately measure the absorbed dose at the phantom surface. A similar observation was made when irradiating at angles of 0–75°, as well as for other field sizes. The response of the individual MOSkin detectors was quite reproducible, with a narrower range of responses than the 15.2 – 20.2% obtained by Scalchi.

REFERENCES:

[1]*P. Scalchi Characterization of a new MOSFET detector configuration for in vivo skin dosimetry Med. Phys. 1571–78.*

INTRA-OPERATIVE RADIOTHERAPY WITH A MINIATURE X-RAY SOURCE

P. Lanzon, S. Behin-Ain, N. Caswell and D. Waterhouse

Department of Radiation Oncology, Sir Charles Gairdner Hospital, Perth, Australia

INTRODUCTION: A miniature 50kV x-ray therapy device has been in clinical use for intra-operative radiotherapy of breast tumours in this Hospital since 2001 with a total of 130 patients treated. An international clinical trial (Targit), is currently accruing patients to assess the clinical efficacy of this device for the treatment of breast cancer.
The device generates 30-50 kV x-rays with currents of 5-40uA at the tip of a needle-like probe. The dose distribution is isotropic and a range of solid plastic spherical applicators of diameter 1.5-5cm are used for patient treatment.

DISCUSSION: The following aspects of the use of this device will be presented:
Dosimetric characteristics: HVLs are of the order of 0.1 mm Al unattenuated and 0.5-0.9 mm Al attenuated (10 mm solid water) for the 30-50kV beams respectively. The dose rate with an applicator varies between 0.1-0.5Gy/min at 1cm depth in water for the 50kV 40μA beam and the dose fall-off with depth in water varies approximately as the cube of the distance. Beam isotropy is within 10% except in the backward direction near the probe itself. Dose output is stable over time within 2% variation per annum.
Quality assurance: Pre-treatment QA includes probe straightening, isotropy, internal and external radiation monitor checks, output constancy.
Radiation Safety: For pre-treatment QA, the device accessories provide complete shielding; lead screens are used during patient treatment.
Treatment procedure: For breast treatments, a single dose of 6Gy is delivered at 1cm depth in tissue with treatment times ranging from 20-50 minutes.
Clinical Trial: The Targit clinical trial, which commenced in 2001, has 17 participating centres in Europe, Canada, USA and Australia (Perth and Melbourne). The randomised trial has accrued almost 900 patients to date with a target of 2200.
Radiobiology
Other clinical applications: Liver metastases

INVESTIGATION OF THE DOSIMETRIC EFFECTS OF NON-UNIFORM BACKSCATTER FOR AN AMORPHOUS SILICON EPID

C. Lee[1,2], P. Greer[2,3] and F. Menk[2]

[1]*Central Coast Radiation Oncology Centre, Gosford, Australia*
[2]*University of Newcastle, Newcastle, Australia*
[3]*Calvary Mater Newcastle Hospital, Newcastle, Australia*

INTRODUCTION: Images acquired with the Varian aS500 amorphous silicon EPID contain inherent dosimetrically significant artefact due to backscatter from the non-uniform design of the mechanical supporting structure. The flood-field calibration (FF) only compensates for this effect when the entire panel is exposed. For smaller field sizes, the FF becomes invalid as the backscatter conditions used in its acquisition are different to that of the smaller field being imaged. The aim of this work is to characterise the spatial distribution and magnitude of the backscattered component in an EPID acquired image then use a simple mathematical solution to remove it, thereby improving the dosimetric accuracy of the EPID.

METHODS: A narrow slit (0.3 cm × 30 cm) of 6MV radiation from a Varian 21EX linear accelerator was used to expose a small number of rows across the entire width of the aS500 image detection unit (IDU). A series of images were acquired by stepping the IDU in 1 cm increments in between exposures. Each image was acquired over 100 MU, at a source to detector distance of 120 cm.

The maximum pixel reading and the FWHM value of each slit were recorded. An array of values were built up which enabled the construction of a "topographical map" of the pixel values thus displaying the extent to which regions of the IDU are affected by the non-uniform backscatter.

RESULTS: Figure 1 shows the variation in pixel response along the midline (superior-inferior) of the aS500 EPID. As the figure shows, the inferior side of the EPID panel is more sensitive than the superior side for small field widths. Similar results have been obtained for planes parallel to the midline, suggesting that the non-uniformity in the aS500 construction is primarily superior to inferior.

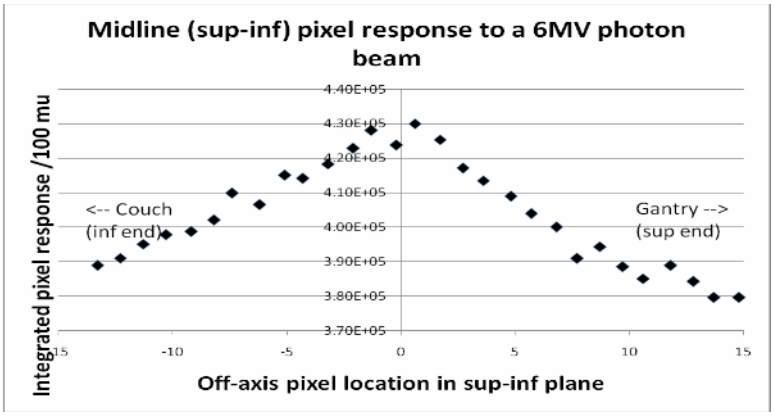

Figure 1. *Graph of the pixel response along the mid-line of the aS500 EPID when exposed to a constant source of radiation.*

DISCUSSION & CONCLUSIONS: The results above show the difference in backscatter component of the flood-field calibration image and the small field at each pixel location. As the major backscatter components are in the superior end of the EPID, these suggest that the backscatter component in the flood-field is over-compensating for backscatter in smaller fields in this direction. Further work will be undertaken to remove the flood-field from acquired images to examine the backscatter to a pixel without its influence.

INTRA-OPERATIVE RADIATION THERAPY – IORT

C.Lee[1] and P.Yuile[2]

[1]*Central Coast Radiation Oncology Centre, Gosford, Australia*
[2]*Mater Misericordiae Hospital, Crows Nest, Australia*

INTRODUCTION: IORT is a treatment modality whereby the tumour is excised and the tumour bed and appropriate margin is irradiated with a single fraction from a megavoltage electron beam (typically to a dose of 10 – 25 Gy) in order to sterilize any residual microscopic disease. Disease free tissue can be mobilised out of the treatment field and held out by a rigid applicator, typically cylindrical in shape. IORT is not limited to the abdomen but the vast majority of cases worldwide are abdominal tumours.

METHODS: Our experiences at the Mater Misericordiae Hospital involved placing a cylindrical aluminium applicator over the target volume. This defined the area to be irradiated and also served to hold the disease free tissue out of the field. A TLD was placed in the centre of the field for dosimetric verification. Once the applicator was in place, the patient, whilst still under anaesthesia, was moved out of the sterile surrounds of the operation theatre, transported through the hospital, into the radiotherapy department. The standard electron applicator of the Varian 2100C was discarded in favour of a specifically designed collimator system. Precise alignment of the applicator with the central axis of the beam is problematic. There was a

gap between the collimator system and the applicator protruding from the patient. The patient is still on the operating theatre table which is not designed to be finely adjusted in the longitudinal, lateral and vertical planes.

RESULTS: During the period from 1993 to 2003, 12 patients received between 10 – 18 Gy. An additional 3 cases were aborted at time of surgery due disease spread.

Table 1. *Summary of clinical IORT cases treated at the Mater Hospital, Crows Nest.*

Tumour Site	Dose	Electron Energy	Follow up
Pancreas	10 Gy	9 MeV	Deceased – Liver failure
Pancreas	10 Gy	9 MeV	Deceased - Mets
Synovial sarcoma HG	12.5 Gy	9 MeV	No evidence of disease – 6 yrs
Sigmoid/Bladder (Rec)	15 Gy	9 MeV	Deceased - Mets
Sarcoma - high grade	10 Gy	9 MeV	No evidence of disease – 5.5 yrs
Sarcoma - high grade	12.5 Gy	9 MeV	Deceased - Mets
Rectum (Rad)	15 Gy	9 MeV	No evidence of disease – 5 yrs
Ewings Sarcoma	15 Gy	12MeV	Deceased - Mets
Rectum (Rad)	15 Gy	12MeV	No evidence of disease – 2 yrs
Malig. Schwannoma	15 Gy	12MeV	Deceased - Mets
Malig. Schwannoma	10 Gy	12MeV	
SCC anal canal (Rec)	15 Gy	9 MeV	LF 12 mos
2nd field	18 Gy	9 MeV	D Mets

DISCUSSION & CONCLUSIONS: IORT failed to take off as a viable treatment option in Australia. There are several reasons for this, most notably is the debate as to the clinical benefit of IORT and the lack of remuneration (less than $50 for 5-8 hours work). Also, there was major disruption in the hospital in general because a patient with an open wound and under general anaesthetic was being transported through the corridors. We also found that we didn't have support in the surgical fraternity due to the length of time the procedures were taking (reduced case load for surgeons and anaesthetists) and the disruption it was causing to the running of the operating theatres. On the positive side, we had our successes in that we encountered no increase in infection nor did we have any emergency situation outside the operating theatre.

COMPUTED RADIOGRAPHY FOR CHECKING SOURCE POSITION AND DWELL TIME IN HDR BRACHYTHERAPY: AN ALTERNATIVE TO RADIOGRAPHIC FILMS

M. Madebo, P. Roxby, A. Haworth, J. Cramb, and T. Kron

Peter MacCallum Cancer Centre, Melbourne, Australia
mebratu.madebo@petermac.org

Background: Alternatives to radiographic film for quality assurance (QA) in radiotherapy are required as film processors are phased out of hospitals in favour of digital imaging equipment. Challenges in using Computed Radiography (CR) for this application include high sensitivity compared with film and the light-proof cassette which normally encloses the imaging plate and moves the front surface of the plate away from radiation sources.

Objective: To investigate the usefulness of a Fuji Capusla XL CR equipment, as a replacement for film for autoradiographic tests in high dose rate (HDR) brachytherapy.

Methods: The areas of interest for autoradiographic tests are source position and dwell times. Measurements were performed using a Nucletron Microselectron mHDR at a dose rate of about $2cGym^2hr^{-1}$. The sensitivity of the CR reader was reduced to allow measurements of doses up to 3Gy for external beam radiotherapy QA. We investigated the use of CR as a QA tool for testing the accuracy of source positions and dwell times. In-house made collimator, which is an alternative strip of 1.2 mm lead and 1.47 mm Perspex, is used for determining the accuracy of source position for dwell position spacings of 2.5 mm and 5.0 mm. The distance of the source to the surface of the CR (hight of collimator) is 7.9 cm. A 3.1 mm lead is placed between source and CR plate to avoid saturation. Appropriate In-house made collimation is used to avoid primary radiation from one dwell location to another. In all cases, 20 cm stainless steel pro-guide is used. With proper collimation between dwell positions, the accuracy of dwell position and dwell time is checked against that set by the treatment planning system. The minimum visually observable distance between dwell positions (without collimation) has also been determined.

Results and discussion: The high sensitivity of the CR system allows assessing source anisotropy in the images and transit dose in the pathways. The minimum visually observable distance between two source positions without collimation is found to be 7.5 mm. We have also confirmed the linearity of dose with dwell time within less than 3%. A transit (pathway) dose is also observed in the CR image and is being measured to determine its clinical significance to patients. From our investigation, CR was found to be an acceptable alternative to film for autoradiography-based quality assurance and comprehensive results and methods used will be presented at the conference.

COMPARISON OF TWO RADIOTHERAPHY RESPIRATORY GATING DEVICES

J. McNamara[1], P. Metcalfe[1] and M. Williams[1,2]

[1]*Centre for Medical Radiation Physics, University of Wollongong, Wollongong, Australia*
[2]*Illawarra Cancer Care Centre, Wollongong, Wollongong, Australia*

INTRODUCTION: Lung tumours have been found to move up to 5 cm due to respiratory motion. [1] This can cause large artifacts and inaccurate delineation of target volumes in CT based treatment plans. Respiratory gating abates this problem by allowing only selected portions of the breathing waveform to be reconstructed, between specified time intervals, or specified amplitudes. The Illawarra Cancer Care Centre currently utilises the ANZAI AZ-733V respiratory gating system coupled with the Siemens Sensation Open scanner for radiotherapy treatment purposes. The Real time Position Monitoring (RPM) system (Varian Medical Systems, Palo Alto, CA) has been purchased for use with the Varian linear accelerators in the clinic. In order to utilise gating for treatment purposes it is necessary to ensure that the two gating systems correlate.

METHODS: The ANZAI respiratory gating system, consisting of a belt with a strain gauge, was placed at the same external chest wall location as an infrared camera-based motion-tracking system, (RPM, Varian). A time stamp was devised and the respiratory waveforms recorded simultaneously for a cohort of 5 staff volunteers. The breathing waveforms were also collected for the external surrogates placed at separate chest wall locations.

RESULTS: The correlation was found to be 91.3%-96.8% when both the ANZAI pressure sensor and the RPM infrared motion-tracking device were placed in the same location on the chest wall. When placed in separate locations the results varied greatly for individuals, correlation ranging from 59.6%-96.2%. A phase shift between markers in separate locations was noted in 3 of the individuals.

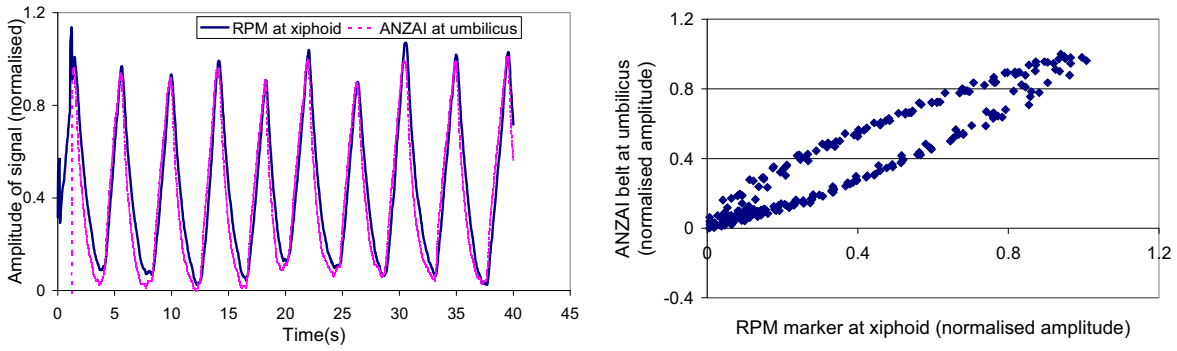

Figure 1. *(a) Comparison of breathing waveforms for ANZAI and RPM systems vs time. (b) Scatter plot of ANZAI vs RPM waveforms illustrating reduced correlation due to phase shift.*

DISCUSSION & CONCLUSIONS: When placed in the same position, the breathing waveforms obtained from the RPM respiratory gating system and the ANZAI belt correlate reasonably well. The importance of marker positioning between planning and treatment was made apparent by the variation in results due to location. Phase shifts between markers positioned on the xiphoid and umbilicus can be attributed to independent motion of ribcage and abdomen. [2] Further research into chest wall motion and the adequacy of external surrogates to model internal tumour movement is needed.

REFERENCES:

[1]*P. Keall (2006) Medical Dosimetry, 31, 2: 152-162.*
[2]*K.Konno, J. Mead, (1968) Journal of Applied Physiology, 24: 544-548.*

EUD OBJECTIVES FOR IMRT PROSTATE PLANS

P. Metcalfe[1], N. Hardcastle[1], A. Miller[2] and K. Foo[2]

[1]*Centre for Medical Radiation Physics, University of Wollongong, Australia*
[2]*Illawarra Cancer Care Centre, Wollongong, Australia*

INTRODUCTION: IMRT has proven efficacy in head and neck cancer treatment. Plans and clinical trials show parotid gland sparing and reduced Xerostomia[1]. Due to cost reimbursement differences Australian centres have been somewhat slower than US centres in examining the merits or not of IMRT prostate plans versus conformal prostate plans. Effective Uniform Dose (EUD)[2] has been found to be useful as a planning objective tool.

METHODS: Plan trials were compared using dose volume histograms (DVH's) for conformal versus IMRT and conformal versus EUD optimised IMRT plans using a radiotherapy treatment planning tool (Pinnacle version 8.0 with DMPO). EUD is a way of weighting the mean dose with a biological parameter. The EUD formulas are:

$$EUD = \left(\frac{1}{N} \sum_{i=1}^{N} D_i^a \right)^{\frac{1}{a}} [1] \qquad F = \prod_j f_j \; [2] \quad \text{for organs at risk} \quad f_j = \frac{1}{1 + \left(\frac{EUD}{EUD_0} \right)^n} \; [3]$$

Where in eqn [1] N is the number of voxels, D_i is the dose in the *ith* voxel, and a characterises dose-volume effect. The EUD formalism is easily differentiable see eqn [2] which makes it a good candidate as an inverse planning objective function tool for IMRT. For organ at risk see eqn [3] n is the weight which indicates the structure dependent endpoint[3].

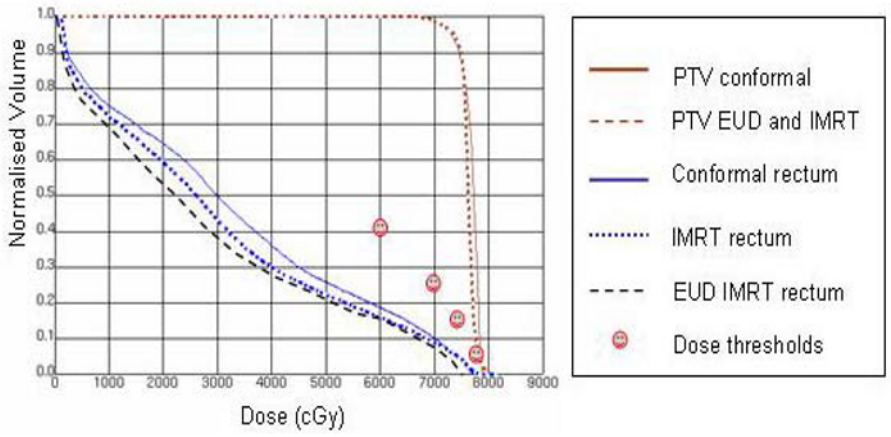

Figure 1. *DVH comparison conformal versus IMRT and EUD IMRT.*

DISCUSSION & CONCLUSIONS: Fig 1 shows all plan trials display rectal DVH's well below suggested clinical trial dose thresholds (e.g., Pollack et al.[4]). With a comparative five field IMRT prostate plan using several dose objectives rectal doses are lower than the conformal plan trial comparison (see fig 1). We have also produced an even lower DVH to rectum using a single effective uniform dose (EUD) objective to 50Gy with a=6 (see EUD IMRT fig 1). A homogeneous target dose can also been met using two EUD objectives[3]. All three plan trials had an efficiently low monitor unit MU/dose ratio (nominally 400 MU/200cGy) hence the time overheads between conformal and IMRT dose delivery are converging. However there are other issues to consider. These include prostate inter-fraction movement and the different temporal distribution between conformal and IMRT dose delivery.

REFERENCES:

[1]*Lee N. et al. (2002) Int. J. Rad. Onc. Biol. Phys. 53: 12-22.*
[2]*Niemierko A. (1997) Med. Phys. 24: 103-110.*
[3]*Wu Q. et al. (2002) Int J. Rad. Onc. Biol. Phys. 52: 224-235*
[4]*Pollack A.et al. (2002) Int. J. Rad. Onc. Biol. Phys. 53: 1097-1105.*

EVIDENCE FOR INTENSITY MODULATED RADIOTHERAPY (IMRT)

P. Metcalfe[1] and M.J. Williams[2]

[1]*Centre for Medical Radiation Physics, University of Wollongong, Australia*
[2]*Illawarra Cancer Care Centre, Wollongong, Australia*

INTRODUCTION: IMRT has proven efficacy in head and neck cancer treatment. Plans and level II clinical trials show parotid gland sparing and reduced Xerostomia[1]. While level III clinical trials comparing conformal with IMRT treatment of the head and neck clinical sites may or may not be successfully recruited, the technique is being widely adopted by most centres using an "equipoise" approach.

METHODS: *Head and Neck* - Plan comparisons clearly show reduced dose to parotid glands with associated reduced xerostomia, while follow up needs to proceed for some years as yet there is no evidence to suggest different local recurrence rates. The credence given to a trial can be grouped into various levels of evidence. *Level III-1* evidence is obtained from well designed pseudo-randomized controlled trials. The evidence for head and neck IMRT is probably currently *Level III-1*. On the flip side there is some discussion that IMRT may slightly increase the risk of secondary cancer formation[2]. It is becoming increasingly important to provide QA for trials using an associated level III dosimetry survey of centres participating in

clinical trials. There is a proposal to do an Australasian level III dosimetry study involving an "Inter-Comparison of Australian Radiotherapy IMRT Systems (ICARIS)".
Prostate - While a prostate dose escalation report showing reduced rectal toxicity in the IMRT arm represents a historical cohort study (Level III-II evidence), these results showing 14% versus 2% grade II rectal toxicity are somewhat compelling[3]. Hence another level III dosimetry survey linked to an IMRT prostate dose escalation trial is another future possibility. A pioneering level III dosimetry survey of Australasian centres has been successfully completed in association with a TROG prostate trial[4](not IMRT). This provides an excellent framework for future level III dosimetry studies.

DISCUSSION & CONCLUSIONS: *Head and Neck* - With the introduction of monoclonal antibody agents such as cetuximab which act independently of radiation enhancement[5], it is likely the added advantage of applying concurrent boosts with IMRT will also be exploited more in future with accelerated regimens. Hence associated dosimetry studies of these complex IMRT treatments becomes essential.
Prostate-While the adoption of IMRT for prostate treatment in Australia has been slow this is not the case for most overseas centres. With the establishment of several phase III hypofractionation trials for prostate treatment[6] it is perhaps pertinent that IMRT treatment for prostate be re assessed in Australia as it may add some dose sparing value over and above that established using image guided radiotherapy (IGRT) techniques alone. Once again an associated IMRT level III dosimetry study associated with a prostate hypofractionation trial would be a very useful QA tool.

REFERENCES:

[1]*Lee N., Garden A., Kramer A., Xia P. (2005) RTOG 0225: A phase II study of intensity modulated radiation therapy (IMRT) +/- chemotherapy for nasopharyngeal cancer.*
[2]*Hall E., Wuu C. (2003) Radiation induced second cancers: the impact of 3D-CRT and IMRT. Int. J. Rad. Oncol. Biol. Phys. 56: 83-88.*
[3]*Hanks G.E., Krall J.M., Hanlon A.L., Asbell S.O., Pilepich M.V., Owen J.B.*
(1994) Patterns of care and RTOG studies in prostate cancer: Long term survival, hazard rate observations, and possibilities of cure. Int. J. Rad.. Oncol. Biol. Phys. 28: 39–45.
[4]*Ebert M. (2007) Private Communication.*
[5]*Bonner J., Harari P., Giralt J., Azarnia N. et al. (2006) Radiotherapy plus cetuximab for squamous cell carcinoma of the head and neck. N. Engl. J. Med. 354: 567-578.*
[6]*Pollack A., Hanlon A., Horwitz E., Feigenberg S. et al. (2005) Dosimetry and preliminary acute toxicity in the first 100 men treated for prostate cancer on a randomized hypofractionated dose escalation trial. Int. J. Rad. Oncol. Biol. Phys. 18:115-120.*

IMPLEMENTATION OF IMAGE-GUIDED 6D PATIENT POSITION CORRECTION INTO CLINICAL ROUTINE

J. Meyer[1,2], M. Guckenberger[2] and J. Wilbert[2]

[1]*Department of Physics & Astronomy, University of Canterbury, Christchurch, New Zealand*
[2]*Department of Radiation Oncology, University Hospital Wuerzburg, Germany*

INTRODUCTION: Kilo-voltage X-ray tubes attached to the gantry of a linear accelerator allow X-ray volume imaging of radiotherapy patients on the treatment couch (Fig. 1). With these so-called cone-beam computed tomography (CBCT) scanners anatomical information can be obtained at the time of treatment. Co-registration between the initial planning CT and the CBCT gives information regarding differences in patient set-up and organ positions. Having obtained this information the patient position can be corrected accordingly by either a standard couch (typically 3 translational corrections) or by means of a robotic couch with 6 degrees of freedom (3 translational and 3 rotational corrections). In this work the process of implementing CBCT image-guidance and subsequent 6D position correction into clinical routine is described.

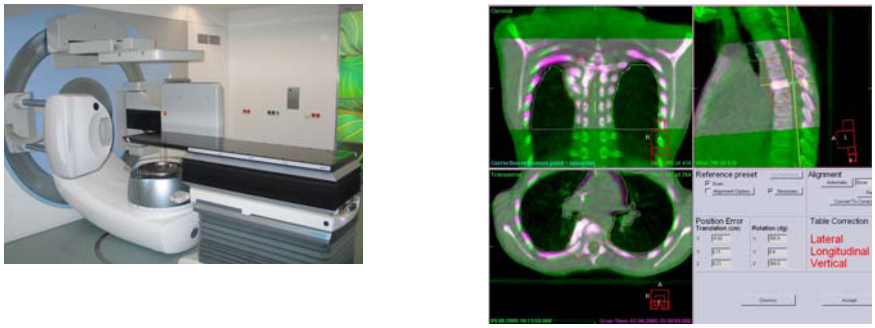

Figure 1. *a) Linac with cone-beam CT and robotic hexapod table; b) Rigid body image registration in 6D between CT and CBCT*

METHODS: To compare the differences between the established method and CBCT both orthogonal portal images (anterior, lateral) and CBCTs were taken on an Elekta Synergy S with X-ray volume imaging (XVI) for a number of patients

[1]. Independently, a CBCT phantom study was conducted to evaluate the accuracy of 2 different image registration algorithms, the reproducibility of the mechanical parts of the CBCT system and subsequent 6D position corrections by means of the robotic hexapod couch (Medical Intelligence) [2]. Last but not least the relative merits of 6D versus 3D position correction was analysed by simulating different clinical scenarios in a treatment planning system.

RESULTS & DISCUSSION: The accuracy of CBCT compared well to orthogonal portal images. CBCT showed advantages for soft tissue visualisation but is also less vulnerable to inter-observer differences. The phantom studied revealed sub-millimetre and sub-degree position accuracy for the combination of CBCT and robotic couch (mean error of <0.2mm and <0.2º). The grey value match was able to detect smaller artificially induced translational and rotational errors compared to the bone match. For elongated target volumes and sharp dose gradients both translational and rotational errors can lead to underdosage in the target volume and increased dose to the adjacent organs-at-risk.

CONCLUSIONS: Image-guided adaptive radiotherapy has been successfully implemented into clinical routine. The method has been compared favourably to the current standard and in addition it was found that sub-millimetre and sub-degree accuracy is reproducibly achievable with the hard- and software investigated. Patients with elongated target volumes and patients for which steep dose gradients are required will befit most from image-guided radiotherapy and 6D position correction.

REFERENCES:

[1]*Guckenberger M, Meyer J, Vordermark D, Baier K, Wilbert J, Flentje M., (2006) Int J Radiat Oncol Biol Phys. 65(3):934-42*
[2]*Meyer J, Wilbert J, Baier K, Guckenberger M, Richter A, Sauer O, Flentje M., (2007) Int J Radiat Oncol Biol Phys. 67(4):1220-8.*

MODELLING TUMOUR TRAJECTORIES AS A FUNCTION OF RESPIRATORY MOTION

J. Meyer[1,2], K. Lenz[1], P. Wilson[3], J. Wilbert[2], M. Guckenberger[2], A. Richter[2] and K. Baier[2]

[1]*Department of Physics & Astronomy, University of Canterbury, Christchurch, New Zealand*
[2]*Department of Radiation Oncology, University Hospital Wuerzburg, Wuerzburg, Germany*
[3]*Department of Mathematics, University of Canterbury, Christchurch, New Zealand*

INTRODUCTION: Intra-fractional movement of lung tumours necessitates considerable treatment margins around the lesion to ensure sufficient dose coverage. These margins are referred to as internal target volume (ITV). The ITV can be several folds larger than the actual planning target volume (PTV) for comparable stationary tumours. Consequently this results in a high dose to the surrounding lung tissue. Gating the treatment, breath hold or even compensating for the tumour movement in real-time has the potential to reduce margins and hence spare healthy tissue [1]. To accomplish this safely it is essential to know the exact tumour position over time to prevent target misses. In this work several models are investigated with respect to their suitability to correlate external respiratory signals with tumour movement.

METHODS: Data for the modelling were based on hypo-fractionated stereotactic lung treatments and were acquired with the Wuerzburg Adaptive Tumour Tracking System (WATTS). Respiratory signals were acquired in two different ways. One was by means of a pressure sensitive belt (Anzai) around the abdomen of the patient and the other was by means of spherical reflectors placed on the abdomen. The reflectors were tracked at a high frame rate with an infra-red tracking camera (Polaris) [2]. With the former a 1D respiratory signal was obtained and with the latter a 3D vector representing the motion of the abdomen. The tumour trajectory was obtained by tracking the tumour in consecutive megavoltage portal images at a rate of approximately 3 images per second [3]. Several different algorithms were applied to model the relationship between the external respiratory signal and internal tumour motion. The models were applied retrospectively and investigated in terms of how well they could reproduce the tumour path given a respiratory signal and whether one of the two respiratory signal was more suited than the other. In a further comparison it was examined whether the breathing pattern changed over a period of several treatment fractions, i.e. whether the same models could be applied for every treatment fraction.

RESULTS & DISCUSSION: The relationship between respiration and tumour movement can be modelled very accurately with a resulting root-mean-square error (RMS) of below 1mm. Models based on the 3D respiratory signal were superior to the 1D respiratory signal in describing tumour motion not along the main axis of tumour movement. This resulted generally in smaller RMS errors. Variations in model fit between consecutive treatment fractions were observed. They are likely to be due to differences in placement of the reflectors/belt but might also be due to a change in the breathing pattern of individual patients.

CONCLUSIONS: In conclusion it is possible to model the correlation between respiratory motion and the tumour trajectory. More work is necessary to understand and accommodate the changes in the relationship between the breathing signal and tumour movement over consecutive fractions.

REFERENCES:

[1]*M. Engelsman, G. C. Sharp, T. Bortfeld, R. Onimaru, and H. Shirato, (2005) Phys Med Biol; 50, 477-490.*
[2]*J. Meyer, K. Baier, J. Wilbert, M. Guckenberger, A. Richter, and M. Flentje, (2006) Acta Oncol; 45, 923-934.*
[3]*J. Meyer, A. Richter, K. Baier, J. Wilbert, M. Guckenberger, and M. Flentje, (2006) Med Phys; 33, 1275-1280.*

INTRODUCTION – THE DEVELOPMENT OF IMRT TO 2007

L. D. Oliver[1]

[1]*Department of Radiation Oncology, Royal North Shore Hospital, St Leonards, Australia*

INTRODUCTION: The goal for external beam radiotherapy is to deliver a controlled dose of megavoltage ionising radiation sufficient to eradicate the malignancy whilst reducing the dose to the surrounding normal tissue as much as possible. The means of treating the patient improved significantly around 1990 with the advent of 3-dimensional imaging techniques and more sophisticated beam shaping using multileaf collimators (MLC) to define the target and shield organs at risk (OAR).

METHODS: The MLC replaced cumbersome shielding blocks, automatically shaped the linear accelerator high energy beam and made conformal radiotherapy a much improved standard of radiotherapy practice. The MLC and other similar devices promulgated a huge amount of physics research, development and quality assurance work for intensity modulated radiotherapy (IMRT) techniques. Old conventional methods of IMRT such as metal wedges, compensators and even the dynamic wedge were replaced by the dynamically moving collimators. Thus dynamic IMRT became a new tool that could replace conventional 'open, static beams'. Multiple fields of varying intensity beamlets were able to produce very complex target-dose shapes. The OAR dose, in most cases, was limited well below their tolerance whilst the target was elevated to much higher doses.

RESULTS: By 1998, dynamic treatment techniques were extensively reported in the literature with excellent reviews published since then[1,2]. Many overseas treatment centres have reported a number of IMRT clinical trials. However, other initiatives have also evolved to be an integral part of IMRT. Inverse planning, dose optimisation algorithms, IMRT for moving targets, image-guided and gated radiotherapy, cone beam imaging and transmission dosimetry are all complex adjuncts to consider.

DISCUSSION & CONCLUSIONS: In such a complex use of equipment and treatment techniques, there is a heavy reliance on testing, implementing and monitoring the accuracy of all steps in the treatment process. Medical physics plays a pivotal role to ensure that IMRT planning and treatment dosimetry is in fact what it is claimed to be. Once a protocol is established to verify the dosimetry using an agreed method of treatment, an Australian and New Zealand clinical trial for suitable types of cancer therapy should be established. Without any evidence based trial, it is difficult to show the clinical success of IMRT – Nationally or Internationally.

REFERENCES:

[1]*S. Webb, Intensity-Modulated Radiation Therapy, Series in Medical Physics, Institute of Physics Publishing (2001).*
[2]*Memorial Sloan-Kettering Cancer Center, A Practical Guide to Intensity Modulated Radiation Therapy, Medical Physics Publishing (2003).*

THE IAEA PROGRAMME OF ACTION FOR CANCER THERAPY

L. D. Oliver[1]

[1]*Department of Radiation Oncology, Royal North Shore Hospital, St Leonards, Australia.*

INTRODUCTION: The International Atomic Energy Agency (IAEA) was awarded the Nobel Peace Prize on 10 December 2005. To acknowledge receiving this prestigious award, the IAEA arranged three special workshops in the regions of Asia, Africa and South America[1]. These special events brought together high-ranking delegates from IAEA member countries within their regions. The theme of the *workshop was on human resources development in radiation oncology in the context of cancer control programs.* This paper presents information on the world cancer incidence provided by the International Agency for Research on Cancer (IARC). Details of the IAEA Programme of Action for Cancer Therapy (PACT)[2] are also presented.

METHODS: The IAEA is seeking urgent action with other International health bodies by building partnerships to stop the global cancer epidemic. At the IAEA Asia Pacific Workshop held in Bangkok, Thailand on 4-8 December 2006, delegates met to consider the state of the world's cancer burden and specifically addressed the shortage problem of adequately trained radiation oncology professionals and the need for more radiotherapy equipment. Other meetings followed in Cape Town and Buenos Aires.

RESULTS: Epidemiological research on cancer has shown that, despite an increased knowledge about the prevention and treatment of cancer, the number of new cases continues to grow. Statistics collated by World Health Organisation and the International Union Against Cancer indicate that the world cancer incidence comprises 6.7 million deaths, 10.9 million new cases, and 24.6 million living with cancer. Unless there is a substantial plan of preventative action there could be in the order of a 50% increase to 10.3 million deaths and 16 million new cancer cases by 2020[3,4].

The alarming outcome from this research is that the incidence of cancer was much the same in all countries in 1990. By 2020, two thirds of new cancers will occur in newly industrialised or developing countries where there are critical shortages of radiotherapy equipment and experienced radiation oncology professionals to meet the need.

DISCUSSION & CONCLUSIONS: It is very evident that the gap in cancer incidence is widening between developed and developing countries. Much of this trend is due to the life style and environment in these countries. PACT provides some basic strategies that can reduce the cancer incidence. PACT needs substantial funds to implement it as soon as possible. The Australian and New Zealand governments and radiation oncology professionals should be aware of the need to support other less fortunate Asian and Pacific countries by providing support for personnel training and mentor expertise in future years.

REFERENCES:

[1]*IAEA Nobel Peace Prize Cancer and Nutrition Fund, www.iaea.org/nobelfund*
[2]*IAEA Programme of Action for Cancer Therapy, pact@iaea.org*
[3]*WHO and UICC Publication (2005) Global Action Against Cancer., Geneva.*
[4]*WHO Executive Summary, (2002) National Cancer Control Programme, Geneva.*

PRELIMINARY BEAM SIMULATIONS OF A PROTOTYPE PROTON COMPUTED TOMOGRAPHY SYSTEM

S.N. Penfold[1], A.B. Rosenfeld[2] and R.W. Schulte[3]

[1,2]*Centre for Medical Radiation Physics, University of Wollongong, Australia*
[3]*Department of Radiation Medicine, Loma Linda University Medical Centre, Loma Linda, California*

INTRODUCTION: Proton radiation has many proven advantages in radiation therapy. This is primarily due to its capability to deliver high doses to well defined tumours that lie close to critical structures. However, for proton therapy to be successful, the range of protons in tissues must be accurately known. Currently, proton dose calculations are performed based on image data obtained with X-ray CT (xCT). The use of this mode of imaging partially nullifies the advantages of proton radiation due to the difference in physical interactions between photons and protons. For this reason, proton computed tomography (pCT) has been suggested [1] as a possible imaging modality for proton radiation treatment planning. This paper reports on the GEANT4 simulation results obtained in a measurement of beam profile and reconstruction accuracy for a prototype pCT system. In particular, a cone beam geometry has been specified with the use of only downstream proton tracking silicon strip detectors (SSD's).

METHODS: In order to reduce cost and negate the need for synchrotron radiation, the performance of the proposed geometry has been simulated with the GEANT4 Monte Carlo toolkit. From a measurement of the angular distribution of the proton beam emerging from various thicknesses of lead scattering foil, the location of isocentre of the respective system can be calculated. Isocentre is defined by the downstream point at which the beam displays a FWHM of 5cm. At this point a measurement of the energy profile of the beam is carried out to determine beam quality.
While the accuracy of the most likely path [2] reconstruction algorithm, specific to pCT, has been tested for a flat beam geometry with both upstream and downstream tracker information, its use in the system described above has had to be modified. The accuracy of the calculated path has been tested, again, with the use of GEANT4.

RESULTS: Beam profile and energy profile at isocentre are displayed for one instance of Pb scattering foil in Figure 1.

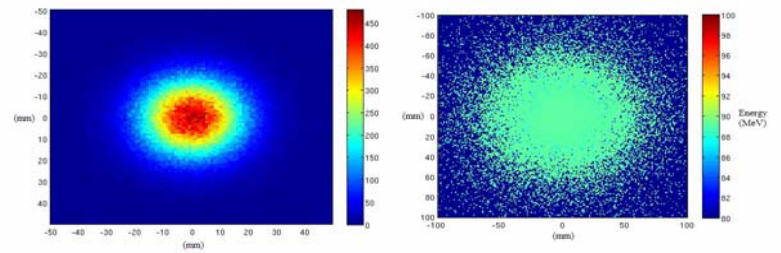

Figure 1. *Beam profile is displayed on the left for a Pb scattering foil thickness of 2.5mm, while the corresponding energy profile is displayed on the right.*

DISCUSSION & CONCLUSIONS: With the use of the GEANT4 simulation toolkit, the effect of lead scattering foil thickness on beam profile and isocentre location was successfully observed. This will be taken into account in the production of the physical system at Loma Linda University Hospital, Proton Treatment Centre.

REFERENCES:

[1]*R. Schulte et al., (2003) Design of a Proton Computed Tomography System for Applications in Proton Radiation Therapy, Nuc. Science Symposium Conf. Rec., IEEE, 3:1579-1583.*
[2]*D.C. Williams, (2004) The Most Likely Path of an Energetic Charged Particle Through a Uniform Medium, Phys. Med. Biol. , 49:2899-2911.*

MEASUREMENT OF DOSE UNDER EYE SHIELDS IN KILOVOLTAGE X-RAY

Sian Price[2], Martin J. Butson[1,2,3], Tsang Cheung[1] and Peter K. N. Yu[1]

[1]*City University of Hong Kong , Dept. of Physics and Materials Science, Kowloon Tong, Hong Kong*
[2]*Illawarra Cancer Care Centre, Department of Medical Physics, Crown St, Wollongong, Australia*
[3]*Centre for Medical Radiation Physics, University of Wollongong, Wollongong, Australia*

INTRODUCTION: Eye shields are used in kilovoltage x-ray treatment of the periorbital region. This is performed to minimize dose delivered to the cornea, lens and retina. The introduction of an eye shield however also introduces effects on dosimetry and scatter conditions of the treatment. This presentations looks at dose under eye shields and some dosimetric effects of the shield on tumour dose.

METHODS: EBT Gafchromic film is used to measure radiation doses around eye shield both in front of in areas such as eye lids and behind to estimate eye dose. EBT was chosen due to its high spatial resolution and its relatively low energy dependence.

RESULTS: Results show that primary beam photon are almost completely removed by the eye shield however significant doses (up to 20% of max) are still present under the eye shield due to back scatter contributions. These values are found to be energy and field size dependant. EBT Gafchromic was found to be a very suitable dosimeter for this region as high spatial resolution is required along with a relatively energy independent detector.

DISCUSSION AND CONCLUSION: Dose under eye shields was found to be significant due to backscatter contributions with energies around the 125kVp to 150kVp producing the highest eye doses. As field size increased the eye dose also increased which was expected due to scattering conditions of kilovoltage x-rays. Of importance for clinical consideration is that there can still be a significant dose under eye shields which cannot be removed no matter what the shield thickness is. Also of clinical importance is the reduced dose to a tumour which is located above the shield due to the variation in backscatter contributions from a high z material compared to water.

KEYWORDS: Radiochromic film, Gafchromic^{TM} EBT, kilovoltage, eye shields

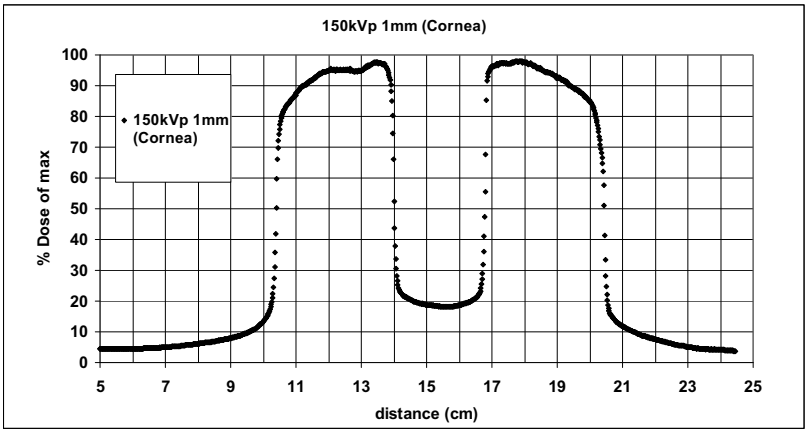

PARTIAL BREAST IRRADIATION USING MAMMOSITE BRACHYTHERAPY – CLINICAL EXPERIENCE

K. Quach[1], R. Nelligan[1], M. Borg[2] and E. Bezak[1]

[1]*Department of Medical Physics, Royal Adelaide Hospital, Adelaide, Australia*
[2]*Department of Radiation Oncology, Royal Adelaide Hospital, Adelaide, Australia*

INTRODUCTION: A feasibility study has been performed regarding the practicality, efficiency and safety of MammoSite brachytherapy as an accelerated partial breast irradiation (boost phase) for early stage breast cancer following conservative surgery[1]. Potential advantages of MammoSite brachytherapy are: high localised dose with rapid falloff for normal tissue sparing, minimum delay between surgery and RT, catheter moves with breast, improved local control, no exposure to staff (compared to LDR), likely side-effects reduction and potential cost and time saving (eg for country patients).

METHODS: Six patients received 9-10 Gy dose at 1 cm from the Mammosite balloon (MSA, Proxima Therapeutics, USA) surface in two fractions 6 h apart. EBRT to the whole breast commenced 1-5 days following brachytherapy. MammoSite treatments were planned using Plato Nucletron Brachytherapy Insight TPS, using patient CT and X-ray images. A single dwell position was determined in the centre of the balloon and treatment was delivered using Nucletron Microseletron HDR unit with Ir-192 source. Simulator and Mobile II images were taken before each fraction to confirm the dwell position and the balloon diameter before each fraction. TLDs positioned on the breast surface were used to determine the skin dose (with balloon surface-to-skin distance between 7-19 mm).

RESULTS: All insertions were well tolerated, and scars healed within 3-5 days. Computer planning time took up to 2 h and the HDR treatment lasted ~5-8 minutes per fraction. Planning time decreased to ~25 min for the 6th patient. TLD dosimetry showed that high skin doses were recorded in some areas of the breast surface. Skin doses (Table 1) ranged from 1 to 7 Gy with an average dose ranging from 2 to 4 Gy.

Table 1. *MammoSite TLD dosimetry results.*

Patient no	TLD position / Dose (Gy)						
	1	2	3	4	5	6	Average skin dose (Gy)
1	2.19	3.77	6.36	6.99	2.22	-	4.31
2	1.75	1.89	2.07	2.17	2.2	2.02	2.02
3	2.19	3.77	6.36	6.99	2.22	-	4.31
4	1.44	2.39	5.13	4.96	3.28	2.14	3.22
5	2.82	3.38	1.52	1.11	1.75	2.07	2.11
6	7.46	3.72	1.32	0.93	1.44	3.05	2.99
						Total Avge:	3.16

DISCUSSION & CONCLUSIONS: CT planning was ideal for the optimization of the treatment plans and to ensure that any air pockets had been dissolved. Reactions observed were mild and resolved within 2 weeks of completion of treatment. However, a number of factors (eg long term effects of HDR on normal tissues, the optimal distance to cover beyond the tumour cavity, biological effective dose, graduated inhomogeneity of a single point source, etc) must still be investigated to use this technique as a routine treatment modality.

REFERENCES:

[1] *M. Borg at al, (2007) Australasian Radiology ,51:53-61.*

RADIATION DOSE ENHANCEMENT BY GOLD NANOPARTICLES IN KV RANGE OF X RAYS BEAMS

W.N.W.A. Rahman[1], N. Bishara[1] and M. Geso[1]

[1] *Dicipline of Medical Radiation, School of Medical Sciences, RMIT University*

INTRODUCTION: Increasing the absorbed X ray dose to the targets while sparing the healthy tissue tolerance remains the big challenge in radiotherapy. Techniques are investigated to enhance local control of tumour while preserving more efficiently the normal tissues. Application of gold nanoparticles to enhance dose in targets offers considerable promise due to photoelectric interaction. The flux of photoelectrons, characteristic x rays and Auger electrons produce a highly localized dose enhancement in the targets. In this study, we experimentally demonstrated dose enhancement produced by the gold nanoparticles *in vitro* and the optimum energy required to increase absorbed x ray doses are also been investigated. The dose enhancement is investigated via cell survival curves.

METHODS: Experiments were performed with the mouse endothelial cells irradiated with 65 kV photon beams from PANTAX MXT 225 superficial therapy machine. Different gold nanoparticles concentrations and different photon energies were tested. The cell survival curves for the cells treated with the gold nanoparticles were compared to the control.

RESULTS: Estimation of dose enhancement factor (DEF) and its variation with photon energy is depicted in the Figure. Maximum dose enhancements are observed around 40 kev and reaching about 160 of DEF when gold nanoparticles concentration is 100%. Slightly lower dose enhancement values were obtained empirically in this work using a 65 kV x-ray beam. Cell survival curves with and without nanoparticles are compared. Lower survival rates are observed when cells are mixed with gold nanoparticles solutions.

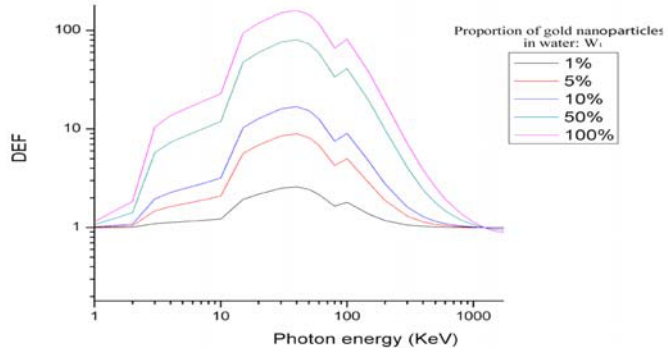

DISCUSSION & CONCLUSIONS: Similar trend of dose enhancement variations with beam energy and gold concentrations were observed in both theoretical and experimental data. The results show that gold nanoparticles enhance the sensitivity of MEC cells to kilovoltage X-ray beams. It can be concluded that dose to the tumours can be enhanced in the presence of the gold nanoparticles for the external beam radiotherapy and highest enhancement is obtained at optimum energy as predicted from the absorption calculations and also at optimum gold concentration.

REFERENCES:

[1]*S Corde, A. J., JF Adam, AM Charvet, JF Le Bas, F Esteve , H Elleaume, J Balosso (2004). "Synchrotron radiation-based experimental determination of the optimal energy for cell radiotoxicity enhancement following photoelectric effect on stable iodinated compounds." British Journal of Cancer 91(3): 544-551.*

WHAT ACCURACY IS REQUIRED OF PREDICTED TRANSMITTED DOSE MAPS FOR EPID DOSIMETRY IN BREAST CRT?

P. Reich[1,2], E. Bezak[1,2] and M. Mohammadi[3]

[1]*Department of Medical Physics, Royal Adelaide Hospital, Adelaide, Australia*
[2]*School of Chemistry and Physics, University of Adelaide, Adelaide, Australia*
[3]*Department of Medical Physics, Hamadan University of Medical Sciences, Hamadan, Iran*

INTRODUCTION: There are two main approaches to EPID dosimetry. One approach involves a back-projection of an EPID dose map to a plane inside a patient CT data set followed by a systematic reconstruction of delivered dose in 3D[1]. The second approach compares an EPID dose map measured during treatment with a predicted or calculated 'EPID' dose map based on the patient's treatment planning data[2]. Both procedures are known to have limitations in their ability to accurately verify patient treatment delivery. In the latter approach, 4 % agreement between EPID dose maps predicted by a TPS and actual EPID dose measurements under heterogeneous phantom conditions have been reported[1]. Given this difference, it remains to be shown what level of accuracy in transmitted dose calculations is required for detecting true differences in planned and delivered doses. The aim of this particular study was to simulate patient positioning errors combined with a range of possible breathing excursions of breast CRT treatments as reported in the literature and to determine whether differences in resultant transmitted dose difference maps exceed 4 %.

METHODS: CT scans from a patient archive were used to plan two treatment techniques; namely a supraclavicular (SC) breast CRT technique and an opposing tangents (OT) technique. A water equivalent EPID model was incorporated into each of the plans and the transmitted dose was calculated for each of the beams in the two plans using Pinnacle TPS. Patient breathing excursions were simulated by shifting the beams with respect to the CT data and patient positioning errors were simulated likewise. Dose difference (DD) maps were then calculated to quantify any differences detected in transmitted dose.

RESULTS: In the SC technique, simulated breathing excursions of 2.1/10.6 mm combined in the ant/post and lateral directions produced transmitted DDs (from the tangential fields only) greater than 10 % at the surface of the breast. Combining breathing with positioning errors of 2.5 mm along the superior/inferior axes had no additional effect on the DD maps. For the anterior-posterior field, breathing excursions of 2.1mm/10.6 mm parallel to the beam central axis, produced dose differences less than 4 %. When combined with positioning error of 2.5 mm along the superior-inferior axis, dose differences exceeded 4 % but only for a few pixels. Results were nearly identical for the OT technique.

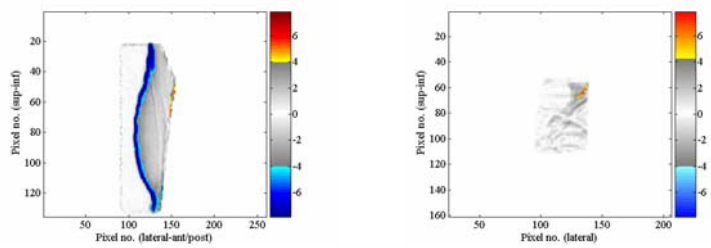

Figure 1. *Transmitted DD maps. (a) OT technique: lateral tangent field; 2.1 mm breathing excursion (anterio-lateral direction), (b) ST technique: anterio-posterior field; 2.1 mm breathing excursion (posterior direction) combined with 2.5 mm positioning error (inferior direction).*

DISCUSSION & CONCLUSIONS: The current accuracy of 4 % in predicted EPID dose maps relative to measured EPID maps under heterogeneous conditions may be acceptable for detecting possible breathing and/or set up errors relating to breast CRT treatments.

REFERENCES:

[1]T.R. McNutt *et al*, (1995) *Med Phys,* 23:527-35.
[2]M. Wendling *et al* (2006) *Med Phys* 33:259-73.

OPTICAL FLUORESCENCE BACKGROUND IN OPTICAL FIBRE SCINTILLATOR DOSIMETERS

L. Reinisch[1], T. Chen[1], M.A. Alhabden[1], P. Butler[1], S. Alzaidi[1], G. Sorell[2] and M. Bird[2]

[1]*Department of Physics and Astronomy, University of Canterbury, Christchurch, New Zealand*
[2]*Department of Medical Physics and Bioengineering, Christchurch Hospital, Christchurch, New Zealand*

INTRODUCTION: We investigated the use of small scintillators attached to optical fibres to use as dosimeter or small area detectors. Background signals induced in the optical fibres were filtered with interference filters.

METHODS: We investigated three different scintillators (580, 490 and 420 nm), silica and plastic fibres irradiated in a 6MV photon beam from a Varian 600 C linear accelerator. The scintillator was fashioned as a cylinder, 3 mm in diameter and 10 mm long. This was fixed to the 1 mm optical fibre. The scintillator and fibre was irradiated as a function of angle and compared to the fibre, alone, irradiated a function of the incident angle. Exposures of 1 to 1024 monitor units were investigated. 8 cm of solid water was placed below and 1.5 cm of solid water was above the dosimeter. The scintillator signal was separated from the background with an interference filter and the light detected with a photodiode.

RESULTS: While the scintillator showed a linear response over the range of exposures measured, the radiation as a function of incident angle was not flat. The geometry is defined with 0˚ to be irradiation delivered perpendicular to the optical fibre. Irradiation angles pointing away from the photodiode are positive and those angles pointing towards the photodiode are negative. A slight increase in the signal of the fibre alone is noted as the radiation is angled towards the photodiode. A more significant increase in the signal from the scintillator and optical fibre when the radiation was angled towards and away from the photodiode.

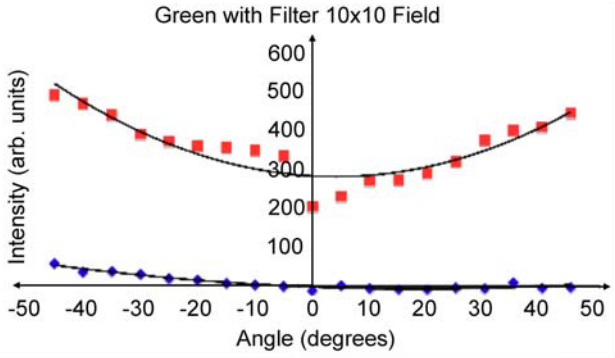

Figure 1. *Measured signal as function of incident angle. The squares are from irradiating the scintillator and optical fibre. The diamonds are from irradiating only the fibre.*

DISCUSSION & CONCLUSIONS: Although the optical filters are effective in blocking most of the Cherenkov radiation and fluorescence created in the optical fibre, there is still a significant change in the signal as a function of the incident angle when both the scintillator and optical fibre are irradiated. We can model this angular dependence of the signal as optical fluorescence in the scintillator created by the Cherenkov radiation. This background cannot be filtered with our optical filter system. This background is also not compensated in systems using two optical fibres with a scintillator on only one of the fibres.

IMRT DOSIMETRY VERIFICATIONS USING Portal Vision aS500^{TM} IMAGES AND Dosimetry Check^{TM}

L. W. Steven, R. A. Chappell, A. Nicolau and Chuan-Dong Wen

W. P. Holman Clinic, Royal Hobart Hospital, Hobart, Australia

INTRODUCTION: Clinical dosimetry verification of IMRT treatment has become major task for medical physicists and various methods have been introduced and practised routinely. We are commissioning a method of dosimetry verification using EPID images applied within Dosimetry Check^{TM}.It is complementary to our clinical QA procedures using RadCalc^{TM} for MU check, MapCheck^{TM} for intensity modulation and a chamber for absolute measurement at one location in a phantom. We have observed a good match between planned and 'delivered' dose in those head and neck cases we have studied, with somewhat poorer match in 'forward-planned' breast cases.

METHODS: MLC files are exported from the treatment planning system (Pinnacle$^{3\ TM}$ –*Philips Medical Systems*) and used to obtain integrated EPID images (Portal Vision aS500 – *Varian Medical Systems*). Each raw image is calibrated and renormalised to generate a dose map which is in turn deconvolved to incident fluence using a kernel with parameters fitted to the specific linac and EPID used (in our case, Varian 600C, 23EX and aS500)[1]. This reconstructed incident fluence is used

with the patient CT data set to compute the 3D dose distribution. These processes are accomplished using Dosimetry Check™ (*Math Resolutions, LLC, Columbia, Maryland, USA*).

The dose distribution can be compared in 2D and 3D with those of generated by the planning system. Tools for dose comparison are provided in Dosimetry Check™, these include dose volume histograms and 'gamma analysis' [2, 3].

RESULTS:

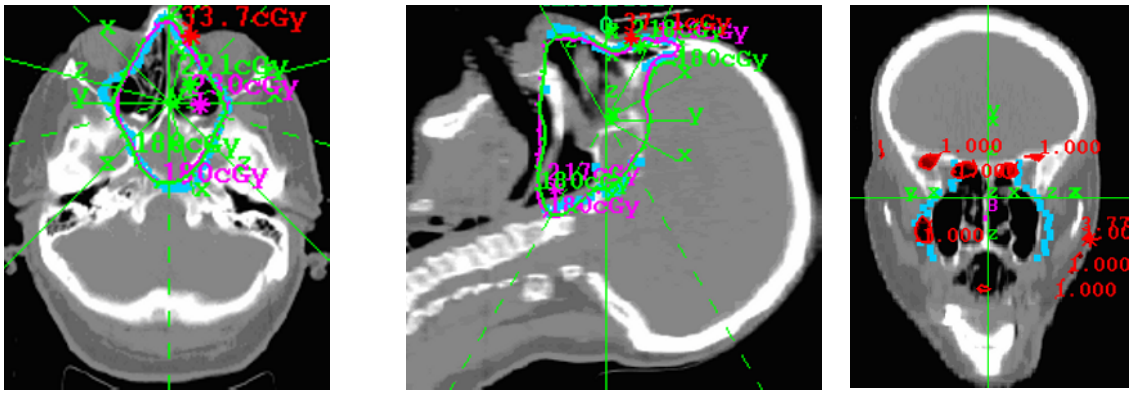

An IMRT H&N 7-Beam Non-coplanar Clinical Case Dose and Gamma Distributions

DISCUSSION & CONCLUSIONS: Dosimetry Check™ has the potential to be effective, accurate, and efficient EPID-based tool for dosimetry verification. It has the potential to save significant time and effort in performing QA, while providing the clinician, physicist and therapist with a clinically relevant comparison of intended and delivered radiation dose. The commissioning process and future work of Dosimetry Check™ will be discussed.

REFERENCES:

[1] *A method for deconvolution of integrated electronic portal images to obtain incident fluence for dose reconstruction Wendel D. Renner et al JACMP, Vol.6 No.4 Fall 2005.*

[2] *A technique for the quantitative evaluation of dose distributions Daniel A. Low et. al. Med.Phys.25 (5), May 1998.*

[3] *Evaluation of the gamma dose distribution comparison method Daniel A. Low et al Med. Phys.30 (9), September 2003.*

THE INCLUSION OF PET IMAGING IN INTENSITY MODULATED RADIATION THERAPY TREATMENT PLANNING FOR HEAD AND NECK CANCERS

R. Smith[1], B. Van Every[2], P. Jones[1], C. Evans[1], T. Mills[2], M.J. Kelly[2] and S. Davis[1]

[1] *William Buckland Radiotherapy Centre, The Alfred Hospital, Melbourne, Australia*
[2] *Nuclear Medicine Department, The Alfred Hospital, Melbourne, Australia*

INTRODUCTION: Intensity modulated radiation therapy (IMRT) allows curative doses to be delivered to a target volume that is typically in the region of critical anatomical structures. The inclusion of molecular imaging to provide further pathological information, not seen in regular CT simulation images, has been proposed to aid target volume delineation.

This work evaluates the usefulness of including PET images in IMRT treatment planning for head and neck cancer sites. We address the practical issue of how to accurately register a PET-CT data set with a radiotherapy planning CT data set. We also assess how to interpret the PET information and how this can be incorporated in the contouring of target volumes.

METHODS: A GE Discovery VH PET/SPECT/CT hybrid scanner located at The Alfred Hospital Nuclear Medicine department was used to acquire co-registered PET and CT data sets with the patient placed in the radiotherapy treatment position. Fiducial markers were used to fuse the PET-CT data to the radiotherapy planning CT data set. The Eclipse treatment planning system displayed all image sets together, allowing the radiation oncologist to consider the information provided by PET, while marking treatment volumes. The influence of PET information on the outlined treatment volumes was then assessed.

RESULTS: The results presented here are the initial 9 patients simulated using CT and PET-CT image sets and consequently treated with IMRT. Three patients had further treatment volumes added as a result of PET showing unrecognized metastatic spread to regional lymph nodes. Structural and PET imaging data showed concordant findings in 5 patients, and in the last case PET was unable to confirm treatment volumes because the tumour was not FDG avid.

DISCUSSION & CONCLUSIONS: This project requires close collaboration between the radiotherapy department and the nuclear medicine department. The process relies on accurate fusion between PET-CT and simulation CT data sets. To date, we have successfully treated eight head and neck patients with IMRT when PET information has aided the radiation oncologist in defining target volumes.

NON-CLINICAL LABORATORY EVIDENCE RELATED TO INTENSITY MODULATED RADIATION THERAPY

Natalka Suchowerska[1,2]

[1]*Department of Radiation Oncology, Royal Prince Alfred Hospital, Australia*
[2]*School of Physics, University of Sydney, Australia*

Intensity Modulated Radiation Therapy (IMRT) has rapidly been accepted into clinical practice without first going through clinical trials on the assumption that delivered dose is a sound predictor of radiobiological response. It is argued that the improvement in dose distribution which maximizes the radiation dose to the tumour, while avoiding critical healthy structures, must give a better clinical outcome. However, IMRT introduces three new variables and the clinical effects of these remain uncertain. The first of these is the high spatial modulation of the radiation beam, the second is the temporal modulation of the radiation delivery and the third is the change in the radiation beam spectrum as a function of collimator position.

Spatial modulation cannot be ignored given the recent evidence that un-irradiated cells may die because of an association with irradiated cells. This challenges the fundamental concept that cell survival following exposure to ionizing radiation is restricted to DNA damage in the irradiated cells. This non-local effect has been termed the bystander effect. Experimental evidence using a therapeutic energy beam has shown that in-vitro tumour cell response to dose non-uniformities is significantly affected by bystander effects. Existing models of tumour and normal tissue response commonly used in radiotherapy are based on the assumption that cells respond independently and their response depends only on local energy deposition. This view of cellular dose-response leads to the development of mechanistic models which do not include bystander effects. The consequences of temporal modulation have been extensively discussed in the recent literature. However most of these publications are of a theoretical nature and do not fully address the clinical implications. Furthermore these discussions do not consider the changes in beam quality as a function of collimator position.

The non-clinical laboratory evidence related to IMRT will be presented and new experimental data focusing on the radiobiological effects will be discussed.

In order to explore mathematical models that incorporate non-local effects and temporal modulation we need to better understand the radiobiological consequences, to quantify these effects and assess their implications for modern radiation therapy. A better understanding of the complex nature of tissue response to therapeutic irradiation will enable us to more accurately predict the clinical response. This new knowledge will identify opportunities to improve treatment techniques and therefore patient outcomes.

PROBABILITY OF NORMAL TISSUE COMPLICATIONS AND RISK OF SECOND CANCER FOLLOWING PROSTATE CANCER RADIOTHERAPY

R. Takam[1,3], E. Bezak[1,3] and E. Yeoh[2,4]

[1]*School of Chemistry and Physics, The University of Adelaide, Adelaide, Australia*
[2]*School of Medicine, The University of Adelaide, Adelaide, Australia*
[3]*Medical Physics Department, Royal Adelaide Hospital, Adelaide, Australia*
[4]*Radiation Oncology Department, Royal Adelaide Hospital, Adelaide, Australia*

INTRODUCTION: Normal tissue complication probability (NTCP) and risk of developing second cancer for rectum and bladder following standard dose schedule (2 Gy/fx for 64 Gy) EBRT, hypofractionated (2.75 Gy/fx for 55 Gy) EBRT, HDR-BT monotherapy (4*9.5 Gy), LDR-BT (I-125) and combined treatment (std. EBRT + HDR-BT) modality for prostate cancer have been assessed using differential dose-volume-histograms (DVH) from patients' plans. Relative seriality model and modified competition model were used to assess NTCP and risk of second cancer, respectively.

METHOD: Rectal and bladder differential DVHs obtained from corresponding treatment planning system for each treatment technique were exported and converted to biologically effective dose[1] (BED)-based DVHs and equivalent dose[2] (D_{EQ})-based DVHs. In case of combined treatment modality, a pair of rectal D_{EQ}-based DVHs for each modality (Std. EBRT and HDR-BT) was combined together bin by bin to produce a rectal D_{EQ}-based DVH for combined treatment modality. Relative seriality NTCP model[3] and competition model[4] were applied to rectal and bladder DVHs obtained as mentioned above to assess NTCP and risk of second cancer. Radiobiological parameters such as α/β ratio, D_{50}, s, and k for rectum were obtained from several sources.

RESULTS:

Treatment Technique	Rectum		Bladder	
	NTCP (%)	Risk of 2nd cancer (%)	NTCP (%)	Risk of 2nd cancer (%)
Standard dose schedule (2 Gy/fx) EBRT	2.8 ± 1.0 (1.1 – 4.1)	8.7E-03 ± 1.4E-02 (2.0E-03 – 4.0E-02)	1.9 ± 0.2 (1.6 – 2.3)	2.2E-03 ± 2.9E-03 (1.8E-04 – 8.2E-03)
Hypofractionated (2.75 Gy/fx) EBRT	1.3 ± 0.2 (1.1 – 1.6)	2.1 ± 2.2 (0.1 – 6.0)	0.7 ± 0.2 (0.4 – 0.9)	1.3E-03 ± 1.6E-03 (7.4E-05 – 4.2E-03)
HDR-BT monotherapy (4*9.5 Gy)	0.5 ± 0.4 (0.0 – 0.8)	5.2E-05 ± 8.7E-05 (2.6E-07 – 2.1E-04)	-	-
LDR-BT (I-125)	0.7 ± 0.4 (0.0 – 1.7)	2.2E-04 ± 2.8E-04 (8.9E-06 – 1.3E-03)	-	-
Combined treatment (Std. EBRT + HDR-BT)	0.3 ± 0.1 (0.0 – 0.5)	6.0E-02 ± 9.7E-02 (8.4E-03 – 2.9E-01)	-	-

Table 1. *Rectal and bladder average NTCP (%) and risk of second cancer (%) following various treatment techniques for prostate cancer.*

DISCUSSION & CONCLUSION: In average, probability of severe rectal complications following brachytherapy monotherapy (HDR-BT and LDR-BT) as well as combined treatment modality is lower than that following external beam radiotherapy (standard dose schedule and hypofractionated). Risk of rectal second cancer was quite low in all techniques except hypofractionated EBRT. Observation from differential DVHs suggested that irradiation of rectum with doses around 4 Gy where the risk reaches maximum may contribute to an elevation in risk of rectal second cancer. Bladder NTCP and risk of bladder second cancer following hypofractionated EBRT are lower than that following standard fractionated EBRT. It was suggested that it is desirable to choose a treatment plan which results in high doses irradiation to small volume of normal tissue than a plan which causes low doses irradiation to a larger volume of tissue since this would increase several fold the risk of second cancers[4].

REFERENCES:

[1]*R.G. Dale (1985) Brit J Radiol, 58: 515 – 528.*
[2]*S. Nag & N. Gupta (2000) Int J Rad Oncol Biol Phys, 46: 507 – 513.*
[3]*M. Zaider, et al. (2005) Int J Rad Oncol Biol Phys, 61: 702 – 713.*
[4]*A. Dasu, et al. (2005) Acta Oncol, 44: 339 – 347.*

DIFFERENCES BETWEEN DOSE TO WATER AND A RANGE OF POLYMER GEL DOSIMETERS IN COMMON CALIBRATION TECHNIQUES

M.L. Taylor[1], R.D. Franich[1], J.V. Trapp[2] and P.N. Johnston[1]

[1]*Applied Physics, RMIT University, Melbourne, Australia*
[2]*School of Physical and Chemical Sciences, QUT, Brisbane, Australia*

INTRODUCTION: Gel dosimetry is a method for validation of three-dimensional (3D) dose distributions for radiotherapy techniques involving high dose gradients. Polymer gel dosimeters work on the principle of radiation induced cross-linking of constituent monomers distributed uniformly in a gel matrix, which is proportional to the dose absorbed. A variety of polymer gel dosimeters exist, such as polyacrylamide gel (PAG) and normoxic dosimeters such as MAGIC, MAGAS and MAGAT. Gel dosimeters are often used for relative dosimetry; however for absolute information it is necessary to calibrate each batch of gel individually. In principle, this is undertaken by irradiating gel with varying doses, with the assumption that the doses received are equivalent to that in water under the same conditions. A dose calibration curve is then constructed by association of the presumed dose at such points with the corresponding relaxation rate values obtained via MRI, or with Hounsfield units from x-ray computed tomography, attenuation coefficients from optical computed tomography, or similar.

METHODS: Here, six contemporary, published modes of gel calibration are investigated via the Monte Carlo technique in terms of the influence of the composition of the gel and its containment vessel on the dose absorbed, as compared to dose in water alone. The DOSRZnrc user code for EGSnrc was employed, allowing dose to be scored in detailed cylindrical geometries.

RESULTS: The majority of calibration methods result in doses that match the dose to water to within one percent, ranging up to several percent depending on the gel formulation. Calibration methods and gels that yield the closest matches to water equivalence are described.

DISCUSSION & CONCLUSIONS: The study has shown that several gel calibration methods performed under well defined conditions yield results that approach clinical acceptance. Methods using long test tubes coaxial with the beam give the largest differences.

THREE DIMENSIONAL DOSE VERIFICATION FOR IMRT USING AMORPHOUS SILICON EPIDS

T. Tehovnik[1, 2], P. Greer[1, 3], M. Carolan[2, 4], W. Ansbacher[5] and P. Metcalfe[2]

[1]*Department of Radiation Oncology, Calvary Mater Newcastle, Newcastle, Australia*
[2]*Centre for Medical Radiation Physics, University of Wollongong, Wollongong, Australia*
[3]*Department of Mathematical and Physical Sciences, University of Newcastle, Newcastle, Australia*
[4]*Illawarra Cancer Care Centre, Wollongong Hospital, Wollongong, Australia*
[5] *British Columbia Cancer Agency, Victoria, BC, Canada*

INTRODUCTION: A 3D method[1] for IMRT verification has been recently developed that acquires an EPID image for each field that will represent the mid-plane dose in a cylindrical virtual phantom. The image is convolved with a kernel to convert the EPID image to the dose at the radial depth of the virtual phantom, and contour corrections applied. A 3D dose matrix within the phantom is then reconstructed using attenuation and divergence corrections to compare to the planned dose distribution. This will provide a faster and more accurate method for verification. The aim of this project is to implement and further develop this method by modifying the kernel correction and by also studying the effect of detector sag with gantry angle. Initial measurements were made to benchmark the accuracy of the method against conventional dosimeters.

METHODS: Film measurements in a flat solid water phantom parallel to the beam axis were made at 100cm SSD with the gantry rotated to 90º to minimise air gaps and with a further 2º offset. The 3D EPID method (EPIdose) program was altered by removing the contour correction. An SSD correction was applied to EPIdose for differing depths for the 10x10cm^2 field size. Both film and EPIdose profiles at depths of 1.5, 5, 10, 20 and 30cm for a 6MV beam were then compared to diode profile measurements taken previously in the department.

RESULTS: Figure 1 and Figure 2 shows the comparison of diode, film, and EPIdose program profiles at the optimised depth of 10cm and also at 5cm respectively.

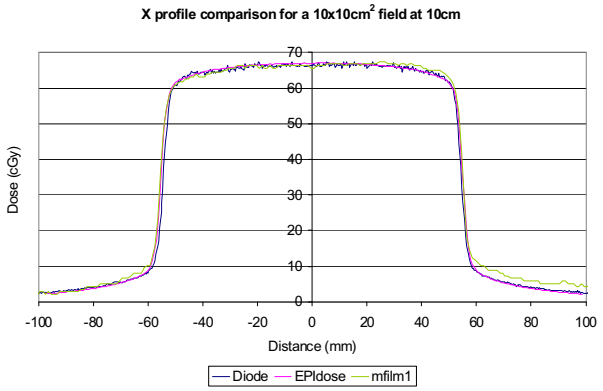

Figure 1. *Profile comparison of diode, EPIdose, and film measurements for 10cm depth.*

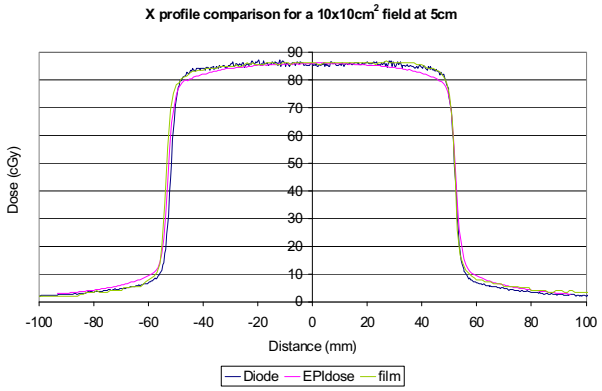

Figure 2. *Profile comparison of diode, EPIdose, and film measurements for 5cm depth.*

DISCUSSION & CONCLUSION: With the preliminary results of the profile comparisons in solid water, it was observed that the EPIdose kernel is optimised for 10cm depth. At other depths, the EPIdose profile differs from both film and diode measurements. We aim to alter the kernel that is being used so that we are matching at depths, and also compare film profile measurements in our cylindrical phantom.

REFERENCES:

[1]*W. Ansbacher, "Three-dimensional portal image-based dose reconstruction in a virtual phantom for rapid evaluation of IMRT plans," Med. Phys. 33, 3369 - 3382 (2006).*

HIGH DOSE-RATE BRACHYTHERAPY FOR SUPERFICIAL LESIONS; SKIN AND ORAL MUCOSA APPLICATIONS

L. Wee[1], P. Rampant[1], S. Sarudis[3] and C. Hartman[2]

[1]*Department of Medical Engineering & Physics, Royal Perth Hospital, Perth, Australia*
2Perth Radiation Oncology, Wembley, Australia
[3]*Karolinska Institute, Stockholm, Sweden*

Radium “moulds” were one of the earliest applications of radionuclides in radiation therapy. It was often the only form of radiotherapy available until the advent of implantable radionuclide sources and x-ray tubes. The radiobiological and dosimetric traditions of radiotherapy were established for mould brachytherapy, then expanded to address the diversity of modalities we possess today.

Brachytherapy for superficial lesions of the skin and oral mucosa is experiencing something of a quiet revival in recent times. The appeals of brachytherapy – the ability to shape conformal volumes of high radiobiological effective dose; sparing of normal structures from incident and leakage radiation; short overall treatment time) – are still highly relevant today, either as "boost" treatments in tandem with external beam radiotherapy and as a sole radiotherapy modality of surgical margins following excision.

The widespread use of computer-controlled after-loading sources, computerised dosimetry and image-guidance in current brachytherapy practices provides compelling motivation for the revival of the above brachytherapy techniques.
In this paper, I discuss the developmental work carried out at Royal Perth Hospital in the area of high dose-rate brachytherapy for two clinical applications; applicators for superficial skin lesions and post-excision mould brachytherapy of the oral mucosa. I wish to highlight the potential contributions of medical physicists in a multi-disciplinary effort centred on the safe and effective delivery of the radiation dose.

The salient points I wish to examine are; how empirical statements about geometry such as the Manchester distribution rules should be used as the starting point for applicator design, the applicability of automated dwell-weight optimisation as a means of moving onwards from empirical systems and why a medical physicist should always have a grasp for the potential effects of uncertainties in source delivery.

ANALYSIS OF INTER- AND INTRA-FRACTION BREATHING PATTERNS USING A SPIROMETER

M. Whitaker[1, 2], S. Todd[1], M. Kenny[1], J. Whitaker, J. Hagekyriakou[1] and T. Kron[1, 2]

[1]Department of Physical Sciences, Peter MacCallum Cancer Centre, Melbourne, Australia
[2]Royal Melbourne Institute of Technology, Melbourne, Australia

INTRODUCTION: Radiotherapy treatment to lung, liver and breast cancer patients may be adversely affected by the movement of the target due to respiration. This may be corrected for by performing gated radiotherapy, where the beam is only turned on when the patient is in a particular phase or amplitude of the breathing cycle[1].
It is therefore essential that the location of the target be established or predicted, so that maximum dose can be delivered to the tumour whilst minimising dose to the surrounding normal tissue. There are several commercially available methods for monitoring respiratory movement.
In this study, using an in-house designed spirometer[2], we determine the key parameters[3] required to reproduce patients breathing patterns for the purpose of developing a model to predict diaphragmatic and chest wall motion[1]. The key parameters are: breathing frequency, maximum amplitude of inhale and exhale, asymmetry of the breathing pattern and of particular clinical importance, the maximum time spent in a particular state of breathing volume: the duty cycle.

METHODS: The spirometry data of three volunteers of similar age and health were captured with the volunteers in a prone position, emulating a typical treatment setup. Data was collected over 1 minute and 15 minutes on multiple occasions over several days. From the resulting breathing patterns, the four key parameters were derived and compared between inter- and intra-fraction breathing patterns.

RESULTS: Breathing frequencies were noticeably different between the three volunteers, whilst the intra-fractional difference within each volunteer remained minimal. Significant differences were also observed for asymmetry of the breathing pattern and the maximum and minimum amplitude between volunteers. The differences in breathing patterns between volunteers was significantly larger than the intra-volunteer variation in repeat measures over several days.

DISCUSSION & CONCLUSIONS: The breathing patterns of the volunteers showed consistency both inter- and intra-fraction within each volunteer, whilst a comparison of the breathing patterns between volunteers showed marked differences. We conclude that spirometry can be used to reproducibly measure the respiratory parameters which form the basis of gating or motion adaptive radiotherapy. These parameters may be used to develop a model to predict the patient's respiratory movement during radiotherapy treatment.

REFERENCES:
[1]S.S. Vedam, P.J. Keall, V.R. Kini. and R. Mohan (2001) Med Phys, 25:2139-2146.
[2]T. Zhang, M.J. O'Brien, T.R. Mackie and B. Paliwal (2003) Med Phys 30: 3165-3171.
[3]X.A. Li, C. Stepaniak and E. Gore (2006) Med Phys 33: 145-151.

EVALUATION OF HEAD SCATTER FACTOR FORMULAS

P. A. White and C. A. J. Norvill

Department of Radiation Oncology, Prince of Wales Hospital, Randwick, Australia

INTRODUCTION: Output factors are commonly obtained from measurements. An alternative is to derive equivalent squares using generic formulas. Two formulae commonly used are:

$$EqSq. = 4 \times \frac{Area}{Perimeter} \quad (1),$$

$$EqSq. = \frac{(A+1)XY}{AX+Y} \quad (2)[1],$$

where X and Y represent the lower and upper collimator jaws respectively, and 'A' is a machine dependant factor that can be determined experimentally. These equations are commonly used for manual monitor unit calculations in hand planning and checking treatment plan accuracy. The aim of this project was to compare these formulae for a range of treatment set ups.

METHODS: A mini-phantom and ion chamber was used to measure head scatter factors on a Siemens Oncor linear accelerator. These were then converted to sets of equivalent squares using a linear interpolation model. Equivalent square values were also derived using both equations. For equation 2 a range of 'A' values were examined. It was found that A = 1.9 minimised the difference between calculated and measured equivalent squares. Doses were then calculated using measured and derived equivalent squares for a range of field sizes and depths, and compared using measured data as the reference.

RESULTS: Figure 1 shows the percentage difference in dose accuracy for the 4A/P formula compared with that given by Vadash and Bjarngard (1993)[1]. For the majority of field sizes and depths, it was found that equation 2 performed better than 4A/P, by as much as 5%.

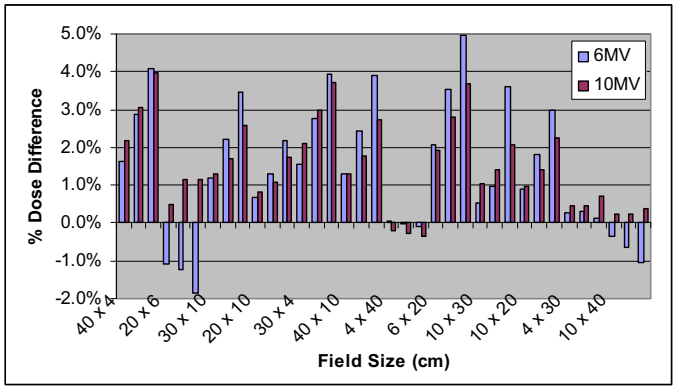

Figure 1. *Graph showing the % dose error in 4A/P relative to results using the equation 2. Data has been normalised to measured values for both formulas.*

DISCUSSION & CONCLUSIONS: The accuracy of two formulas commonly used to calculate equivalent square values have been evaluated. It was found that the Vadash and Bjärngard formula gave improved accuracy over 4A/P of up to 5% when calculating doses for a variety of field sizes and depths.

REFERENCES:

[1] *P. Vadash, and B.E. Bjärngard. An equivalent-square formula for head scatter factors, Med. Phys, 20 (3): 3733 – 734, 1993.*

GEL DOSMIETRY FOR MICROBEAM RADIOTHERAPY USING RAMAN SPECTROSCOPY

C.J. Wong[1], W. Patterson[2], C. Powell[3], G. Qiao[3], D. Solomon[3], J. Crosbie[4] and M. Geso[1]

[1] *Department of Medical Radiation, RMIT University, Bundoora, Australia*
[2] *Radiation Oncology Victoria, East Melbourne, Australia*
[3] *Department of Chemical & Biomolecular Engineering, University of Melbourne, Parkville, Australia*
[4] *William Buckland Radiotherapy Centre, Alfred Hospital, Melbourne, Australia*

INTRODUCTION: Microbeam Radiotherapy is an irradiation technique with many very narrow beams (μm range) of high intensity. However, the measurement of the dose delivered in this way is a challenging task for dosimeters. In this work, gel phantoms irradiated with microbeams from a synchrotron were used to determine the peak-to-valley ratio of the dose distribution.

METHODS: Gel phantoms were irradiated with microbeam of high intensity at the SPring-8 synchrotron in Japan. The polymerisation in the gel can be measured at a point using Raman Spectroscopy[1]. The change in Raman spectra at

positions across the polymerised regions of the gel was obtained using a 514 nm laser. Raman Spectroscopy measurements are indicative of the polymerisation, which is proportional to the dose deposited.

RESULTS: Figure 1 demonstrates a linemap over the surface of such a gel dosimeter irradiated with microbeams as measured using Raman Spectroscopy. This figure shows the Raman spectra of the polymerised regions have changed compared to the unirradiated regions between the narrow beams.

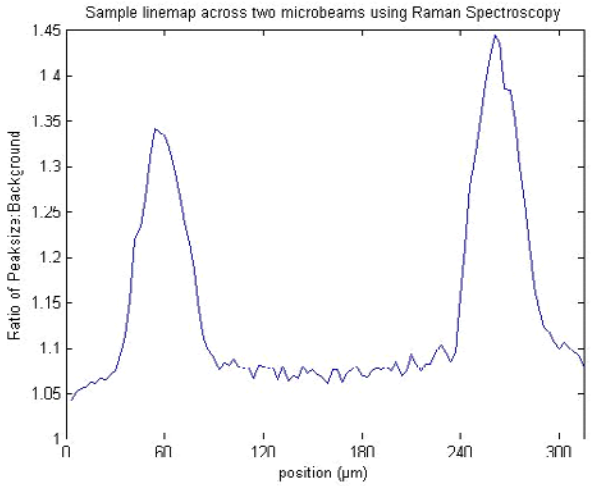

Figure 1. *A sample Linemap in 3 µm steps demonstrating the change in the size of the peak located at 2936 cm^{-1} with position.*

The peak-to-valley ratio was found to be approximately 20:1. This is slightly lower than results obtained using special-type gafchromic film dosimetry.

DISCUSSION & CONCLUSIONS: These results demonstrate that Raman Spectroscopy can be used to measure the dose distribution from microbeams.
The effect of monomer movement may become relatively important at these field sizes. Investigations are underway to measure this effect using X-ray phase contrasting techniques. Additionally, the colouration of gel when polymerised is a limit to Raman Spectroscopy measurements at depth and methods of overcoming this are being investigated.

REFERENCES:
[1]*L. Rintoul et al (2003), Appl. Spectrosc.,57:51-57.*

SMALL SEGMENT DOSIMETRY: IMPLICATIONS FOR IMRT

J. Yuen[1], N. Hardcastle[2] and P. Metcalfe[2]

[1]*Department of Medical Physics, St. George Hospital, Sydney, Australia*
[2]*Centre for Medical Radiation Physics, University of Wollongong, Sydney, Australia*

INTRODUCTION: Small segments in intensity modulated radiation therapy (IMRT) are used to shape the dose into more conformal shapes. Frequently, this involves high dose gradients as well as segments as small as 1x1 cm^2. There are potential issues with uncertainty in the dosimetry of small MLC fields that are addressed in this study.

METHODS: Small segments down to 1x1 cm^2 were measured using a small volume ionization chamber (PTW 31015 Pinpoint) and a diamond detector (PTW 60003 Diamond). Measurements of penumbra width were then compared with the standard (PTW 31002 Semiflex 0.125 cm^3) ionization chamber data. The data is processed and is then modelled in a radiotherapy treatment planning system (Pinnacle version 8.0). The data measured includes variation of MLC field size, depth, jaw position, detector volume size, chamber offset, and leaf junction offset.

RESULTS: The leaf junction dose was accounted for in the Pinnacle measurement procedure with a chamber offset but our study found that an offset in the leaf junction was able to reduce the leaf junction dose to 30% of its original value with a 2 cm shift on either side of the central axis –this avoided measurement of off-axis profiles with the chamber offset. A comparison of the PDD with and without leaf junction offset revealed that the collimator jaw position could increase the dose at d_{max} at jaw positions decreasing the dose at depths more than 5 cm consistently by 2% (for jaw positions above 2x2 cm^2 in a 1x1 cm^2 MLC field). The correlation between detector size and penumbra width was found to be linear$^{(1)}$ but the

linear model varied with depth and MLC field size. The penumbra width is known to increase with depth as well as increasing MLC field size[2].

DISCUSSION & CONCLUSIONS: Linear fit of the detector volume with the penumbra (80-20% width values) can produce consistent effective zero volume chamber penumbra values, but with varying penumbra shapes (due to various factors such as energy-response). The gradient correlating volume size to field size is are slowly varying. Methods to account for these effect include simplistic scaling of profiles using the linear fit, more complicated convolution kernels[3, 4], or the use of smaller volume detectors to begin with to minimise extrapolation errors. In addition, the measurement setup relating to the MLC junction offset and jaw position was taken into account. Lastly, Monte Carlo simulations (1 mm resolution) and comparison between a measured small segment setup and the model will give a valuable comparison between variations in small segment dosimetric procedures.

REFERENCES:

[1]*Laub WU, Wong T. The volume effect of detectors in the dosimetry of small fields used in IMRT. Med. Phys. 2003; 30:341-347.*
[2]*Pawlicki T, Ma C-MC. Monte carlo simulation for MLC-based intensity-modulated radiotherapy. Medical Dosimetry 2001; 26:157-168.*
[3]*Garcia-Vicente F, Delgado JM, Peraza C. Experimental determination of the convolution kernel for the study of the spatial response of a detector. Med. Phys. 1997; 25:202.*
[4]*Pappas E, Maris TG, Papadakis A, et al. Experimental determination of the effect of detector size on profile measurements in narrow photon beams. Medical Physics 2006; 33:3700-3710.*

DIAGNOSTIC IMAGING / RADIATION PROTECTION

INVITED TALK

PRACTICAL PATIENT DOSE SAVING: CR AND DR IMAGING SYSTEMS

David J. Dowsett

Consultant Medical Physicist, The Institute of Radiological Sciences, Dublin, Ireland
medphys@indigo.ie

INTRODUCTION: Since the introduction of digital imaging systems into diagnostic radiology they have been quickly accepted as a replacement for film. Computed Radiography (CR) uses an imaging plate which must be first processed by a laser scanning system. Direct Radiography (DR) uses a more complex electronic detector but gives instant images. It was anticipated that both systems would yield lower radiation dose, however results have generally been disappointing. Theoretical considerations suggest that there is still room for improvement.

METHODS: In Ireland a number of hospitals have adopted filmless diagnostic radiology departments using either CR or DR or a mix of both. This report presents patient radiation dose clinical audits from two large university hospitals (300 to 400 beds), two private hospitals (300 beds) and a maternity hospital (300 beds). The data has been collected over a period of three years from a simple clinical audit which gives: patient identity, age, clinical history and exposure details taken from the display (entrance surface dose and dose area product). European Directives require that all new x-ray equipment display patient dose preferably in mGy. Further data[1] were obtained from a U.K. report obtained from a large number of hospital sites. Comparisons between more recent Irish and slightly earlier U.K. dose measurements have been made.

RESULTS: CR imaging systems have not shown significant dose reductions when compared with recent fast film/screen systems. Some results from Irish DR imaging systems are shown in the box graph (Figure 1.). Specifically some dose reduction is seen but in general results have been disappointing. Early work[2] investigating film/screen imaging was modified and applied to digital detectors in order to both understand the limitations of detector materials and suggest areas that may give room for improvement.

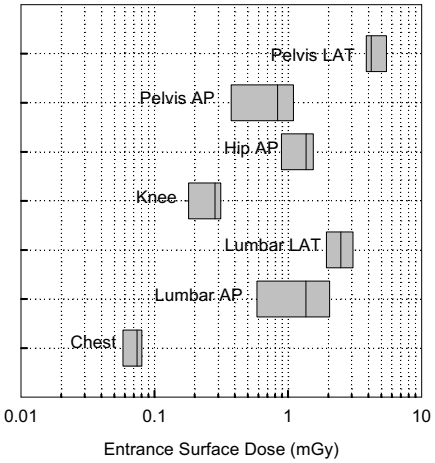

Figure 1. *Doses from some DR studies.*

DISCUSSION & CONCLUSIONS: Although some hospitals have reported dose reductions after introducing digital imaging systems this has not been generally experienced. The main benefits in dose reduction have been indirect, such as more secure record keeping and reduced repeat investigations. "On the job" staff training has allowed both CR and DR systems to be quickly accepted and incorporated into radiology routine but there is an urgent need for more formal staff training seminars given by physicists, so that mechanisms for further dose reduction can be explored.

REFERENCES:

[1] *D Hart MC Hiller, BF Wall. Doses to Patients from X-ray Imaging in the UK: 2005 Review.*
[2] *DJ Dowsett Towards a limitation of Radiation Exposure Levels in Diagnostic Imaging (PhD Thesis)*

INVITED TALK

WISE PRECAUTIONS FOR RADIATION SAFETY

David J. Dowsett

Consultant Medical Physicist, The Institute of Radiological Sciences, Dublin, Ireland
medphys@indigo.ie

INTRODUCTION: When considering department radiation safety many aspects must be considered that are not at first obvious but could lead to serious complications. Regular radiology departmental meeting should be held where potential hazards can be discussed with radiology staff. The hazard to pregnant patients and staff should be high on any agenda and protocols regarding low radiation exposure levels to non-radiological hospital staff (nurse and secretarial) should be constructed. Installation of new x-ray equipment or replacing old equipment requires a review of radiation shielding and safety. Upgrading CT machines to multi-slice models or replacing existing multi-slice machines will involve increased radiation spill from the broader cone beams.

METHODS: Routine inspections of diagnostic radiology departments in Ireland have yielded information about hidden dangers/potential hazards regarding, not only radiation safety but also general department safety records (electrical and chemical). Increasing workloads have required immediate revision of local safety rules in order to reduce radiation exposure.

RESULTS: Many radiology departments seen were more than 30 years old and previously specified radiation shielding was inadequate. The functional illiteracy of the adult population (>20%) has caused problems with notices and where clinical investigations require informed consent. In certain instances successful litigation has been brought against hospitals by patients and staff.

DISCUSSION & CONCLUSIONS: Observing the evolution of radiation safety in Irish hospitals has been an instructive process. It is evident that staff training programmes must be introduced on a regular basis for both radiographers, technicians, radiologists and othe hospital clinical staff. Strict clinical audits must also be introduced so that radiology staff understand how their department compares with reference doses.

INVITED TALK

THE ECONOMICS OF DOSE REDUCTION

David J. Dowsett

Consultant Medical Physicist, The Institute of Radiological Sciences, Dublin, Ireland
medphys@indigo.ie

INTRODUCTION: The comprehensive study of department design and subsequent department performance can save considerable present and future financial outlay. The size of x-ray rooms is critical for optimum safety since distance between source and operating area is more effective for dose saving than expensive shielding. Partition or block walls are also part of the equation as well as the number of shielded doors.

METHODS: The design of two large radiology departments containing conventional x-ray, mammography, nuclear medicine and PET/CT has been undertaken over the last few years. Wall and door shielding was calculated from published work[1]. Shielding for large and small dental suites was also specified. Architects, x-ray machine manufacturers, builders and shielding suppliers have been encouraged to attend Planning Committees so that optimum shielding can be specified before building commenced. An initial reference design value of 0.3mSv per year was used for public areas and 1mSv per year for radiology staff.

RESULTS: The first consideration should be the estimation of clinical workload since this will influence shielding required now and in the near future. One radiology department anticipated a growing catchment area (new town) and this influenced room design and construction. Moveable partitions were specified so that room size could be altered. An established department that changed from film to digital imaging achieved space saving by dumping their film processor equipment and chemical store; two adjacent x-ray rooms expanded into this free space.

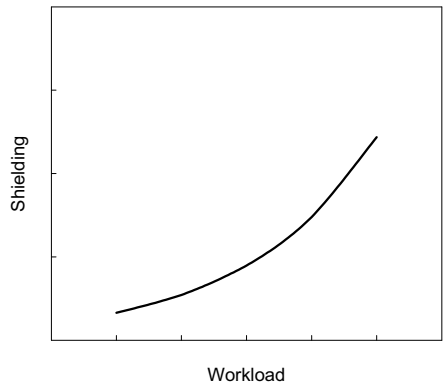

Figure 1. *Clinical workload determines the amount of shielding and will influence costs.*

Nuclear medicine departments were mostly not shielded except when waiting or reception rooms were next door. Wall dosimeters deployed for 3 month periods confirmed that low dose levels were being maintained , in spite of high activity levels. Architects who did not employ a qualified radiation protection adviser always over specified shielding; in some instances when it was entirely unnecessary. Nuclear medicine and PET/CT staff dose can be much reduced with staff training[2].

DISCUSSION & CONCLUSIONS: Failing to employ a medical physicist as radiation protection adviser results in excessive radiation shielding being specified with consequent high cost which cannot be recovered. An overall linear design gives ergometric benefits and effectively separates non-radiation from radiation areas.

REFERENCES:

[1]*Radiation Shielding for Diagnostic X-rays. BIR/IPEM Report. British Institute of Radiology 2000.*
[2]*Roger Price (Personal Communication 2007)*

INVITED TALK

RENEWABLE ENERGY AND SUSTAINABLE DEVELOPMENT

Philip Jennings

Division of Science and Engineering, Murdoch University, Murdoch, WA

Human society is facing a set of major challenges, including resource depletion, global warming and over-population. As a result the question of sustainability has become the central issue of our time. We are just beginning to understand what sustainability means and the symptoms of unsustainable practices are still prevalent.

Energy is the lifeblood of modern industrial society. It powers our homes, factories, hospitals and vehicles. Our quality of life is based on machines, powered by cheap, abundant energy and there is no obvious way that we could do without them. However our current sources and uses of energy are causing serious social, economic and environmental problems and the search is now underway in earnest to find alternative sources and to reduce consumption. Some people believe that "clean coal" and nuclear power are the answers to this dilemma, but others point out that these are both fossil fuels and will not provide long term answers to our energy needs.

Renewable energy has been used by human society for thousands of years for traditional purposes, such as lighting, heating, agriculture and transport. However, since the industrial revolution we have come to depend more on fossil fuels and electricity to support our modern lifestyle. The challenge for renewable energy advocates is to demonstrate how such sources can be used sustainably to produce the sort of energy that modern society requires.

This talk will review the renewable energy resources of Australia and the progress that has been made in harnessing them for energy supply. Attention will also be paid to the question of sustainability and the need to carefully design and assess all new technologies to avoid repeating the mistakes of the past.

ACTION LEVELS WHEN CREMATION FOLLOWS TREATMENT WITH IN VIVO OR IMPLANTED RADIOACTIVE SOURCES

M. Aerts

Radiation Health Branch, Department of Health, Australia

INTRODUCTION: The NHMRC *Code of Practice for the Safe Handling of Corpses Containing Radioactive Material* refers briefly to the question of cremation following the death of a patient containing radioactive materials. However, the Code no longer reflects current radioisotope use, and also does not distinguish between the different source forms (sealed or unsealed) or address the nature of incorporation of the radioactive substance in the body and how that will affect the post-cremation fate of the material.

This paper proposes an approach to be used in examining the action that might be required when cremation follows radioisotope therapy, and looks at those isotopes and procedures in current clinical practice that might be affected.

METHODS: The approach is:

- If the radioisotope is in a form or compound or has had pharmacokinetics such that it will survive the cremation process and end up in the cremation ashes: Compare the residual activity in the body with (the less stringent of) the IAEA Exempt Activity or Exempt Activity Concentration.

(Applies, for example, to unsealed radioisotopes incorporated in mineral bone or to sealed radioactive seeds encapsulated in substances of very high melting point.)

- If the radioisotope is in a form that is non-persistent through the preparation of the cremation ashes but will be emitted through the chamber and flue of the cremation furnace: Compare the residual activity in the body with 1,000 x the IAEA Exempt Activity.

(Applies, for example, to unsealed ^{131}I.)

RESULTS: This approach has been applied to radioisotopes used or proposed for use for the treatment of bone metastases (^{89}Sr, ^{153}Sm or ^{188}Re), to permanent seed implants (^{125}I), and to large activity IV or oral radioisotope therapies (^{90}Y, ^{131}I or ^{188}Re).

Times for which precautions are relevant for the particular radioisotope and use are given, along with the relevant action which may range from excision of implant tissue before cremation to precautions by crematorium workers and storage of ashes.

DISCUSSION & CONCLUSIONS: The approach, action levels and actions have been approved in Western Australia by its radiation regulatory authority.

The practical implications are that only the ^{89}Sr palliative bone therapy treatments constitute an occasional but regular situation where radiation safety precautions are required during cremation and where storage of the ashes may be required for some months. The other therapies only rarely lead to situations requiring precautionary actions for cremation, and unless large quantities of ^{131}I are involved, can usually be dealt with before the cremation by means such as a wait of a few days or excision of the implant/infusion tissue.

REFERENCES:

National Health and Medical Research Council (1986): Code of Practice for the Safe Handling of Corpses Containing Radioactive Material, NHMRC Radiation Health Series #18.

SKIN DOSE ASSESSMENT IN CARDIOLOGY

A. Blair

Department of Medical Physics and Bioengineering, Christchurch Hospital, New Zealand

Interventional Cardiology is a branch of cardiology that treats vascular and heart conditions using fluoroscopically guided catheters. Since it offers many obvious advantages over conventional open surgery its use has exploded in recent times. The Centre for Disease Control reports that 1.3 million cardiac catheterisation were performed in 2004 in the United States[1]. Maximum skin doses for IC procedures vary widely from ~100-700 mGy [2] and in very rare cases be over 10Gy. Dose monitoring and dose statistics have become a hot topic in the community with commissions such as the DIMOND consortium reporting dose reference levels for certain procedures[3]. Measurement of skin dose is not trivial and an accurate estimate usually requires vendor made hardware. Since few labs have such devices clinicians have resorted to recording the only information they have available, that is KAP and total fluoroscopic time. While these can provide indications of risk they are far from accurate for many reasons. For my Masters Thesis I am looking at ways to accurately measure skin dose especially practical methods. In this talk I will cover why this work is relevant and useful along with a brief introduction to skin injury and statistics. Then two methods for dose assessment will be discussed. One using a new Radiochromic film Gafchromic ® XR-RV2[4] of which the characteristics will be discussed. The second using the information contained in the DICOM image files to reconstruct the exposure. Preliminary results will also be presented.

REFERENCES:

[1]*National Centre for Health Statistics, Series 13 No. 162- National Hospital Discharge Survey: 2004 Annual Summary With Detailed Diagnosis and Procedure Data.*
[2]*E. Vano et al, Skin dose and dose-area product values for interventional cardiology procedures, BJR 74 (2001), 48 -55.*
[3]*Digital Imaging: Measures for Optimizing Radiological Information Content and Dose http://www.dimond3.org/WEB_DIMOND3/home.htm*
[4]*International Specialty Products, New Jersey.*

MEASURING CYCLOTRON BEAM ENERGY BY IRRADIAITON OF COPPER FOILS

J. Burrage[1], R. Fox[2], R. Price[3], J. D'Souza[3] and S. Siddiqui[4]

[1]*Department of Medical Engineering and Physics, Royal Perth Hospital, Perth, Australia*
[2]*School of Physics, University of Western Australia, Perth, Australia*
[3]*Department of Medical Technology and Physics, Sir Charles Gairdner Hospital, Perth, Australia*
[4]*Department of Applied Physics, Curtin University of Technology, Perth, Australia*

INTRODUCTION: Experiments involving irradiation of molybdenum in a standard medical cyclotron at Sir Charles Gairdner Hospital (SCGH) yielded results that indicated the beam energy differed from the nominal 18 MeV. To rule out beam energy as a contributing factor to the anomalous results it was resolved to measure the energy by irradiating a stack of copper foils and measuring the activity of each.

METHODS: Two irradiations were performed. In each, a stack of 8 natural copper foils, each 0.1 mm thick, were bombarded with protons for 30 seconds at 7.5 and 5 μA respectively. A solid target holder, designed and built at SCGH, was used to hold the disks. After bombardment, a germanium detector was used to measure the activity of ^{65}Zn on each disk,

produced by the $^{65}Cu(p,n)^{65}Zn$ reaction. A model was designed that used stopping power and cross section data to predict the activity on each disk. By using this model, the beam energy could be inferred by altering the initial proton energy until the differences between measured and predicted activities were minimised. Beam alignment was checked by post-irradiation placement of the Cu disks on radiotherapy film.

RESULTS: Results from the first run indicated a beam energy of 18.3 MeV and those from the second 17.7 MeV. Yields for the first run were substantially lower than predicted, whereas yields for the second run were within 15% of predicted values apart from the last disk which had very low levels of activity and hence a large percentage error (515%). Figure 1 shows the predicted and measured values of activity per disk when normalised to the maximum activity. Results of the beam alignment checks indicated that the beam was aligned centrally.

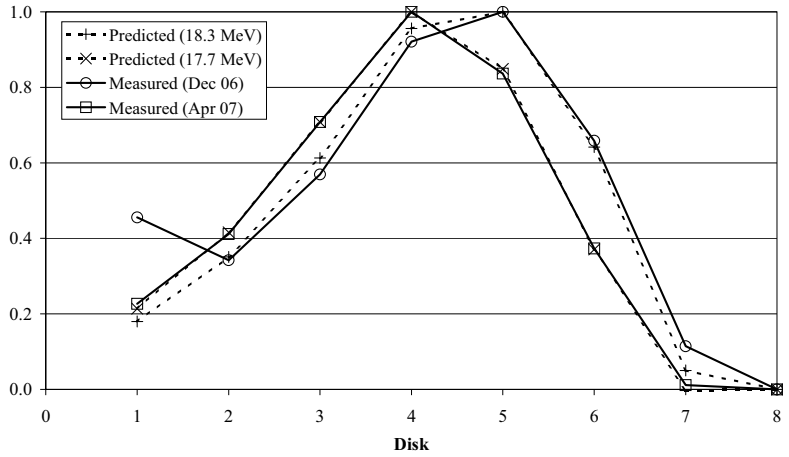

Figure 1. *Predicted v measured yield of ^{65}Zn per Cu disk, normalised.*

DISCUSSION & CONCLUSIONS: The experiment verified that the beam energy was within ±0.5 MeV of that expected. The cause of the lower than expected yield for the first run is unknown, but it suspected to be due to errors in beam current measurement. Work is ongoing in this area. The experiment also continued successful application of the solid target holder designed and built in-house.

ACKNOWLEDGEMENTS: Thanks to Tom Deans, Murray Bottomley, David Cryer and Sun Chan (SCGH) for their valuable assistance in this project.

UNUSUAL SCATTER RECORDINGS IN A DIGITAL OPG/CEPHALOMETRY ROOM

D. Causer

Department of Medical Engineering and Physics, Royal Perth Hospital, Perth, Australia

INTRODUCTION: The A personal dosimeter sited in the OPG/Cephalometry room of an Orthodontic Clinic had been recording doses of up to 90 µSv in a three month period whereas those sited in similar rooms in other clinics were always below the minimum reporting level of 10 µSv. The dosimeter was attached to the hand switch controlling the x-ray unit and was therefore taken outside into the corridor by the operator while exposures were being made. An investigation of the causes of the elevated dose levels was undertaken.

METHODS: The lead equivalence of relevant protective barriers was estimated using a ^{99m}Technetium source and a three-month survey of doses inside and outside the room was undertaken with TLD area monitors. These indicated that dose rates in the corridor outside the x-ray room were higher than others measured on the inside walls. Scatter measurements were performed using the head of a RANDO phantom to further investigate these results.

RESULTS: The lead equivalence of the walls of the x-ray room was estimated at around 0.1 mm for ^{99m}Technetium gammas which is consistent with the use of two sheets of Gyprock or similar material in the walls. This is also consistent with the design recommendations of the Radiological Council of WA for dental intra-oral or OPG rooms. The dose survey results were unexpected showing higher dose rates outside the room than within. Scatter measurements indicated that the scatter doses were generally higher for an OPG scan than for a cephalometric view and were consistent around the room. The scatter from a cephalometric view was only a quarter of that than from an OPG in the forward direction but was increased by more than tenfold in the backward direction and there was also an elevated level towards the door.

DISCUSSION & CONCLUSIONS: It was concluded that the doses recorded in the corridor were due to scatter through the door, which was higher in this direction for cephalometric views. It could also be possible that the operators were standing in

the doorway whilst children were being scanned. They were not in the habit of closing the door during exposure. It was recommended that a window be fitted in the door so that it could be closed whilst exposures were being made.

PAEDIATRIC CT DOSES USING MONTE CARLO

M. Caon

School of Nursing & Midwifery, Flinders University, Adelaide, Australia

INTRODUCTION: The calculation of dose from computed tomography (CT) examinations CT requires: a model of anatomy that geometrically defines the position in space of the boundary between one tissue or organ and the next (a computational model). It requires a computer program (a Monte Carlo code) to move individual x-ray photons through the geometry of the anatomical model. This program uses random numbers to sample the known probabilities that certain scattering events will happen and what the resulting outcome will be. Some features of the CT scanner such as its beam shaping filter are required, as is the x-ray energy spectrum from the CT scanner tube.

ANATOMICAL MODELS: Geometrical (MIRD) style "anthropomorphic" computational models were the first produced. They were clever attempts at using 3D mathematical formulae to represent organs. "Reference adults" were constructed of average stature, and "reference" child models were rescaled from the adult versions. These "mathematical" models were constructed before modern medical imaging machines were able to show us the wonderful images that CT & MRI can produce. Real children however don't look like a MIRD model. Now we use slice or tomographic 2D pixel images and extend the images into the space between slices to form "voxel" or tomographic models.

SOURCES OF MEDICAL IMAGES FOR MODELS: Serendipity has delivered some images sets for voxel models of children eg leukaemia patients (Zankl) or cadavers (Zankl, Lee). Existing de-identified data sets from extensive CT examinations of real patients can be used (Caon) but these may cover only the torso. It is possible to build composite models from the images of several individuals – rescaled in size if necessary. The UHF series of models were constructed from the images of a 9 mo male, a 4 yo female (which lacked arms & legs), an 8 yo female, an 11 yo and a 14 yo – the latter three had the heads from a different patient attached (Lee). The five also have the rescaled arms and legs of a Korean male "grafted" on. Recently, the emergence of combined PET-CT scanners and their use to image children head to foot has provided a source of medical images fro a complete individual. Making a voxel model involves segmenting the image - a very time consuming due to need to repetitively process each image and the large number of images involved. Automatic segmentation is yet to be achieved.

DOSE FROM VOXEL MODELS: A range of anatomical models is required so one can be matched to the patient of interest. The details from a range of contemporary CT scanners is required along with the means to handle their mAs modulation. These would need to be packaged into a user-friendly, portable, PC-based unit, for use in clinic by radiographers where scanner, scanning protocol, anatomy to be scanned can be input and following an MC calculation a list of organ doses (and effective dose) can be output.

REFERENCES:

Caon, M., Bibbo, G. & Pattison, J. (1999) Phys Med. Biol, 44(9), 2213-2225
C. Lee, J. L. Williams, C. Lee W. E. Bolch, (2006) Phys. Med. Biol. 51 4649–4661
Zankl, M, Veit et al. (1988) Radiat Environ Biophys 27:153

DANGERS OF MEDICAL RADIATION - ARE THEY REAL?

R. Fox[1,2]

[1]*Royal Perth Hospital, Perth, Australia*
[2]*School of Physics, University of Western Australia, Crawley, Australia*

INTRODUCTION: Since early last century it has been well known that ionising radiation is hazardous. More recently there has been increasing evidence that the risk of radiation induced cancer occurs even at quite low doses. Despite this, statements that appear to indicate that radiation risks are absent at low doses continue to be propogated. This paper looks at the evidence for there being risks of radiation induced cancer at the doses expected from typical procedures in radiology.

METHODS: The major evidence for the link between cancer and radiation is the analysis of the Japanese "atomic bomb" data. More than 10 years ago a paper was published [1] that indicated that risks were significant even in the dose range 5-20 mSv. More recently a study on 400,000 radiation workers [2] receiving a mean cumulative dose of approximately 20 mSv (90% of those being less than 50mSv) also demonstrated cancer risks that were statistically greater than those expected in that population of workers and which predicted risks that were actually 3 times higher than (although statistically compatible with) the "atomic bomb" data.

RESULTS: Typical doses for single diagnostic procedures in medicine range up to about 30 mSv, however organ doses may be significantly higher than this. In addition, the type of radiation and its delivery timescale are directly comparable with the

data analysed in reference [1]. At this radiation dose, both quoted papers indicate that the risks of cancer induction are significantly higher than the ICRP estimates would suggest, although both have large errors that encompass the ICRP figures. It is argued that these data provide substantial evidence, although not proof, that such medical procedures induce a small risk of cancer induction.

DISCUSSION & CONCLUSIONS: Despite the fact that it is true that no-one has, nor probably ever will, prove that radiation has in any particular case caused cancer, this does not excuse misleading statements being made that would imply that no harmful effects from radiation at these doses have been demonstrated. Although there may be no absolute certainty, radiation physicists have a responsibility to make sure that where relevant, the community and especially their medical colleagues are fully aware of potential risks.

REFERENCES:

[1]*Pierce DA, Shimizu Y, Preston DL, Vaeth M, Mabuchi K. (1996) Studies of the mortality of atomic bomb survivors. Report 12, Part I. Cancer: 1950-1990. Radiat Res, 146:1-27.*
[2]*E Cardis et al. (2005) Risk of cancer after low doses of ionising radiation: retrospective cohort study in 15 countries Brit Med Jnl, 331: 77-82.*

MAGNETIC FRACTIONATION OF MALARIA-INFECTED ERYTHROCYTES; VARIATIONS WITH CHLOROQUINE RESISTANCE

S.L. Hackett[1], J. Hamzah[2], T.M.E. Davis[2] and T.G. St Pierre[1]

[1]*School of Physics, The University of Western Australia, Perth, Australia*
[2]*School of Medicine and Pharmacology, The University of Western Australia, Perth, Australia*

INTRODUCTION Malaria parasites ingest iron in the form of haemoglobin, releasing large quantities of haem. The parasites detoxify the haem primarily by sequestering it into crystalline haemozoin. Haemozoin formation accounts for almost 100% of ingested haem iron in chloroquine sensitive (CQS) parasites, whereas chloroquine resistant (CQR) parasites appear to convert less than 50% of ingested haem iron into haemozoin. Several experimental techniques exploit the relatively large paramagnetic susceptibility of malaria-infected cells as a means of sorting cells or investigating haemoglobin degradation. However, the source of the dramatic increase in cellular magnetic susceptibility during parasite growth has not been unequivocally determined.

METHODS We magnetically enriched *Plasmodium falciparum* cultures and directly measured the magnetic susceptibility of cell contents. The different forms of haem iron present in the erythrocytes were quantified spectroscopically. Further separations were performed such that, by controlling the fluid velocity through the column, only cells with more than a critical amount of paramagnetic iron were extracted from a suspension of infected and uninfected red blood cells.

RESULTS Parasites were enriched up to 33-fold, as illustrated in Figure 1. In the standard 3D7 laboratory strain (CQS), we found that mature parasites converted approximately 60% of host cell haem iron to haemozoin and this product was the primary source of the increase in cell magnetic susceptibility. The volumetric magnetic susceptibility of the magnetically enriched cells was found to be $0.15 \pm 0.03 \times 10^{-7}$ relative to the suspension medium, accounting for the significant enrichment of mature-stage parasites observed. Enrichment of cells containing mature parasites was significantly greater in two CQS than two CQR strains.

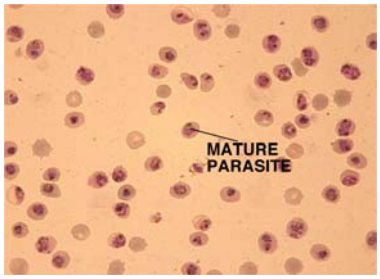

Figure 1. *Erythrocytes infected with mature parasites extracted by magnetic separation.*

DISCUSSION AND CONCLUSIONS The results of the magnetic susceptibility measurements on the cell contents of the CQS strain 3D7 indicate that haemozoin production is the primary cause of increased magnetic susceptibility of the infected erythrocytes. The cause of the reduced magnetophoretic mobility observed in the two CQR strains is yet to be identified. The results suggest the possibility of using magnetic separation columns in identifying CQR strains of *P. falciparum*, potentially in a diagnostic or research setting. Chloroquine remains one of the best-tolerated and most affordable antimalarials, so if resistance to chloroquine could be identified before patient treatment this would enable more effective treatment. The low cost of instrumentation and labour make magnetic separation columns an attractive option for malaria research. Our study

also underlines the need to identify and quantify the forms of iron in CQR and CQS parasite strains as the fate of haem iron will have implications in understanding the mechanisms of chloroquine resistance.

EVALUATION OF COMPUTED RADIOGRAPHY (CR) AND DIGITAL RADIOGRAPHY (DR) IMAGE QUALITY AGAINST THE EUREF GUIDELINES

I. Honey[1], P. Clinch[2], C.P. Lawinski[2] and A. Mackenzie[2]

[1]*Medical Physics and Bioengineering Department, Christchurch Hospital, Christchurch, Canterbury, New Zealand*
[2]*KCARE, King's College Hospital, London, UK*

INTRODUCTION: In the UK National Health Service Breast Screening Program (NHSBSP) the predominant imaging technique remains film/screen. However there is a gradual move towards digital imaging technologies. Before a system can be considered for use by the NHSBSP it must undergo technical and clinical evaluation. The technical evaluation must meet the requirements of EUREF[1]. In this work the image quality of several systems is compared against these guidelines.

METHODS: Four CR systems (Agfa CR-85, Fuji FCR Profect CS, Kodak DirectView CR 850, Konica Minolta Regius 190) and one DR system (SECTRA MicroDose) were assessed. A CDMAM phantom was positioned in the centre of a 4 cm Perspex stack. For the CR systems six images were acquired using factors giving a mean glandular breast dose (MGBD) close to the maximum acceptable values given by EUREF. For the DR system six images were acquired using the factors suggested by the system for a compressed breast thickness of 6cm (which is a radiologically equivalent thickness to the CDMAM phantom and perspex). Two images each were score by 3 experienced observers for each system. A nearest neighbour correction was performed.

RESULTS: *All systems tested met the EUREF acceptable levels for of threshold gold thickness detectability using the CDMAM phantom. Of all the tested systems the Fuji FCR Profect exhibited the highest detail detectability. The SECTRA images were acquired at between 21% and 38 % of the EUREF acceptable MGBD (as compared to approximately 90% for the tested CR systems). However the SECTRA system was operating at close to maximum tube factors so the scope for improvement of image quality was limited.*

DISCUSSION & CONCLUSIONS: All the systems tested were shown to meet the EUREF acceptable levels. The SECTRA system achieved this at very low dose levels, meaning significant patient dose reduction would be possible. This dose reduction is made possible by the scanning and photon counting technologies employed by SECTRA. These technologies allow more efficient scatter removal and virtually eliminate all noise sources except quantum noise and structure noise. It should be noted that these results are purely based on contrast phantoms and clinical verification of these findings is required.

REFERENCES:

[1]*European guidelines for quality assurance in breast cancer screening and diagnosis, 4th edition. European Commission, 2006.*

MEASURING AND MONITORING RADIATION DOSE RECEIVED BY EYE DURING ROUTINE MANUAL DISPENSING OF RADIOPHARMACEUTICALS FOR PET STUDIES

C. Jeffery[1] and T. Tuchyna[1]

[1]*Department of Medical Technology and Physics, Sir Charles Gairdner Hospital, NEDLANDS, Australia*

INTRODUCTION: Monitoring of radiation exposure received by the eye was not performed routinely in almost four years of radiopharmaceutical production for PET studies at SCGH, as preliminary studies and research from similar facilities indicated that the dose received was small (with whole body and finger radiation exposure of greater potential impact), and because of a lack of readily available monitoring equipment. Since then, whole body and finger doses for the RAPID (Radiopharmaceutical Production and Development) team have been well-defined, so attention has turned to monitoring eye exposure, since there is a risk of the formation of cataracts from manual dispensing. Approximately 2850 patient doses are dispensed annually to SCGH and SKG PET centres, with a typical patient dose of ~370MBq activity (±10%). The patient dose is drawn into a sterile disposable 5mL plastic syringe from a bolus of up to 100GBq of an ^{18}F radiopharmaceutical (a Capintec is used for accurate measurement of activity), behind an angled lead glass shield (lead equivalents = 48mm), which has a lead body (50mm of lead shielding). The bolus is contained in a 25mL glass vial, which is stored in a lead pot (35mm of lead shielding) that swivels.

METHOD:

Several electronic dosimeters were investigated, with the Aegis ED2 Personal Extremity Dosimeter chosen as the most appropriate dosimeter. The ED2 has a small silicon solid state detector probe attached to a cable, which can be comfortably positioned on the forehead between the eyes by use of a head strap. The probe can detect β, γ and x-ray radiation (γ is of importance with ^{18}F). The display unit shows both the instantaneous dose rate (μSv/h or mSv/h, range 0μSv/h to 30mSv/h) and accumulated dose (μSv or mSv, range 0μSv to 10000mSv). The software graphs the data logged against time.

A sampling regime was developed based on dispensing 3000 patient doses annually, with a sampling period of covering approximately 10% of the expected dispensing duties per person, followed by linear extrapolation of the data obtained to estimate the annual eye radiation dose exposure. Dispensing duty is shared between two members of the RAPID team (out of six) per day, with the person rostered first typically dispensing 8 patient doses (on average), plus any patient dose requested by SKG. Each team member dispensed approximately 1/6 patient doses (500 of 3000), so the ED2 was worn whilst dispensing 50 patient doses. At 8 patient doses dispensed per person per day, this required that the device be worn for 6.25 days, so it was deemed that a monitoring period of two weeks was appropriate, with the ED2 positioned on the forehead between the eyes. The greatest potential for radiation exposure is experienced in the early dispensing shift, so monitoring was performed by this team member.

RESULTS: In order for radiation exposure to the eyes to reach regulatory limits, an individual's daily dose needs to be greater than 2.5mSv per day. Results indicate that doses received dispensing are less than 100μSV per individual per collection period (average 5 hours), for the data available (23 weeks). This is less than 4% of the regulatory exposure limit. The amount of radiation detected correlates positively with the number of doses dispensed, but does not necessarily correlate with the total activity of the ^{18}F bolus, which suggests that technique is more significant.

DISCUSSION: The radiation exposure received by the eye is now routinely monitored. The use of the ED2 has led to users modifying their manual dispensing techniques using the principles of time, distance and shielding. Generally, the greatest amount of exposure is received during the first few patient doses dispensed each day, and the person on first shift receives a greater dose of radiation (both total accumulated dose and dose per number of patient doses dispensed), since the bolus is hot and it is more difficult to dispense a small volume accurately. Problems with the ED2 have been experienced – these include the probe being sensitive to electromagnetic fields from mobile or cordless telephones (a cordless telephone is used to communicate patient dose orders) and being prone to recording a spike in the data when knocked. There have also been issues with prolonged 'overload' due to a malfunction that is most likely with the cable.

OPPORTUNITIES FOR AUSTRALIA TO EXPAND ITS INVOLVEMENT IN THE NUCLEAR FUEL CYCLE

P.N. Johnston

Applied Physics, RMIT University, Melbourne, Australia

On 6 June 2006, the Prime Minister announced the appointment of a taskforce to undertake an objective, scientific and comprehensive review of uranium mining, value-added processing and the contribution of nuclear energy in Australia in the longer term. The Review of Uranium Mining Processing and Nuclear Energy in Australia was completed and submitted to the Prime Minister on December 29, 2006 and he promptly released the report.

Australia's demand for electricity will more than double before 2050. Over this period, more than two-thirds of existing electricity generation will need to be substantially upgraded or replaced. The additional capacity will need to be near-zero greenhouse gas emitting technology if Australia is just to keep greenhouse gas emissions at today's levels. Many countries confronted by similar issues have considered the use of nuclear power for some of the following reasons:

- the relative cost competitiveness of nuclear power versus the alternatives
- security of supply and independence from fossil fuel energy imports
- diversity of domestic electricity production and reduction in volatility arising from input fossil fuel costs; and
- reduction in greenhouse gas emissions and subsequent effects on global climate.

The world's first civilian nuclear reactor commenced operation in 1955. According to the International Energy Agency (IEA), today there are 443 nuclear reactors operating in 31 countries, producing 15 per cent of the world's electricity.

Australia has 38 per cent of known low cost global reserves of uranium and has 23 per cent of global production, Australia is well positioned to increase production. This presentation will discuss Australia's opportunity to increase production of uranium and to become a participant in the wider nuclear fuel cycle and the Government's response of April 28, 2007.

ROUTINE MEASUREMENT OF THE FWHM OF CT SCANNER RADIATION DOSE PROFILES. IS IT NECESSARY?

F.J. Thomson

Radiology Department, Auckland City Hospital, Auckland, New Zealand

INTRODUCTION: It is generally accepted that measurement of the slice thickness radiation dose profile is a necessary step in determining the performance of a CT scanner and is a regulatory requirement in all developed countries. What is less obvious, is the need for repeated measurement of the FWHM of the profile after the initial acceptance test. In New Zealand, an annual measurement is required [1], while AAPM Report No.74 [2] recommends that "This test should be performed monthly to semi-annually at all available slice thicknesses".

METHODS: Unlike many countries which require the measurement of dose in 16 cm and 32 cm diameter PMMA phantoms, the New Zealand Code specifies that "the CTDI shall be measured in air at the isocentre". In addition to being very easy to measure with a pencil ionization chamber, this parameter is doubly useful because it is the basis for calculating the effective dose for any particular patient study using the ImPACT Excel spreadsheet programme and the NRPB SR250 data sets. If the dose to air for each slice thickness is measured, it can be compared with the corresponding FWHM of the dose profile. In all scanners measured to date, this relationship is very linear. Usually, the measured CTDI in air for each slice thickness does not change significantly from one routine QC assessment to the next. Hence, if the dose ratios for the range of slice thicknesses have not changed, it is an absolute certainty that the corresponding FWHMs have not changed either.

The FWHM of the dose profile has been measured using a low sensitivity CR imaging plate read in an Agfa ADC Compact system using the Flat Field option and Exposure Class 50. [3]

RESULTS: The measured FWHM is plotted against relative dose to air for a typical CT scanner QC assessment. The predicted FWHM is obtained from the linear regression equation. The agreement is not quite so good in a scanner where the profile is asymmetric outside the main peak due to the presence of extra-focal radiation.

Table 1. *Comparison of measured FWHM of dose profile and value predicted from dose ratio for a Siemens Volume Zoom CT scanner.*

Nominal slice thickness [mm]	Average dose ratios	Measured FWHM [mm]	Predicted FWHM [mm]	Difference [mm]
4 x 5 = 20	1.000	21.82	21.81	0.00
2 x 8 = 16	0.772	16.86	16.87	-0.01
4 x 2.5 = 10	0.549	12.01	12.01	0.00
4 x 1 = 4	0.266	5.86	5.83	0.03
2 x 0.5 = 1	0.117	2.59	2.61	-0.02

DISCUSSION & CONCLUSIONS: To answer the question posed in the title, in my opinion, the FWHM of the dose profile should be measured once only at acceptance, and subsequent QC assessments should only require dose measurements. Of course, if the measured CTDI in air changes, then further investigation is required. It is unreasonable to suggest that the FWHM must be measured at monthly intervals.

REFERENCES:

[1] *Code of Safe Practice for the Use of X-rays in Medical Diagnosis, NRL C5 (1994), National Radiation Laboratory, Ministry of Health, New Zealand*

[2] *AAPM Report No.74 Quality Control in Diagnostic Radiology (2002), Published for the American Association of Physicists in Medicine by Medical Physics Publishing*

[3] *Thomson FJ, Measurement of CT scanner Dose Profiles in a Filmless Department, Australas Phys Eng Sci Med 28 (3): 179 – 183, 2005*

HIP RADIOGRAPHIC IMAGE-DERIVED MORPHOMETRIC & TRABECULAR STRUCTURAL PHENOTYPES IN A LARGE GROUP OF DIZYGOTIC TWIN PAIRS: METHODOLOGY

R.I Price[1,2], S.G. Wilson[1,2], M. Bottomley[1], I. Sweetman[2], S. Bailey[1], C. Leatherday[1] and T.D. Spector[3]

[1] *Sir Charles Gairdner Hospital*
[2] *University of Western Australia, Perth, Australia*
[3] *Twin Research Unit, Kings College London, London, UK*

Genetic linkage analysis of twins phenotyped for multiple traits is a proven approach for gene discovery (Wilson *et al*. Eur J Hum Genet. 2006 14(3):340-8). Studies of osteoporotic fracture in families show it is under genetic control. However BMD is an incomplete descriptor of bone fragility, not accounting for shape or trabecular structure, which are aspects of "bone quality"; a problematic contributor to bone strength. Structural analysis of plain radiographs favourably discriminates hip-fracture cases. This study of female twins (n= 650) examines new methods for determination of gross morphometric and trabecular-structural phenotypes from pelvic radiographs.

Proximal femoral (PF) images were digitised (600 dpi) and subjected to an algorithm that established a femoral neck (FN) axis by determination of femoral-head centre and midpoint of FN. Femoral shaft (FS) axis was determined analogously. Derived variables described: gross shape of PF, its cortical structure plus several 12x12mm regions-of-interest (ROI) for image "texture" analyses, positioned relative to PF. Fast Fourier transform (FFT) power spatial-frequency spectra were determined for each ROI using a novel thresholding algorithm based on maximisation of the power-spectral variance coefficient between all angles; comparing favourably with traditional noise-reduction methods.

Intra- and inter-operator reproducibilities (CV%; n=100 in duplicate) were similar, but strongly dependent on the phenotypic variable: FH diameter (0.8%), bone widths (1-1.5%), ROI position (<1%), inferior and superior FN cortical thicknesses (8-10%).

These improved semi-automated methods are suitable for application to large groups of proximal femoral images and potentially provide new and important phenotypes for the study of bone structure and fracture.

THE AUSTRALASIAN CLINICAL MEDICAL PHYSICS AND BIOMEDICAL ENGINEERING WORKFORCE

W.H. Round

Department of Engineering, University of Waikato, Hamilton, New Zealand

INTRODUCTION: In August and September of 2006 a survey of the medical physics and biomedical engineering work force was carried out in Australia and New Zealand. This was done to obtain a precise snap-shot of the workforce at that time.

METHODS: To ensure that as complete coverage of the workforce as possible would be obtained, effort was put into ensuring that as many as possible of the clinical medical physicist and biomedical engineer positions would be accounted for. Initially all of the Branch Chairmen of the Australasian College of Physical Scientists and Engineers in Medicine (ACPSEM) were asked to list contact details of all of the chief or principal physicists and biomedical engineers in all of the clinical departments in their branches. The lists were to contain the details of those in the private as well as the public sector, and those outside the hospital-based medical sector who may be carrying out duties such as overseeing radiological quality control that a hospital-based physicist may typically do.

The lists were to include all chief or principal physicists and biomedical engineers whether or not they were members of the ACPSEM to ensure a full coverage of the workforce.

A survey document was then emailed to each of the chief or principal physicists and biomedical engineers that asked them to provide for each of their established positions

- The jurisdiction in which they worked (i.e. New Zealand or the Australian state or territory).
- The years of relevant experience that the person had since passing their first degree.
- The base salary or total remuneration package (TRP) of the person occupying the position.
- The fraction of full time spent in each of the disciplines of radiation oncology physics, radiology physics, nuclear medicine physics and biomedical engineering.
- Whether or not the position was vacant.

The survey recipients were continuously lobbied until a complete data set was obtained.

RESULTS: 495 positions (equivalent to 478 equivalent full time (EFT) positions) were captured by the survey. Of these 268 EFT were in radiation oncology physics, 36 EFT were in radiology physics, 44 were in nuclear medicine physics, 101 EFT were in biomedical engineering and 29 EFT were attributed to other activities. The survey reviewed the experience profile, the salary levels and the number of vacant positions in the workforce for the different disciplines in each Australian state and in New Zealand.

DISCUSSION & CONCLUSIONS: Analysis of the data identifies staffing shortfalls in the various disciplines and demonstrates the difficulties that will occur in trying to train sufficient physicists to raise staffing to an acceptable level.

A REVIEW OF CT RADIATION DOSE IN QUEENSLAND HOSPITALS

D. Schick

Biomedical Technology Services, Brisbane, Australia

INTRODUCTION: Over the past few years Queensland Health has replaced many of its computed tomography (CT) systems – predominantly with the multi-slice Philips Brilliance series (16 and 64 slice) scanners. Given the common system platform across multiple sites, hospital physicists and radiographers have taken the opportunity to review scan techniques and their associated radiation dose, with a view to determining and sharing "preferred" scan protocols. A survey of Dose Length Product (DLP) and scan technique data has been undertaken, collated, compared with other published data, and preliminary conclusions drawn regarding possible scan technique modifications.

METHODS: Data collection has occurred in two phases. A preliminary survey was circulated as a Microsoft Excel spreadsheet to senior CT radiographers from participating hospitals in late 2006. This phase of the survey requested data entry for head, abdo/pelvis with contrast, and CTPA studies. The data required was DLP as reported on the scanner console and default scan technique (kV, mAs or mAs_{eff} per rotation, reconstructed slice thickness, dose modulation used). DLP data was recorded for as many (adult) patients as practicable for each scan type.

In part due to growing interest in this project following collation and reporting of the first phase results, the survey spreadsheet was modified and expanded to include a wider range of commonly performed examinations. DLP and scan technique data from 6 hospitals (8 scanners) and for 6 commonly performed scan types have been collated and reported back to system users. Median DLP for each exam category has been derived, and principally compared with the local diagnostic reference levels (LDRL) suggested by Heggie[1] and the DRLs specified by the NRPB (UK)[2].

RESULTS: In many respects the data reflects the fact that an optimization process has not yet been applied to these multislice scanners ie. doses are frequently above DRLs. Of the 42 median DLPs determined (across the 6 hospitals) from the survey data, only 6 of these are less than the relevant LDRL suggested by Heggie. Furthermore there was significant variance in technique and dose amongst the CT systems even with respect to scanners of the same make and model. Subsequent discussions and presentation of this data at a Queensland hospitals CT reference group meeting has resulted in some scan protocol changes.

DISCUSSION & CONCLUSIONS: The survey highlights the need for optimisation of scan technique on CT equipment. For the most part, the surveyed CT scanners had been recently commissioned with technique determined by a combination of manufacturer recommendations and experiences during the applications training phase. Despite this, significant variance in technique and dose exists as noted above. Acceptance and performance testing undertaken by medical physicists has not focussed on issues of patient dose from clinical scans but rather compliance with manufacturer's specifications such as noise, MTF and CTDI. Further work is required to optimise CT dose in a structured and controlled manner across the participating sites and is currently in the planning stage.

REFERENCES:

[1] *J.C.P. Heggie, J.K. Kay, W.K. Lee, (2006) Australasian Radiology, 50: 278-285.*
[2] *P.C. Shrimpton, M.C. Hillier, M.A. Lewis, M. Dunn. (2005) Report No.: NRPB-W67. National Radiological Protection Board, Didcot.*

A NATIONAL DOSIMETRIC SURVEY OF COMMON SCANNING PROCEDURES FOR PAEDIATRIC CT EXAMINATIONS

A. Wallace[1], K. Sibelle[2], R Budd[2], S. Goergen[3] and J. Heggie[4]

[1] *Medical Engineering and Physics Department, Austin Health, Heidelberg, Australia*
[2] *Department of Medical Imaging and Radiation Sciences, Monash University, Clayton, Australia*
[3] *Department of Radiology, Monash University, Clayton, Australia*
[4] *Medical Engineering and Physics Department, St. Vincent's Hospital, Fitzroy, Australia*

INTRODUCTION: The growing recognition of the increased risk of stochastic injury to paediatric patients from MSCT investigations has prompted a survey sponsored by RANZCR QUDI program, Austin Health and Monash University to review paediatric doses for some of the most common investigations undertaken in MSCT paediatric practice.

METHODS: A cohort of 8 specialist Radiology paediatric sites were initially chosen across Australia. A senior Radiologist from each site was personally contacted and then sent an explanatory letter and invitation to submit data. The survey forms included a data sheet requiring acquisition protocol parameters (kVp, mAs, pitch, beam width, reconstructed slice thickness, etc) and a phantom graphic sheet requiring the marking of the inferior and superior acquisition margins. Survey forms were supplied for each of 13 common CT acquisitions to be tested.
Response data was input into CT-Expo Version 1.5.1., a CT dosimetry calculation engine, to determine Dose-Length Product (DLP (mGy.cm)) and Effective Dose (ED (mSv)). Data was collected, calculated, blinded and collated into various presentations that were given at a QUDI seminar in November, 2006[1].

RESULTS:. A total of 6 of the original 8 surveyed sites responded (75% compliance) using 5 types of MSCT platforms (2x Philips Brilliance 64, 1x GE LightSpeed Plus 4, 1x GE LightSpeed Pro 16, 1x Siemens Sensation 16, 1x Siemens Sensation 64). Subsequently an additional site, not originally invited to submit data but having significant expertise in paediatric radiology also submitted survey forms (1x Toshiba Aquilion 64). Data showed a range of dose efficiencies spread across the surveyed sites. The acquisition protocols also varied significantly across the sites having an important bearing on the dose delivered. An indicative Diagnostic Reference Level (DRL) was calculated using the 5th ranked value of DLP as a measure of current dose delivered per procedure. A measure of the spread of DLP values per procedure ranged from a minimum of less than 2x for a Head-Trauma acquisition (372 – 520 mGy.cm) to 14x for a Chest-Trauma acquisition (28 – 388 mGy.cm).

DISCUSSION & CONCLUSIONS: Survey data indicates a significant variation in acquisition protocols for various MSCT investigations across system platforms and site boundaries. Consequent dose efficiencies and inefficiencies are also apparent. This large variation could be addressed by the implementation of a substantive national survey to establish current practice and dose prior to establishing more definitive DRL values. The implementation of a dose optimisation information program would also be of benefit as an information source for all CT practices in Australia.

REFERENCES:

[1] *QS10.i Paediatric CT Dose Survey, http://www.ranzcr.edu.au/qualityprograms/qudi/projects.cfm#QS10.i.*

A REAL-TIME MONITORING STUDY OF THE PERSONAL DOSE RECEIVED BY A NUCLEAR MEDICINE TECHNOLOGIST (NMT) ADMINISTERING FDG IN A HIGH PATIENT THROUGHPUT PET CENTRE

P. U[1], A. Wallace[1], K. Hickson[2] and J. Bradley[2]

[1]*Medical Engineering and Physics Department, Austin Health, Heidelberg, Australia*
[2]*Nuclear Medicine & Centre for PET, Austin Health, Heidelberg, Australia*

INTRODUCTION: With the increasing success and developing applications of PET-CT, especially in relation to Oncology Staging, it is possible that the number of PET scans may overtake traditional gamma camera scanning as the major scanning procedure. This rapid growth in PET studies has already resulted in an increasing radiation exposure cost to NMT'. Previous personnel dosimetry surveys by our group have established the increasing dose impacts of PET and PET-CT investigations to staff(*1, 2*).

METHODS: This project has used, a real-time, solid-state, 2 second resolution, personal dosimeter to monitor the occupational Hp(10) equivalent dose of NMT' managing FDG patients.
A detailed manual mapping of the patient management procedure, time dependence and distance relationships to the sources of exposure and their magnitudes was undertaken.

RESULTS: Experimental results show, that a junior NMT may spend on average 52% of the close contact time (<2 m) with the patient when administering an FDG dose compared to 36% of that time for the senior NMT. This results in an average daily dose of 15 μSv and 11.4 μSv respectively.
Post-administration, escorting the patient into the scanner room and setting-up the patient on the bed, takes approximately 27% of the junior NMT time to perform, which results in an average daily dose of 7.8 μSv. The senior NMT takes approximately 33% of their time for the same task, with an average daily dose of 10.3 μSv.
Removing the patient from the scanner room and escorting them from the department takes about 21% of the junior NMT time giving 6.2 μSv of dose and 31% or 9.7 μSv for the senior NMT.

DISCUSSION & CONCLUSIONS: At the conclusion of this study the typical daily dose received by NMT staff, working in close contact with FDG patients is approximately 29 μSv for junior NMT (4-5 mSv/yr) and 31.4 μSv (5-6 mSv/yr) for senior NMT. Currently this centre is performing approximately 3,400 FDG injections per year plus 50 511 keV research injections of various positron emitters. This dose load is spread across 3 dedicated PET NMT', 1.5 EFT NMT rotating through PET and 1 EFT registrar physician.

REFERENCES:
[1]*F. O. Roberts et al., J Nucl Med Technol 33, 44 (Mar, 2005).*
[2]*C. N. Robinson, J. G. Young, A. B. Wallace, V. J. Ibbetson, Health Phys 88, S17 (Feb, 2005).*

CLINICAL / BIOMEDICAL ENGINEERING TALKS

INVITED TALK

TITLE: ANTIMICROBIAL RESISTANCE, CAN WE RISE TO THE CHALLENGE?

Keryn Christiansen

Department of Microbiology & Infectious Diseases, PathWest Laboratory Medicine, Royal Perth Hospital, Perth, Australia

Resistance to antibiotics was recognised soon after the introduction of penicillin in the 1940's. For the following 40 years the development of new antimicrobial agents kept pace with the emergence of resistance. That has now changed and we are potentially facing a future where untreatable infections become common place, where we return to pre-antibiotic era challenges in patient management.

What is antimicrobial resistance: There are many mechanisms that bacteria can employ to render antibiotics useless. Some are due to point mutations on the bacterial chromosome but more significantly many are carried on mobile genetic elements that are 'promiscuously' transferred to other bacteria, often of unrelated species and genera. Resistance can occur due to changes in the binding site for antibiotics, by enzymatic degradation of the antibiotic, by changes in permeability of the bacterial cell membrane or by activation of efflux pumps.

Why does it occur: Resistance genes occur in nature or due to exposure to antibiotics – the use of antibiotics selects for the resistance genes. The higher the use, the greater the selective pressure. Amplification then occurs by transmission of the resistant bacteria between patients or members of the community. Poor infection control, poor hygiene, and crowded conditions facilitate transmission.

Where does it occur: Resistant bacteria traditionally have been associated with hospitals and certainly there are many examples – Methicillin Resistant Staphylococcus aureus (MRSA), Vancomycin Resistant Enterococcus (VRE), and Resistant Gram negatives. Resistant bacteria also occur within the community – multi drug resistant Streptococcus pneumonia (commonest bacterial cause of pneumonia), multi drug resistant tuberculosis and more recently community associated MRSA.

What can be done: Management of antimicrobial resistance has been aimed mainly at reducing the selective pressure by stopping unnecessary use of antibiotics and interrupting transmission. Development of new antimicrobials is now also receiving attention. Infection control in the hospital is extremely important, both to prevent introduction of resistant organisms and in the control and eradication of outbreaks. Antibiotic stewardship programs are also being employed within hospitals. Community programs are less well developed but do exist.

How can you contribute: Knowledge is essential – both within the working sphere and as a member of the community. Knowing how transmission occurs, and thus how to prevent that occurring, knowing that antibiotics have a role in the treatment of bacterial but not viral infections. Knowing that a personal contribution to the fight can be made by not asking for antibiotics for treatment of a 'cold'.

DESIGN OF A MULTI-CHANNEL INTRALUMINAL IMPEDANCE SYSTEM

S. Afkari[1-2], G. Hebbard[1] and M. Fowler[2]

[1]*Biomedical Engineering Department, Royal Melbourne Hospital, Melbourne, Australia*
[2]*Gastroenterology Department, Royal Melbourne Hospital, Melbourne, Australia*

INTRODUCTION: Esophageal function testing and monitoring are important clinical tests in patients presenting with esophageal symptoms. The gold standards to evaluate the motor function of the esophagus and diagnose gastro-esophageal reflux are manometry and pH esophageal monitoring respectively. However, these techniques offer only indirect information about intra-esophageal bolus and/or liquid movement and presence[1].

Multichannel intraluminal impedance (MII) is a relatively new technique allowing detection of intraluminal bolus movement in the gastrointestinal tract without the use of radiation at a much lower cost[2]. In clinical applications it can be combined with manometry and/or pH studies, allowing better evaluation of bolus transit and non-acid gastro-esophageal reflux abnormalities[3]. A new 16 channel MII monitoring system has been designed for clicnial research in conjunction with manometry and pH studies.

METHODS: Impedance testing depends upon measurement of changes in resistance (in Ohms) to alternating electrical current when bolus passes a pair of metallic rings mounted on a catheter. In an empty tubular organ (esophagus) the electrical current between the two rings is conducted by the few ions present in and on the esophageal mucosa. Liquid containing boluses with an increased number of ions have a higher conductivity and as a result will have lower impedance values [1]. The impedance stays at this low value as long as the bolus is present; returning to baseline once the bolus is cleared

by a contraction (swallow). Gas passing will produce a rapid rise in the impedance due to its poor electrical conductance compared to liquid.

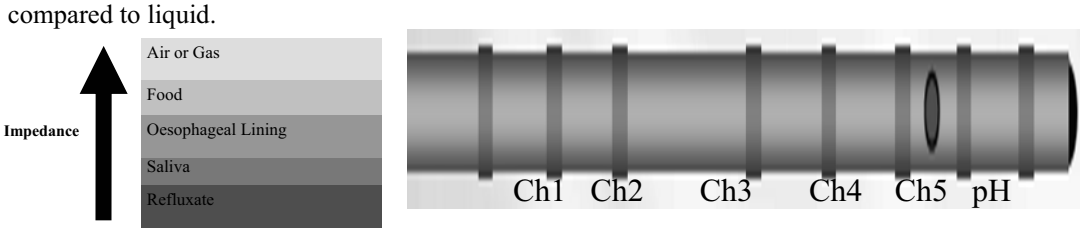

Figure 1. *Impedance change (left) and test catheter[3] (right).*

Measuring impedance at multiple sites (multichannel) allows for bolus movement and velocity determination based upon bolus entry and exit.

RESULTS: The designed system was tested in vistro using various, valued resistors and liquids (water, saline, and alcohol). Preliminary results show the designed system has a rapid rise of impedance due to air between two electrodes (typically above 33000 ohms) followed by a rapid return to baseline in presence of oral mucosa (typical value of 10000 ohms).

DISCUSSION & CONCLUSIONS: The system differs to others by using only one signal generator and current source for multi-channel recording. The system allows direct recording of information about intra-oesophageal bolus and/or liquid movement, velocity and bolus entry point.

REFERENCES:

[1]*H. Nguyen, Multiple Intraluminal Electrical Impedancometry for Recording of Upper GI Motility; The American Journal of Gastroenterology; Volume 94; Number 2; 1999.*
[2]*M. Vela, Simultaneous Intra-esophageal Impedance and pH Measurement of Acid and Nonacid Reflux: Effect of Omeprazole; Gastroenterology 2001; 120:1599-1606.*

OVERGROUND WALKING PERFORMANCE BY MEANS OF NEUROMUSCULAR STIMULATION: A NEW MOTION SENSOR-DRIVEN STRATEGY

G.P. Braz[1,2], M. Russold[1], R.M. Smith[2] and G.M. Davis[1,2]

[1]*Rehabilitation Research Centre, The University of Sydney, Australia*
[2]*Disciplinine of Exercise and Sport Science, The University of Sydney, Australia*

INTRODUCTION: Even after over 30 years of functional electrical stimulation (FES) research, there is still not a widely accepted closed-loop strategy to control gait. Consequently for this reason, the practice of FES gait remains primarily restricted to the use of open-loop (OL) systems.

METHODS: We developed a novel closed-loop (CL) strategy based on a finite-state algorithm that processed kinematic feedback from four compact motion sensors placed over the lower limbs (Fig. 1). This strategy automatically controlled knee extension via quadriceps and gluteus stimulation during the stance phase of gait and managed the stimulation delivered to the common peroneal nerve during swing-phase [1]. The performance of this strategy and that of an OL system was contrasted on two male paraplegics: one skilled (S1) and another regular FES-walker (S2), both experienced users.

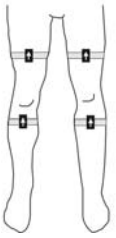

Figure 1. *Experimental setup of four compact motion sensors strapped to the subject's thighs and shanks. The sensors provided absolute angular displacements in the sagittal plane, which was used as feedback information to modulate the stimulation sequences required to evoke gait.*

RESULTS: In a protocol consisting of three walks over a 10m pathway, our skilled subject completed it with both strategies, while our regular user only completed 64% and 93% of the total distance with OL and CL respectively. In OL, this happened mainly because of the time spent regaining knee extension after a fatigue-driven knee buckle when the quadriceps stimulation was increased manually. This operation interrupted gait frequently, resulting in most cases in a slower cadence for both subjects. Conversely, the number of steps per meter did not vary significantly between both strategies.

Overall, the gait quality scores reported by the subjects using a visual analogue scale favoured the CL strategy, probably due to the automation of knee extension.

Table 1. *Overground walking performance. The distance field denotes the maximal walking length in case the subject was not able to walk the complete 10-m pathway.*

Trial	Distance (m)			Cadence (steps·min^{-1})			Step length (steps·m^{-1})	Gait Quality Score
	1st	2nd	3rd	1st	2nd	3rd		
S1-OL	10	10	10	14.27	21.08	20.39	4.2	5
S1-CL	10	10	10	24.70	25.54	20.31	5.1	8
S2-OL	8	5.9	5.3	7.63	9.68	6.40	3.2	7
S2-CL	10	10	7.95	8.84	9.43	10.63	3.1	9

DISCUSSION & CONCLUSIONS: With a relatively simple setup of sensors, our CL strategy demonstrated its feasibility in a clinical setting, significantly improving the performance of our regular user. Also important, CL enhanced key technical aspects in relation to current OL systems: it required less user intervention and accounted for the inter-subject differences in their stimulation requirements.

REFERENCES:

[1]*Braz G P, Russold M, Smith R M, Davis G M (2006) Motion Sensors Feedback in FES Gait: A Novel Control Strategy, Proc. 2006 World Congress on Medical Physics and Biomedical Engineering, Seoul, pp 2738-41.*

INVESTIGATION OF INTRAVASCULAR ULTRASOUND TO ESTIMATE THE PSEUDOELASTIC MATERIAL PROPERTIES OF ARTERIES AND VEINS

V. Cartwright[1] and P. Langhorne[2]

[1,2]*Department of Physics, University of Otago, Dunedin, New Zealand*

INTRODUCTION: In recent years improvement has been made in the understanding of the biomechanical properties of blood vessels. Experimental data used to develop mathematical models of blood vessel wall material have focused on arteries with few exceptions. Since the development of coronary artery bypass graft surgery, which often utilises venous graft material, better understanding of the vein's biomechanical properties is needed. Experimental equipment used in this study was developed, in part, to investigate the biomechanical properties of veins.

METHODS: Material parameters resulting from the mathematical modelling of porcine arteries and human saphenous veins were compared using two different methods: 1) the traditional method of photographic and direct measurement of the external dimensions, along with the assumption of incompressibility to approximate the inner dimensions; 2) the use of intravascular ultrasound to obtain the inner and outer dimensions of the vessels. An experimental apparatus was constructed to measure circumferential and axial stress-strain data for such arteries and veins. Constitutive equations were developed using strain energy density functions based on the assumption of pseudoelasticity[1]. An exponential form of constitutive equation was fitted to the circumferential and axial stress-strain data, which resulted in a set of four material parameters for each method. A comparison of the sensitivity of both sets of material parameters was investigated with regard to conversion and reference data variations, data from repeated experiments, experiments fitting more than one axial strain, and experiments testing the variation in elastic properties. Levels of venous disease were determined for each specimen using histological classification assigned in accordance with reporting standards[2]. Each venous specimen was given a numeric grade from 0 (no sign of venous disease) to 6 (acute venous disease with active ulceration). The disease classification for the porcine arteries used in this study was unknown. Two statistical evaluations were made for both sets of material parameters. One evaluation compared ten porcine arteries and eight veins that ranged from 2 to 5+ in numeric grade. Another statistical evaluation compared a group with two veins (numeric grade 0) and three veins (numeric grade 2) to a group of five veins with numeric grades ranging from 2+ to 5+.

RESULTS: The traditional method was vulnerable to inaccuracy in the calculation of reference data, which is reliable to within approximately 5%, resulting in a 17% discrepancy in circumferential and axial stresses. Vulnerability found for the intravascular ultrasound method was caused by a combination of reference data and intravascular ultrasound conversion factor inaccuracies resulting in a 7% discrepancy in circumferential and axial stresses. Stress discrepancies influenced the values of the resulting material parameters. Statistical evaluations were made using Student's *t* test. The results for the comparison between ten porcine arteries and eight human saphenous veins with numeric grade from 2 to 5+ were as follows: one material parameter was found to be significant using the traditional method and two material parameters were found to be significant using the intravascular ultrasound method. For the comparison between five veins with numeric grades ranging from 0 to 2 and five veins with numeric grades ranging from 2+ to 5+ no significant difference in the material parameters was found using the traditional method. For this comparison the data may indicate a significant difference for

one material parameter using intravascular ultrasound; however, the grouping of the specimens and a shortage of healthy specimens may have had an adverse influence on these results.

DISCUSSION & CONCLUSIONS: The intravascular ultrasound method was more robust, and in the comparison between arteries and saphenous veins two significant material parameters were found using this technique. For the comparison between the material parameters of healthy and diseased veins the number of healthy veins in this study was not sufficient to be conclusive.

REFERENCES:

[1]*Y. C. Fung, K. Fronek, P. Patitucci, (1979) Am. J. Physiol, 262: H544-H552.*
[2]*J. M. Porter, G. L. Moneta, (1995) Journal of Vascular Surgery, 21:635-645.*

IONTOPHORESIS OF ANTIBIOTICS INTO SEGMENTAL ALLOGRAFTS

Robert Day[1], Kasia Michalak[1], Steve Megson[2], Piers Yates[3,4] and David Wood[3,4]

[1]*Medical Engineering & Physics, Royal Perth Hospital, Perth, Australia*
[2]*Pioneer Valley Hospital, Mackay, Queensland, Australia*
[3]*Perth Orthopaedic Institute, Perth, Australia*
[4]*Department of Orthopaedics, University of Western Australia, Australia*

Background: Deep infection of cortical allograft bone is a disastrous complication with a reported prevalence ranging fro 0% to 33% of allografts. Most of these infections occur early (< 6 months) and are thought to originate from perioperative contamination or wound complications. Iontophoresis, where the diffusion of ions in solution is enhanced by an external potential difference, can be used to load antibiotics directly into the bone graft to prevent perioperative infection. This study reports the results of the first clinical trial of iontophoresis treated allografts.

Methods: From June 1997 onwards all patients who were scheduled to undergo reconstructive allograft surgery at a university-affiliated teaching hospital consented to receive iontophoresed allografts. To date 42 tubular allografts from the Perth Bone and Tissue Bank have been loaded with antibiotics using iontophoresis and implanted into 39 patients, 3 patients receiving 2 segmental allografts each. Indications for allograft insertion were limb salvage for musculoskeletal neoplasm (17) and poor bone stock associated with infection (13) or revision arthroplasty (12). Whenever possible, samples of blood serum and fluid from the drain alongside the graft were obtained and assayed for antibiotic levels.

Results: Currently 33 patients with 36 allografts have an average follow-up of 3.4 years (12-84 months). There have been no early deep infections and all but 5 allografts remain *in situ*, resulting in an allograft retention rate of 86.1% (31/36). Eight patients have died but their final review data has been included in the study. Three of the 8 deaths were from metastatic disease related to a primary musculoskeletal tumor. The remaining 5 patients died of medical problems unrelated to their allograft surgery (mean age at death 84 years). Postoperative serum antibiotic levels were very low with gentamicin remaining below 0.5 mg/l and flucloxacillin remaining below 1 mg/l. Drain antibiotic levels remained above the minimum inhibitory concentration of each antibiotic — at 48 hours gentamicin averaged 5.97 mg/l and flucloxacillin averaged 2.23 mg/l. There were 2 late deep infections, both of which occurred more than 10 months after allograft implantation in patients who had previously sustained periprosthetic fractures. Both cases were infected with organisms that would normally be considered commensal and both presented acutely on previously satisfactory constructs. The union rate for the cohort was 92%.

Conclusions: There were no early deep infections of the allografts and no complications attributable to the iontophoresis technique. Our results demonstrate that iontophoresis is a promising technique for supplementing allograft bone with antibiotics.

ROBOTICS AND AUTOMATION - THE FUTURE

P. Deuchar

CEO. Argon Technology Pty Ltd, Western Australia

INTRODUCTION: In an increasingly complex world, leading edge robotics and automation offer opportunities not only to improve efficiency but to address skilled labour shortages. The challenges we face are whether we choose to invest in these solutions using our own intellectual and financial capital or whether we buy in solutions. Australians have well developed industries which should see us continue to spring innovative and competitive products and services using our own resources.

METHODS: What follows is the industry experience of a Western Australian Engineering company working and developing in the field of robotics and automation, facing the challenges in solving the next generation of industries problems. With innovations aimed at greenfields research or translation research into traditionally brownfields industries. The focus the ability to develop technology transfer initiatives & provide the greater industry with advancing technologies.

Let us look at how robotics and automation in industrial environments and mining laboratories has application to chemical and medical laboratories. We can and should challenge the boundaries of traditional tertiary disciplines and let's consider the advantages that can bring. That is, from the perspective of how technological advances bring together specialisations within the same disciplines and between different disciplines, like mechanical and electrical engineering and between disciplines like engineering, science and medicine.

RESULTS: Let's follow this on a bit and look at some questions like 'Who do you employ today to get a job done?' and 'How much foresight do you have when planning your production processes, and investing in solid local industry expertise to aid these processes?' How do we change a mindset, or paradigm, to expand on the exampling of the Australian medical world leading breakthroughs? The topic outlines opportunities for local technology development raising the question of why invest in overseas technology and it surfaces the challenges faced in technology development, including the inspiration to do it, expertise, the IP challenge and of course funding. We have it at home, look no further!

PHOTO DYNAMIC THERAPY FOR NON-MELANOTIC SKIN CANCER USING A XENON-ARC SOURCE FOR BOTH FLUORESCENCE AND TREATMENT

J. Hagekyriakou

Peter MacCallum Cancer Centre, East Melbourne, Victoria, Australia

INTRODUCTION: Photo Dynamic Therapy (PDT) for the treatment of Non-Melanotic Skin Cancer may be accomplished by the topical application of a photosensitizing compound, such as 5-Aminolevulinic Acid (5 ALA), or an ester formulation of the acid base, (eg 5 ALA Methyl Ester), in order to induce accumulation of a natural photosensitiser Protoporphyrin IX, (PPIX), within the cell cytoplasm. At approximately 3 hours post application, the PPIX may be activated by illumination at specific wavelengths, inducing cell death via the production of singlet Oxygen free radicals. A variety of light sources may be used to activate the PPIX, provided the power output at the specified wavelength is sufficient to deliver the required energy within a 10-20 minute interval and yet be harmless to normal (non-sensitized) skin. On application of Ultra Violet A (UVA) or Violet light to the affected lesion, just prior to illumination, photosensitization may be demonstrated by the presence of a distinctive Red fluorescence. During treatment, the PPIX molecule breaks down as a consequence of photochemical reactions. At the end of treatment, the absence of the UVA or Violet induced Red fluorescence validates the completeness of the treatment; rendering further illumination, ineffective.

METHODS: Patients presenting with Non-Melanotic Skin Cancer at the Peter Mac Callum Cancer Centre were treated using the following technique. The lesion was scraped using a scalpel blade or a small curette, in order to remove loose crust and debris from the surface. The topical photosensitizing compound 5 ALA Methyl Ester, METVIX Cream, (GALDERMA Australia), was then applied over the entire lesion, extending over the normal skin, and covered with a transparent occlusive dressing Tegaderm, (3M) for a period not less than 3 hours. The patient subsequently returned to the clinic whereupon the dressing was removed, excess cream wiped from the surface, and illumination was applied. The light source used was a Polilight 500, (ROFIN Australia), a multiple wave band, high intensity, tuneable light source, which utilises a group of interference filters to shape the output spectrum to a band covering 570 – 650 nm,("Orange" light), corresponding to the peak absorption band of PPIX. A dose of at least 40 Joule/cm^2 was delivered from the source using a 6-8 mm diameter Liquid Light Guide. Light coupling and transfer efficiency is much greater when using a large diameter light guide, compared to that of an optical fibre, for non-laser type of application. The ROFIN Polilight source also provided illumination capability in the UVA (350 ± 30 nm) or Violet light (415 ± 20 nm) part of the spectrum, which provides observation and photographic recording of the Induced fluorescence before, during and after the end of treatment.

RESULTS: The majority of the patients treated, using PDT, presented with the following skin lesions: - Superficial Basal Cell Carcinoma (sBCC), Nodular BCC, Actinic Keratosis (AK) and Bowens Disease. A few less common skin conditions, such as Paget's extra mammary, Porokeratosis, Actinic Cheilitis, Cutaneous T-Cell Lymphoma and Papillary Lymphoma, were also treated using the above technique. Treatment outcome, based on Substantial Reduction or Complete Elimination of the induced Red fluorescence, was observed in 100% of cases. In some patients where a significant amount of Red fluorescence was detected following the delivery of the prescribed surface energy, the active part of the lesion was further boosted until the fluorescence was essentially eliminated. Long term outcome, in patients who have been evaluated thus far, indicates that the treatment can generate excellent cosmetic results, relative to other treatment modalities, commonly prescribed for these skin conditions, such as Surgery, Cryotherapy or Radiotherapy. Patients, who have relapsed within the treated area, may be retreated using PDT, without additional complications; such as those experienced as a consequence of previous non-PDT type treatments.

CONCLUSION: Photodynamic therapy using a Xenon–Arc source, providing "Orange" light for treatment and UVA or Violet light for Fluorescence detection, in combination with 5 ALA Methyl Ester, for the treatment of Non-Melanotic skin lesions such as BCCs AKs and Bowen's disease is very effective. Long term outcomes are comparable to those of Surgery, Cryotherapy or Radiotherapy, but with significantly better cosmetic outcomes.

MECHANICAL DESIGN AND DRIVING MECHANISM OF AN ISOKINETIC FUNCTIONAL ELECTRICAL STIMULATION-BASED LEG STEPPING TRAINER

N.A. Hamzaid[1], C. Fornusek[1], A. Ruys[2] and G.M. Davis[1]

[1]*Rehabilitation Research Centre, Discipline of Exercise and Sport Science, The University of Sydney, Australia*
[2]*School of Aerospace, Mechanical and Mechatronic Engineering, The University of Sydney, Australia*

The mechanical design of a constant velocity (isokinetic) leg stepping trainer driven by functional electrical stimulation-evoked muscle contractions was the focus of this paper. The system was conceived for training the leg muscles of neurologically-impaired patients. A commercially available slider crank mechanism for elliptical stepping exercise was adapted to a motorized isokinetic driving mechanism. The exercise system permits constant-velocity pedalling at cadences of 1-60 rev·min^{-1}. The variable-velocity feature allows low pedalling forces for individuals with very weak leg muscles, yet provides resistance to higher pedalling effort in stronger patients. In the future, the system will be integrated with a computer-controlled neuromuscular stimulator and a feedback control unit to monitor training responses of spinal cord-injured, stroke and head injury patients.

A SYSTEM TO ASSIST THE ANALYSIS OF PERIPHERAL NEUROPATHY

B. Hayes[1], P. Junor[1] and T. Day[2]

[1]*Electronic Engineering, La Trobe University, Melbourne, australia*
[2]*Clinical Neurophysiology, Royal Melbourne Hospital, Melbourne, australia*

INTRODUCTION: Three aspects of human physiology that have a possible association are: small fiber nerve function, (measurable via EMG recordings of the sympathetic skin response), vascular blood flow to the skin (monitored using combined Laser Doppler flowmetry and iontophoresis) and sweat production. Measurement of sweat production may provide a useful indicator of peripheral neuropathy and disease.

METHODS: A sudorometer, constructed to measure sweat production, passes atmospheric air through a flow regulator[1] after desiccation with anhydrous calcium sulfate. Air pressure is monitored using a silicon pressure sensor[2] (Freescale Semiconductor); temperature and humidity are monitored using a combined sensor[3]. The stream of gas of known pressure, humidity and temperature is then passed through a sweat cell attached to the skin, allowing evaporation of sweat: this gas stream (having modified humidity and temperature) is then resampled by separate temperature and humidity sensors. The volume of sweat produced is then calculated using the ideal gas law.

RESULTS: Preliminary bench testing of the sudorometer using a model for the evaporative effect of sweat on the epidermis is depicted below. Initial results demonstrate the ability to detect a small step change in humidity.

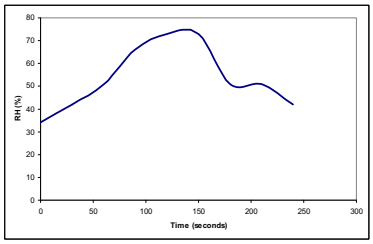

Figure 1. *ΔRH Time Curve In Response to Step Change.*

DISCUSSION AND CONCLUSION: We have developed a unique method suitable for monitoring sweat production in patients suffering conditions leading to peripheral neuropathy. We intend using this to investigate the relationship between sweat volume/production rate and clinically-established assessment of peripheral neuropathy. We hope that this measurement of sweat production may assist analysis of peripheral neuropathy and other disease associated with diabetes.

REFERENCES:

Low PA. Laboratory evaluation of autonomic function. In: Low PA, ed. Clinical autonomic disorders: evaluation and management. Second Edition. Philadelphia: Lippincott-Raven, 1997: 179 – 208.

[1]*DFC, Aalborg Orangeburg, New York, USA*
[2]*MPX 5100, Freescale Semiconductor Texas, USA*
[3]*SHT11, Sensirion Inc. California, USA*

PROJECT MANAGEMENT (PM) STRATEGIES FOR CLINICAL ENGINEERING

S. Hiremath[1] and B. Anderson[2]

[1]*Medical Technology Management Unit, Princess Margaret Hospital, Perth, Australia*
[2]*Perfect Project Palnning, Perth, Australia*

INTRODUCTION: A 'project' is defined as a planned set of tasks, implemented by an effective schedule to achieve specific outcomes within the targeted time period and budget. Project Management is the planning, scheduling and controlling of project activities to meet the set objectives of the projects on time and within the budget. There are specific strategies recommended by Project Management Institute (PMI) to achieve these goals. However in clinical engineering circles often the 'reactive' maintenance strategies are used in preference to PM techniques. This paper describes author's experience in implementing PM strategies.

Quality expert Dr.J.M.Juran [1] defines a project as a problem 'scheduled for solution'. This definition forces us to recognize that projects are aimed at solving the problems and failure to properly set the scope, objectives and metrics for the project often leads to problems related to performance, cost and quality. This is explained by Dennis Lock [3] as the 'triangle of objectives' as shown in fig1. The Earned Value Management (EVM) principles are applied in our project to achieve highest possible quality at the least cost and on time.

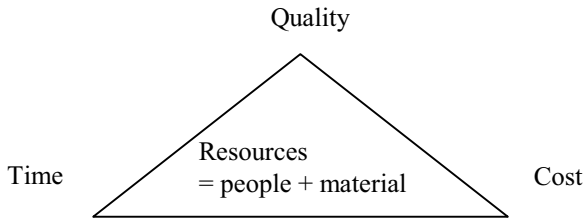

Figure 1. *Triangle of objectives.*

METHODS: A case of EVM is presented by Henderson, Kym [2] in his paper 'Earned Schedule in Action'. This paper describes an approach achieving a high and very direct level of cost and schedule integration for a project. We have used a similar approach by using Plan, Organize, Implement, Network and Train (POINT) strategies. POINT project followed the recommended iterative method of using MSP as follows: Assign Tasks, Durations, Links, Resources, Cost, test Leveling (TDLRCL). This allowed the calculation of EV and ES as a measure of improvements achieved in the maintenance program as a result of POINT project. These EV and ES analysis were applied during the quarterly review of the project performance, to ensure that the project was on schedule and there were no cost escalations or delays. MSP provided very good reports in terms of cost and schedule variance on the go. The reports are graphical and are easily understood.

RESULTS: POINT project achieved cost containment of 2-4% for maintenance budget within two years.

DISCUSSION & CONCLUSIONS: PM strategies work with Clinical engineering as well as they do with large projects, such as building the roads, if strategic PM is used effectively.

REFERENCES:

[1]*Godfrey, A. Blanton and Juran, J. M. Juran's Quality Handbook: 5th Edition, ISBN 0-07-034003-X.*
[2]*Henderson Kym, Earned Schedule in Action, 'The Measurable News', "Summer" 2004.*
[3]*Lock, Dennis, Project Management: 7th Edition, ISBN 0-566-08225-X 2000.*

REDUCING WRONG GAS DELIVERY TO PATIENTS

Glenn Kennett

Flinders Biomedical Engineering, Flinders Medical Centre, Bedford Park, Australia

INTRODUCTION: Accidental delivery of the wrong gas to patients is a world wide[1] problem that can result in severe adverse patient outcomes. Air and oxygen are often located side by side at bedsides in hospitals being indexed incompatible until they reach the end of each flow meter where the threads, hose nipples and patient tubing are interchangeable. Air or oxygen can be delivered incorrectly to patients.

BACKGROUND: Flinders Medical Centre has identified and tracked wrong gas delivery to patients over the past 2 years. There have been 12 Advanced Incident Management System (AIMS) reports of adverse events: 8 involved MET (Medical Emergency Team) intervention and 1 required admission to ICU. Personally witnessing an incident during installation of "AIR Guards" and medical staff feedback indicate the mix up of gases occurs far more frequently than reported. The majority of incorrect connections occurred when patients returned from a procedure or were transferred from another clinical

unit. Contributing factors include incorrect nipple colours on 30% of flow meters involved in incidents, poor lighting and equipment or curtains obscuring the gas panel.

METHODS: A team of various disciplines investigated solutions to this problem. A number of strategies of error proofing and error reduction were considered each with varying risks, barriers and costs.

RESULTS: The preferred error reduction option chosen was "AIR Guard" developed through Flinders Biomedical Engineering (FBE). The prototype "AIR Guard" was developed and 500 units produced and deployed throughout Flinders Medical Centre. The aim was to produce a simple operating, permanent, strong, cleanable, clearly labelled, colour coded and physical barrier able to be post-fitted to all common flow meter brands.

Figure 1. *Air clearly different to oxygen.*

Figure 2. *Attaching patient tube with AIR Guard.*

DISCUSSION & CONCLUSIONS: The FBE "AIR Guard" creates a permanent and obvious difference between air and oxygen by providing a strong visual and physical barrier for users of medical flow meters, to assist with a more conscious choice of gases. Oxygen has been left unchanged and is freely accessible for emergency use.
"AIR Guards" were implemented in July 2007 and are now in the evaluation phase. AIMS reports will monitor further incidents to evaluate the effectiveness of "AIR Guards" and a user satisfaction questionnaire will be undertaken 6 months from installation.

REFERENCES:
[1]*Laura Landro, The Wall Street Journal, Hospitals Scramble To Prevent Errors, Redesign Devices, June 27, 2007; Page D3.*

BAD MEDICINE RESULTING FROM BAD SCIENCE

P. Kolb

Rehabilitation Engineering, Royal Perth Hospital, Perth, Australia

From time to time medicine comes up with some really bad practices originating in flawed science. Some personal experience derived from working in the health care industry has uncovered several interesting examples. Although these may not have had significant consequences, there is now in progress a development that does. In fact, it promises to parallel and even eclipse the gruelling introduction of helicobacter theory in the medical treatment of ulcers.

Over the past 17 years a simple education program (Buteyko) designed to reverse chronic hyperventilation (CHV) (1)has had astonishing success as a complementary therapy for asthma. With published clinical trials (2) boasting figures of up to 96% average reduction in bronchodilator usage for a therapy that is 100% dependent on patient compliance, it has won acclaim from patients and the media (3-7). The Australian Federal Department of Health and Ageing together with the National Asthma Council has investigated 40 complementary therapies for asthma (8). Without looking into the theory, they have determined that this is the only complementary therapy that is "probably" effective in reducing medication for asthma while at the same time reducing asthma symptoms. Yet this inexpensive education program is being withheld from asthma patients (6,9) for reasons that are based solely on some questionable science.

The dispute is over the validity of lung function tests, which show no improvement with this therapy. However, since the theoretical basis for this therapy is the reversal of chronic hyperventilation, it is argued that these tests, which rely on hyperventilation manoeuvres, are meaningless and unscientific. In the meantime, the current symptomatic treatment approach to asthma is perpetuated in the name of "science" (9).

This scientific misrepresentation has implications that go way beyond asthma. Since Da Costa (10) discovered bizarre and debilitating multi-symptomatic disorders in battle fatigued soldiers during the American Civil war in 1863, the list of disorders that can be attributed to chronic hyperventilation has grown and has been well documented in the medical

literature (eg 11,12). Since that time, those doctors who understand CHV have lamented the scant attention paid to this serious medical condition by their colleagues (eg 11,12).

While it takes more than good science to progress the traditionalist medical establishment, the dissemination of good science and the challenging of bad science is clearly one of the major educational roles of engineers and scientists in medicine.

REFERENCES:

[1]*Kazarinov VA, "Buteyko Method: The experience of implementation in medical practice", The biochemical basis of KP Buteyko's theory of the diseases of deep respiration, EDITOR: Buteyko KP; PUBLISHER: Patriot Press Moscow; 1990; PAGES: 198-220.[RUSSIAN].*
[2]*Bowler S, Green A, Mitchell C, "Buteyko breathing and asthma: a controlled trial", Medical J of Australia, VOL 169, December 1998, 575-578.*
[3]*Australian Television Channel 9: A Current Affair 10/03/1993.*
[4]*Australian Television Channel 9: A Current Affair 22/03/1993.*
[5]*Australian Television Channel 9: A Current Affair 09/05/1994.*
[6]*Australian Television Channel 9: Sunday Program (Part 2) 11/02/1996.*
[7]*BBC1 Northern Ireland: QED: Breathless*
[8]*"Asthma and Complementary Therapies: a guide for health professionals. "Australian Government department of Health and Ageing, 2005.*
[9]*Asthma Australia: "Position statement on Buteyko 1999."*
[10]*DaCosta JM, "On irritable heart: a clinical study of a form of functional cardiac disorder and its consequences.", Am J Med Sci, VOL 61, 1871, 17-53.*
[11]*Lum LC, "Hyperventilation: The tip and the iceberg", J Psychosom Res, VOL 19, 1975, 375-383.*
[12] *Magarian GJ, Middaugh DA, Linz DH, "Hyperventilation Syndrome: a diagnosis begging for recognition", West J Med, VOL 138, 1983, 733-736.*

THE LUCKY BED – OR WHY DEVICE CONFIGURATION MATTERS

P. L. O'Meley

Department of Biomedical Engineering, Royal Prince Alfred Hospital (SSWAHS), Camperdown, Australia

INTRODUCTION: The routine safety testing of medical devices is a burden we all bear grudgingly because lots of effort is expended with little or no impact on patient safety or risk reduction. There are several aspects of device inspections that receive little attention but can be vitally important – inspection and verification of device configuration and device condition. A case study is presented where configuration and condition was literally a matter of life and death.

METHODS: The author was recently involved in the investigation of a patient death in a large metropolitan CCU. The investigation was to determine if a failure of alarms on a patient monitor was implicated in a patient death. It was reported that the alarm was not triggered at the bedside or central.

Investigations started with the bedside monitor. Firstly it was observed that the bedside alarm was set to zero volume. It was then quickly established that two nearby beds were similarly set. A large number of tests were conducted to verify the alarm was triggered for a variety of lethal ECG rhythms. It was triggered in every case (but obviously remained silent).

During each bedside test the central station alarm function was also verified. Alarms reached the central but the alarm indication on the screen was not obvious and the sound was obscured by the multiple other simultaneous alarms from other beds (each also without obvious screen indication). The screen colour was "washed-out" so the alarming sector was almost invisible. Staff relied on observing a small "tick" mark near the bed label to determine which sector was in alarm. During tests it was also found that there was no strip recording (recorder paper was being wasted so it was removed) and there was no routine review of alarms to be printed and attached to notes (the printer was disconnected as it only printed black pages). These following the alarm there was no record of the alarm.

During the investigation staff present at the time were interviewed. Most staff were certain that no alarm was transmitted from bed to central and it was also confirmed that there was no power outage that could interrupt network traffic. During one interview, when the investigator was offering an opinion about the safety of zero volume bedside alarms by expressing the view that he would not like to be admitted to such a unit, "Would you?" he asked. "I'd want to be admitted to bed 2 – that's the lucky bed!" was the somewhat surprising reply. Other staff agreed that bed 2 was "lucky".

We then examined Bed 2 in more detail and found audible bedside alarms. Checks of every other bed showed they all had silent alarms. Further investigation revealed that Bed 2, the "lucky bed", had been repaired some years earlier and it was now set to factory defaults – Middle Level Bedside alarms. Unit configuration had not been restored because Biomed staff at the time (now moved on) had not been aware the repair had affected alarms config so had not restored unit configuration. Subsequent inspections had not noticed the difference – nor had nursing staff – except to notice the bed was "lucky". In this way a technically incompetent repair had actually saved lives.

To try and understand how things came to this we investigated the complete history of the unit. It was established that Zero volume alarms were set at installation (1997) following a Nursing request. (The author notes that this is a common request in

CCU – "to enable patients to sleep"). The zero volume alarms were noted during End-of-Warranty Testing in 1998 but were left as they are. For nearly a decade, it seems, these devices have been silently killing patients.

RESULTS: The investigation was forced to conclude that the device was functioning as it was designed and configured. The problem was a multitude of seemingly small, unrelated performance degradations and decisions had combined to mask the state of the patient.

DISCUSSION & CONCLUSIONS: Periodic Testing of devices in "systems" should take account of system performance. Devices configured for life critical alarms should not be silent (changes to alarm limits should allow patients to rest). Device condition must be included in scheduled inspections.

REFERENCES:

[1]*AS3551:2004. Btechnical Management Programs for Medical Devices, Standards Australia.*

BIOMEDICAL ENGINEERING DEPARTMENT STAFFING MODEL

P. L. O'Meley[1] and S. Scahill[2]

[1]*Department of Biomedical Engineering, Royal Prince Alfred Hospital (SSWAHS), Camperdown, Australia*
[2]*Department of Biomedical Engineering, Liverpool Hospital (SSWAHS), Liverpool, Australia*

INTRODUCTION: During facility planning or resource review there is a need to have a method of determining staffing numbers that is simple and sufficiently robust to be defensible. Since workload drives staff numbers and device numbers drive workload (through breakdown, testing, and PM) and staff themselves drive workload (supervision, travel and efficiency) we reasoned that by knowing how many devices a facility had we could predict workload and staff requirements.

METHODS: We starting by examining many ways of determining device numbers for future (or unfamiliar) facilities and it quickly became obvious that bed numbers are the easiest metric to access and the simplest to use. We then reasoned that the relationship between devices and beds would be an S shape because small facilities are low tech and big facilities have large wards devoid of many devices. We then plotted our current data (Devices vs Beds) from all SSWAHS major facilities. We then performed a series of simple regressions to arrive at a relationship between beds and devices fitted to an S curve.

To determine resource requirements we created a very simple model that builds up workload according to device numbers. Our historical data was collected over a range of sites over more than a decade. We used the historical data to determine the rate of failure per device, the time per repair, the time per test. We used the minimum number of available hours per employee (i.e we assumed every sick day is taken and the one weeks LSL is taken every year). We allowed for travel to remote sites for single breakdowns and single trips to perform multiple routine tests. We used simple calculations to predict travel times over given distances. Combining local and remote work gives staff required to service multiple sites from one workshop. Because of the ability to predict resources across a spread geography we call it the Area Biomedical Engineering Service Model, or ABES Model.

Our model only included general Biomedical Equipment (the historical data did not include imaging or IT systems). It is our experience that staffing in these areas is built up case-by-case from contract expenditure reduction or similar. The model does not address the issue of Professional Engineers.

RESULTS: The best relationship we found between Device Numbers (D) and Hospital Beds (B) was a third order polynomial (R2 = 0.978) as follows;

$$D = -0.00002B^3 + 0.0258B^2 + 2.0898B \quad (1)$$

Lower order models had lower regression numbers and higher order models unacceptable tails.

With simple averages from historical data we found; each repair was one hour, each test 0.33 hours and each device had 0.4 repairs per annum. With all leave taken (sick, annual, pub hol, ADOs, family etc) and two weeks training, each employee has 900 hours p.a. To cover the workload of those absent the minimum self-sustaining group is four staff, so we used this as the supervisor ratio (i.e. 3 TOs per STO). Combining these parameters it is possible to predict staffing needs for onsite activities.

Table 1. *Predictions for 150 and 350 Bed Hospital in Hypothetical Group Using ABES Model.*

Beds	Devices	Fail (est p.a.)	Fail (per mth)	Repair Hours	Test Hours	Dist to Offsite BME	Travel Visits	Total Hours	Tech TO (FTE)	Admin (FTE)	STO (FTE)
150	663	265	22	265	221	10	27.6	36.1	522.1	0.6	0.1	0.2
350	2653	1061	88	1061	883	0	0.0	0.0	1944.6	2.2	0.6	0.7

DISCUSSION & CONCLUSIONS: A simple model for predicting staffing needs for any given hospital has been developed. The ABES model is grounded in reality and historical data enabling users to have confidence in predictions from its use. We are currently using this model to successfully argue for more staff at some sites whilst maintaining staff at others.

INSTRUMENTATION OF A LARYNGOSCOPE FOR THE MODELLING OF FORCES FOR THE STUDY OF OPERATOR TECHNIQUE

G. Nicholls[1], C. Reed[1], R. Day[1], D. Guy[1] and M. Waddington[2]

[1]*Department of Medical Engineering and Physics, Royal Perth Hospital, Perth, Australia*
[2]*Department of Anaesthesia, Royal Perth Hospital, Perth, Australia*

INTRODUCTION: The device presented here is not a new idea – however the engineering approach taken here is! Other published designs – although successfully implemented, have involved extensive delicate remodelling and alteration of the laryngoscope including insertion of springs and strain gauges, physical detachment of faces and extensions of the grip tube to provide a beam for the transducer mounting. These devices generally required bulky cables feeding a board of electronics external to the Laryngoscope to produce output measurements. In some designs, this altered the operator's handling of the device while other designs only measured a single axis of force.

The design brief was to instrument a standard laryngoscope with minor physical modification for a non-clinical training environment (using a manikin to reduce patient variability issues), to provide simultaneous axial and bending force moment measurement irrespective of operator grip. The produced tool is also capable of detecting teeth contact – another factor not considered in other designs All required electronics are incorporated in the Laryngoscope handle. This was complimented by the power of a PC with real time display & acquisition software with multi-operator waveform selectable comparison review interface.

The engineered tool has formed the measurement basis of several studies at RPH with successful publications resulting.

METHODS: The laryngoscope forces were modelled using CosmosWorks™, with the calculated strain distribution used to position the gauges. A narrow slot was machined through the head of the laryngoscope using Electrical Discharge Machining (EDM) to produce a thin membrane, to which the four 120Ω quarter-bridge strain gauges were bonded. All required electronics including strain bridge amplifiers, completion resistors & regulated power to the circuit and blade light globe were incorporated in the handle. This improved the signal-to-noise ratio and allowed a thin, flexible cable to be used. The analogue signals were digitised (National Instrument USB 6008 DAQ) to be further processed & calibration compensated using custom LabVIEW™ software.

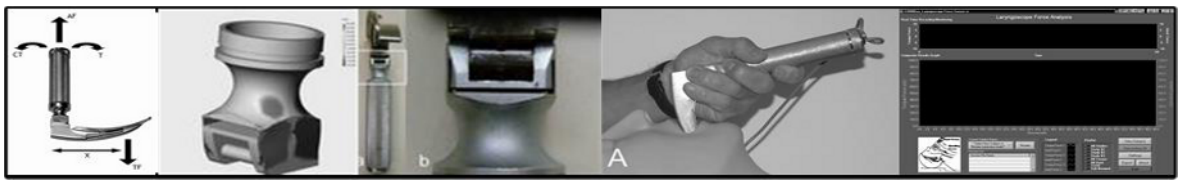

Figure 1. *Laryngoscope force modelling, instrumentation, parameters of measurement, and application interface.*

The laryngoscope was calibrated with known masses at a several distances to accommodate leverage effects on blade insertion length. The LabVIEW™ based application stored operator demographics, real time run data and run time-calculated parameters.

RESULTS: The study returned excellent bending force measurement results. However, the large bending force had cross coupling effects and interaction with the axial force measurements, causing increased variance.

DISCUSSION & CONCLUSIONS: The modelled and developed laryngoscope tool confirmed the two forces could be successfully measured. The LabVIEW™ application software provided a medium for the acquisition and review of the comparison of operator's techniques. Although the axial readings had a large variance, they still provided a comparable trend waveform for comparison analysis.

Possible future development would look at resolving the axial force problem through better strain gauge isolation and incorporating video capabilities into the laryngoscope blade. We are also investigating wireless signal transmission, to make the unit self-contained and able to be utilised as a tool in clinical environments for improved patient care.

TRIAXIAL ACCLEROMETER PILOT STUDY DESIGNED TO STUDY THE GAIT OF VESTIBULAR PATIENTS

G. Pendharkar[1], S. Marin[2], R.E. Mayagoitia[3] and P. Percival[4]

[1,4]*Department of Electrical and Computer Systems Engineering, Monash University, Victoria, Australia*
[2,3]*Centre of Rehabilitation Engineering, Academic Department of Physiotherapy, King's College London*

INTRODUCTION: Vestibular patients often experience spinning vertigo associated with balance problems. The symptoms of imbalance often affect their gait [1] and it is important to determine the severity of vestibular disorders experienced by a patient. The vertigo questionnaire is a standard form used by a physiotherapist to assess the severity, giving useful

information on a vestibular condition [1] but is subjective. Accelerometers have proven to be a reliable tool for the description of gait cycle characteristics using trunk accelerometry [2] and would provide objective data on a patients' performance in standardized tests to determine the severity of vestibular disturbance.

METHODS: Six healthy subjects (age 21 – 42 years) participated in the trials. The two trials consisted of a standard functional test in the gait lab and a free walking test (with a pair of triaxial accelerometers attached to their bodies) over a defined route consisting of crowded and non-crowded streets with regular and irregular surfaces. An XSens Technology MTx sensor was placed at the small of the back and another on the most posterior aspect of the head, both wired to an XBusMaster (wireless transmitter). The XBusMaster was interfaced using a Bluetooth transmitter to the receiver in a laptop where the acceleration data was stored. The head and trunk acceleration signals were sampled at 100Hz in real time and recorded as the subjects walked over the defined route. The accelerometer data for the whole route was divided into smaller sectors and filtered at 10Hz using a low-pass Butterworth filter. The average of the root mean square (RMS) values of the medio-lateral (ML) acceleration signals were calculated and normalized against each subject's speed for the sector under study. This allowed comparisons between the head and trunk accelerations for the various sectors of the free walk.

RESULTS: Table 1 compares the average RMS values of the trunk and the head ML accelerations for the various sectors of the free walk.

Table 1. *Average and standard deviation of RMS value of the ML acceleration for all subjects. The sectors indicated by a and b have the same length. T-tests compare surface conditions.*

	Sector Characteristics	Trunk Acceleration (m/s^2)±SD	Head Acceleration (m/s^2)±SD	t-test p trunk	t-test p head
1a	Surface: smooth	0.79± 0.17	0.46± 0.12	0.011	0.08
1b	Surface: cemented	0.91±0.14	0.59±0.10		
2a	Street: crowded	0.86±0.27	0.62±0.11	0.44	0.27
2b	Street: non-crowded	0.80±0.21	0.57±0.10		
3a	Surface: irregular	0.92±0.20	0.59±0.10	0.001	0.15
3b	Surface: regular	0.82±0.21	0.58±0.10		

DISCUSSION & CONCLUSIONS: In agreement with previous studies [3,4], the average RMS value of the ML acceleration for the trunk is increased for the more difficult floor surface conditions ($p \leq 0.05$) while the head showed no differences ($p > 0.05$). This suggests that the trunk stabilized the movement of the head. We would argue that vestibular patients, depending on the type of sensory loss, would either have reduced gait speed represented by reduced average trunk ML acceleration or the average head ML acceleration could be more than the trunk as compared to normal subjects to compensate for the sensory loss during a free walking test. These tests are planned for late 2007.

REFERENCES:

[1] *V.B. Pothula, F. Chew, A.K. Sharma (2004), Clinical Otolaryngol, 29: 179-182.*
[2] *R.Moe-Nilssen, J.L. Helbostad (2004) Journal of Biomechanics, 37:121-126.*
[3] *H.B. Menz, S.R. Lord, R.C. Fitzpatrick (2003) Gait & Posture, 18:35-46.*
[4] *J.J. Kavanagh, R.S. Barrett, S. Morrison (2003) Gait & Posture, 20: 291-298.*

PROPOSED WIRELESS SENSOR QA MONITORING SYSTEM WITH WEB BASED MANAGEMENT FOR RPH PATHWEST LABS

C. Reed[1], G.Nicholls[1] and J.Ivey[2]

[1]*Department of Medical Engineering & Physics, Royal Perth Hospital, Perth, Australia*
[2]*PathWest, Department of Pathology, Royal Perth Hospital, Perth, Australia*

INTRODUCTION: Changes to regulatory standards has increased the workload for QA monitoring of laboratory devices at RPH PathWest. This has been mainly due to the manual nature of hand written data recording, which is staff intensive and prone to errors. A fully automatic wireless system has been proposed to improve the efficiency and accuracy of this activity.

METHODS: The proposed system is based on the IEEE 802.15.4 ZigBee Standard. This is a wireless bi-directional communication topology that has been specifically designed to monitor very large scale networks. ZigBee's low power, cycle and data rates coupled with it's reliable, self healing and self organising abilities make it ideally suited to the monitoring of large numbers of sensors distributed throughout the Labs infrastructure. ZigBee was also designed to work in parallel with existing 802.11 WiFi infrastructure with minimal interference and has very good wireless and network security. All data traffic will be recorded in standard ODBC compliant central database, through a fully integrated HMI/SCADA solution. This will allow client computers to view current and historical data trends, alarms, network status and the ability to generate QA reports through a standard Web Browser interface.

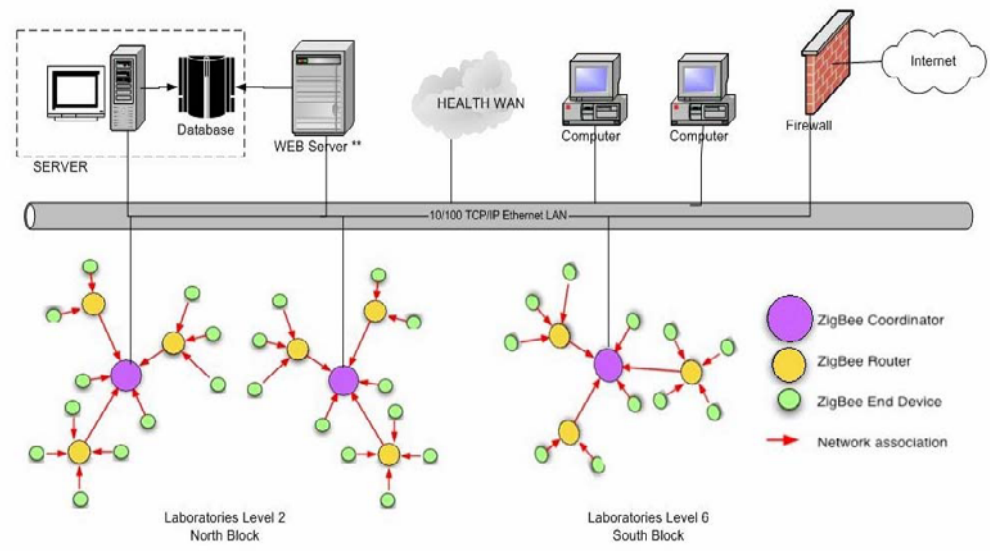

Figure 1. *ZigBee Wireless Network Layout.*

RESULTS: A preliminary feasibility study identified 241 digital Jumbo temperature devices currently being used in Labs and that a further 220 devices (Cyro, Deep Freezers, Pressure, CO_2, Humidity) also needed to be monitored. For the current Jumbo system it has been estimated that the running and labour costs over a 5-year period for manual recording, management, documentation and maintenance would conservatively amount to $420,000, compared to a similar sized ZigBee system of around $220,000 to install and $75,000 in running costs. The ZigBee system can also be extended to monitor all identified devices (461) and the additional parameter types.

DISCUSSION & CONCLUSIONS: The industrial standard ZigBee solution will provide a cost-effective, robust and low maintenance system. It can be installed in stages as the budget becomes available and can be easily relocated to new sites - an important consideration with the possibility that RPH may shift locations in the near future. The adoption of the system is not without risks. This cutting edge technology is yet to be proven in an Australian health environment. Calibration practices may need to change once NATA validation and acceptance has been secured. If these risks are addressed the potential benefits are enormous for QA activities to become an on-line, real-time, automated system.

VALIDATION OF A NEW HAND GRIP DYNAMOMETER

K.J. Reynolds[1], D. Chapman[1] and N. Massy-Westropp[2]

[1] *Flinders Medical Devices & Technologies, School of Informatics & Engineering, Flinders University, Adelaide, Australia*
[2]*Division of Health Sciences, University of South Australia, Australia*

INTRODUCTION: The measurement of grip strength is a widely used clinical assessment tool for evaluation of hand strength. However, devices that are currently used have a number of limitations associated with them. Working with primary and allied healthcare professionals, the Flinders Medical Devices & Technologies research group at Flinders University has developed a new device for measurement of hand grip strength [1]. The objective of this study was to validate the new Flinders dynamometer against the Jamar dynamometer, which is generally accepted as the 'gold standard' grip strength measuring device [2].

METHODS: Ethics approval for the study was obtained from Flinders Clinical Research Ethics Committee. Two different devices were used for the study, the Flinders dynamometer and a Jamar dynamometer. Both dynamometers were calibrated prior to and again after the trials, using known weights suspended from the dynamometer's handle. Weights were suspended at a number of locations along the handle to assess the effect of force location. All measurements using the Jamar were made using the second handle position which has comparable grip dimensions to the Flinders dynamometer.

Thirty subjects aged between 18 and 50 were recruited for the trials. Subjects performed all grip strength measurements in the seated position as recommended by the American Society of Hand Therapists [3]. The dial of the Jamar dynamometer, and screen of the Flinders dynamometer were turned away from the subjects during the trial so that they could not see the display.

Each subject performed a total of 12 contractions in the session, three on the Jamar and three on the Flinders dynamometer, for both hands. Each contraction was at maximal effort, sustained for a period of 10 seconds. Subjects were given a 30-second recovery period between contractions. The order of hand use (right or left) was randomised, as was the order of dynamometer use (Flinders or Jamar).

Results from the Jamar consisted of a single maximum grip strength value for each contraction. The Flinders dynamometer delivered a 10-second force recording for each contraction from which the maximum value was obtained. For each subject, the average of the three trials on each hand for each dynamometer was calculated.
Data was analysed using the method of Bland and Altman [4]. Bias and variability including 95% confidence intervals (CIs) were calculated.

RESULTS: Calibration results for both dynamometers revealed a high accuracy up to 60kg with the force applied to the centre of the beam. The Flinders dynamometer became insensitive above 60kg, but this was thought to be due to a mechanical 'stop' that had been incorporated in the device design. The Jamar dynamometer showed considerable sensitivity to the location of the applied force, with a variation of up to 20% in force measurement along the length of its handle. Variation in measurement along the length of the Flinders dynamometer handle was less than 5%.
Clinical trials showed a small overall bias of 15N (Jamar - Flinders) with a standard deviation of 40N. The Flinders dynamometer showed more repeatability across each set of 3 readings than the Jamar.

DISCUSSION & CONCLUSIONS: Calibration results up to 60kg showed the Flinders dynamometer to be accurate and less influenced than the Jamar by the location of the applied force. The clinical measurements indicate a good degree of agreement between both methods of measurements, and indicate that the Flinders dynamometer warrants further investigation as a clinical tool for hand grip strength measurement.

ACKNOWLEDGEMENTS: The authors acknowledge the assistance and contribution of Morgan Dean, Kira Evans, and Lauren Brown from Australian Science and Mathematics School in Adelaide.

REFERENCES:
[1]*Chapman D et al. (2006) Australas Phys Eng Sci Med, 29:53-6.*
[2]*Shechtman O et al. (2003).J Hand Ther. 16:36-42.*
[3]*Fess EE. (1992) Grip strength. 2nd edn Chicago: American Society of Hand Therapists.*
[4]*Bland JM and Altman DG. (1986) Lancet; i:307-10 .*

A VIRTUAL REALITY TOOL FOR TEACHING ANATOMY

G.S. Ruthenbeck[1], C.S. Carati[2], I.L. Gibbins[2] and K. J. Reynolds[1]

[1]*School of Informatics & Engineering, Flinders University, Adelaide, Australia*
[2]*School of Medicine, Flinders University, Adelaide, Australia*

INTRODUCTION: It is commonly understood that the learning process is enhanced by 'doing' – i.e. a hands-on interactive approach. Neural substrates, such as neuronal networks associated with new knowledge acquisition, are most effectively laid down when the mind, hand and eye are all involved in the learning experience. In learning anatomy, comprehension of complex anatomical structures and their biomechanical behaviour is traditionally learnt from textbooks and 2D graphics, supplemented by practical classes involving human cadavers and skeletons. In these classes, under the guidance of an expert tutor, students manipulate anatomical material, and the hand, eye and mind combine to produce three dimensional 'imaginings' of how the various parts of the body fit together and interact. However, cadavers and expert tutors may not always be accessible, particularly at times and places outside formal anatomy classes, or in environments where there is no access to appropriate material. A solution is to supplement the physical tutor with a virtual one, providing an environment familiar to a generation raised on computer games and immersive computerised technologies. This project aims to develop a virtual reality teaching tool for anatomy. In this demonstration of the technology, the user can manipulate parts of a human skull.

METHODS/TOOLS: The VR anatomy skull 'jigsaw' uses a skull model (courtesy of M. Kirov, New York University) of 13 separate parts. Control of the position and orientation of skull parts is provided using a Sensable Phantom Omni (6DOF) input device. The software uses Extensible Markup Language (XML) to define all scene elements (lights, cameras, objects) and the scene-graph. The software is written in C/C++ using open-source tools (Ogre3D, OPCODE, OgreHaptics).
On opening the software program, the skull pieces appear in their correct anatomical location. The assembly can then be deconstructed manually (one bone section at a time) using the Phantom Omni input device, or randomly deconstructed by pressing a key.
The user can select an individual object by touching it virtually in the scene with the Phantom Omni stylus. Touching an object causes the name of the structure to be displayed (e.g. 'Mandible'). When an object is touched it highlights (changes colour) and remains so for several seconds. Clicking the stylus button grabs the object (which is visually confirmed by another colour change). The user can then manipulate and re-position the object in 3D virtual space. By relocating all 13 objects, the user can effectively build and re-build the skull, and can visualise the skull and its component parts from any direction. The learning experience is enhanced by the use of stereoscopic rendering to allow visualisation in 3D.

RESULTS: The developed application successfully demonstrates the concept of using a 3D virtual reality jigsaw to teach anatomy. The '3D jigsaw' allows anatomical structures to be identified, manipulated and accurately located in virtual 3D space.

DISCUSSION & CONCLUSIONS: We are currently arranging to trial the software with undergraduates in the Flinders University School of Medicine. This trial will evaluate the learning experience of medical students, and compare learning outcomes between students using the virtual reality skull jigsaw, conventional 2D graphics, and hands-on practical classes with real skulls.

There are some examples of the use of 3-D interactive virtual tools for teaching anatomy already available [1,2]. However the use of the Phantom Omni interface device successfully addresses some of the shortcomings of interfaces used previously. The software is written using open-source tools. Consequently the software is robust, extensible and feature rich and can be built to run on all popular operating systems.

REFERENCES:

[1]*F. Ritter, B. Berendt, B. Fischer, et al (2002) Virtual 3D Jigsaw Puzzles: Studying the Effect of Exploring Spatial Relations with Implicit Guidance (2002), Mensch und Computer, 363 - 372.*

[2]*R. A. Schmidt, C.A. Wrisberg (2004) Motor Learning and Performance: A Problem Based Learning Approach, 3rd ed. Human Kinetics.*

MONITORING PATIENT OUTCOME AFTER HIP AND KNEE ARTHROPLASTY - WHY, HOW AND WHAT BENEFITS ARE ACHIEVED

K.E. Sloan, MSc, and R.J. Beaver, MBBS, FRACS (Orth)

Joint Replacement Assessment Clinic and Elective Orthopaedic Department, Royal Perth Hospital

INTRODUCTION: The Royal Perth Hospital (RPH) Joint Replacement Outcomes Project, and its assessment tool, the Joint Replacement Assessment Clinic (JRAC) commenced in 1998. It was initiated to independently measure outcome of hip and knee replacement surgery conducted within the hospital.

METHODS: All primary and revision (after 2000) total hip and knee replacement patients are functionally assessed at pre-op, 3,6,12 months, 2, 5yrs post surgery and every 5 yrs there after until the patient dies or the implant fails. The Harris Hip Score or Knee Society Score, SF36, WOMAC and patient satisfaction are collected, together with details of diagnosis, operative procedures, and complications. At this time there are over 3,000 operations under review with some having been followed for more than 5 years.

RESULTS: A summary of the demographic and operative data shows that there are slightly more females than males for both types of operations, while the average age is higher for hip than knee replacement. The most common diagnosis is osteoarthritis, and the most used implant is the Duracon for the knee, and the Exeter stem for the hip. Hip replacement patients are generally more satisfied than knee patients, although over 80% of both groups are very satisfied with their replacement.

Analysis of the outcome scores has revealed that improvement for both primary hip and knee replacements occurs mostly in the first 3 to 6 months after surgery with a plateauing effect seen between 1 and 2 years post-surgery. Revision hip and knee replacements do not perform as well as the primary operation. Comparisons between cemented and non-cemented implants, between different types of implants and between patella resurfaced knees and non-resurfaced ones have revealed little difference at 5 years post-surgery.

In addition two research projects will be presented. Changes in selected gait parameters after hip and knee replacement surgery were examined using data from 73 primary hip and 91 primary knee replacements, followed up via JRAC. These results provide a natural history of hip and knee replacement up to 1 yr post surgery and can be used to assess the effectiveness of clinical interventions to improve walking function.

The second project is a comparison of health status prior to hip and knee replacement surgery, using standardised outcome data from JRAC and a number of centres in Australia and around the world. Clinically relevant differences were found between centres indicating differences in practise, access and resources, which has implications for future planning.

CONCLUSIONS: Data from this project is used to provide feedback to both patients and surgeons on the progress of the patient, help guide patient expectation and improve patient care by providing a standardised method of assessing outcome. Research projects are also undertaken to review and improve practise.

REFLECTIONS ON CAPACITY BUILDING AND MENTORING IN DEVELOPING COUNTRIES

David A.W. Smith* and Mavis E. Smith

This paper provides reflections, observations and learning about approaches to capacity building in developing countries, and in particular mentoring. Whilst the experiences discussed relate largely to medical equipment and technical support capacity building, the approaches taken and the emerging themes are relevant in a broader context.

Many countries including Australia provide aid funding for the provision of training and technical support in developing countries. Health, along with education are seen as high priority areas with a focus on outcomes such as economic growth, reduction in poverty and sustainability of activities and systems once aid funded support is removed or decreased.

The need for improved scientific and technical capacity relating to health in countries such as Papua New Guinea and Vanuatu has been recognised to ensure that health system development, structures, service delivery and workforce development are realistic, appropriate and sustainable. Virtually all capacity building projects rely on key elements of training, mentoring, coaching and facilitating in various forms depending on the needs of the recipients and timeframes involved.

Approaches to the provision of aid funding includes longer term capacity building and development projects (a number of years) as well as shorter term approaches including targeted inputs to individual countries (weeks rather than months) with a growing focus on regional development and rotating input to selected countries within a particular region. The short term approach (compared to a longer term approach) presents a number of challenges particularly with regard to the provision of effective mentoring. For example, relationship building in which frank discussion of problems and solution can be achieved, role modelling, and establishing effective communication approaches (particularly in the context of cultural perspectives) are more difficult to achieve in a short term scenario.

A number of reflections and observations are offered on capacity building and mentoring experiences by way of comparison of Papua New Guinea and selected countries in the Pacific. Strengths, weaknesses, challenges and lessons learnt are discussed.

Address for David Smith. Medigraf Graphics & Engineering Pty Ltd 8A Henderson Ave Malvern Victoria 3144

NOVEL INTERFACE PRESSURE SENSORS FOR EVALUATING BRASSIERE DESIGN FOR BREAST SURGERY PATIENTS

M.C. Smith[1], J. Hobbs[2], R. Woolford[3], A. Moseley[4] and N. Piller[5]

[1, 2,3] *Flinders Biomedical Engineering, Flinders Medical Centre, Australia*
[4,5] *Lymphoedema Assessment Clinic, Surgical Oncology Unit, Flinders Medical Centre and Department of Surgery, Flinders University, Australia*

INTRODUCTION: Measuring the pressure under brassiere straps and panels demands thin, flexible pressure transducers. The need for thin sensors to have a smooth interface with curved surfaces excludes most existing pressure sensor technologies from this application. Continuous measurement of strap pressure and tension could be used to evaluate new brassiere designs, which may then reduce lymphoedema during the recovery of breast surgery patients. The need for a low-cost, thin, flexible, smooth sensor for continuous pressure measurement was identified.

METHODS: A capacitive sensor was developed and optimised for this application. The dimensions of the sensor were adapted through several iterations to increase sensitivity and flexibility while decreasing thickness. Appropriate shielding, cabling and amplification were also developed to transmit the small variations due to pressure changes in the range 0-80 mmHg. Prototype sensors were calibrated using purpose built rigs and software and evaluated on flat and curved surfaces. An algorithm was developed to relate strap tension and pressure without referring to surface curvature.

RESULTS: For measurement of low pressures, it has been difficult to choose an appropriate dielectric/strain material for this sensor. Materials were excluded based on their incompressibility and inelasticity. Most closed and open-cell foams were not sufficiently elastic and caused drift in prototypes. Rubber mouldings showed some success, though encapsulated static charge produced an offset when flexed.

Sensor faces needed to be made very smooth for measurements on curved surfaces. Protrusions produced offsets during curved-surface tests. Preliminary investigations showed that the sensors were sufficiently stable and sensitive enough to record continuous variations in pressure. The effects of patient breathing and movement were able to be recorded, as was the relationship between strap tension and pressure during strap lifting (figure 1).

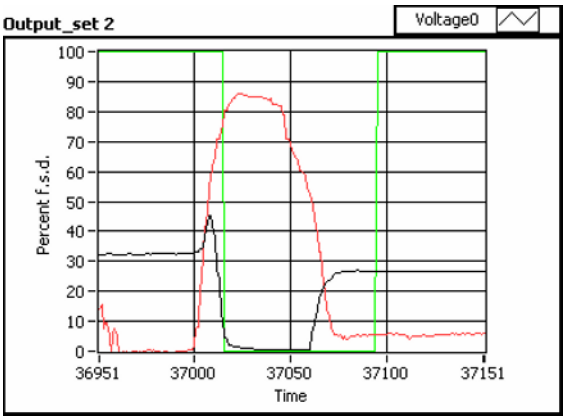

Figure 1. *Strap tension and pressure during lifting.*

DISCUSSION & CONCLUSIONS: It was found that an optimal sensor design incorporates capacitor plates that are thin, flexible and connected electrically within a completely smooth, shielded sensor package. While efforts must continue to decrease sensor thickness and remove offsets due to sensor flexion, this type of sensor shows promise in the continuous measurement of curved interface pressures under brassiere straps and similar garments. Knowledge of these pressures will aid research into the relation between brassiere design and lymphoedema in breast surgery patients.

WORKSHOP: TRENDS IN CLINICAL EQUIPMENT AND INFORMATION TECHNOLOGY

Workshop Synopsis

There have been dramatic changes in the design of medical equipment over the last ten years or so and change continues to accelerate. Increasingly, clinical equipment systems and the need for integrated clinical data, corporate data and personal information are blurring the lines of responsibility. The major shift from stand alone equipment to systems based technologies has a knock on effect in terms of how we manage the technology and whether the biomedical engineer is adequately equipped for the task. How do we define the future, how do we plan for it, what is our role in co-operation with the IT specialist, are we meeting clinical expectations - these are all questions that will form the future.

The object of the Workshop is to explore some of these challenges and to cause us to question our directions, hopefully in a positive way.

The Worshop will be anchored by Dr.Elliot Sloane, from Villanova University in the USA. Dr.Sloane has an extensive clinical engineering background in both the University and Industry, with wide ranging interests in biomedical informatics, health systems engineering and technology assessment. Dr.Sloane's plenary address is scheduled for 0830.

The introduction will be followed by four sessions covering;

- a review of how BME-IT systems are managed across health sectors in Australia,
- an insight into clinical expectations as to future need in areas of critical care
- a glimpse into where the Industry is heading and likely trends from both the US and Europe
- a quick look at how corporate IT systems and whole of health demand may influence directions.

In each case it is intended that the presentations will be forward looking, challenging and provocative in the hope that this will stimulate enthusiastic participation in the final panel session and ensuing IT standards workshop. The panel session should be an opportunity to develop ideas, air frustrations and to challenge the accepted dogmas.

Session 1: (0930-1030). Three 20 minute papers from experienced BME practitioners working in the field.

The object is to give an overview of how the "new" technology is being managed in three areas: WA (Mike Lovett), QLD (Tony Cowan) and NSW (Willy Vandenberg). The intent is to discover the similarities and differences between the jurisdictions in respect of how the systems are designed, managed and the role of BME in the process. What is the extent of system development, inter-departmental and hospital connectivity, what is the level of integration with other corporate IT systems and the working relationships with IT and ICT organisations and professionals.

Session 2: (1100-1230), Three 30 minute papers from senior Clinicians working in the field and with a strong interest in the development of BME-IT technologies, medical information systems and improved management of clinical data: Faculty includes;

- Dr.Cyrus Edibam, Senior Consultant, Intensive Care, RPH
- Dr.Richard Riley, Clinical Assoc.Prof and Director of the Centre for Anaesthetic Skills and Medical Simulation UWA.
- Dr.Daniel Fatovich, Assoc.Prof. in Emergency Medicine UWA and Senior Emergency Physician RPH.

The intent is to discover whether there is a gap between the expectation and aspirations of clinicians working in the field and the BME understanding of where the technology is heading. The issue may be less to do with the technology and more to do with addressing the needs of the Clinical team. There is an increasing demand for clinical information, the need to integrate patient data from clinical equipment and corporate sources and the requirement for this to be available at a variety of sites including the bed side. Do we have this right ? Issues relate to the type and availability of data, the timeliness of information, the capacity to identify essential trends and events, the organisation of equipment and equipment systems to meet increasing demands on facilities and resources. Does the BME fraternity understand these aspirations, are we listening or are the clinical imperatives being lost as we grapple with rapid change, financial restraints and responsibility issues.

Session 3: (1400-1530), Three 25 minute presentations from Industry partners, closely involved with relevant technologies and practices. These include;

- GE Healthcare. Presenter to be confirmed
- Siemens Ltd.(Aust) - Medical Solutions. Mr.David Brown, Sales Manager, Medical Information Technology
- Hospira. Ms.Nicole Kennedy

The intent is to discover where Industry research and development is leading the medical equipment - IT trend in to the future. This will be explored by three representatives from the sector, involved with a range of technologies and coming from different backgrounds. What are the issues that are going to drive change? Are some of the accepted givens such as Dicom, bandwidth constraints etc.. going to survive in to the future? What will be the effect of trends toward globalisation, wireless technologies, bedside information systems, etc.? What role will regulation play and will this vary between the US and Europe (or elsewhere). Where do emerging powerhouses such as India and China fit in the scheme of things and what effect are they having. Importantly, do these trends meet (ie. respond to) or do they drive clinical expectation, do they impose unexpected change and are we ready for it.

Session 4: (1600-1730), A 30 minute presentation by Marcus Young will be followed by panel discussion and a summation from Dr.Elliot Sloane.

Marcus Young (Incarta IT) provides a unique perspective, with a foot in both the BME and IT camps. He has worked in both biomedical engineering (three dimensional visualisation for monitoring cardiac electrical activity and is currently consulting to the public and private health sectors in the application of information technology in clinical practice. It is intended that Marcus will explore the effect that whole of health initiatives (eg. e-health, smartcard technologies, centralised health records, etc.) will have on hospital systems and procedures. Are these factored into our planning, do they impinge on clinical equipment systems and who/how will we manage them ?

Hopefully, the aforesaid content will demand a forthright and robust panel discussion and contribution from the floor to complete the day.

WORKSHOP: BME ASSISTANCE TO DEVELOPING AND RECOVERING COMMUNITIES

Workshop Synopsis

Most BME departments and professionals have received requests for assistance from people working with communities who are in the process of development or who are recovering from the devastation of occurrences such as earthquake, tsunami or aggression. These requests may be from government agencies, NGOs working in the area, service organisations or individuals. The requests may be in relation to the need for medical equipment or the resources to support equipment already in the field. We have all grappled with the dilemma of wanting to respond positively, but not knowing quite what is the best way to act.

Previous ABEC conference sessions have dealt with the difficult business of providing donated equipment into regions in need and how this should be managed. The intent of this symposium is to look at the difficult process of supporting equipment in these areas, whether it be by training the local population or by providing Australian expertise in to the area. In defining an “area” we tend to think of the overseas need, but perhaps the same principles apply to support we provide into some of our more remote regions within our own country.

The impetus to address this topic arose from an opportunity to discuss Australian support with a visiting group from the Aceh province of Indonesia. Overwhelmingly, their expressed concern was not for donated equipment, but was to do with the vexed problem of assisting them to install, commission and maintain equipment provided as part of the recovery program in the region. This was not a request for a short term fix but was for a sustainable effort with long term benefit.
In contemplating a Workshop it was apparent that we had people who could define the need; people working in the field. We also have colleagues who have experience in responding to the need; people working in areas such as PNG, the Solomon Islands and the Pacific. We have successes and no doubt we have some failures that can be a salient lesson upon which to base a future.

The workshop brings together a faculty including;

- **Professor Michael V. Henderson, Chairman, Technology & Industry Advisory Council.** Michael has an active role with TIAC in relation to Indonesia and is working with AusAid and the Indonesian authorities to establish medical and hospital support systems in the region. Michael, along with others in the medical community in WA, is a strong advocate of the need for BME support as an essential element of the various medically based programs needed to assist long term recovery in the region. Michael will define a difficult problem and is looking for the BME community to assist with the solution.
- **Mr.Graham Forward, Consultant Orthopaedic Surgeon, representing ADFA (Australian Doctors for Africa).** ADFA is a family based initiative developing a capacity, supported by medical practitioners in WA, to provide practical aid into areas of Africa including Ethiopia and Somalia. Like a lot of organisations, ADFA has confronted the situation where equipment in these areas, while it may exist, is often unserviceable or at best, is unreliable. Service support is often marginal, even in established centres and the best of areas. Again, Graham’s group can define the problem and is seeking a long term and reliable solution as to how Australia can assist in this regard.

- **Bruce Morrison.** Bruce has been Project Director of the Pacific Medical Equipment Maintenance Project, Provincial Biomedical Engineer on the PNG Medical Equipment Management Project, Technical Advisor and Commissioning Specialist on the Taveuni Community Health Project and is currently Project Director of the Interim Pacific Medical Equipment Maintenance Activity.(an AusAID funded project providing clinical engineering support in the Pacific.) He brings to the forum experience over 8 years in Papua New Guinea and the Pacific in the delivery of medical equipment centred aid projects.

Bruce has provided facility design, developed specifications, procured medical equipment, tools, test equipment, components and spare parts for BMETs in the developing countries. He has developed policies & procedures, provided training and mentoring for BMETs and clinical staff and performed hands-on equipment repairs & testing.

His experience indicates that the;

- Challenges in developing countries are immense and include getting the support of the country's Ministry of Health, getting right people to train and mentor, keeping them once they are trained, ensuring they have access to money for spare parts and communications, ensuring they have access to service information and ensuring they are pro-active in their service provision.
- Problems include the educational level of the designated technicians, their work ethic or lack of it, the lack of a maintenance culture, lack of a spare parts or maintenance budget, staff employed on a casual basis and a lack of any succession planning.
- Solutions tried to date include regular BMET visits to repair and provide on-the-job training, attachments to BME departments in Australian and New Zealand hospitals, short courses and training workshops, sponsorship to complete TAFE and/or university qualifications, mentoring and vendor sponsored/equipment specific courses.
  Bruce would like to see the Forum develop a mechanism for helping the BMETs when aid organisations go missing, change focus or just aren't there.
- **David Smith.** David and his work in the area of overseas assistance, is well known to the ABEC meeting, with significant presentations on the topic. He brings an extensive experience to the forum, his views summarised in the attached abstract of his presentation.
- **Mike Denison.** Director of Facilities Maintenance Austin Health & Logistics Delegate, Australian Red Cross. Mike is also well known to ABEC through his work in the field and through his contributions on the topic. Mikes contribution will concentrate on emergency and disaster response opportunities, conflict/disaster situations, training and skills requirements, the need for cultural awareness, security/OHS issues in relation to workers in the field and comment on the major players.

The contributions will be followed after morning tea (an ideal opportunity to prepare) by a joint panel discussion and robust comment from the floor. What would we like to achieve and what are some key questions;

- Is there a clear way forward and is it possible to design an adequate response for the profession ?
- Is there a role that the College of Biomedical Engineers can play in entrepreneuring an organised, adequate and lasting response ?
- Can we now define some of the key elements that would form a terms of reference in addressing this challenge ?
- Has the forum gone any of the way toward addressing the problems posed by the contributors to the forum.

BIOMATERIALS TALKS

INVITED TALK

ADVANCES IN HEART VALVE TISSUE ENGINEERING

W.M.L. Neethling

Fremantle Heart Institute (Cardiothoracic Surgery, School of Surgery and Pathology, UWA), Fremantle Hospital, Celxcel Pty Ltd, Perth, Australia

Materials to replace malfunctioning or diseased heart valves have been under investigation for more than 45 years. Presently, there are two primary choices for heart valve substitutes: mechanical and xenogeneic bioprosthetic (tissue) valves. Cryopreserved allograft (human) valves are also used but to a lesser extent because of limited supply. Drawbacks to mechanical devices include the need for life-long anticoagulation therapy, bleeding disorders and sub-optimal flow dynamics. Tissue heart valves, display better haemodynamics but have shorter lifetimes due to complications with calcification and leaflet wear.

During the past 15 years, tissue engineered heart valves have been proposed by physicians and scientists to be the ultimate solution for treating valvular heart disease. The main principle of a tissue engineered heart valve is to create a heart valve which can be repopulated in vitro or in vivo to eventually develop into a living organ, able to respond to growth and physiological forces in the same way as native heart valves.

Two main approaches have been attempted: regeneration and repopulation. Regeneration involves the use of a resorbable matrix which is expected to remodel in vivo and yield a functional valve composed of cells and connective tissue proteins of the patient. Repopulation involves the implantation of a decellularised valve matrix (human or animal tissue) which is expected to repopulate (in vitro or in vivo) by patient cells, creating a living organ with proper function and durability. Factors such as the unpredictable resorption rate, enzymatic degradation, and immunoreactivity are some of the main problems which are continuously being addressed in order to create the ultimate biomaterial for heart valve replacement therapy.

An alternative to resorbable and decellularised heart valves is the fabrication of complex hybrid structures through manipulation of biological molecules. Specific building blocks of the original valve morphology are fabricated and joined together in order to form a specialised valve structure.

Application of stem cells and progenitor cells are currently being regarded as the way of the future. Considerable evidence exists that matrices seeded with the relevant cells incorporate and offer therapeutic benefit. However, the use of autologous cells, cell expansion and preimplantation cell culture “management” is not always the preferred approach in the medical valve and therapeutics industry.

Today, heart valve tissue engineering can be regarded as an advanced multi-disciplinary science, which is aimed at the development of a specialised biomaterial for the treatment of heart valve disease. The clinical performance of these biomaterials is largely dependent on the joint efforts of clinicians, bioengineers, cell biologists and pathologists, all focused on the manufacturing of a functional and durable heart valve substitute.

INVITED TALK

CELLULAR & TISSUE BASED PRODUCTS FOR CLINICAL THERAPY

M.J. Sturm

Cell & Tissue Therapies WA(CTTWA), Royal Perth Hospital, Perth, Australia

One of the emerging areas of health care that is at the interface between research and development and advances in clinical treatment is the manufacture of cellular and tissue based therapies. This is an exciting and expanding field that is developing at a dramatic rate with both demand and diversification of products expected to accelerate to ensure advancements in patient care and therapeutic outcomes. Even so, human heart valves, muscular skeletal tissue, eyes, skin, blood and bone marrow have been successfully processed and used for clinical treatments for more than a decade. It is the experience in manufacturing of these products that is guiding the safe delivery of the emerging biotherapies.

The cellular and tissue manufacturing industry is regulated by the Federal agency, the Therapeutics Goods Administration (TGA), to ensure safety and efficacy of products. The increased activity in the biotherapeutic sector has been recognised by the TGA, which is addressing oversights in current regulation with the development of a framework for the regulation of human cell and tissue based products. All manufacturing for human biotherapeutics will need to be compliant to the Federal government regulation under surveillance of the TGA. This means that manufacturers must be licensed to produce cellular and tissue based therapies, which meet the Code of Good Manufacturing Principles (GMP) and related Tissue Specific

Standards. The facilities in which the biotherapeutics are manufactured must be licensed as compliant to GMP and relevant ISO standards.

CTTWA is a newly established manufacturing unit at Royal Perth Hospital (RPH), developed to meet the demands of current and emerging biotherapies and increased regulatory requirements. CTTWA was created to integrate all cellular and tissue manufacturing at RPH into a single facility to provide an efficient service, compliant to regulation and to deliver a framewok for the continued development of cellular and tissue based therapies to meet future demands of "best practise" clinical care. It comprises of a suite of "clean rooms", qualified, validated, monitored and controlled to strict specifications. CTTWA is accredited by the TGA and is licensed to manufacture homologous cardiac valves for valve replacement and expanded keratinocytes for burns patients. It also performs haemopoietic cell manipulation and cryopreservation for both autologous and allogeneic bone marrow transplantation, as well as manufacturing autologous serum eyedrops for dry eye syndromes. The multidisciplinary nature of the facility in servicing many clinical specialities and sites across the WA health sector provided many challenges in the development and operation of the facility.

INVITED TALK

BURNS CARE FOR THE FUTURE - SOLUTIONS THROUGH COLLABORATION

Clinical Prof Fiona Wood, FRACS, FRCS, AM

Director, Telstra Burns Unit, Royal Perth Hospital, Australia

We are faced with clinical problems on a daily basis. In providing clinical solutions we need to harness the experience and knowledge of today to give the best possible outcome from injury. We also need to learn form experience and question how we can improve all aspects of care. Looking to the future we can postulate how clinical care will advance.

Burns care over the next 50 years may well change radically if we explore the options of multidisciplinary collaboration.

Assessment is key in understanding the extent of injury. Debridement is focused on tissue salvage. Reconstruction balances repair with regeneration.

Investigation of multimodality, multi-scale characterisation, including con-focal microscopy and synchrotron technology will quantify assessment.

Debridement using autolytic inflammatory control techniques with image guided physical methods will ensure the vital tissue frameworks are retained.

Tissue guided regeneration afforded by self-assembly nano-particles will provide the framework to guide cells to express the appropriate phenotype in reconstruction.

To solve the clinical problem a multi-disciplinary scientific approach is needed to ensure the quality of the scar is worth the pain of survival.

In treating burn injury it is vital to consider all aspects of the individuals affected by the trauma. When seeking novel solutions to critical problems it is vital to understand the power of collaboration. With knowledge advancing at an unprecedented pace the answers to many problems are waiting to be connected. Therefore, in the quest for scarless healing, collaboration across traditional boundaries harnessing the power of science and technology into clinical medicine has the potential to improve outcomes.

VALIDATION OF THE SMALL PUNCH TEST IN THE CHARACTERISATION OF THE MECHANICAL PROPERTIES OF HUMAN BONE

J. Bateman[1], T. Bateman[1] and R.E. Day[1,2]

[1]*School of Mechanical Engineering, University of Western Australia, Perth, Australia*
[2]*Department of Medical Engineering and Physics, Royal Perth Hospital, Perth, Australia*

INTRODUCTION: The mechanical properties of human bone are of utmost importance to the bio-medical engineering industry, particularly when bone is used as an implant in the form of bone allograft. These are designed to replace deteriorated or removed cancerous sections of bone. The bone used for this application is dead and is sterilised using gamma irradiation to prevent any infection or disease spreading to the patient, but gamma irradiation can reduce the strength and toughness of the bone. Various methods have been used in the past to assess these properties, however many are limited by the volume of material available for testing. One mechanical test that hasn't been widely applied to human bone is the relatively new, small punch test. This method can be considered a constrained bending test, which evolves into deep drawing as the punch progresses further into the die. To date, it has had immense success in testing fairly small samples of various materials and appears to have the capacity to be further miniaturised. How this test performs on bone is what this study will explore.

METHODS: In order to apply the small punch test on bone, appropriately sized specimens had to be prepared. The bone used was the mid shaft of a femur taken from a young male which was left over from a bone allograft implant. The specimen size required was a disk with diameter approximately 6.3mm and thickness of less than 0.5mm. A slow speed diamond saw was used to cut bone slices with a nominal thickness of 0.3mm, however the produced slices had thicknesses ranging between 0.4 and 0.61mm. Disks were then cut from these slices using an appropriately sized hollow drill bit to core out the required specimen dimensions. Some specimens were oversized and required filing in order to fit into the recess in the small punch rig. Testing took place using the ASTM small punch rig designed for UHMWPE[1]. Once the specimen was placed within the recess (located on the upper die), the lower die was mounted, guided by the alignment pins. The rig was then inverted upright and the three socket head cap screws fastened in place. The hemispherical head punch was then inserted through the upper die and rested on the specimen surface. The test rig was then mounted on a type 5566 INSTRON mechanical testing machine and loaded in compression.

RESULTS: A graph of compressive load versus compressive extension was generated which corresponded to the output data generated by the INSTRON. These plots illustrated a very poor degree of repeatability; however this variation was mainly due to the varying thickness. Maximum Load and Elastic Modulus were highly linearly correlated with thickness (r^2 0.98 & 0.94 considering specimens cored at 85 rpm), indicating that most of the variation in the results was due to varying thickness. However results did differ considerably with small variations in thicknesses.

DISCUSSION & CONCLUSIONS: Surprisingly, it was necessary to ignore the fracture load in this analysis, as testing proved the bone to behave in a ductile manner. The two significantly different coring speeds implemented in preparation were found to have a substantial effect on results. To remove this inconsistency the data for each speed was analysed separately. It was found that coring at 85rpm produced more consistent results than coring at 1000rpm. This study has demonstrated that the Small Punch Test is a valid method for determining the mechanical properties of human bone. The variation in load-displacement curves was largely explained by the strong linear relationships with specimen thickness. However results are extremely dependent on specimen thickness, therefore in order to further validate this method specimens with constant thickness must be able to be produced.

REFERENCES:

[1] *ASTM F2183-02 Standard Test Method for Small Punch Testing of Ultra-High Molecular Weight Polyethylene Used in Surgical Implants.*

DESIGN CONSIDERATIONS IN THE DEVELOPMENT OF MAGNETIC NANOPARTICLES FOR MRI CONTRAST ENHANCEMENT

M.R.J. Carroll[1], R.C. Woodward[1], M.J. House[1], T.G. St. Pierre[1], J.D. Goff[2], N. Pothayee[2], J.S. Riffle[2], L. Dan[3] and R. Amul[3]

[1]*School of Physics, The University of Western Australia, Perth, Australia*
[2]*School of Chemistry, Virginia Polytechnic Institute and State University, Blacksburg Virginia, USA*
[3]*School of Chemical Sciences and Engineering, The University of New South Wales, Sydney, Australia*

INTRODUCTION: Since its development in the mid 1970s, Magnetic Resonance Imaging (MRI)[1] has become a widely used diagnostic tool, particularly for soft tissue imaging where the technique generates anatomical detail with millimetre-scale resolution. Contrast agents provide the opportunity to extend the versatility of MRI by enhancing the contrast between different tissue types. Contrast enhancement can improve the effectiveness of MRI as both a tool for scientific studies (molecular and cellular tracking and imaging)[2] and as a diagnostic tool[3].

In most cases the variation in signal intensity developed by MRI contrast agents is due to the magnetic properties of the agents. The contrast agents produce a variation in the local magnetic field which can act to increase both the longitudinal (R_1) and transverse (R_2) relaxation rates of the protons. In a very simplified picture, the greater the variation in the local magnetic field the greater the change in the relaxation rates. MRI contrast agents take 2 basic forms, the first is paramagnetic ions such as gadolinium, the second is magnetic nanoparticles. The contrast from magnetic nanoparticles is generally higher for a variety of reasons owing to the interplay between structure, size relative to the diffusion correlation distance of water, and magnetic properties.

METHODS: In this study we are developing a series of design considerations for the optimisation of magnetic nanoparticles for use as contrast agents in MRI. Two key models are used for the prediction of proton transverse relaxation rates: (i) a motional averaging model and (ii) a static dephasing model[4]. A series a model nanoparticulate contrast agents based on polymer-coated magnetite particles have been characterised by magnetic measurements, transmission electron microscopy, electron diffraction, small angle x-ray scattering, small angle neutron scattering, and dynamic light scattering. Parameters from these measurements are used in the models to assess the degree of agreement between predicted proton relaxation rates and those measured at 1.5T (a common clinical MRI field strength).

RESULTS AND DISCUSSION: In general the trends in the experimental measurements match the behaviour predicted by the models. However, some agents show relaxivities that differ significantly from the modelled behaviour. Two factors that

can confound the current models are (i) uncontrolled clustering of nanoparticles in some systems and (ii) porous structures in the polymer coatings.

Other issues that need to be considered in the design of magnetic nanoparticle contrast agents are stability of nanoparticles, toxicity (particularly in terms of *contrast specific toxicity*), functionality and the lifetime of agents within the body.

REFERENCES:

[1]*P.C. Lauterbur (1973) Nature, 242, 190-191.*
[2]*J. W. M. Bulte, D. L. Kraitchman, (2004), NMR Biomed, 17, 484-499.*
[3]*M. G. Harisinghani et al., New Eng. J. Med., 348, 2491-2499.*
[4]*P. Gillis et al., Mag. Reson. Med. (2002) 47, 257-263.*

COMPLEX ACETABULAR RECONSTRUCTION USING SLM

Robert Day[1,2], Noel Jones[1,2] and Prof. David Wood[3]

Medical Engineering & Physics[1], Royal Perth Hospital, Australia
Mechanical Engineering[2] and Orthopaedics[3], University of Western Australia, Australia

Hip replacement is a very successful operation, but not in every case. If the joint fails there can be destruction of the bone, either due to the loosening of the implant, infection or sometimes the effort required to remove the old component. This is a particular problem if it occurs in the acetabulum (the socket part of the hip joint), as there is often not enough bone to support a new socket. One solution to this problem is to reconstruct the missing acetabulum with a metal cage to support a new socket. Commercial devices are available to do this, but these require fitting to the patient at the time of surgery, prolonging the operation and increasing the chance of complications. The fit of these devices is rarely perfect, and in particular it is difficult to place the fixing screws into the best of the remaining bone.

Custom made cages do not suffer from these problems, but their complicated shapes, and in particular the need for screw holes at odd angles, make them difficult to manufacture with conventional machining methods. Casting methods can be used, but these are time consuming and difficult with the alloys used for medical implants. Recently freeform manufacturing methods have become available for medical grade alloys, and this seemed to offer a solution to our clinical problem.

The cages were designed using medical imaging data of the damaged bone and a variety of software systems. All cages were made by MCP-HEK using Selective Laser Melting (SLM) in a medical grade alloy (Ti–6Al–7Nb ISO 5832-11). Post manufacturing heat treatment was performed at Royal Perth Hospital. The initial microstructure of the SLM produced alloy showed an α′ (alpha prime) martensitic structure with the presence of build defects. A range of heat treatments was examined to improve this structure, and a β solution treatment and aging procedure chosen as being likely to give the best service life.

Four cages for three patients (one with a cage in each hip) have been implanted, and three remain in place with a maximum follow-up of 14 months. There has been one failure (the most recent cage), due to early weight bearing, in the patient who had two cages. Average surgical time and blood loss has been reduced, compared to other reconstruction methods. At surgery the fit of all cages has been rated as good or excellent. There are two more cages being designed, and another candidate patient has been identified.

Custom reconstruction cages made with SLM are a promising tool for the reconstruction of challenging acetabular defects. These cases are not rare, as our series of six patients in two years demonstrates, and the conventional treatment options can often have a poor outcome. More work remains to be done to streamline the design process and to optimise the material properties for this application. Further heat treatment and fatigue studies are planned, along with close clinical and radiographic followup of the implanted devices.

TRABECULAR BONE REMODELLING

K. J. Reynolds[1], T. M. Cleek[1], L. M. Burrow[1] and N. L. Fazzalari[2]

[1]School of Informatics & Engineering, Flinders University, Adelaide, Australia
[2]Bone & Joint Research Lab, Institute of Medical and Veterinary Science, Adelaide, Australia

INTRODUCTION: The skeleton is a dynamic organ as bone constantly undergoes maintenance, repair, and adaptation through the cellular process of bone remodelling. The balance between osteoclast resorption and osteoblast formation results in the increase, decrease, or maintenance of total bone mass. Studies suggest that peak bone mass in both sexes is attained by the third decade of life, after which net decreases 0.4 to 1.4% per year are observed, caused by an imbalance between resorption and formation [1,2]. Bone loss rates for women around the menopause are particularly elevated, usually doubled, due to oestrogen deficiency. In cancellous bone, this net bone loss results in thinning of trabeculae, increased trabecular separation, destruction of supporting trabeculae, and perforation of trabecular structural elements [3]. To investigate changes

in bone mass and architecture, a computer algorithm was developed to simulate the 3D remodelling process in cancellous bone.

METHODS: A bone remodelling algorithm was developed in Matlab (Mathworks, Inc) for use with 3D microCT datasets. There are three modifiable parameters which include:

- Total number of remodelling cycles (activation frequency)
- Resorption cavity depth (osteoclast activity) - causes any trabecular perforation
- % of cavity refilled (osteoblast activity) - sets net loss/gain for each remodelling cycle.

Twenty-two samples of human cancellous bone from the lumbar spines of thirteen individuals were scanned with a Skyscan 1076 μCT machine at a voxel resolution of 15.63μm. A central volume of 400x400x400 voxels was extracted from each reconstructed dataset and analysed with the CTAnalyser program provided by Skyscan, to yield a limited population sample of structural parameters in spinal cancellous bone. The remodelling algorithm was applied to a limited number of datasets for a simulation of 500,000 remodelling cycles (resorption depth: 60μm, % refilled: 93.3%). Five runs were completed per dataset and coefficients of variation were calculated for structural parameters including bone volume, bone surface, trabecular thickness, trabecular separation, trabecular number and degree of anisotropy. Two methods were explored to demonstrate the ability of the algorithm to produce variability in structural parameters with simulated remodelling. The first was to alter resorption and formation input parameters within the range of measured biological values [4]. The second was to set a preferential direction for surface voxel selection.

RESULTS: The simulations produced variations in structural parameters consistent with those observed from real data. The simulations on a single dataset setting a preferential direction for voxel selection yielded a range in variation from random voxel selection results. The largest variation was observed in the degree of anisotropy.

DISCUSSION & CONCLUSIONS: A new 3D bone remodelling algorithm was successfully applied to human spinal microCT datasets with high repeatability. Comparison of simulated changes with a small cross-sectional human dataset indicated considerable population variability in parameters for a given bone volume fraction. It has been observed that there is a preferential resorption of horizontal struts in vertebral bodies with increasing age [6]; accordingly, results indicated the most anisotropic structure after remodelling in the Z (vertical) direction, which would be preferentially reducing struts oriented in the X-Y (horizontal) plane. Given the anisotropic structure of bone, directional dependence is not unexpected and points to the importance of considering targeted remodelling in response to load. A longitudinal study using an animal model of bone loss is underway which will allow further algorithm refinement to simulate temporal changes in trabecular bone architecture.

ACKNOWLEDGMENTS: Thanks to Dr. Ian Parkinson for providing microCT spinal samples courtesy of IMVS. Project supported by ARC Grant DP0663271

REFERENCES:

[1]*B.L. Riggs et al. (1986) J Clin Invest 77:1487-91.*
[2]*J.W. Davis et al. (1992) J Bone Miner Res 7:719-25.*
[3]*L. Mosekilde, (1990) Bone Miner 10:13-35.*
[4]*S. Tayyar et al. (1999) Bone 23:733-739.*
[5]*L. Moskilde, (1988) Bone, 9:247-250.*

IMPLANT SURVEILLANCE!

E Swarts, E R Scull and A Kop

Department of Medical Engineering and Physics, Royal Perth Hospital, Perth, Australia.

INTRODUCTION: There is currently a bewildering array of implants available to the surgeon. In Australia over 140 different hip stems, 120 acetabular components and 50 knee prostheses are currently used. Each device is supposedly a marked improvement on its predecessor, or has some innovative material or design advantage over its competitor (according to the manufacturer). How do we test these claims? Apart from pre-clinical testing, implant tracking and retrieval analysis is possibly the most effective way of monitoring the design and performance of implant devices. Information on implant longevity, usage, failure rates and biomaterial performance is vital to the device selection process and therefore patient outcomes.

Over a period of 35 years, the Royal Perth Hospital Retrieval Laboratory has accumulated data from in excess of 5000 implant retrievals (predominantly hip and knee arthroplasties). This is complemented with implant insertion and removal data obtained via an implant tracking program in operation for more than ten years. Where recurrent failure or abnormal performance of a device or material is detected, the large archive of retrieved devices provides a comprehensive database on implant design, materials, and manufacture, as well as clinical details of the procedure.

METHODS: All removed devices are sent to the retrieval laboratory for verification, analysis (if necessary) and storage. Indications for analysis include implant damage or failure, surgeon request or previous failures of similar devices.

Assessment of material quality is determined with reference to implant standards. Following failure analysis, a summary report is made available to the surgeon, manufacturer and regulatory authority when required. A major focus of the retrieval studies is to identify both success and failure modes of generic designs.

The Theatre Management System (TMS), available in all major public hospitals in Western Australia, contains a purpose built Implant Tracking module. This module allows tracking of the implants by linking the unique patient medical record number to the implant components, surgeon, procedure, operation date and hospital for both insertion and removal events.

In order to review insertion and removal data, an implant activity report is generated. Specific or generic implants can be searched for and implant trends can be ascertained for the major public hospitals.

RESULTS: Preliminary investigations of the implant tracking data indicate changing trends in implant usage over the past 10 years. Often surgeon preference is a major influence, however more recently, compliance with a tender for primary hips and knees in public hospitals in WA, have appeared to dictate usage trends[1]. Whilst recurrent failure or abnormal performance of a device or material may be detected by implant tracking, it is through the retrieval studies that modes of failure are determined. Poor microstructure and/or sub-optimum design factors are commonly featured in recurrent failures[2,3,4]. In contrast, low wear rates of LCS mobile bearing components demonstrate the benefits of good design principals[5].

In summary, implant tracking and analysis plays an important role in improving quality and design of devices. In our experience, serious adverse implant events have been averted and regular feedback to both surgeon and implant manufacturers have proven beneficial in improving patient outcomes.

REFERENCES:

[1] *A. Kop, E. Swarts, (2006) ANZ J. Surg 76:1068*
[2] *E. Swarts et al. (2001) J. Arthroplasty 16: 927*
[3] *E. Swarts, (2007) J. Biomed. Mater. Res. subm*
[4] *L. Lam, et al. (2007) Acta Orthop subm*
[5] *A. Kop, E. Swarts, (2007) Acta Orthop 78: 364*

INTELLECTUAL PROPERTY

INTELLECTUAL ASSETS IN THE MEDICAL WORLD - IDENTIFYING, MANAGING AND COMMERCIALISING INTELLECTUAL PROPERTY

Mark Pulllan

Watermark Patent and Trade Mark Attorneys

Almost every business, university and institution, generates intellectual property (IP) in one form or another. Hospitals and their various scientific and technical departments are no exception.

IP can arise in many guises, from a new product or process (invention), a new or revised product or service name (trade mark), or "know how" linked to internal processes (trade secret), or might even be "bought in" or arise through collaboration with business partners.

Regardless of its origin, IP represents a valuable asset to an institution or business, either as a means to obtain a direct income stream e.g. through licensing, through share value (adding value to the company's bottom line), or as an asset to attract funding through tax concessions, government grants, or capital investment.

Many institutions and businesses invest significant amounts of time, resources and money into developing products, systems and processes to establish an income stream, credibility, market share, and growth potential. Much of that investment can be lost or given away simply by not putting in place procedures that capture, look after and use IP to its full potential. Often IP is given away, or more likely, allowed to leak away or for others to own it, for free.

It is important for every institution and business to recognize the need to own, identify, protect, manage and exploit their IP, whilst at the same time preventing third parties benefiting from the same developments.

With a focus on medical services, this presentation seeks to provide an awareness of what is IP, how to identify it, own it, manage it and exploit it, in order to gain an exploitable benefit and return on money, time and resources invested in projects.

SYNCHROTRON WORKSHOP

INVITED TALK

IMAGING AND RADIOTHERAPY WITH SYNCHROTRON X-RAYS

R. Lewis

Director, Monash Centre for Synchrotron Science, Monash University, Clayton, Australia

Australasia's first synchrotron has just been opened in Melbourne. Victoria. It is the most powerful and flexible source of X-rays in the Southern Hemisphere

A beamline specifically designed for research into medical imaging and radiotherapy is currently under construction on the Australian Synchrotron and will open up a host of research opportunities for Australasian Medical Physicists.

The use of a Synchrotron for imaging and therapy research offers us a window into what may become possible in the clinic and many of the the results are spectacular.

An overview will be given of the research areas that are driving the construction of the Imaging and Therapy beamline. Specific examples include;

- Low dose X-ray image sequences of lungs that reveal alveolar structure and the first breaths after birth
- Sub micron resolution computed tomography scans
- Angiography
- Radiotherapy that is effective on high grade gliomas by increasing single fraction doses more than one hundredfold tumour yet still sparing normal tissue

In addition to novel methodologies in imaging and radiotherapy the Australian synchrotron is already being used to determine the molecular structures of proteins and will be able to provide several new methods for characterising tissue biopsies.

NANOPARTICULATE IRON OXIDE DEPOSITION IN IRON LOADED MAMMALIAN TISSUE BY SMALL ANGLE SYNCHROTRON X-RAY SCATTERING

E.Bovell[1,2], C. Buckley[3], W. Chua-anusorn[2], D. Cookson[4], N. Kirby[5], M. Saunders[6] and T. St Pierre[2]

[1]*Medical Technology & Physics, Sir Charles Gairdner Hospital, Australia*
[2]*School of Physics &* [6] *Centre for Microscopy & Microanalysis, University of Western Australia, Australia*
[3]*Applied Physics, Curtin University of Technology, Australia*
[4]*Australian Synchrotron Research Program, Argonne National Laboratory, USA*
[5]*Australian Synchrotron Project, Victoria, Australia*

INTRODUCTION: Iron overload diseases such as haemochromatosis and thalassaemia affect a large fraction of the world's population. Excess iron is toxic and accumulates in tissues in the form of iron(III) oxyhydroxide associated with the iron storage compounds ferritin and haemosiderin. The physical form of the iron is of particular importance since it is expected to reflect the biological and environmental conditions of deposition. Size distribution determines the surface to core iron ratio, which is in turn expected to determine the molar toxicity of cellular deposits. Despite its significance, a method for characterising the physical form of iron oxide deposits in bulk tissue samples has been lacking, until now.

METHODS: We have exploited the brilliance and monochromaticity of synchrotron radiation to study iron oxide deposition. The liver and spleen from a series of rats (n=64), iron-loaded under three different regimes for various durations to result in a variety of iron-loaded conditions. Two methods of sample preparation were utilized for small angle x-ray scattering (SAXS) at ChemMatCARS at Advanced Photon Source; 1) Samples were freeze-dried and ground to form pellets of tissue for bulk analysis by anomalous SAXS (ASAXS), 2) Samples were wax embedded and sectioned to 1 mm thickness to study local variation in the tissue by scanning SAXS. From radiography we know the distribution of iron is uneven on the mm length scale. We have applied scanning ASAXS to investigate the local variation in iron deposition within a tissue.

RESULTS: ASAXS at the iron K-edge afforded chemical sensitivity and the ability to measure iron oxide particle size in bulk tissue samples. The most likely particle diameter (±SD) for spherical iron oxide deposits is 6.4 ± 0.3 nm. The brilliance of the photon source allowed timely collection of 2D maps to reveal element- and dimension-specific images where nanoparticulate iron deposits give rise to image intensity.

DISCUSSION & CONCLUSIONS: No appreciable difference in particle size could be found with duration of iron loading, loading regime or organ type and the ferritin protein shell is therefore likely to be the primary determinant of particle size. The SAXS maps compare well with radiography and reveal significant heterogeneity in nanostructure over mm distances, depending on iron loading condition.

A METHOD OF DOSIMETRY FOR SYNCHROTRON MICROBEAM RADIATION THERAPY USING RADIOCHROMIC FILMS AND MICRODENSITOMETRY

J.C. Crosbie[1,2], I.D. Svalbe[1], P.A.W. Rogers[3], N. Yagi[4] and R.A. Lewis[1,2]

School of Physics[1], Monash Centre for Synchrotron Science[2] & Monash Institute of Medical Research[3], Monash University, Clayton, Australia
Japanese Synchrotron Radiation Research Institute[4], Hyogo, Japan

INTRODUCTION: Normal tissue displays an exceptional tolerance to high doses of radiation (hundreds of Gy) when delivered as a microplanar array of synchrotron-generated x-rays. Furthermore, MRT has been shown to cause significant tumour growth delay and in some case complete ablation. The biological effects of MRT on tissue are not fully understood. This is further complicated by difficulties in performing accurate dosimetry. The majority of dosimetry performed for MRT has been Monte Carlo simulations. The aim of this work was to utilise film dosimetry and microdensitometry to measure the peak-to-valley dose ratios (PVDRs) for synchrotron microbeam radiation therapy.

METHODS: Two types of radiochromic film of different sensitivity were irradiated with peak in-beam doses of between 16 Gy and 800 Gy. The films were sandwiched in a solid water phantom and irradiated at the BL28B2 beamline at the SPring-8 synchrotron in Japan. The x-ray beam from this beamline is produced by a bending magnet and delivers a high flux polychromatic x-ray beam (median energy 110 keV) at approximately 100 Gy/sec. The x-ray beam from the synchrotron was segmented spatially into microplanar arrays of very narrow beams approximately 30 microns wide, with a peak-to-peak separation of 200 microns. The HD-810 and EBT varieties of radiochromic film were used to measure peak dose and valley dose respectively. All films were analysed on a microdensitometer.

RESULTS: The measured PVDR varied with depth in the solid water phantom. The mean peak-to-valley dose ratio was 52 (range 37-61). This value is in close agreement to PVDRs calculated by other microbeam radiation therapy researchers in Europe, using Monte Carlo simulations.

DISCUSSION & CONCLUSIONS: The peak-to-valley dose ratio is an important biological parameter in MRT. It is likely that the observed palliative and curative effects of MRT on tumours and the sparing of normal tissue to very high doses of radiation are a consequence of the PVDR. The results of this work points to a method of experimentally verifying Monte Carlo simulations for synchrotron microbeam radiation therapy

HIGH DOSE SYNCHROTRON MICROBEAM RADIATION THERAPY OF NORMAL MOUSE SKIN: AN IMMUNOHISTOCHEMICAL STUDY OF DNA REPAIR, PROLIFERATION AND APOPTOSIS

J.C. Crosbie[1,2], L. Cann[3], K. Rothkamm[6], S. Ruwanpura[5], S. Meachem[5], I.D. Svalbe[1], R.A. Lewis[2], N. Yagi[4] and P.A.W. Rogers[3]

School of Physics[1], Monash Centre for Synchrotron Science[2] & Monash Institute of Medical Research[3], Monash University, Clayton, Australia.
Prince Henry's Institute[5], Clayton, Australia.
Japanese Synchrotron Radiation Research Institute[4], Hyogo, Japan

INTRODUCTION: Synchrotron Microbeam radiation therapy (MRT) is based on observations that normal tissue displays a remarkable resistance to necrosis when irradiated with parallel, thin slices of a microplanar X-ray beam. Additional findings suggest that tumour tissue is destroyed at the same levels and distributions of doses that leave surrounding normal tissues relatively undamaged. The biological effects of MRT are not well understood. The aim of this study was to identify suitable histological and immunohistochemical markers of the acute damage to normal mouse skin from high dose MRT.

METHODS: Experiments were performed at the SPring-8 synchrotron, Japan. The beam (median energy 110 keV) was segmented spatially into microplanar arrays of very narrow beams approximately 30 microns wide, with a peak-to-peak separation of 200 microns. The raised dorsal skin-flap of normal mice was irradiated with single fraction, unidirectional, synchrotron microbeam radiation or broadbeam radiation of increasing doses (200 Gy, 400 Gy and 800 Gy). Mice were culled at intervals of 6, 12, 24, 48 hours or 5 days post irradiation. Skin sections were harvested and fixed in formalin and returned to Australia. Histological and immunohistochemical staining was performed on formalin-fixed, paraffin-embedded tissue sections at laboratories in Australia and the UK.

RESULTS: At 48 hrs post-irradiation with a broadbeam of radiation, there was a significant reduction in cellular proliferation for 400 Gy and 800 Gy. By 5 days post-irradiation with broad-beam radiation, severe tissue damage was observed, including; necrosis, epidermal denuding, significantly damaged hair follicles and sebaceous glands. In contrast, at 48 hrs post-irradiation with MRT there was an increase in proliferation of epidermal cells in the irradiated regions. The increase in proliferation was also observed at 5 days for the 400 Gy and 800 Gy MRT groups. Apoptotic and pyknotic cells appeared at 12 and 24 hours post irradiation and were more numerous for broadbeams compared to microbeams. Immunohistochemical staining for phosphorylation of histone H2AX (gamma-H2AX), a marker for DNA double-strand breaks, revealed intense 'stripes' or 'tracks' of positive staining at locations where microbeams had traversed the tissue. The

tracks appeared to become wider and less distinctive with time (out to 48 hrs), presumably as irradiated cells were cleared from the region and the DNA repair was completed. In addition, we have also used gamma-H2AX as a biodosimeter to quantify the dose in the valley regions between microbeam peaks. In irradiated monolayers of human fibroblasts approximately 3% of the peak MRT dose is delivered to central 'valley' regions.

DISCUSSION & CONCLUSIONS: This work confirms and extends previously published observations by other MRT research groups in Europe and the USA showing that high dose synchrotron microbeam radiation therapy confers a sparing effect on normal tissue compared to broad beam radiation fields. The gamma-H2AX immunohistochemical stain has proven to be a most useful marker of radiation-induced damage for MRT in skin tissue. We have now extended this to perform double stains of DNA repair and other cellular processes in both normal and tumourous tissues.

TRACKING IMPLANTED CELLS USING SYNCHROTRON BASED X-RAY IMAGING

C. Hall[1], E. Schultke[2], L. Rigon[3], S. Rigley[2], R. Menk[4], F. Arfelli[5], E. Bovell[6], G. Tromba[4], A. Round[7], S. Crittell[8], R. Griebel[2], and B. Juurlink[2]

[1]*Monash University, Melbourne, Australia*
[2]*The University of Saskatchewan, Saskatoon, Canada*
[3]*INFN, Trieste, Italy*
[4]*Sincrotrone Trieste (Elettra), Italy*
[5]*The University of Trieste, Trieste, Italy*
[6]*Sir Charles Gairdner Hospital , Perth, Australia*
[7] *DESY, Hamburg, Germany*
[10]*Liverpool University, Liverpool, UK*

INTRODUCTION: Synchrotron sources provide a bright beam of x-rays with qualities that are very difficult to obtain in any other way. Although initially thought of as facilities for the physical sciences several attempts over the last few decades have been made to exploit synchrotron storage rings in medical x-ray imaging. Around the world there are now several machines that can claim to have imaged human patients using synchrotron light. The brilliance, monochromaticity, and ability to tune the x-ray wavelength suggested to our group the possibility of visualising small groups of cells inside a living organism. Cell tracking in animal models is of great interest in disease progression studies. It is usually performed using histological methods and by sampling a cohort of study animals at intervals. However, the need for histological assessment prevents the study of progress in a single animal. An ideal methodology for this would be to image small clusters of cells, within the animal without invasion or radiation damage. Some initial tests using animal models of glioma and synchrotron CT imaging have provided tantalising evidence that this might be possible.

METHODS: Wistar rats were injected transcranially with gold labelled C6 glioma cells. After 10 to 14 days incubation the cranium and spine were imaged using monochromatic synchrotron x-ray CT. Imaging was performed at the SYRMEP facility on the Elettra storage ring source in Trieste, Italy using a 24 keV monochromatic fan beam.

RESULTS: High resolution CT sets were obtained which clearly show contrast in regions where the glioma was thought to be developing. This was later confirmed with histology. In the initial CT data doses of 2-3 Gy were used. However a low dose protocol has been devised which will bring the imaging method into a regime where the visibility of the lesion will be retained whilst dropping the dose significantly.

THE AUSTRALIAN SYNCHROTRON AND THE IMAGING AND MEDICAL THERAPY BEAMLINE

D. Häusermann

Australian Synchrotron, Monash Centre for Synchrotron Science and CSIRO

Australasia's first The Australian Synchrotron is a state-of-the-art 3rd generation synchrotron light source. Five out of the first nine beamlines are in the commissioning phase, some already receiving users. The imaging and medical therapy (IMT) beamline belongs to the next group. The availability of this facility for the medical community will strengthen many existing research programmes and benefit new user groups who have not accessed and used synchrotron radiation before.

The medical research program priorities are high quality phase-contrast imaging, tomography and novel radiotherapy techniques. These require a high flux of high-energy x-rays, a long source-to-subject distance and a wide beam. The beamline will be 150 metres long for high contrast imaging with a 60 cm wide beam to handle large subjects such as sheep and patients. Clinical trials are expected to begin two to three years after opening the facility.

The project will include a satellite building, part of the 'long beamline', which will receive beam in early 2009 and cater for high-resolution phase contrast imaging of large objects. Four radiation enclosures are planned in the main synchrotron building, three are currently under construction. They will receive beam in mid-2008. The first experiment enclosure is optimised for high-flux radiotherapy and fast time resolved imaging; the second for semi-quantitative imaging of medium size samples, and point-projection imaging using focusing optics for quantitative phase-contrast imaging with higher spatial

and temporal resolution. All experiment enclosures will have near-beam surgery facilities for fast preparation-to-measurement animal transfers, and animal holding facilities will be provided.

Capabilities to be added later include diffraction enhanced imaging, K-edge subtraction imaging, micro-beam imaging using propagation-based and fluorescence techniques, hard x-ray microscopy and ultra-small-angle scattering.

After a general introduction to synchrotron radiation and the Australian facility, the technical aspects of the IMT beamline project will be summarized. Special emphasis will be given to shielding requirements and the safety aspects of the medical research program, including clinical. The process for applying for beamtime and generally accessing the synchrotron will be presented.

INTRA-OSTEON DISTRIBUTION OF OSTEOCYTE LACUNAE IN HUMAN CORTICAL BONE ASSESSED BY SYNCHROTRON RADIATION MICRO-CT

C. David L. Thomas[1], David M. L. Cooper[2], John G. Clement[1], Andrew G. Peele[3] and Kevin Hannah[3]

[1]*School of Dental Science, University of Melbourne, Melbourne, Australia*
[2]*Department of Orthopaedics, University of British Columbia, Vancouver, BC, Canada*
[3]*Department of Physics, LaTrobe University, Melbourne, Australia*

Introduction: Progressive improvement in the resolution of micro-computed tomography (micro-CT) systems has facilitated the analysis of bone structure at ever smaller scales. In biological terms this has allowed the analysis of trabecular architecture, the cortical canal network, and osteocyte lacunae. Synchrotron radiation micro-CT is currently the only reliable modality for imaging the smallest level of this hierarchy – osteocyte lacunae. Osteocytes are believed to be the primary mediators of mechanotransduction, calcium homeostasis, and remodeling in bone. Variability in osteocyte density associated with age, sex, and disease has been reported from histological studies; however, relatively little is known regarding the 3D distribution of osteocytes within bone or, more specifically, within individual osteons. The purpose of this preliminary study was to develop analytical methods for measuring the intra-osteonal spatial distribution of osteocyte lacunae and apply this to a human cortical bone specimen.

Methods: A 2mm x 2mm x 35mm specimen of femoral midshaft cortical bone from a 20 year old male was imaged at beamline 2BM of the Advanced Photon Source, Argonne National Laboratory. A serial image dataset with isotropic resolution of 1.6μm was generated using 1/8degree angular steps and averaging four frames at each step. Photon energy was 26.4keV. ImageJ (http://rsb.info.nih.gov/ij/) was employed to assess the 2D relation between the osteocyte lacunae and the osteonal canals through the serial images of a 0.63 mm3 volume of interest (Fig. 1).

Results: More than 10,000 osteocytes were counted in the volume of interest. Lacunar concentration was high directly adjacent to the osteonal canals then dropped off to its lowest point at 10-15 microns. From this point the number of osteocytes increased logarithmically (Fig. 2) to 130 microns from the canal surface – roughly the expected distance to the outer osteonal border. This finding of a non-uniform distribution of osteocyte lacunae within cortical bone potentially has far reaching significance for modelling the mechanical and fluid flow properties of bone as well as the regulation of cortical remodeling and its role in osteoporotic bone loss. Future goals include the development of 3D methodology and analysis of a range of human cortical bone across the lifespan.

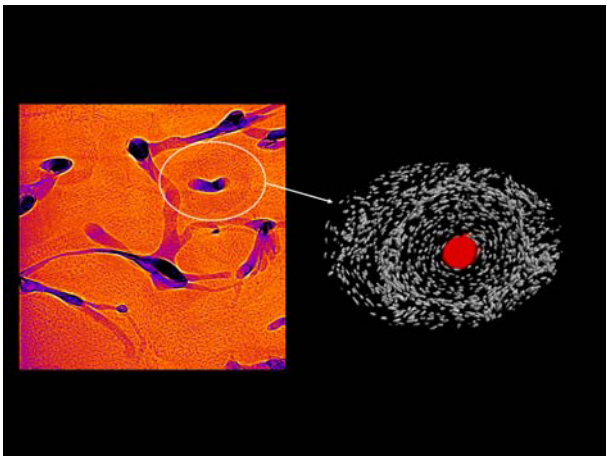

Figure 1. *3D rendering of the study volume with extracted osteocyte lacunae and pore.*

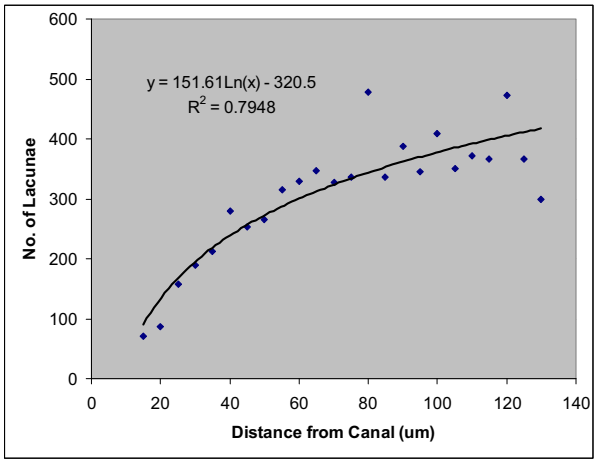

Figure 2. *Graph of osteon count vs distance from pore surface.*

TOWARDS THE CLINICAL APPLICATION OF PCI

I.M. Williams[1], K.K.W. Siu[2], S.A. Hart[3], Y. Chong[2], R. Gan[2], X. He[2] and R.A. Lewis[1,4]

[1]*School of Physics, Monash University, Australia*
[2]*Department of Medical Imaging and Radiation Sciences, Monash University, Australia*
[3]*Southern Breast Clinic, Southern Health, Australia*
[4]*Monash Center for Synchrotron Science,Monash University, Australia*

INTRODUCTION: Although synchrotron-based Phase Contrast Imaging (PCI) has generated significant interest, the technique has yet to be implemented in the clinical environment for routine diagnostic or screening imaging. We seek to determine whether available medical equipment can produce PC enhanced images which are diagnostically better than images taken with the conventional contact geometry.

METHODS: A micro-focus (100 µm spot size) Molybdenum X-ray source with 0.03 mm Molybdenum filtration was installed at a local hospital. Tissue samples, excised masses and mastectomies, were obtained directly from surgery, compressed in a saline bath and imaged at three geometries. The geometries employed were the conventional mammographic contact arrangement with the sample at 65 cm from the source, the Konica phase contrast geometry and a third, optimized phase contrast geometry. The optimised solution was formulated from a ray-line optics argument that produced a solution which can be applied to any source-detector combination. An initial scoring trial was performed with five images sets, each with three images. Images were scored by pair-wise comparison allowing scorers to determine that one image was better, equal or worse than another. Analysis was performed with a binary approach in which the null hypothesis assumed that all the images were of the same quality.

RESULTS: The initial results from the first scoring trial are shown in figure 1. Results for the full trial of seventy-seven samples will be presented.

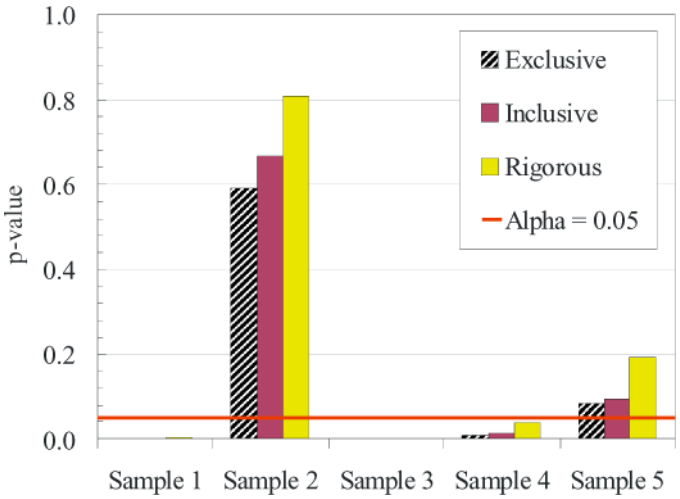

Figure 1. *Significance of the binary score by sample number for the Monash:Konica comparison with all three analytical techniques. The exclusive technique removes the cases in which the two relevant images were judged to be equal in quality, the inclusive ascribed 0.5 to each of the 'better than' and 'worse than' bins while the exclusive technique assigned all equal outcomes to the Konica is better than Monash bin.*

DISCUSSION & CONCLUSIONS: Data accumulation is ongoing and the full spectrum of results with the corresponding analysis will be presented.

POSTERS

RADIOTHERAPY POSTERS

COMMISSIONING AND EVALUATION OF DOSE DISTRIBUTION VOLUMES USING RESPIRATORY GATED TREATMENT

J. Barber[1, 2], S. White[1], S. Yau[1] and C. Baldock[2]

[1]Nepean Cancer Care Centre, Penrith, Australia
[2]Institute of Medical Physics, School of Physics, University of Sydney, Sydney, Australia

INTRODUCTION: Respiratory gating is a method of collecting temporal information relating movement caused by the respiratory cycle and incorporating this into radiotherapy planning and treatment. By incorporating temporal information into patient planning data, the uncertainty of inter-fraction organ position can be reduced. This leads to a reduction in plan margins and hence allows a tumour region to be treated while reducing the dose to surrounding healthy tissue. Retrospective gating may be performed by analysing a patient's anatomical information during their breathing cycle and finding the optimal point in the cycle for treatment. Dose distributions in three dimensions are useful to fully quantify the dosimetric benefits of a gated delivery compared to a non-gated delivery, and can be achieved with both Gafchromic EBT films and polymer gels. This work compares the dose distributions obtained using conformal radiotherapy for a static and moving patient, to a retrospective-gated treatment. Both conformal three-dimensional and intensity-modulated plans are investigated. This dosimetric analysis was undertaken as part of the respiratory gating commissioning process.

METHOD: Commissioning of the respiratory gating process involves the use a phantom with periodic motion, a CT scanner capable of creating 4D datasets, a respiratory cycle tracking system and a gated therapy beam delivery system. The dosimeters are placed in an in-house phantom designed to simulate a respiratory cycle by approximation to a 1D sinusoid. A GE 4DCT (LightSpeed RT) scanner collects phantom image information for planning purposes, while the movement is tracked by the Varian RPM system. Using the Pinnacle treatment planning system, conformal and IMRT dose distributions are planned [1]. Each plan is delivered for 3 cases: static and moving phantoms with no gating, and a moving phantom with gated treatment. The dosimetry of each case is then compared by gamma analysis.

DISCUSSION AND CONCLUSIONS: It can be shown that respiratory gating can deliver desired dose distributions to a given volume while reducing the dose to surrounding regions in an ideal setup. While having dosimetric advantages, other factors to consider in gating such as extended treatment time, accuracy of patient tracking and possible radiobiological effects. Continued investigation of the clinical viability of gating for thoracic and breast patients needs to be performed [2].

REFERENCES:

[1]*P. Keall, et al (2006) Medical Dosimetry 31:152-162.*
[2]*R. Frazier, et al (2004) Int J Rad Onc Bio Phys 58:1041-1047.*

INITIAL CLINICAL EXPERIENCE WITH PROSTATE MARKER SEEDS AND ON-BOARD IMAGING FOR DAILY POSITIONING AT RPA

J. Booth, P. Aston, K. Francis, G. Hruby and C. Kwong

Department of Radiation Oncology, Sydney Cancer Centre, Sydney, Australia

INTRODUCTION: Prostate marker seeds are to be used for daily patient positioning of prostate patients at Sydney Cancer Centre. We have initiated a two phase pilot study to investigate their impact on prostate contouring, seed migration, seeds visibility in MV images, treatment time, to assess positioning accuracy, kV imager reliability and treatment efficacy. The first phase has 10 patients being imaged daily (kV daily and MV for 20 fractions) and (if intervention required) moved only using bony anatomy following local protocol. During this phase we establish whether the seeds migrate during treatment, and we quantitate the variability of prostate position within the pelvis. During the second phase we shift patients daily based on implanted marker identification in orthogonal kV images (if the shift is greater than a tolerance set using data from Phase 1).

METHODS: Prostate marker seeds are implanted by a Urologist ~10 days prior to CT acquisition. The Urologist records the size of the prostate and marker positions based on ultrasound guidance during insertion which is used by the Radiation Oncologist for contouring. Marker seed positions and centroid positions are documented on orthogonal DRRs and compared with seed positions in daily OBI images. Therapists note the daily table shift for matching to bony anatomy and to seeds. Separate databases are used to document each set of data. On treatment, Therapists use a stop watch to record the time taken from when the patient walks in the treatment suite to when they start treatment and also total time.

RESULTS: Our experience with seed migration matches that of the literature with negligible migration during the 7 week treatment course. The extra time taken to image and reposition the patient reduces quickly once the treatment staff becomes familiar with the system and we aim to use 15 minute appointments. Stark differences were found between the match to

bones vs match to seeds datasets for particular patients. We will also report of the service reliability of the OBI in a clinical setting.

DISCUSSION & CONCLUSIONS: Preliminary results show that prostate marker seeds and online positioning create a large advantage in the precision of prostate treatments. This will lead to this cohort of patients receiving higher doses with reduced PTV margins.

CLINICAL ISSUES ARISING FROM ELECTRON MONTE CARLO ALGORITHM IN ECLIPSE

J. Booth[1], J. Xia[2] and E. Claridge Mackonis[1]

[1]*Sydney Cancer Centre, Royal Prince Alfred Hospital, Sydney, Australia*
[2]*Institute of Medical Physics, Department of Physics, University of Sydney, Sydney, Australia*

INTRODUCTION: Varian Medical Systems have released an implementation of the Macro Monte Carlo method for electron dose calculation known as electron Monte Carlo. A number of Centres have already commissioned this application[1]. In this presentation we present our commissioning of the application leading to the clinical implementation with special focus on its use in a clinical setting. The eMC algorithm presents an increase in sophistication from previous Eclipse electron algorithms. It also presents a reduction in required input data and increases in unknown data handling and verification requirements. Specifically, the clinical interface has a range of calculation variables – which can be quickly reduced once the corresponding accuracy is ascertained. We consider the algorithm accuracy with surface curvature, heterogeneity, extended FSD and junctioning with photon fields for a range of electron energies.

METHODS: We investigated v7.5.18.0 of the eMC algorithm. Calculated dose distributions were compared against measurement for a range of situations using ion chambers and film. Initially, the calculation parameters of the algorithm were investigated for accuracy. Once a reliable subset of calculation parameters were established we investigated clinically relevant arrangements from open applicators to complex shapes and extended FSD with patient surface curvature and real CT scan data. We also compared directly against the Eclipse GGPB algorithm.

RESULTS: Qualitative comparison showed that smoothing is required even for high accuracy calculations. Even using 1% accuracy with a 1mm grid gave poor agreement without smoothing. Using smoothing, 1% accuracy and 1mm grid, the algorithm gave good agreement in many situations with the largest discrepancies seen in regions of sharp gradient and with significant inhomogeneity.
As expected, the calculation time was strongly dependent on precision required and grid size and only marginally by the smoothing selected with a 1%, 1mm calculation of a 10cm applicator taking over 26 minutes compared with a 5%, 2.5mm calculation taking 21 seconds.
The monitor units calculated by eMC were found to be higher than required, compared to measurement, in almost all cases. This is consistent with the strong smoothing applied by the algorithm prior to normalisation.

DISCUSSION & CONCLUSIONS: The eMC calculated dose distributions can be very noisy and this presents issues for normalisation. Even for long, high accuracy, smoothed calculations the PDD might not give 100% in an open reference applicator. Overall, commissioning this algorithm presented challenges with regard to dose normalisation, low energy calculations and the need to handle prescription in non-water material (dose is calculated to material not water). Despite these challenges, the algorithm displayed increase accuracy in the situations considered when compared to the previous GGPM algorithm.

REFERENCES:

[1]*Popple, R. A., Weinberg, R., Antolak, J. A., Ye, S-J., Pareek, P. N., Duan, J., Shen, S. and Brenovich, I. A., 2006, Med. Phys., 33 (6), pp 1540-1551.*

RADIOLOGICAL PROPERTIES OF THE PAGAT GEL DOSIMETER AND THE PRESAGE POLYMER DOSIMETER

S. Brown[1,2], A. Venning[3], Y. De Deene[4], P. Vial[1,2], L. Oliver[1,2], J. Adamovics[5] and C. Baldock[1]

[1]*Institute of Medical Physics, School of Physics, University of Sydney, Sydney, Australia*
[2]*Department of Radiation Oncology, Royal North Shore Hospital, St Leonards, Sydney, Australia*
[3]*Department of Radiation Oncology, Wellington Hospital, Wellington New Zealand*
[4]*MR Department, Ghent University Hospital, De Pintelaan, Belgium*
[5]*Heuris Pharma, Skillman, NJ*

INTRODUCTION: This study has determined the radiological properties of the PAGAT gel dosimeter and the PRESAGE polymer dosimeter using Monte Carlo modelling. The mass density (ρ), mass attenuation coefficients (μ/ρ), mass energy absorption coefficients ($\mu_{en/\rho}$), electron mass stopping powers (S/ρ) and electron mass scattering powers (T/ρ) were calculated and compared to the values of water over the therapeutic x-ray energy range.

METHODS: The mass densities (ρ) were determined at room temperature. The electron to mass density ratio (ρ_e/ρ), the electron density (ρ_e) and the effective atomic number (Z_{eff}) were calculated. Fractional interaction probabilities were calculated for each of the dosimeters and water using the *EXAMIN* and *PEGS4* computer programs. The electron mass collisional ($S_{col/\rho}$) and mass radiative ($S_{rad/\rho}$) stopping powers were calculated using the *ESTAR* computer program. A 6 MV Varian 600C/D linear accelerator was modelled using the *BEAMnrc* Monte Carlo computer program. The depth dose curves for water, PAGAT and PRESAGE were calculated using the *DOSXYZnrc* computer program.

RESULTS: The mass density of the PAGAT gel was 2.6% higher than water and PRESAGE 10% higher than water. The fractional interaction probability differences of PAGAT (plotted as photoelectric, Compton and pair production curves) were found to be less than 4% different from water over the entire energy range. The PRESAGE photoelectric curve was found to be as high as 81% larger than water and the Compton scattering curve as high as 55% larger, over the energy range 10 keV to 1 MeV. The mass attenuation and mass absorption coefficient ratio curves of PAGAT was found to approach unity from less than a 5% difference up to 100 keV and remained less than 1% from 100 keV to 20 MeV. The mass attenuation coefficient ratio curve for PRESAGE showed a large peak between 10 keV and 100 keV, indicating that the mass attenuation coefficient of PRESAGE over this range was as large as 1.5 times that of water. The mass energy absorption coefficient ratio curve for PRESAGE showed a similar peak. The mass scattering power curve for PRESAGE is on average 8.5% less than that the curve for water. The PAGAT curve is on average 1.3% less than the curve for water. The depth dose absolute percentage difference for PRESAGE was below 2% and for PAGAT below 1%. In relative terms, the difference between the dose for the dosimeters and for water increases to 7.6% for PRESAGE and 2.5% for PAGAT.

DISCUSSION & CONCLUSIONS: The dosimeter that exhibited the closest water equivalence was the PAGAT formulation. PRESAGE was found to be the least water equivalent due to its high effective Z value being approximately 17% higher than water. The lack of water equivalence of PRESAGE may be overcome with dosimetric correction factors.

REFERENCES:

[1] *Venning, A.J., Radiological properties of normoxic polymer gel dosimeters. Med. Phys., 2005. 32(4): p. 1047-1053.*
[2] *Guo, P.Y., Adamovics, J. A., Oldham, M., A practical three-dimensional dosimetry system for radiation therapy. Med. Phys, 2006. 33(10): p. 3962-3972.*

FURTHER INVESTIGATION OF ARTEFACTS ASSOCIATED WITH OPTICAL CT FOR GEL DOSIMETRY

S. Brown[1,2], S. Bosi[1], D. Bailey[3], Y. De Deene[4], S. Sarabipour[1] and C. Baldock[1]

[1] *Institute of Medical Physics, University of Sydney, Sydney, Australia*
[1] *Department of Radiation Oncology, Royal North Shore Hospital, St Leonards, Australia*
[3] *Department of Nuclear Medicine, Royal North Shore Hospital, St Leonards, Australia*
[4] *MR Department, Ghent University Hospital, De Pintelaan, Belgium*

INTRODUCTION: Polymer dosimetric gels undergo a change in opacity when exposed to radiation due to the formation of cross-linked polymer chains. Cone beam optical CT can be used to evaluate dosimetric polymer gels such as PAGAT [1]. The aim of this research was to quantify the scatter and absorption of light by opaque gel volumes of various dimensions.

METHODS: The opacity change of a dosimetric gel was simulated by mixing a known concentration of the antiseptic product Dettol (Reckitt Benckister) with gelatin [2]. This mixture could be poured into a cavity in a gelatin volume for optical CT analysis. A gelatine volume was prepared and a glass funnel was used to create a cavity of decreasing circular diameter. The gelatin was allowed to set and a mixture of antiseptic and gelatin was poured into the cavity and allowed to set. The phantom was scanned with a resolution of 0.25 mm per pixel. An optical CT scan of the phantom produced horizontal slices containing a central circular region of a density higher than gelatin with decreasing circular diameter.

RESULTS: The change in central axis and edge attenuation coefficients was plotted and found to increase linearly with the diameter of the antiseptic/gelatin region. The optical attenuation coefficient was plotted against the offset from the central axis for a number of slices of decreasing circular diameter (*Fig. 1*). The optical attenuation coefficient corresponding to a central circular region of 0 mm diameter was extrapolated from the data.

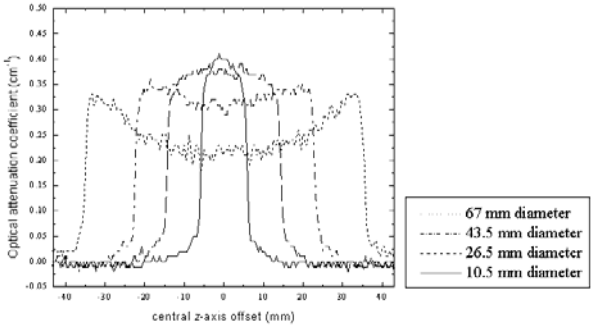

Figure 1. *Attenuation curves for circular antiseptic/gelatin regions of decreasing diameter.*

DISCUSSION & CONCLUSIONS: Larger diameter slices were found to exhibit dishing artefacts, where the central region of the attenuation curve showed a reduction from the values at the edge due to light scatter in the funnel volume. A similar dishing effect has been observed in X-ray CT scans due to absorption and scatter of the X-rays. Lower diameter slices were found to exhibit doming artefacts where the central region flips over and presents as the opposite of the dishing artefacts, with an increased central axis value.

REFERENCES:

[1]*A.J. Venning, B. Hill, S. Brindha, C. Baldock, "Investigation of PAGAT normoxic polymer gel dosimeter using magnetic resonance imaging". Phys. Med. Biol., 50 (2005): 3875-3888*

[2]*S. Bosi, P. Naseri, A. Puran, J. Davies, C. Baldock, "Initial investigation of a novel light-scattering gel phantom for evaluation of optical CT scanners for radiotherapy gel dosimetry". Physics in Medicine and Biology, 52 (2007): 2893-2903.*

MEASUREMENT OF HIGH ENERGY X-RAY BEAM PENUMBRA WITH GAFCHROMIC™ EBT RADIOCHROMIC FILM

Martin J Butson[1,2,3], Tsang Cheung[1] and Peter K. N. Yu[1]

[1]*City University of Hong Kong , Dept. of Physics and Materials Science, Kowloon Tong, Hong Kong*
[2]*Illawarra Cancer Care Centre, Department of Medical Physics, Crown St, Wollongong, Australia*
[3]*Centre for Medical Radiation Physics, University of Wollongong, Wollongong, Australia*

INTRODUCTION: High energy x-ray beam penumbra are measured using Gafchromic™ EBT film. Gafchromic™ EBT, due to its limited energy dependence and high spatial resolution provide a high level of accuracy for dose assessment in penumbral regions. The spatial resolution of film detector systems is normally limited by the scanning resolution of the densitometer.

METHODS: EBT Gafchromic is tested for its ability to measure high energy x-ray beam penumbra with optical density measurements performed with a desktop scanner.

RESULTS: Penumbral widths (80 % / 20 %) measured at Dmax were found to be 2.8 mm, 3.0 mm, 3.2 mm and 3.4 mm (±0.2 mm) using 5 cm, 10 cm, 20 cm and 30 cm square field sizes respectively for a 6 MV linear accelerator produced x-ray beam. This is compared to 3.2 mm ± 0.2 mm (Kodak EDR2) and 3.6 mm ± 0.2 mm (Kodak X-Omat V) at 10 cm x 10 cm measured using radiographic film.

DISCUSSION AND CONCLUSION: Using a zero volume extrapolation technique for ionisation chamber measurements, the 10 cm x 10 cm field penumbra at D_{max} was measured to be 3.1 mm, a close match to Gafchromic™ EBT results. Penumbral measurements can also be made at other depths, including the surface, as the film does not suffer significantly from dosimetric variations caused by changing x-ray energy spectra. Gafchromic™ EBT film provides an adequate measure of penumbral dose for high energy x-ray beams.

KEYWORDS: Radiochromic film, Gafchromic™ EBT, surface dose, penumbra measurements

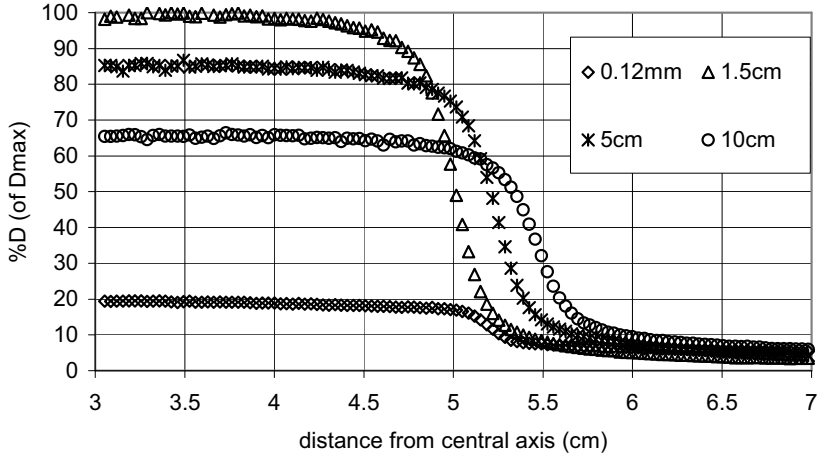

X-RAY ENERGY RESPONSE OF SIRAD RADIATION DOSIMETERS

Martin J Butson[1,2,3], Tsang Cheung[1] and Peter K. N. Yu[1]

[1]*City University of Hong Kong , Dept. of Physics and Materials Science, Kowloon Tong, Hong Kong*
[2]*Illawarra Cancer Care Centre, Department of Medical Physics, Crown St, Wollongong,,Australia*
[3]*Centre for Medical Radiation Physics, University of Wollongong, Wollongong, Australia*

INTRODUCTION: SIRAD (Self indicating Instant Radiation Alert Dosimeter) dosimeters are designed to measure radiation exposure as a personal dosimeter. As the source of radiation is normally unknown, a detector, which exhibits low energy dependence, is ideal for personal dosimetry of x-rays.

METHODS: SIRAD dosimeters have been tested for their optical density to exposure response over the x-ray energy range of 50kVp to 10MV. This relates to a photon equivalent energy of 25.5 keV to 2.2 MeV.

RESULTS: Results have shown that the SIRAD dosimeters optical density to dose response at 25.5 keV is approximately 0.71 ± 0.04 1SD relative to 1 at 1.4 MeV (30% under response). The relationship is a slowly increasing OD response to exposure with increasing x-ray energy.

DISCUSSION AND CONCLUSION: This variation in response is relatively small compared to radiographic films which over responds by 10 to 15 times and similar to Lithium Fluoride Thermoluminescent dosimeters which over respond by approximately 40% over the same energy range. This does produce a limitation in the accuracy of exposure assessment in unknown energy radiation fields however its intrinsic property of automatic visual evaluation of exposure is not significantly compromised.

KEYWORDS: SIRAD dosimeters, radiation dosimetry, energy dependence, dose response, radiochromic film, radiochromic

MEASUREMENT AND PRODUCTION OF ELECTRON DEFLECTION USING: A SWEEPING MAGNETIC DEVICE IN RADIOTHERAPY

N. Damrongkijudom[1], B. Oborn [1], M. Butson[1,2,3], Tsang Cheung[3] and Peter K.N. Yu[3]

[1]*Centre for Medical Radiation Physics, University of Wollongong, Wollongong, Australia*
[2]*Illawarra Cancer Care Centre, Department of Medical Physics, Crown St, Wollongong, Australia.*
[3]*City University of Hong Kong, Dept of Physics and Materials Science, Kowloon Tong Hong Kong*

KEYWORDS: electron contamination**,** surface dose**,** magnetic deflector device

INTRODUCTION: The deflection and removal of electrons produce by a medical linear accelerator has been attained by Neodymium Iron Boron (NdFeB) permanent magnetic deflector device.

METHODS: This work was performed in an attempt to confirm the theoretical amount of electron deflection by monitoring the paths of pure electron beams using radiographic film. Calculated and measured effectiveness of the magnetic field to deflect electrons is performed using monoenergetic high-energy electron beams from 6 MeV to 20 MeV. Small field beams were deflected with magnetic fields with angles measured and calculated based on magnetic field strength produced by the clinical device.

RESULTS: Results show 6 MeV electron measured deflection distance was 18 ± 6 cm and calculated deflection distance was 21.3 cm. For 20 MeV this value was 5 ± 2 cm for measurement and 5.1 cm for calculation.

DISCUSSION AND CONCLUSION: Bending electron contaminations out of the treatment field with these magnetic field strengths are predicted to remove electron with energy up to 6 MeV over 12 cm deflection distances. These magnetic field strengths can reduce surface dose in treatment regions of a patient under irradiation by photon beam and predict to remove all electron contaminations energy up to 6 MeV away from the treatment field of 6 MV photon beam with the radiation field size up to 10 x 10 cm^2. It can give a guide for determining if electron contamination will still be present in the treatment beam at various field sizes.

ENERGY AND DOSE RESPONSE OF XRCT RADIOCHROMIC FILM

Tsang Cheung[1], Martin J. Butson[1,2,3], and Peter K.N. Yu[1]

[1]*City University of Hong Kong , Dept. of Physics and Materials Science, Kowloon Tong, Hong Kong*
[2]*Illawarra Cancer Care Centre, Department of Medical Physics, Wollongong, Australia*
[3]*Centre for Medical Radiation Physics, University of Wollongong, Wollongong, Australia*

KEYWORDS: Radiochromic film, Gafchromic XRCT, radiation dosimetry, energy dependence, dose response.

INTRODUCTION: Gafchromic XRCT film is a relatively new product designed for use in diagnostic energy radiation dosimetry and specifically CT applications.

METHODS: Gafchromic XRCT radiochromic film was assessed over a broad energy range, from kilovoltage to megavoltage x-rays for variations in reflected optical density (ROD) to dose response.

RESULTS: A large energy dependence was found with reflected optical density output for the same delivered dose varying from 7.8±0.35 at 25.5 keV (50 kVp) peaking at 12.1±0.5 at 54 keV (125 kVp) to 0.975±0.03 at 2300 keV (10 MV) when normalised to 1 at 1400 keV (6 MV) energy. Results also showed a high sensitivity to delivered dose compared to other conventional radiochromic films which make it well suited to CT applications where lower applied doses are delivered. With respect to dose response, a 1cGy applied dose produced an approximate net optical density change of 0.3 at 636nm and 0.2 net OD using broad band white light.

DISCUSSION AND CONCLUSION: The energy response is constant (within 3%) in the 36 keV to 69 keV equivalent photon energy range, which corresponds to x-ray tube generating potentials of approximately 100 kVp to 150 kVp. This matches well with beam qualities for diagnostic CT applications. Its sensitivity to dose is well suited for applications requiring low doses such as CT.

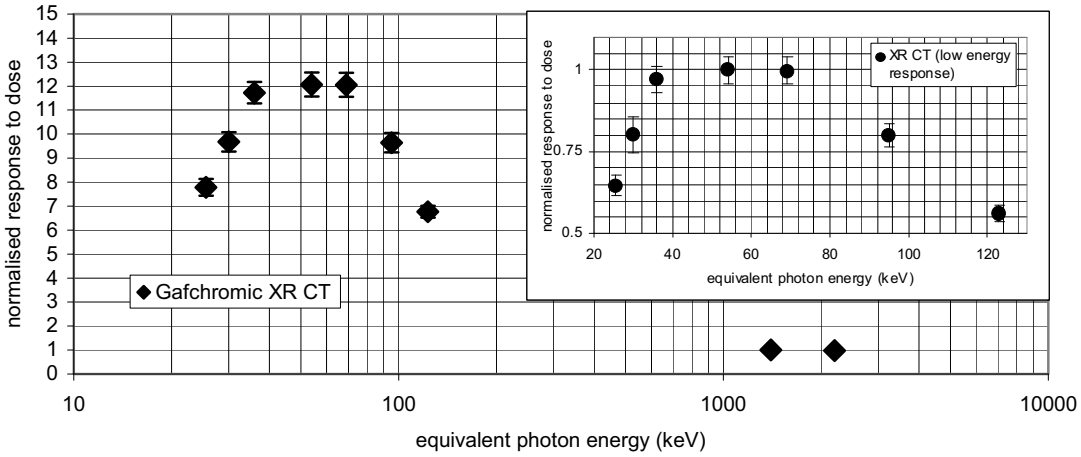

INDEPENDENCE OF CALIBRATION CURVES FOR EBT GAFCHROMIC FILMS OF THE SIZE OF HIGH-ENERGY X-RAY FIELDS

Tsang Cheung[1], Martin J. Butson[1,2,3] and Peter K.N. Yu[1]

[1]*City University of Hong Kong , Dept. of Physics and Materials Science, Kowloon Tong, Hong Kong*
[2]*Illawarra Cancer Care Centre, Department of Medical Physics, Wollongong, Australia*
[3]*Centre for Medical Radiation Physics, University of Wollongong, Wollongong , Australia*

KEYWORDS: Radiochromic film, Gafchromic, EBT, calibration, energy dependence, field size, scatter.

INTRODUCTION: EBT Gafchromic radiochromic film is a relatively new product designed specifically for dosimetry in radiation therapy. Due to the weak dependence of its response on the photon energy (variations are below 10% in the 50 kVp – 10 MVp range), the film is ideal for dosimetry when the photon energy spectrum may be changing or unknown.

METHODS: In order to convert a map of optical densities into a map of absorbed radiation doses, a calibration curve constructed on the basis of standard calibration films is necessary.

RESULTS: Our results have shown that, with the EBT Gafchromic film, one can use the same calibration curve for 6-MV x-ray fields of any size in the range from 5×5 cm^2 up to 40×40 cm^2. This is not the case for radiographic films, such as Kodak X-Omat V, whose response to the same dose varies approximately by 10% depending on the field size in this range.

DISCUSSION & CONCLUSION: This insensitivity of the EBT Gafchromic film to size of the radiation field makes it possible to assess doses delivered by small radiation fields. With the help of this film, it was shown that the output factor for a 0.5×0.5 cm^2 field is 0.60 ± 0.03 relative to the 10×10 cm^2 field.

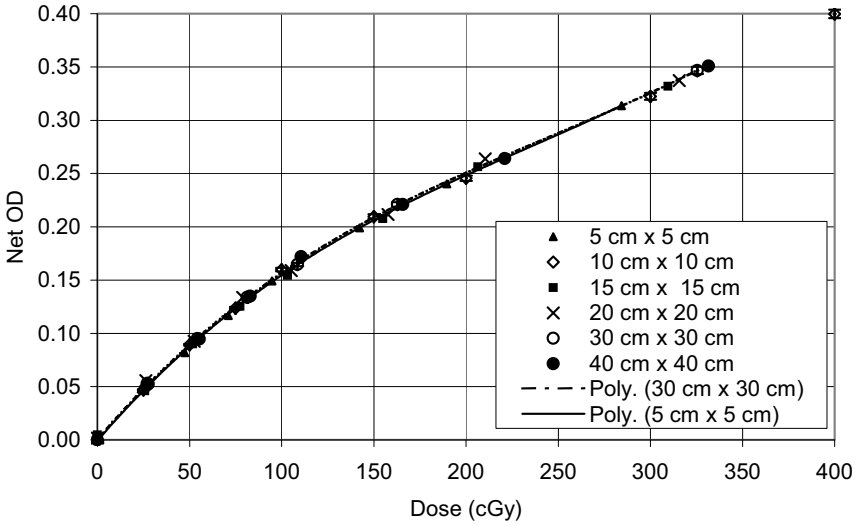

DOES MECHANICAL PRESSURE ON RADIOCHROMIC FILM AFFECT OPTICAL ABSORPTION AND DOSIMETRY?

Tsang Cheung[1], Martin J. Butson[1,2,3] and Peter K.N. Yu[1]

[1]*City University of Hong Kong , Dept. of Physics and Materials Science, Kowloon Tong, Hong Kong*
[2]*Illawarra Cancer Care Centre, Department of Medical Physics, Wollongong, Australia*
[3]*Centre for Medical Radiation Physics, University of Wollongong, Wollongong, Australia*

KEYWORDS: Gafchromic EBT, Radiochromic film, densitometry, pressure

INTRODUCTION: EBT Gafchromic film, a new high sensitivity radiochromic film has been tested to evaluate if external pressure on the film can affect absorption spectra analysis and thus radiation dosimetry.

METHODS: This question arises from the fact that Gafchromic film is often cut into smaller pieces or to certain shapes for dosimetric analysis using scissors which can apply significant pressure to the sides of the film and small film pieces are placed within a solid phantom at depth which can produce significant pressure on the film if appropriate weight distribution procedures are not performed. Films were subjected to external pressure in various sizes to measure any variations recorded in optical density and dosimetry.

RESULTS: As expected, results have shown that films cut by scissors can produce a large increase in OD near the film edge up to 5-10 mm away due to physical damage to the EBT film layers however. Films placed within a solid phantom receiving up to 39.5 kg/cm^2 pressure showed negligible differences in measured absorption spectra compared with control films subject to no external pressure. This equates to negligible external pressure effects for as much as 44 cm of 30 cm x 30 cm solid water placed on a 1 cm^2 area film piece.

DISCUSSION AND CONCLUSION: As such, we recommend based on results herein, that film analysis should be performed with a boundary around every film edge, which can be defined visually based in the film. Also film dosimetry in a phantom can be performed with weights up to 39.5 kg/cm^2 (or 44 cm of 30 cm x 30 cm solid water or equivalent) placed on the film without effecting the absorption spectra and thus dosimetry of radiation beams.

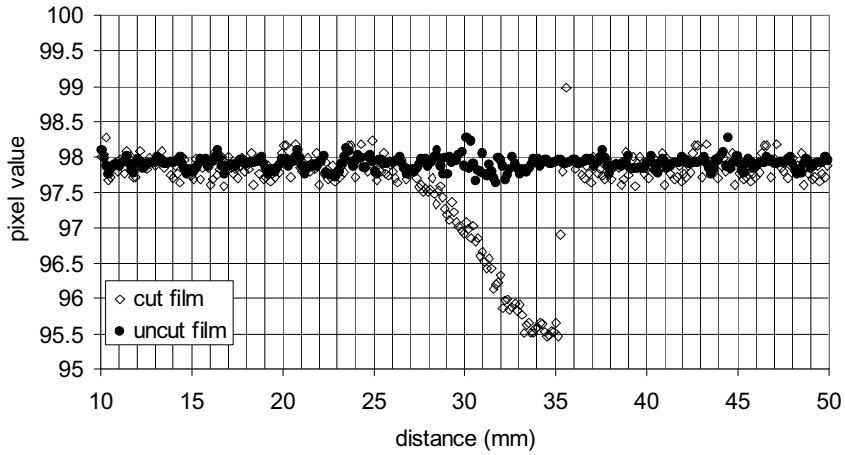

CT-NUMBER DEPENDENCE ON KV/MA SETTINGS – INFLUENCE OF AUTO-MA

M.A. Ebert[1,2], J. Lambert[3] and P. Greer[3,4]

[1]*Department of Radiation Oncology, Sir Charles Gairdner Hospital, Australia*
[2]*School of Physics, University of Western Australia, Australia*
[3]*School of Mathematical and Physical Sciences, University of Newcastle, Newcastle, Australia*
[4]*Department of Radiation Oncology, Newcastle Mater Hospital, Newcastle, australia*

INTRODUCTION: Contemporary 3D radiotherapy treatment planning systems (TPS's) utilise the electron density information derived from computed tomography (CT) images as input to dose calculation algorithms. Typically, the relationship of CT-number to electron density ('CT-ED') is obtained from a calibration performed with reference kV and mA settings on the CT scanner. CT scanners are now available with algorithms for the automatic variation of mA ('auto-mA') with slice position in order to optimise the ratio of image-quality to patient exposure. This constant variation in mA can potentially vary the CT-ED relationship across a patient due to variations in response of the imaging and image-processing system. This study investigated this variation.

METHODS: Using a commercially available phantom with inserts representing a wide range of electron densities, variations in the CT-ED variation with CT kV and mA settings were investigated. This included examining CT number for high atomic number (Z) materials representative of metallic implants, and examining the effect of different reconstruction algorithms available with the GE Lightspeed RT scanner used in this study. Material electron densities (ρ_w^e – relative to water) varied from $\rho_e^w = 0.2$ for lung-at-inhale to $\rho_e^w = 3.7$ for titanium. To examine the effect of auto-mA, a phantom was produced of variable thickness and containing materials representative of soft tissue, air cavities and bone.

RESULTS: A significant dependence of CT number on kV setting was found for electron densities above $\rho_e^w \approx 1.5$ (see Fig. 1). Although variations in CT-ED were also found with mA for very high density materials, it is believed that statistical uncertainty was high for these samples (due to CT numbers almost reaching saturation at those densities).

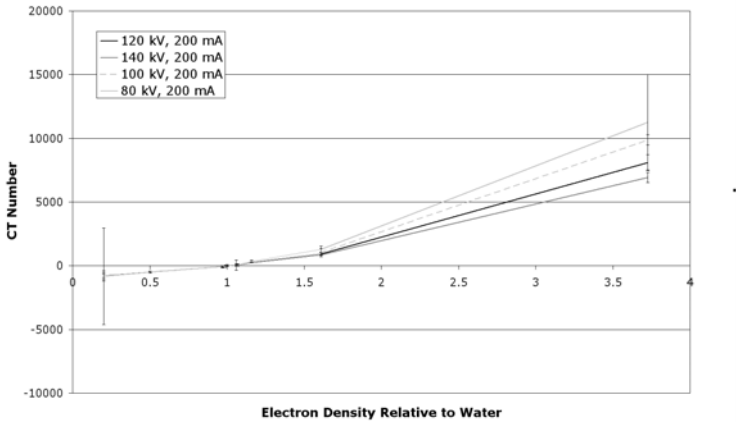

Figure 1. *Comparison of CT-ED relationships with variation in kV.*

With the auto-mA setting, some variation in ED with position along the phantom was found for the bone analogue. However, by comparison with a fixed-mA scan, this was found to be due to an artefact introduced by the variation in thickness of the phantom rather then the automatic variation in mA.

DISCUSSION & CONCLUSIONS: While some variation in CT-ED was found with kV, it was found that for the GE scanner, variations in CT-ED resulting from changes in scanning and/or image processing methods were insignificant. This suggests that extended-range and auto-mA features are suitable for use when obtaining images for radiotherapy treatment planning.

SOFTWARE TO FACILITATE IMPLANT POSITION VERIFICATION FOR PROSTATE HDR BRACHYTHERAPY

C. Fox[1], A. Haworth[2] and S. Van Dyk[3]

[1, 2]*Department of Physical Sciences, Peter MacCallum Cancer Centre, Melbourne, Australia*
[3]*Radiation Therapy Services, Peter MacCallum Cancer Centre, Melbourne, australia*

INTRODUCTION: For HDR brachytherapy treatment of the prostate, catheters are commonly implanted transperineally into the prostate. Since the treatment is fractionated, treatment extends over more than one day. Movement of the implant relative to the prostate is often observed over time, with movements up to 42mm reported. These movements impact negatively on dose coverage and clearly need to be monitored and corrected.

Current practice at PMCC is to treat all HDR prostate brachytherapy patients in two fractions, each of which is verified for implant position. The implant consists of an average of 14 flexible 24cm 5 French proguides which are anchored to a template which in turn is stitched to the patient's perineum. Four gold fiducial markers, each 0.8mm dia and 3mm long, are implanted in the prostate at the time of the HDR implant. At each treatment fraction, an AP image of the implant is compared with a reference image from the planning CT data set and the location of the treatment dose adjusted to compensate for any detected implant movement.
Prior to development of this software, measurements were extracted from reference and treatment images using a software package and compared with the aid of a spreadsheet. This process was complex and error prone.

METHODS: The software was developed in Visual Studio using Visual Basic.NET. Images are imported as bitmaps for both the reference and treatment images and calibrated from the x-ray markers. Fiducial marker positions are entered by a mouse click on the image. Patient details and measurements are stored automatically in tables in a Microsoft SQL Server database. A report may be printed for addition to patient records.

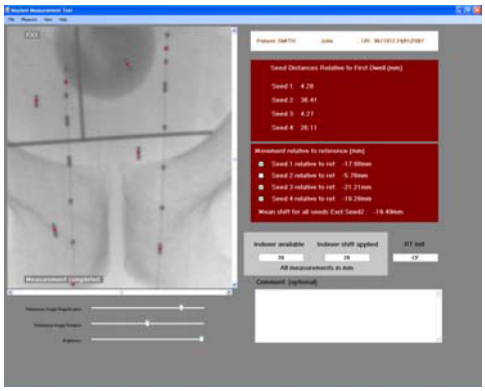

Figure 1. *Screen grab of implant position verification software.*

DISCUSSION & CONCLUSIONS: The software as described has made setup verification simpler and reduced the likelihood of error. Time taken to carry out the procedure has also been reduced.

REFERENCES:
[1]*Martinez A, et al (2001) Int. J. Radiation Oncology Biol. Phys. 49: 65.*
[1]*Hoskin P, et al (2003) Radiotherapy and Oncology 68: 285.*
[1]*Mullankandov E, et al (2004) Int. J. Radiation Oncology Biol. Phys. 58 1066.*

DOSE PERTURBATION CAUSED BY LARGE AIR GAPS CREATED BY IMMOBILISATION DEVICES

A. Gray[1], L. Oliver[2], S. Brown[3] and P. Johnston[4]

[1, 2, 3]*Royal North Shore Hospital, Radiation Oncology, Sydney, Australia*
[1, 4]*RMIT University, School of Applied Sciences, Melbourne, Australia*
[2, 3]*University of Sydney, Sydney, Australia*

INTRODUCTION: When a photon beam passes through a treatment couch or immobilisation device, such as a tilted breast board, it may traverse a large air gap (up to 15 cm) prior to entering the patient. Previous studies [1-4] have investigated the ability of various treatment planning systems (TPS's) to calculate the dose immediately behind small air cavities, such as those within the body. The aim of this study was to investigate the ability of the Eclipse™ pencil beam convolution (PBC) algorithm to calculate the dose behind large air gaps when utilising the equivalent tissue air ratio method of inhomogeneity correction.

METHODS: Central axis depth dose data in water for a 6MV photon beam (Varian Clinac 600), 10 x 10 cm^2 field size and 100 cm source to water surface distance were measured behind a range of air gaps (1 to 15 cm) using a parallel plate ionisation chamber. The air gaps were created by supporting water equivalent RW3 slabs (0.2 to 4 cm thick) above the water surface (see inset in Figure 1). The dose for each setup was normalised to that delivered by 100 monitor units at 5 cm deep. For each setup, dose calculations were performed using the Eclipse™ TPS and DOSXYZnrc software (with a phase space produced by the BEAMnrc Monte Carlo system) and compared to the measured values.

RESULTS: The measured and Eclipse™ calculated dose behind 2 cm RW3 slabs and various air gaps are shown in Figure 1 below. The Monte Carlo and measured results indicate that as the air gap increases the dose reduces at the water surface. For larger air gaps, the dose behind the air gap is also reduced at depth. The Eclipse™ dose was found to be the same for all air gaps and a given slab thickness and does not predict the reduction in dose after the air gap. For the 2 cm RW3 slab, 15 cm air gap case, Eclipse™ overestimated the dose by 52% at the water surface, by ~3% between 4 and 13 cm and by 2% at 15 cm depth in the water phantom. This trend was evident for each setup investigated in this study.

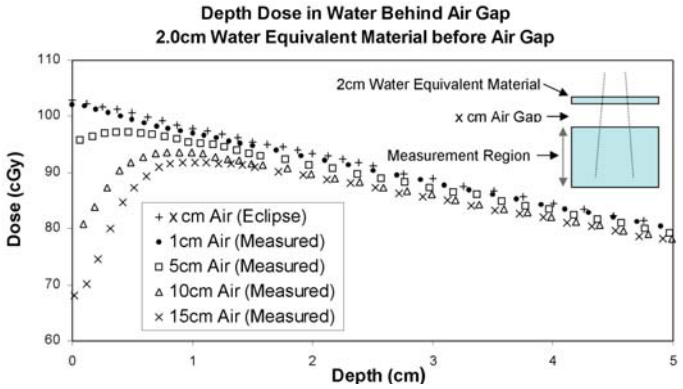

Figure 1. *Depth Dose in Water behind 2.0 cm Water Equivalent Material and Various Air Gaps.*

DISCUSSION & CONCLUSIONS: When a beam passes through a large air gap created by a patient positioning device, the dose to the patient's surface and to depths of 15 cm reduces due to a decrease in scattered radiation to the point of interest. Significant errors can result when using the Eclipse™ PBC algorithm to calculate the dose beyond a large air gap created by a patient positioning device included in the dose calculation.

REFERENCES:

[1]*T. Wong, P. Metcalfe, T. Kron, T. Emeleus, (1992) Aust Phys Eng Sci Med, 15(3):138-146.*
[2]*T. Wong, W. Kan, M. Law, (1996) Aust Phys Eng Sci Med, 19(4):237-247.*
[3]*B.H. Shahine, M.S.A.L. Al-Ghazi, E. El-Khatib, (1999) Med Phys, 26(3):350-355.*
[4]*W. Ding, P. Johnston, T. Wong, I. Bubb, (2004) Aust Phys Eng Sci Med, 27(2):39-48.*

SCATTERED NEUTRON DOSE EQUIVALENT FROM AN ACTIVE SCANNING PROTON BEAM DELIVERY SYSTEM

Draik Hecksel[1], George A. Sandison[1], Jonathan B. Farr[2] and Andrew C. Edwards[3]

[1]*School of Health Sciences, Purdue University, West Lafayette, Indiana, USA*
[2]*Midwest Proton Radiotherapy Institute (MPRI), Bloomington, Indiana, USA*
[3]*Indiana University Cyclotron Facility (IUCF), Bloomington, Indiana, USA*

A stud of neutron production from a novel active scanning proton beam delivery system at the Midwest Proton Radiotherapy Institute (MPRI) has been performed. The neutron dose equivalent was determined using a neutron REM detector at 0, 45, and 90 degrees from the proton beam central axis and for various proton beam energies (127-208 MeV) and scanned field sizes (25-144 cm^2). The maximum neutron dose observed was .43 mSv/proton treatment Gy at 90 degrees from the beam axis for a beam energy of 208.4 MeV and a scanned field size of 144 cm^2. It is still possible to further mitigate this secondary neutron dose during treatment by optimizing parameters within the treatment nozzle and using shielding.

A TEST OF WATER EQUIVALENCY OF SOLID PHANTONS AT LOW PHOTON ENERGIES USING GAMMA RAY TRANSMISSION VALUES

R. Hill[1,2], S. Brown[2,3] and C. Baldock[2]

[1]*Department of Radiation Oncology, Royal Prince Alfred Hospital, Camperdown, Australia*
[2]*Institute of Medical Physics, School of Physics, The University of Sydney, Australia*
[3]*Department of Radiation Oncology, Royal North Shore Hospital, St Leonards, Australia*

INTRODUCTION: The selection of an appropriate solid phantom is critical if water equivalence is required for the dosimetry of lower energy photons. The purpose of this paper was to investigate the water equivalence of several solid phantoms at these energies by comparing gamma ray transmission values using experimental and Monte Carlo techniques.

METHODS: Three solid water-type phantoms and perspex were compared with water. Technetium-99m radionuclide was confined within and collimated by a lead container to produce a narrow beam of photons of 5 mm diameter. The transmitted gamma rays were measured as a function of phantom thickness using a Phillips Skylight gamma camera. An energy window of ±10% was set to exclude low energy scatter. This setup was modeled within the EGSnrc Monte Carlo code V4.2.2 and the FLURZnrc user code. The total fluence was scored after passing through the different phantom thickness. The linear attenuation coefficient was calculated from the resultant transmission curves and compared with published NIST data using the XCOM program.

RESULTS: The measured transmission values for the Plastic Water, RMI-457 Solid Water and RW3 phantoms were in good agreement with those for water, with a maximum difference of 1.5%. However the transmission values through perspex differed by up to 4% as compared to water. The agreement between EGSnrc and measured transmission values was good, with a maximum difference of 1.3% for all phantom materials. The linear attenuation coefficients, μ, were derived from the transmission values using an exponential function and the Sigmaplot software. All the coefficients are presented in table 1. The linear attenuation coefficients derived from measurements and EGSnrc calculations agreed to within 2.4%. For all phantom materials, the NIST linear attenuation coefficient was greater than the measured and EGSnrc calculated coefficients. Differences between experimental values and published NIST data are attributed to the energy resolution of the scintillator crystal within the gamma camera and limitations in the source description for the Monte Carlo calculations.

Table 1. *Linear attenuation coefficients for the five phantoms studied determined using measured and Monte Carlo calculated transmission data and calculated by the XCOM program for gamma rays emitted by a technetium-99m source.*

	Water	RMI-457	Plastic Water	RW3	Perspex
$\mu_{Measured}$	0.148	0.151	0.151	0.149	0.166
μ_{EGSnrc}	0.151	0.151	0.152	0.153	0.170
μ_{XCOM}	0.154	0.154	0.155	0.155	0.177

DISCUSSION & CONCLUSIONS: This work has demonstrated a simple method for testing water equivalency of solid phantoms at low photon energies using gamma ray transmission values determined from measurements and Monte Carlo calculations.

THE EFFECT OF PATIENT SIZE ON THE VISUALIATION OF PROSTATE FIDUCIAL MARKERS IN MEGAVOLTAGE CONE BEAM CT IMAGES

J. Hughes[1, 2], L. Holloway[1], A. Fielding[2] and A. Kneebone[1]

[1]*Liverpool Cancer Therapy Centre, Sydney, Australia*
[2]*Queensland University of Technology, Brisbane, Australia*

INTRODUCTION: Siemens MVision is a new commercially available megavoltage cone beam system that facilitates the acquisition of 3D patient images at the time of treatment utilising the treatment beam. A trial study conducted at the Liverpool Cancer Therapy Centre found that two of the main factors influencing the quality of these images were the radiation dose used and the patient separation[1]. This was particularly evident for the prostate patients where there was also a lack of soft tissue information in the centre of the image. Therefore, this paper aimed to determine the minimum number of monitor units (MU) necessary to visualise prostate fiducial markers given the lack of soft tissue information, and what, if any, increase in dose was needed as patient separation increased to ensure a useable image.

METHODS: Three gold seeds were placed within an anthropomorphic phantom in the approximate location of the prostate. Several cone beam image sets were acquired of this phantom, which has 31.5 cm separation at the prostate using an increasing number of MUs. The Cone Beam (CB) image sets were evaluated to determine at what dose the gold seeds were visible. The anthropomorphic phantom's separation at the prostate was increased using tissue equivalent bolus and wax to 40.1 cm and 49.5 cm and the procedure repeated to assess the effect of patient size.

RESULTS: It was found that the fiducial markers were visible for all thicknesses of patient when images were acquired with the lowest number of MUs. However, there was, as expected, degradation in overall image quality with increasing patient thickness as is illustrated below by the images acquired using 8 MU.

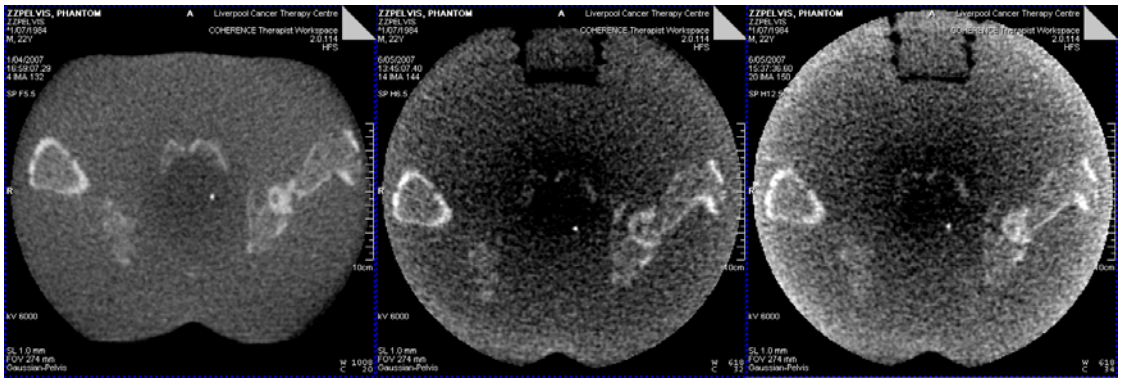

Figure 1. *Images of phantom with 31.5 cm, 41.5 cm and 49.5 cm separation respectively acquired with 8MU.*

DISCUSSION & CONCLUSIONS: The quality of images acquired using Megavoltage Cone Beam CT were sufficient to locate fiducial markers in prostate patients of separations up to 49.5cm using 5MU. Further research is needed to determine the most appropriate uses of MVCB CT to ensure that this system is used to its fullest potential within radiation therapy.

ACKNOWLEDGEMENTS:
Images courtesy of Liverpool Cancer Therapy Centre, Sydney Siemens Medical Services

REFERENCES:
[1]*Fuller M, Rattavong, S, Arts, J and Hughes, J. Introduction of Megavoltage Cone Beam Computed Tomography at Liverpool Cancer Therapy Centre, 4th Annual Scientific Meeting Of Medical Imaging & Radiation Therapy, March 2007.*

EPID AS A DAILY LINAC QUALITY ASSURANCE TOOL

E. Jhala[1] and L. Greig[1]

[1]*Wellington Blood & Cancer Centre, Wellington, New Zealand*

INTRODUCTION: The ability of the electronic portal imaging device (EPID) to acquire a large two-dimensional array of digitized x-ray data in real time is extremely attractive for dosimetric measurements. Due to this ability, the use of EPID for dosimetric quality assurance of linear accelerators in Wellington Blood and Cancer Centre was explored.

METHODS: The output of linac is checked daily using the Keithley tracker. The constancy of the readings day after day is analysed. These readings obtained from Keithley tracker were compared to the response of EPID for 10 consecutive days of measurements.
A patient was set-up in Vision, with two fields. Firstly, a 6 MV open field of 18 x 18cm^2 with 120 MU was delivered on a daily basis. Secondly, the same field with 60^0 EDW was acquired. These were then analysed using Matlab. These images were used to evaluate the constancy of linac output, flatness, symmetry, wedge angle constancy, wedge factor constancy tests for routine linac quality assurance.

RESULTS:

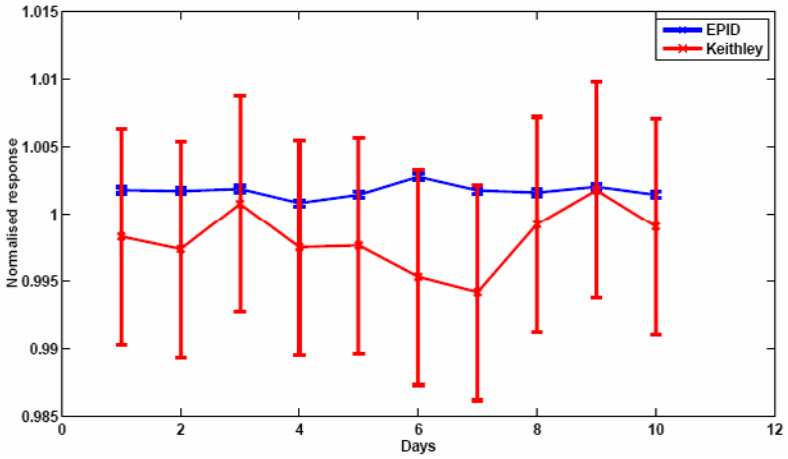

Figure 1. *Comparison of daily linac output constancy measured using Keithley tracker and EPID.*

DISCUSSION & CONCLUSIONS: The EPID's capability to give constant output, flatness, symmetry, wedge angle and wedge factors with high level of accuracy and reproducibility was demonstrated. The use of EPID for linac QA could be simplified by improving the available software analysis tools thus making it more efficient.

A MODELLING INVESTIGATION INTO ALTERED FRACTIONATION FOR IMRT

Ming Kong[1], L. Holloway[1] and D. Forstner[1]

[1]*Department of Cancer Therapy Centre, Liverpool Hospital, Sydney*

INTRODUCTION: Hypofractionation is generally considered as the use of dose per fractions higher than 2.0 Gy, resulting in reduced fractions compared with conventional fractionation[1]. Appropriate hypofractionation has been shown to deliver equivalent treatment in some clinical situations, such as breast, it is also possible that there may be benefits for head and neck by reducing overall treatment time. There is limited research on hypofractionation for Intensity Modulated Radiation Therapy (IMRT). IMRT uses non-uniform beam intensities within a radiation field to provide more degrees of freedom for dose shaping, resulting in dose distributions that conform more tightly around the tumour[2]. Therefore less dose/ fraction is delivered to normal tissues when compared with conventional 3D conformal radiation therapy if the prescription and

fractionation schedule are maintained. Instead of reducing dose/fraction and total dose to normal tissues, maintaining the biological effect to normal tissues for IMRT can be achieved by adjusting the prescription and fractionation schedules. The total dose to the tumour volume could be increased or the number of fractions reduced while delivering the same effect to the normal tissues. This investigation utilises modelling to assess the possibilities for these situations.

METHODS: In this project, the LQ model was utilised. A central feature of the LQ methodology is the quality known as the Biologically Effective Dose (BED). The equation for BED is given below where D is the total dose, d is the dose per fraction and ˜ is a tissue specific parameter.

$$BED = D.[1+ d/(\alpha/\beta)] \quad (1)$$

In this project, BED was used to adjust the treatment fractionation schedules for an IMRT head and neck treatment plan when compared with a conventional head and neck treatment plan. For the conventional plan, a total dose of 70 Gy was delivered in 35 fractions to the target with an α/β of 10 and 50 Gy was given to the brain stem, for which α/β was assumed to be 2. The BED was calculated for the normal tissue for the conventional plan and used as an acceptable value for the IMRT plan. On the IMRT treatment plan, dose per fraction and number of fractions were determined to achieve the same BED to the normal tissues and equivalent or greater for the target as the conventional plan. This was achieved by rearranging equation 1 for the situation of maintaining the standard fraction size to the target and simply increasing the total dose or hypofractionating the dose to the target and delivering the same fraction size to the normal tissues as occurs with conventional treatment plans.

RESULT: It was noted that the BED for the brain stem was reduced from 100 Gy_2 in the conventional plan to 72.8 Gy_2 in the IMRT plan. This is consistent with the expectation of IMRT. The BED for the target in the IMRT plan was increased to 109.4 Gy_{10} when same BED to the brain stem was maintained in both treatment plans and the fraction size to brain stem was maintained. It was found that if the fraction size to the target was hypofractionated for IMRT, the number of fractions could be reduced to 27 with the BED to the target maintained and the BED to the brainstem reduced to 76 Gy_2 If the dose to the target was hypofractionated in this way it would also be possible to increase the BED to the target and maintain the BED to the brainstem.

DISCUSSION & CONCLUSIONS: The increase of BED to the target whilst maintaining the same BED to the brain stem as the conventional plan has the potential to result in improved local tumour control according to this modeling. This however would need to be undertaken carefully to ensure that any normal tissues within the target volume were not adversely affected by the change in fraction size.

REFERENCES:

[1]*Steel, G.Gordon (2002). Basic Clinical Radiobiology. Arnold Great Britain.*
[2]*Jacob, V Dyk (2005). The Modern Technology of Radiation Oncology. Volume 2. Medical Physics Publishing. USA.*

IMRT FOR LARGE TUMOUR VOLUMES

J. Meyer[1,2] and A. Richter[2]

[1]*Department of Physics and Astronomy, University of Canterbury, Christchurch, New Zealand*
[2]*Department of Radiation Oncology, University Hospital Wuerzburg, Wuerzburg, Germany*

INTRODUCTION: Treatment of tumour volumes which are larger than the projected dimension of the multi-leaf collimator can be a challenging problem [1,2]. On a standard linear accelerator straightforward treatment techniques such as abutting fields or extended skin-surface distance can be applied. However, these techniques have considerable disadvantages meaning that patients with large tumour volumes may not be considered for intensity-modulated radiation therapy (IMRT) even though they might benefit from a more conformal treatment technique. In this work a practical IMRT technique is presented that makes it possible to treat large tumours that extend in superior-inferior direction beyond the projected dimensions of the multi-leaf collimator.

METHODS: The technique developed for treating large tumours with IMRT is shown exemplarily for a clinical head-and-neck patient. The patient had a large oropharynx/oesophagus carcinoma and was scheduled for our head-and-neck IMRT protocol with simultaneous integrated boost (SIB). The SIB protocol includes three dose levels in the target ranging from approximately 52Gy in the elective nodal region to 69.9Gy in the boost volume. The superior-inferior dimensions of the target volumes drawn by the clinician were beyond the maximum field size for IMRT planning and delivery.

The technique developed makes use of an odd number of beams. The gantry angle between consecutive beams is constant. The beams with odd indices (1, 3, 5 …) have a common isocentre and the beams with even indices (2, 4, 6 …) have a common isocentre. The two isocentres are placed such that their coordinates only differ in superior-inferior direction. The upper isocentre is placed such that the superior part of the target is covered by the MLC in the beams-eye-view (BEV) and the lower isocentre is placed such that the inferior part of the target is covered by the MLC in the BEV. This results in an interlaced beam arrangement with all beams covering the central part of the target and correspondingly fewer beams covering the superior and inferior edges of the tumour. The technique was applied using 9 beams and compared with a more complex IMRT technique for large target volumes described in literature [2]. The complex IMRT technique employed 14

IMRT beams and also two isocentres. The plans were compared in terms of complexity, dosimetry and the effect of inaccurate translation between the isocentres.

RESULTS: The technique developed as well as the more complex IMRT technique achieved the clinic objectives. Both plans did not violate the planning constraints. Tumour control probability (TCP) and normal tissue complication probability (NTCP) did not reveal any clinically relevant differences. 1mm translational set-up errors between the isocentres did not affect the dose distribution significantly ($\Delta TCP < 0.5\%$, $\Delta NTCP < 4.0\%$). The number of monitor units was 1/3 less for the technique developed than for the competing more complex IMRT technique.

DISCUSSION & CONCLUSIONS: With the interlaced IMRT technique it is possible to treat large tumour volumes without compromising the dose distribution. Due to the interlaced nature of the IMRT beams there are no field junction problems. The technique does not require more beams than a standard IMRT plan and therefore keeps the integral dose to the patient comparable to standard IMRT plans. The technique does not add in complexity except for one isocentre shift. It was shown that the approach is not susceptible to inaccurate isocentre translations. The general idea of interlacing IMRT beams to increase the treatable field size is likely to make it possible to use smaller MLCs, such as micro MLCs, to treat larger target volumes with IMRT. Due to the versatility of the technique it can easily be applied to other clinical regions and is well suited for clinical routine usage.

REFERENCES:

[1]*Q. Wu, M. Arnfield, S. Tong, Y. Wu, and R. Mohan, (2000) Phys Med Biol; 45, 1731-1740.*
[2]*H. K. Malhotra, S. Raina, J. S. Avadhani, S. Deboer, and M. B. Podgorsak, (2005) J Appl Clin Med Phys; 6: 77-87.*

IN VIVO DOSIMETRIC VERIFICATION OF MIDLINE DOSE AND PATIENT SETUP ERRORS FOR IMRT PROSTATE TREATMENT, USING ENTRANCE AND EXIT MOSFETS

J. Meyer[1,2] and A. Richter[2]

[1]*University of Adelaide, School of Chemistry and Physics, Adelaide, Australia*
[2]*Department of Medical Physics, Royal Adelaide Hospital, Adelaide, Australia*

INTRODUCTION: In vivo dosimetry using MOSFETs placed in the entrance and exit beams, with the application of a dose estimation algorithm, is a useful tool to verify midpoint dose. The accuracy of dose prediction for standard 4-beam and step-and-shoot IMRT prostate treatments using this method is investigated using simple and complex phantoms. The suitability of this method to identify patient positioning errors is also investigated.

METHODS: Verification of the suitability of MOSFETs for in vivo dosimetry was performed by checking characteristics such as linearity with dose, field size, angular, dose-rate dependence and reproducibility. A dose-calculation algorithm[1] which takes into account inhomogeneities was chosen to determine midline dose from entrance and exit MOSFET measurements. The accuracy of this method was assessed by comparison with calibrated ion chamber readings using firstly simple phantoms, then phantoms of increasing complexity and inhomogeneity and ultimately lung and anthropomorphic (Rando) phantoms.

Comparisons were made of dose as calculated using MOSFETs+algorithm and ion chamber measurements for a standard 4-beam prostate treatment, including to what extent MOSFETs could be used to detect patient position offsets. The accuracy of the method for IMRT step-and-shoot prostate treatment was evaluated.

RESULTS: Agreement within 1.3% was found between IC measured and MOSFET calculated dose for simple symmetric homogeneous phantoms and within 2.3% for phantoms with symmetric inhomogeneous (e.g. lung phantom). MOSFET calculated dose was within 0.7% of dose predicted by the Treatment Planning System for standard prostate treatment with 4 fields, and accurate within 3.5% for IMRT prostate treatment.

For a phantom in which an inhomogeneity was placed between entry surface and midline, agreement between MOSFETs and IC dose was 3.1%, however when the inhomogeneity existed between midline and exit surface, there was a difference in dose between the two methods of 16.2%.

MOSFETs could detect offsets in position of 1.5 – 2.0 cm, but could not confidently identify setup errors less than 1.5 cm.

DISCUSSION & CONCLUSIONS: MOSFETs were found to be suitable in vivo dosimeters for simple homogeneous and symmetrically inhomogeneous phantoms, and phantoms in which an inhomogeneity exists in front of the midline, but were unreliable when inhomogeneities exist between the midline and the exit surface due to the algorithm not taking into account the *position* of the inhomogeneity. MOSFETs are considered suitable for in vivo dosimetry for radiotherapy treatments involving flat and largely homogeneous target regions, and for dose verification during IMRT prostate step-and-shoot treatments. They can identify patient setup errors larger than 1.5 cm.

REFERENCES:

[1]*D. Huyskens, J. Van Dam, A. Dutreix (1994) Phys. Med. Biol., 39: 1089-1101.*

COMMISSIONING PROCEDURES AND EVALUATION OF IMSURE PROGRAM

T. Pham[1], J. Barber[2], S. Yau[3], S. White[4] and E. Estoesta[5]

[1,2,3,4,5]*Nepean Cancer Care Centre, Nepean Hospital, Sydney, Australia*

INTRODUCTION: To ensure that the patient will be treated with correct doses, it is an essential practice to carry out an independent monitor unit calculation check. The Rad Calc[1] program is currently being used at Nepean Cancer Care Centre. Another program called IMSure[2], which was investigated, also serves the same purpose plus IMRT monitor unit (MU) check. The commissioning procedures for IMSure for photon beams were discussed. In addition, the comparison between the IMSure and Rad Calc data with measured data will be presented.

METHODS: The geometrical characteristics of the linear accelerator (linac) were first set up in the IMSure program. The commissioning of this MU calculation program requires physical data such as: Tissue Maximum Ratio, Off-axis Ratios, Collimator Scatter Factor, Total Scatter Factor and Wedge Factor and others. These data were measured on the linac, analysed on the Wellhofer software and further processed in MS Excel in accordance to the format which IMSure accepts. To further evaluate the accuracy of the MUs calculated using IMSure, the results were compared with results generated from Rad Calc and from previously measured data. A series of data points were measured at different depths, wedges and collimator settings. The same conditions were set up in Rad Calc and IMSure. The percentage differences of Rad Calc and measured data were compared against the percentage differences of IMSure and measured data.

RESULTS: The IMSure and Rad Calc calculated point doses for open fields at central axis agree within 1% with the measured data. Generally, the physical and dynamic wedge point dose calculations for IMSure and RadCalc agree within 2% of the measured data.

DISCUSSION & CONCLUSIONS: The most time consuming task in the commissioning of IMSure program were the data entry and analysis. Wellhofer and MS Excel program were used in these processes. The comparison between IMSure and measured data showed that IMSure's monitor unit calculation algorithm is reliable. Rad Calc's data was shown to provide better agreement with the measured data than IMSure. However, IMSure program has an additional algorithm for IMRT monitor unit calculation. This additional function is subject to further investigation in the near future.

REFERENCES:

[1]*LifeLine Software Inc (2003) Rad Calc Version 4.3, LifeLine Software Inc USA*
[2]*Standard Imaging Inc (2007) IMSure QA Software Version 3.1, Standard Imaging Inc USA*
Khan Faiz M (2003) The Physics of Radiation Therapy 3rd Edition, Lippincott Williams and Wilkins USA

THE USE OF 4DCT TO DEFINE PLANNING TARGET VOLUMES FOR THE TREATMENT OF LUNG CANCER

S. Price[1] and M. Williams[1]

[1]*Department of Radiation Oncology Medical Physics, Illawarra Cancer Care Centre, Wollongong Hospital, Wollongong, Australia*

INTRODUCTION: Respiratory motion poses a significant challenge in achieving optimal dose coverage of lung tumours whilst maintaining adequate sparing of the surrounding healthy lung tissue. Applying nominal margins in the generation of a planning target volume (PTV) with CT data that has been collected as a single random snapshot of the respiratory cycle may be insufficient or excessive in providing optimal tumour coverage. The aim of this study was to quantify, for a single lung cancer patient, the volume difference in the PTV when generated from a complete four-dimensional CT (4DCT) dataset and from limited phases of the 4DCT dataset. The clinical treatment plan was also applied and dose information for the different PTVs was assessed.

METHODS: A 4DCT data set was collected as part of the treatment planning process for a patient with a stage 1B lung tumour in the right hilum. The CT data was collected on a Siemens Sensation Open CT scanner with respiratory gating functionality. The Anzai gating system used in the study consisted of an elasticised belt that was strapped around the patient's torso and a small transducer that inserted between the belt and patient to gauge the change in the tension of the belt during the breathing cycle. A composite PTV was created using clinical target volumes (CTVs) defined over 10% increments of the respiratory cycle with a margin applied for setup uncertainties (PTV_{all}). Additional PTVs were generated from the CTVs defined at the 0%, 50% and 100% points of the inhalation phase (PTV_{3phase}) and at a random point in the respiratory phase (PTV_{random}). The setup margin applied to respective CTVs to determine PTV_{all} and PTV_{3phase} was 5 mm. The margins applied to PTV_{random} were based on the clinical margins developed prior to the use of 4DCT and were set at 12 mm in the lateral and anterior-posterior directions and 17 mm in the superior-inferior direction. The clinical treatment plan was reproduced with each of the different PTVs defined. Dose distribution and dose volume histogram information for each of the PTVs and the combined lung volume were tabulated.

RESULTS: Table 1 shows the results of the study including total volume of the PTVs, dose information and lung volume involved. The volume of lung covered by PTV_{random} was excessive compared to PTV_{all}, however in certain regions PTV_{random}

did not completely overlap with PTV_{all}, indicating despite the large margins they were insufficient to ensure coverage of the tumour defined by PTV_{all}.

Table 1. *Summary of PTVs.*

	Volume (cm^3)	Average Dose (cGy)	Maximum Dose (cGy)	Minimum Dose (cGy)	Lung Volume Included in PTV (cm^3)
PTV_{all}	188.24	6072.6	6474.2	5322.8	85.99
PTV_{3phase}	172.29	6073.4	6474.2	5322.8	73.99
PTV_{random}	318.00	5985.7	6474.2	3807.3	178.32

DISCUSSION & CONCLUSIONS: For this patient the use of a limited set of CT data from different parts of the respiratory phase provided an accurate representation of the tumour location and allowed better definition of the CTV and a reduction in the amount of lung tissue included in the PTV. Generating a PTV from an arbitrary point in the respiratory phase and applying fixed margins resulted in an excessive volume of the surrounding healthy lung tissue receiving dose and did not ensure tumour coverage.

SIMPLE METHODS TO REDUCE DOSE IN CONE BEAM CT

P. Roxby[1], J. Cramb[1], F. Foroudi[2], C. Fox[1], A. Haworth[1] and T. Kron[1]

[1]*Department of Physical Sciences, Peter MacCallum Cancer Centre, Melbourne, Australia*
[2]*Department of Radiation Oncology, Peter MacCallum Cancer Centre, Melbourne, Australia*

INTRODUCTION: Cone beam computed tomography (CBCT) is a three-dimensional imaging modality which has recently become available on linear accelerators. It enables both adaptive and image guided radiotherapy techniques where images are taken on several, or all, treatment fractions. The dose should be as low as reasonable achievable to comply with legislation and to minimise the significant risk of inducing an additional tumour as the number of scans increases.

METHODS: Four methods of dose reduction were investigated for a CBCT-equipped Varian Trilogy linear accelerator with CBCT 2.0 software. These were i) reducing the number of projections, ii) use of an additional 0.15mm thick copper filter on the tube side of the supplied bow tie filter, iii) setting the X-ray blade sizes so that only the truly necessary volume of tissue is irradiated and iv) reducing the beam current (mA).
Doses were measured at the centre and periphery of a 32cm diameter CTDI (CT Dose index) phantom with a Farmer type ionisation chamber. Image quality was assessed using a CATPHAN phantom and by asking the clinician contouring structures which scan (conventional or copper filter) was preferred and whether the latter was adequate for contouring.

RESULTS: The default settings for a half-fan CBCT scan were 650 projections, 125 kV, 80 mA, 25 ms per projection. Dose in the CTDI phantom was 2.37 cGy at the isocentre and 5.33 cGy at the periphery. Results : i) Reducing the number of projections was not practical with the current software release. ii) The copper filter reduced dose by 32% at the centre of the CTDI phantom and 36% at the periphery. Images with the copper filter were preferred, perhaps due to the better image uniformity. iii) A table giving blade settings for combinations of scan length and patient thickness proved practical and saved 5-6 cm length (sup-inf) of unnecessary irradiation. iv) Image quality was just acceptable with the larger patients and default mA settings. A CATPHAN phantom showed small increases in noise (6 rather than 7 1% contrast test objects visible) with 50% of the default mA. There appears scope to reduce the beam current for smaller patients.

DISCUSSION & CONCLUSIONS: Simple methods to reduce the effective dose to patients undergoing CBCT are easy to implement. Some methods increase image quality and the others do not significantly reduce it.

EVALUATION OF THE DOSIMETRY OF A BRACHYTHERAPY SURFACE MOULD BY IONIZATION CHAMBER AND MONTE CARLO METHODS

H. Seo[1], M. Haque[2], R. Hill[1, 2] and C. Baldock[1]

[1]*Institute of Medical Physics, School of Physics, University of Sydney, Australia*
[2]*Department of Radiation Oncology, Royal Prince Alfred Hospital, Sydney, Australia*

INTRODUCTION: Iridium-192 is the most commonly used radionuclide for brachytherapy treatments. Most treatments involve insertion of the source into the body under full scatter conditions. However the one possible brachytherapy use is the treatment of the epithelium using a surface mould, typically on the head, hand, arm or leg. In these cases, the use of the surface mould allows one to deliver the dose on a curved contour. The treatment planning system assumes full scatter conditions and that all tissues are water equivalent. Due to the property of the radioactive sources of having high dose gradient and emitted photons having a low energy allows an effective treatment of superficial lesions or neoplasm but it also

makes the brachytherapy dosimetry difficult. This paper will evaluate the dosimetry of the brachytherapy surface mould by experimental and Monte Carlo methods.

METHODS: A microSelectron HDR remote brachytherapy unit was used to deliver the Iridium-192 source to the dedicated catheters by means of stepping with varied dwell times. Virtual Water ^{TM} (Med-Cal) was used as water equivalent media to provide the scatter material. The catheter was placed on top of 50 mm of Virtual Water, and levelled by several mm of dental wax. Doses were measured using a PTW Roos chamber, connected to a Unidos Electrometer, as a function of thickness of the Virtual Water on top of the catheter and wax. The thicknesses of the Virtual Water, between the source and the Roos chamber, were also varied in order to evaluate the position dependence of the source to the chamber. The experimental setup was modelled within the EGSnrc Monte Carlo and the DOSRZ user code. The dose was calculated at the depth of the Roos chamber with the different thicknesses of Virtual Water above the source. The Iridium-192 source was assumed to be an isotropic point source within the phantom. A total of $2x10^8$ initial histories were used to achieve good statistical uncertainty.

RESULTS: The maximum variation in response between no scatter materials to the 50 mm of scatter material on the top of the catheter was of the order of 3%. For the distances of 5 mm and 10mm between the catheter and the chamber, the maximum percentage deviations in backscatter were 1.1% and 2.7% respectively. The Monte Carlo simulation results have shown that the variation in dose due to the different thickness of scatter material was 0.6%.

DISCUSSION & CONCLUSIONS: The results indicate that the thickness of scatter material around the Iridium-192 source can reduce the dose at an interest point, with the Monte Carlo results showing less variation in dose. The next step will be to define an improved model of the source within EGSnrc.

REFERENCES:

[1]*L.Duggan, M.Butson, S.Howlett, J.Denham, T.Kron, (2000) Australasian Physical & Sciences in Medicine, Volume 23 Number 1: p15-20.*
[2]*J.Pérez-Calatayud, D.Granero, F.Ballester (2004) Med. Phys. 31 (7) July 2004: p2075-81*

EFFECTIVE ATOMIC NUMBER AND THE CHARACTERISATION OF GEL DOSIMETERS

M.L. Taylor[1], R.D. Franich[1], J.V. Trapp[2] and P.N. Johnston[1]

[1]*Applied Physics, RMIT University, Melbourne, Australia*
[2]*School of Physical and Chemical Sciences, QUT, Brisbane, Australia*

INTRODUCTION: For dosimetry in a clinical environment, water equivalent detectors are desired. Water equivalence is often considered in terms of electron density, mass density and an 'effective atomic number', Z_{eff}, and so a material matching the attenuation properties of water is said to have the same Z_{eff} as water. Despite this 'water equivalence', there is no guarantee that either scattering or the dose distribution in such a medium will be the same as in water. This paper reviews several commonly employed methods of evaluating Z_{eff} and discusses their limitations, as well as providing more appropriate, energy-dependent values of Z_{eff}.

METHODS: A review of key literature associated with calculation of the effective atomic number has been conducted. Studies in the field of gel dosimetry most commonly attempt to quantify gels using, amongst other things, a single value of Z_{eff}. However, Z dependency varies with the photon energy and interaction process. Hence, we have calculated, using mass attenuation coefficient data (Hubbell and Seltzer 1995) the effective atomic number of gel dosimeters as a function of photon energy.

RESULTS: The most commonly employed method of the determination of Z_{eff} is that of Mayneord (1937), which is still quoted in contemporary radiation therapy textbooks (Khan 2003). It is found that this and other published rules for Z_{eff} have limited regimes of applicability. This study presents Z_{eff} as a function of photon energy, and results show that some gels have properties similar to water over a large range of energies, whereas others are systematically higher, lower or show different energy dependence.

DISCUSSION & CONCLUSIONS: During studies of gel dosimeter calibration, differences between gels and water were quantified in terms of density and Z_{eff}, however the latter parameter is ultimately of limited value.

REFERENCES:

[1]*Hubbell FH and Seltzer SM 1995 Tables of x-ray mass attenuation coefficients and mass energy-absorption coefficients from 1 keV to 20 MeV for elements Z = 1 to 92 and 48 substances of dosimetric interest NIST-5632.*

MONTE CARLO MODELLING OF HYPOXIC HEAD AND NECK SQUAMOUS CELL CARCINOMA AND RADIOTHERAPY

W. Tuckwell[1], E. Bezak[2] and E. Yeoh[3]

[1,2]*School of Chemistry and Physics, University of Adelaide,Adelaide, Australia*
[1,2]*Medical Physics Department, Royal Adelaide Hospital, Adelaide, Australia*
[3]*Radiation Oncology, Royal Adelaide Hospital, Adelaide, Australia*

INTRODUCTION: A Monte Carlo cell propagation model has been developed to simulate tumour growth and radiotherapy treatment for head and neck squamous cell carcinoma (HNSCC). The inclusion of an oxygen distribution and reoxygenation dynamics simulate radiobiological hypoxia in the tumour, allows the model to predict radiation therapy local control rates for the individual patient and for the average population for different fractionation schedules.

METHODS: Radiation cell kill is modelled though random hits of the tumour cells, and continues for each treatment fraction until a set percentage of cells have experienced a double hit and are programmed to die. The percentage of cells killed is based on SF2 data from the literature[1]. Modelling of hypoxia has been achieved through, in-vivo HNSCC oxygen distribution data from the literature[2] for a tumour with substantial hypoxia, measured using the Eppendorf electrode method. The radiation response of individual cells is dependent on the oxygen level of the cells as well as its proliferative status. Reoxygenation between fractions has also been considered. The tumour cell survival using a standard 2 Gy per fraction schedule is shown in figure 1.

RESULTS: The stem cell percentage and the degree of hypoxia are the parameters most influential on the final tumour growth rate in the model. For a tumour with a doubling time of 50 days, the final stem cell percentage is 1 to 2 % of the total cell population. For a moderately hypoxic tumour the effect on the tumour growth rate and the number of fractions required to achieve local control (zero stem or "stem like" cells remaining) is significant.

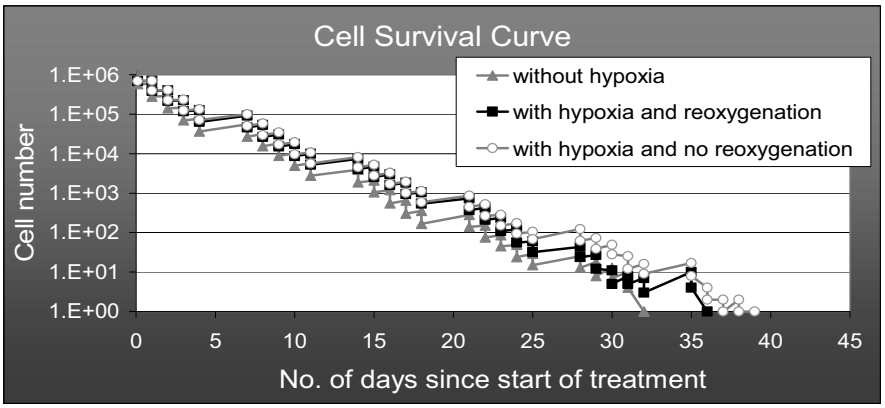

Figure 1. *Hypoxic versus non-hypoxic cell kill, with and without re-oxygenation in the model.*

DISCUSSION & CONCLUSIONS: An efficient and biologically plausible tumour growth and radiotherapy treatment model has been developed. The algorithm uniquely combines epithelial cell hierarchy, random nature of the biology, and specific cell kinetic and oxygenation data. The model in its current state provides evidence that cell hierarchy, hypoxic status and reoxygenation dynamics of the individual patient are vital for predicting the response to fractionated RT. Continuing development of the algorithm includes accelerated repopulation and reoxygenation and necrosis dynamics during accelerated and/or hyperfractionated fractionated radiotherapy.

REFERENCES:

[1]*T. Bjork-Eriksson, et al (2000) Radiosensitivity (SF2) is a prognostic factor for local control in head and neck cancers, Int J Radiat Oncol Biol Phys, 46: 13-9.*

A COMPARISON OF PORTAL DOSIMETRY AND DOSE TO WATER MEASUREMENTS OF IMRT BEAMS

Philip Vial[1, 2], Peter Hunt[1], Peter B. Greer[3, 4], Lyn Oliver[1, 2] and Clive Baldock[2]

[1]*Royal North Shore Hospital, Sydney, Australia*
[2]*Institute of Medical Physics, University of Sydney, Sydney, Australia*
[3]*Newcastle Mater Hospital, Newcastle, Australia*
[4]*University of Newcastle, Newcastle, Australia*

INTRODUCTION: Portal dosimetry is being considered as the sole measurement required for pre-treatment verification of intensity modulated radiation therapy (IMRT) beams at Royal North Shore Hospital. In order to make clinical judgements based on portal dosimetry results we need to understand the relationship between portal dosimetry and dose to water results. This work compares dosimetric measurements using portal dosimetry and dose to water measurements for dynamic multileaf collimator (dMLC) radiotherapy beams. In particular we investigated dMLC beams that contain energy variations due to the radiation filtering and scatter caused by a multileaf collimator (MLC). The response of an amorphous Silicon (aSi) Electronic Portal Imaging Device (EPID) for dMLC beams was evaluated in comparison with ion chamber dose to water measurements.

METHODS: We used a commercially available portal dosimetry system to calculate predicted EPID images. Uniform intensity dMLC beams were created that contained different fractions of dose delivered from MLC transmitted radiation. These beams were used to measured EPID response vs. MLC transmission fraction at the central axis, across the beam profile, and with changes in field size. We also created dMLC fields with large intensity modulations at the central axis and off-axis positions. The experiment was repeated by comparing the dose to water calculated by the treatment planning system (TPS) and dose to water measurements with an ion chamber in a water tank. Experiments were confined to 6 MV photon beams delivered at 400 monitor units per minute on a Varian linear accelerator equipped with a Millennium 120 leaf MLC and an aS500 model EPID.

RESULTS: The maximum changes measured in EPID response compared to ion chamber dose to water measurements for fields with different MLC transmission fractions was as follows: 20% at the central axis of a 10 cm x 10 cm field, 15% change in the off-axis ratio at 17.5 cm from the central axis, and 15% change in the field size output factor for a 14 cm x 36 cm field size. For the highest MLC transmission dMLC field (0.06 cm leaf gap) the ion chamber dose to water measurements differed from TPS dose to water calculations by up to: 3.4% at the central axis of a 10 cm x 10 cm field, 11% at 17.5 cm off-axis, and up to 15% error in the field size output factor for a 14 cm x 36 cm field size. For the modulated dMLC beams the predicted portal dose images were on average (39.2 ± 11.6) % higher than the acquired EPID image signal in the very low dose regions as compared to the dose to the corresponding dose to water errors. The large local percent errors for portal dosimetry in low dose regions were within 3% relative to the maximum field dose.

DISCUSSION & CONCLUSIONS: The TPS used in this work models the MLC transmission with a single constant value. The change in EPID response to MLC transmission variations must be modelled if portal dosimetry results are to provide an accurate indication of dose to water for IMRT beams. Our experiments demonstrate large local percent errors in both dose to water calculations and in portal dosimetry calculations when the MLC transmission and scatter effects are not modelled accurately to account for off-axis and field size effects.

CLINICAL IMPLEMENTATION OF THE SIEMENS VIRTUAL WEDGE

L. Zhu[1,2], J. Cramb[1] and P. Phung[3]

[1]*Department of Physical Sciences, Peter MacCallum Cancer Centre, Melbourne, Victoria, Australia*
[2]*Tattersall's Cancer Centre at Epworth, Melbourne, Victoria, Australia*
[3]*Radiation Oncology Victoria, Melbourne, Victoria, Australia*

INTRODUCTION: The Siemens virtual wedge is delivered by varying the dose rate while moving Y jaw at a constant speed. The value for the virtual wedge factor is 1±0.05 at the central axis and a reference depth as specified by Siemens. Such a large uncertainty is not acceptable for clinical use. It has been reported that the virtual wedge factor depends on dose rate and dose calibration for both high and low dose pages, jaw speed and monitor units[1, 2]. Investigation during the commissioning of our Primus linacs showed that the virtual wedge factor could be significantly different from 1 depending on also the asymmetry and monitor unit of the treatment field especially for the steeper wedge angles. After almost four years of clinical experience, rules for virtual wedge have been established to maintain the dosimetry accuracy while keeping the physics time for measuring the virtual wedge factor as low as possible.

RESULTS: Figure 1 and Figure 2 show the average values and variation range of the virtual wedge factor for clinical treatment fields with virtual wedge angle up to 30 degrees. For treatment fields with 45° and 60°virtual wedges, the variations were found to be larger. Significant dependences on monitor units and field symmetry have been observed.

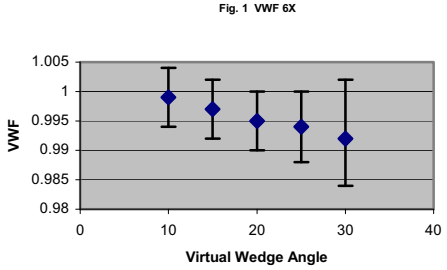

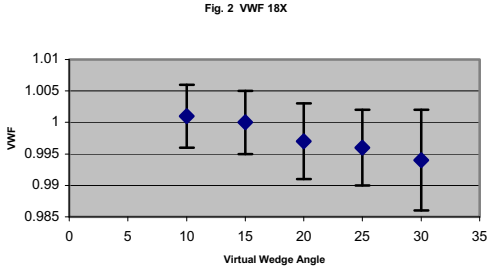

To make sure that the error for the virtual wedge factor is less than ±1%, we have set the following rules.

- For virtual wedges of angle up to 30°, average wedge factors can be used if the values for both Y jaws are larger than 2cm and smaller than 10cm.
- For the 45° virtual wedge a ton beam, an average wedge factor can be used if the nd an 18MV pho absolute difference between Y1 and Y2 is less than 3cm.
- The virtual wedge factor will be measured by physics if the monitor units are smaller than the switch points [1].

The virtual wedge factor will be measured for all 60° wedges and also 45° wedges that do not meet the rule No.2.

DISCUSSION & CONCLUSIONS: The Siemens virtual wedge factor depends on many treatment parameters. The XiO planning system may not be capable of accurately modelling the virtual wedge factor in some situations.

REFERENCES:

[1]*X. R. Zhu, M. T. Gillin, K. Ehlers, F.Lopez, D. F. Grimm and J. J. Rownd, "Dependence of virtual wedge factor on dose calibration and monitor units". Med. Phus. 28 (2) , 174-177 (2001).*
[2]*J. V. Santvoort, "dosimetric evaluation of the Siemens Virtual wedge" Phys. Med. Biol. 43 2651-2663 (1998).*

RADIOLOGY PHYSICS POSTERS

IMPROVING THE ESTIMATION OF DOSES RECEIVED DURING MAMMOGRAPHY

Kent J. Gregory[1], John E. Pattison[2] and Giovanni Bibbo[3]

[1]*Department of Medical Physics, Royal Adelaide Hospital, Adelaide, Australia*
[3]*Division of Medical Imaging, Women's & Children's Hospital, North Adelaide, Australia*
[1,2,3]*School of EIE – Applied Physics, University of South Australia, Mawson Lakes, Australia*

INTRODUCTION: Breast cancer screening programmes are now operating in many countries. This involves millions of mammograms being conducted every year. It is important that image quality and dose to the patient are optimised such that cancer detection is maximised and the possibility of cancer induction is minimised. Quality control test protocols and performance standards for mammographic x-ray units were published by the American College of Radiology (ACR) to satisfy these requirements[1], and these have been accepted in many countries including Australia[2]. These protocols include the evaluation of several quantities that are derived from exposure measurements; half-value layer (HVL), radiation output rate (ROR), average glandular dose (AGD) and automatic exposure control reproducibility (AECR). The ACR protocols require that these quantities be evaluated using exposure measurements taken in a specified manner, such as using an appropriately calibrated ionization chamber and electrometer.

METHODS: This study examined the measurement uncertainties of HVL, ROR, AGD and AECR for Mo/Mo x-ray units. These four quantities are subject to various error sources, depending on the quantity being evaluated, the test equipment used and whether or not corrections were applied. Given that Mo/Mo x-ray beams are low energy, the exposure measurements upon which these quantities depend are subject to some unique error sources. This is particularly the case with regard to the type of exposure meter used. The analysis of the uncertainties was performed in accordance with the International Organization for Standardization Guide[3], as described in Gregory, *et al.*[4] for medical x-ray unit exposure measurements. This involves identifying the error sources of HVL, ROR, AGD and AECR, and quantifying the uncertainty parameters, standard uncertainty, u and sensitivity coefficient, c, associated with each quantity. Then the relative importance of an error source is given by the term $(c.u)^2$. The analysis identified the error sources that make the largest contributions to HVL, AECR, AGD and ROR and, equally, error sources that were not so important.

RESULTS & DISCUSSION: Values of $(c.u)^2$ were calculated for various combinations of test equipment and applied corrections[5], and four error sources were identified that would reduce the uncertainties of HVL, ROR and AGD measurements. They were to use Al attenuators of at least 99.9% purity (for HVL); use a well calibrated exposure meter (for ROR); to make exposure measurements on the central-axis of the x-ray beam (for AGD); and to interpolate values of the dose conversion factor (for AGD). AECR measurement errors were found to be small and could not be reduced further. Also identified were error sources that have no significant effect on the measurement uncertainties. For HVL measurements, using attenuator increment sizes less than 0.2 mm (if corrected for increment size) or 0.1 mm (if not corrected); correcting for impurities in high purity attenuators; and correcting for beam angulation; each did not significantly improve measurement uncertainty.

CONCLUSIONS: The measurement uncertainty of a quantity can be reduced by choosing a method with error sources having the lowest possible values of $(c.u)^2$. Improvements in corrections for any error sources will result in lower $(c.u)^2$ values, but an overall improvement in measurement uncertainty is best attained by reducing the largest $(c.u)^2$ value.

REFERENCES:

[1]*R. E. Hendricks, et al., (1999) American College of Radiology, Mammography Quality Control Manual. ACR: Reston VA.*
[2]*Royal Australian and New Zealand College of Radiologists, (2002) Mammography Quality Control Manual. RANZCR: Sydney.*
[3]*International Organization for Standardization, (1995) Guide to the expression of uncertainty in measurement. IOS: Geneva.*
[4]*K. J. Gregory, G. Bibbo, J. E. Pattison, (2005) Australas. Phys. Eng. Sci. Med. 28:131-139.*
[5]*K. J. Gregory, J. E. Pattison, G. Bibbo, (2006) Med. Phys. 33:687-698.*

THE EFFECT OF AXIAL PHANTOM LENGTH ON SCATTERED RADIATION DOSE FROM A CT PROCEDURE

A. Baali[1], E. Bovell[2] and J. Atkinson[2]

[1]*Université Paul SABATIER de Toulouse, France*
[2]*Medical Technology & Physics, Sir Charles Gairdner Hospital, Nedands, Australia*

INTRODUCTION: Manufacturers of CT equipment provide an estimate of the scattered radiation dose during a procedure with a 2-D isokerma map. The isokerma maps are used in radiation safety calculations, including; radiation shielding requirements and dose rate to personnel. The cylindrical Perspex CTDI phantom (30 cm diameter, 15 cm length), used for this type of measurement is likely to result in an overestimate of the scattered dose rate owing to its limited axial length. The project aimed to determine the suitability of the Perspex CTDI phantom in approximating the scattered dose rate around an abdominal CT procedure by quantifying the dose with changing axial phantom length.

METHODS: Electronic dosimeters (Aloka-112) were tested for suitability to measure scattered dose from single CT exposures at 140 kVp, 4 cm width and 400 mAs. For all measurements, detectors were maintained at a source to detector (SDD) of 48 cm. Scatter data were collected from the CTDI phantom placed at the isocentre of the scanner as per the manufacturer's method. To quantify the effect of limited axial phantom length, doses were measured using a variable length of phantom between the scanner isocentre and the detector, herein referred to as the phantom length. Two phantoms were studied with different methods of altering phantom length; 1) Two adjacent CTDI phantoms, incrementally displaced axially, resulting in phantom lengths ranging from 2.5 to 27.5 cm and 2) The Anthropomorphic phantom, Rando, prefabricated in 2.5 cm slices was incrementally assembled to result in phantom lengths ranging from 2.5 cm to 35 cm. The fully assembled Rando closely approximates an abdominal CT patient.

RESULTS: The Aloka-112 provided dose measurements from a single exposure with a precision of 1% and was deemed suitable for measuring scatter doses. The dose collected from the Perspex CTDI phantom is very similar to the dose variation obtained from the Rando anthropomorphic phantom, in despite of the differences in geometry and constitution, they scatter the primary beam in the CT scanner similarly (see Figure 1). Both phantoms show a significant reduction in scattered dose with increasing axial phantom length. Irradiating the CTDI using the manufacturer method (phantom length 7.5 cm) resulted in a scatter dose of 173 µSv. By contrast, a dose of 27 µSv was measured from the fully assembled Rando (phantom length 35cm).

CONCLUSION: The Perspex CTDI overestimates the scatter dose from abdominal CT procedures along the axis of the scanner by up to six times owing to its limited length.

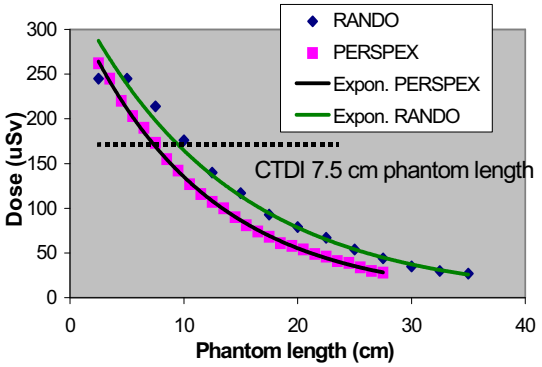

Figure 1. *Scattered dose as a function of the Rando and Perspex phantom length.*

DESIGN AND PERFORMANCE OF A DEVICE TO MEASURE LEAD EQUIVALENCE OF STRUCTURAL SHIELDING

M. McManus[1,2], E. Bovell[2] and D. Cryer[2]

[1]*School of Physics, University of Western Australia, Perth, Australia*
[2]*Department of Medical Technology and Physics, Sir Charles Gairdner Hospital, Nedlands, Australia*

INTRODUCTION: Required structural shielding, as specified by the Radiation Safety Act, is calculated and installed as new equipment is purchased by the hospital. We set out to measure all shielding in the hospital and create a database of this information. Our aim was to design a device to make the measurements quickly and accurately which conforms to the ALARA principles.

METHODS: A SmartIon detector was used to measure the attenuation of the gamma rays generated by a source of Tc-99m (400 MBq). Technetium is readily available from the Nuclear Medicine department at SCGH and its short half life makes it easy to dispose of safely. A rig was designed that shields the source and gives the option of securing it to the rig or removing easily. The rig is mobile, keeps the source and detector aligned and has adjustable height and source-to-detector distance. Measurements were made comparing the calculated lead equivalence to known thicknesses of lead.

RESULTS: Figure 1 shows the performance of the rig for a range of actual lead thicknesses. For lead between 1 - 2 mm the rig provides estimates of lead equivalence, accurate to 5%. For lead of thickness 0.5 – 1 mm and

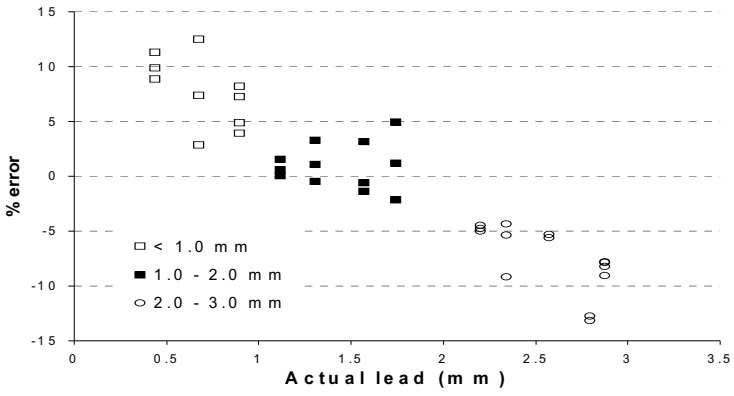

Figure 1. *Performance of the rig over a range of lead thicknesses.*

2 – 3 mm the rig is accurate to 15%. Diagnostic radiation equipment uses relatively low energies and is often shielded with barium plaster or besser bricks. The high energy of Tc-99m makes it unsuitable to measure these materials.

DISCUSSION & CONCLUSIONS: The rig we built enabled expedient measurement of most barriers. The measurements were accurate, optimised to within 5% in the clinical range of 1 – 2 mm Pb. Above 3 mm of lead a 400 MBq soure is not intense enough to penetrate and a larger source would be needed.

ACKNOWLEDGEMENTS:
Thanks go to Tony Warwick and staff in the Department of Nuclear Medicine for their support in the supply of Tc-99m.

NUCLEAR MEDICINE POSTERS

NON-INVASIVE APPROACH FOR RESPIRATORY MOTION GATING IN PET: DIGITAL PHANTOM EVALUATION

Jianfeng. He[1,2], Graeme O'Keefe[2], Gareth Jones[2], Tim Saunder[2], Sylvia Gong[2], Moshi Geso[1] and Andrew Scott[2]

[1]*School of Medical Science, RMIT University, Melbourne, Australia*
[2]*Department of Nuclear Medicine & PET for Centre Austin Hospital, Melbourne, Australia*

INTRODUCTION: PET imaging in oncology has an important role in diagnosis and treatment planning. However, PET still has some problem facing respiratory motion issue. Respiratory motion can be compensated by gating techniques and so improve image quality of PET. In this study, a data-driven gating method was investigated. We have developed a data-driven gating method that utilizes the geometric sensitivity properties of 3D PET. The geometric sensitivity gating (GSG) method has been simulated using GATE (GEANT4 Application Tomographic Emission) and NCAT (NURBs(Non Uniform Rational B-Splines) CArdiac Torso) software

METHODS: With geometric sensitivity gating method, the respiratory motion phases could be gated from list-mode data in terms of the distribution of counts of coincidences. The simulation processing has five steps: first, setting up GATE in terms of Philips Allegro PET detection characteristics and the NCAT phantom parameters; second, running GATE to obtain the phantom projection data as list-mode data; third, gating list-mode data into one frame by proposed method; next, converting the gated frame data into UGM sinogram format; last, obtaining reconstruction from sinogram data. All simulations are running with a total of 37MBq source activity in the phantom. In addition, GSG method has also been tested on list-mode data acquired from the clinical acquisition.

RESULTS: All simulation results are presented by reconstructed images. Geometric and NCAT plotting curves of frame counts with the static and the motion are obviously different due to geometrical sensitivity distribution. If phantom with no respiratory motion simulated, the frame counts are constant whilst with respiratory motion enabled, the frame counts exhibit an oscillatory trend consistent with the respiratory motion parameters

DISCUSSION & CONCLUSIONS: A limitation of GSG is that it is insensitive to non-axial motion. However, for respiratory motion, the organs motion is largely in the axial direction. Computer simulations show that GSG data-driven method can compensate simulated respiratory motion and that the reconstructed images are improved. The results of simulation show good agreement with GSG testing on the clinical acquisition.

REFERENCES:

[1]*S. Jan, G. Santin, D. Strul, S.Staelens, K. Assie, D. Autret, S. Avner, R. Barbier, M. Bardies, P. M. Bloomfield, D.Brasse, V. Breton, P. Bruyndonckx, I. Buvat, A. F. Chatziioannou, Y. Choi, and e. al, GATE Users Guide: GATE-Geant4 Application for Tomographic Emission: a simulation toolkit for PET and SPECT:http://www.lphe.epfl.ch/GATE/, 2005.*
[2]*W. P. Segars, "Development of A New Dynamic NURBS-Based Cardiac-Torso(NCAT) Phantoms" in Biomedical Engineering and Department of Radiology: Ph.D disseration, The University of North Carolina, 2001, pp. 221.*

VALIDATED WITH THE MONTE CARLO CODE 'GATE'

K. Willowson[1, 2], D. Bailey[1, 2] and C. Baldock[1]

[1]*Institute of Medical Physics, School of Physics, University of Sydney, Australia*
[2]*Department of Nuclear Medicine, Royal North Shore Hospital, Australia*

INTRODUCTION: Quantitative SPECT imaging refers to the determination of radiopharmaceutical concentrations inside the body. Accurate quantitative image reconstruction relies on corrections for degrading factors, specifically scattered and attenuated gamma rays. This work uses information acquired with X-ray CT to implement transmission dependent scatter correction and non-uniform attenuation correction to achieve quantitative SPECT, which can be applied to clinical situations. These quantitative methods are being validated with GATE – a Monte Carlo simulation program.

METHODS: A program was written to implement Transmission Dependent Scatter Correction (TDSC) (1) on SPECT/CT images for the radionuclide Tc-99m. The CT data are first transformed to linear attenuation coefficient (μ) maps using the

relationship between Hounsfield units and μ values, based on the work of Brown et al. (2). The TDSC method uses this μ-map to calculate a scatter fraction for each voxel in the image, based on the system's scatter build-up function. The acquired SPECT data are convolved with an experimentally measured scatter function, and then multiplied on a pixel-by-pixel basis with the calculated scatter fraction, before being subtracted from the original projection data to leave scatter corrected data. These data can then be corrected for attenuation using the co-registered, transformed CT image to produce an attenuation correction factor map. Quantitative analysis can be done using GATE to compare two simulations. An initial simulation acquired with all physical processes which then undergoes scatter and attenuation correction can be evaluated in a quantitative manner against a second, ideal simulation, acquired with no scatter or attenuation present.

RESULTS: *Figure 1* is the resulting GATE simulation of a single-slice voxelized brain phantom. A profile in the X direction gives a quantitative measure and distribution of the counts, which will provide a means to compare simulated results under different conditions in a quantitative manner.

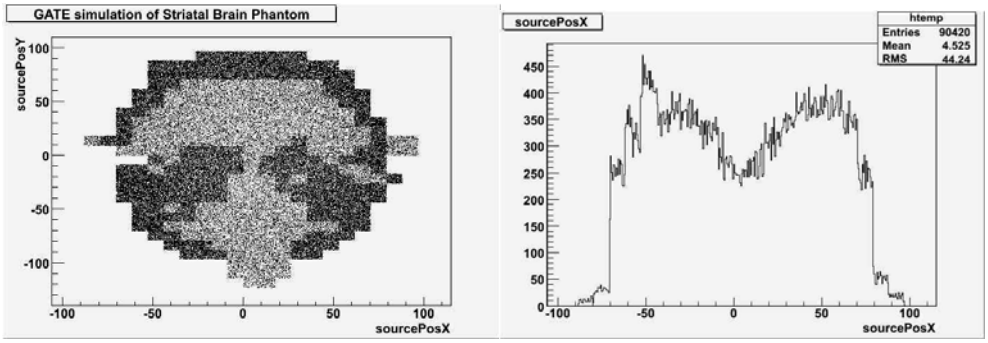

Figure 1. *Resulting GATE simulation of a voxelized Brain Phantom, and the resulting profile.*

DISCUSSION & CONCLUSIONS: GATE offers a unique opportunity to validate quantitative methods, as it realistically models photon transport and image formation, with the additional benefit that physical processes can be selectively ignored. This investigation using GATE will potentially offer an initial validation of the CT-based quantitative SPECT methods developed in this work, and further validation will be sort with a clinical study before clinical application of the methods.

REFERENCES:

[1]*S.R. Miekle, B.F. Hutton, D.L. Bailey, (1994) A Transmission Dependent Method for Scatter Correction in SPECT, J Nucl Med, 35:360-367.*

[2]*S. Brown, D. Bailey, C. Baldock, (2006) An Investigation of the Relationship Between Linear Attenuation Coefficients and CT Hounsfield Units, Australas. Phys. Eng. Sci. Med, 29(1): 140 (abstract).*

CLINICAL ENGINEERING POSTERS

DESIGN OF A MULTI-CHANNEL INTRALUMINAL IMPEDANCE SYSTEM

S. Afkari[1-2], G. Hebbard[1] and M. Fowler[2]

[1]*Biomedical Engineering Department, Royal Melbourne Hospital, Melbourne, Australia*
[2]*Gastroenterology Department, Royal Melbourne Hospital, Melbourne, Australia*

INTRODUCTION: Esophageal function testing and monitoring are important clinical tests in patients presenting with esophageal symptoms. The gold standards to evaluate the motor function of the esophagus and diagnose gastro-esophageal reflux are manometry and pH esophageal monitoring respectively. However, these techniques offer only indirect information about intra-esophageal bolus and/or liquid movement and presence[1].

Multichannel intraluminal impedance (MII) is a relatively new technique allowing detection of intraluminal bolus movement in the gastrointestinal tract without the use of radiation at a much lower cost[2]. In clinical applications it can be combined with manometry and/or pH studies, allowing better evaluation of bolus transit and non-acid gastro-esophageal reflux abnormalities[3]. A new 16 channel MII monitoring system has been designed for clicnial research in conjunction with manometry and pH studies.

METHODS: Impedance testing depends upon measurement of changes in resistance (in Ohms) to alternating electrical current when bolus passes a pair of metallic rings mounted on a catheter. In an empty tubular organ (esophagus) the electrical current between the two rings is conducted by the few ions present in and on the esophageal mucosa. Liquid containing boluses with an increased number of ions have a higher conductivity and as a result will have lower impedance values [1]. The impedance stays at this low value as long as the bolus is present; returning to baseline once the bolus is cleared by a contraction (swallow). Gas passing will produce a rapid rise in the impedance due to its poor electrical conductance compared to liquid.

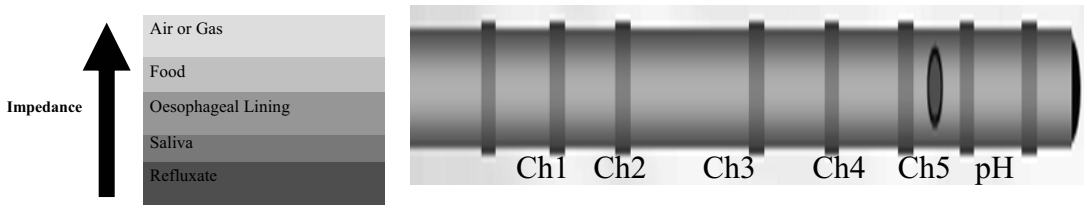

Figure 1. *Impedance change (left) and test catheter[3] (right).*

Measuring impedance at multiple sites (multichannel) allows for bolus movement and velocity determination based upon bolus entry and exit.

RESULTS: The designed system was tested in vistro using various, valued resistors and liquids (water, saline, and alcohol). Preliminary results show the designed system has a rapid rise of impedance due to air between two electrodes (typically above 33000 ohms) followed by a rapid return to baseline in presence of oral mucosa (typical value of 10000 ohms).

DISCUSSION & CONCLUSIONS: The system differs to others by using only one signal generator and current source for multi-channel recording. The system allows direct recording of information about intra-oesophageal bolus and/or liquid movement, velocity and bolus entry point.

REFERENCES:

[1]*H. Nguyen, Multiple Intraluminal Electrical Impedancometry for Recording of Upper GI Motility; The American Journal of Gastroenterology; Volume 94; Number 2; 1999.*

[2]*M. Vela, Simultaneous Intra-esophageal Impedance and pH Measurement of Acid and Nonacid Reflux: Effect of Omeprazole; Gastroenterology 2001; 120:1599-1606.*

STRUCTURAL GEOMETRICAL ACCURACY USING A CUSTOM BUILT ANTHROPOMETRIC PHANTOM OF THE PROXIMAL FEMUR

B.C.C. Khoo[1], T.J. Beck[2], J.W. Wearmouth[1], K.P. Singer[3] and R.I. Price[1]

[1]*Medical Technology and Physics, Sir Charles Gairdner Hospital, Perth, Australia*
[2]*Department of Radiology, Johns Hopkins University, Baltimore, MD, USA*
[3]*School of Surgery and Pathology, University of Western Australia, Perth, Australia*

INTRODUCTION: Material and structural properties influence bone strength. Structural strength via the geometry may be determined through imaging methods, though there is no commercially available phantom to assess structural geometrical accuracy. This paper describes an anthropometric femur structural geometrical phantom and it's testing on Dual energy X-ray Absorptiometry (DXA), peripheral Quantitative CT (pQCT) and whole-body CT scanners.

METHODS: Phantom neck cortex is made in six segments with varying elliptical outer contours and fixed inner circular contour. Along major axis, cortical thickness ranges from 0.5mm to 4mm. Cortical shell is made from bone equivalent dental plaster formulation, "trabecular core" of commercially available trabecular substitute equivalent to mineral density of 200 mg/cm^3. Conically shaped shaft cortex was filled with paraffin wax to simulate fatty marrow. Phantom was scanned with Hologic QDR 1000W DXA, QDR4500A DXA, StratecXCT2000 pQCT and GE-LightSpeed 64 Multi-slice whole body CT scanners. Algorithms were written specifically to generate structural geometrical variables (e.g. cross-sectional area, CSA; section modulus, Z and width, W) across the four scanners using projection principles.

RESULTS: Coefficients of determination, R^2 values were high in all modalities, best in CT. Errors ranged to 37% in bone CSA, Table 1.

Table 1. *Average % errors and R^2 for DXA, whole-body CT and pQCT against phantom dimensions (Column 1) shown for the structural variable CSA.*

Bone CSA	QDR1000W	QDR4500A	Whole-body CT	pQCT
R^2	*0.977*	*0.953*	*0.991*	*1.000*
1.426	9%	37%	-17%	19%
1.621	4%	29%	-17%	15%
2.013	1%	21%	-5%	14%
2.208	2%	31%	-8%	13%
2.795	-14%	5%	1%	10%
3.773	-10%	15%	-3%	8%

DISCUSSION & CONCLUSIONS: CT errors were generally systematic and probably amenable to algorithm improvement. This anthropometric phantom appears to be a viable standard for testing accuracy of bone geometry measurements across conventional imaging modalities.

DEMAND FLOW SYSTEM – A SYSTEM ALOWING SPONTANEOUS BREATHING DURING HIGH FREQUENCY VENTILATION

V. Kopelent[1], M. van Heerde[2], K. Roubik[1], F.B. Plötz[2] and D.G. Markhorst[2]

[1]*Faculty of Biomedical Engineering, Czech Technical University, Prague, Czech Republic*
[2]*Dept. of Pediatric Intensive Care, VU University Medical Center, Amsterdam, The Netherlands*

INTRODUCTION: Maintenance of spontaneous breathing in mechanically ventilated patients augments ventilation perfusion matching and cardiopulmonary function, reduces sedative requirement and shortens intensive care stay [1-4]. In larger children and adults spontaneous breathing during high-frequency oscillatory ventilation (HFOV) is currently advocated but usually not well tolerated because of patient discomfort. In an earlier study we showed that this is explained by a high level of imposed work of breathing (WOB). In this bench test we assessed the effect of a Demand Flow System on imposed WOB during HFOV.

METHODS: An ASL 5000 (IngMar Medical, Pittsburgh, PA) is a digitally controlled real time breathing simulator, allowing to create various types of breath including spontaneous ventilation. The ASL5000 was connected to a modified HFOV ventilator (3100 B SensorMedics, Yorba Linda, CA) via a standard breathing circuit and endotracheal tubes of various sizes. A developed system called Demand Flow System was assembled with the use of a flow valve of a conventional ventilator (AVEA, VIASYS, Palm Springs, CA). Inspiratory and expiratory airway flow and pressure at various places were sampled. Spontaneous breath rate and volume, tube size and ventilator settings were simulated as representative for the pediatric to adult range. Imposed WOB was calculated using the Campbell diagram.

RESULTS: For simulations for an adult subject (VT 500ml) the level of imposed WOB was 1.3 J/l using continuous bias flow. With the use of the Demand Flow System the overall level of imposed WOB was reduced to 0.4 J/l. Simulations of shallow breathing of an adult subject (VT 300ml) yielded values of imposed WOB of 0.90 J/l using continuous bias flow. With the use of the flow demand valve the overall level of imposed WOB was reduced to 0.3 J/l. Mean reduction imposed WOB was in the interval (45% – 69%). Lowest possible imposed WOB that could be accomplished with the Demand Flow System was 0.3 J/l in adult simulations. Fluctuations in mean airway pressure on account of spontaneous breathing were markedly reduced.

DISCUSSION & CONCLUSIONS: Using the Demand Flow System in HFOV the imposed work of breathing can effectively be reduced. As WOB of a healthy adult is 0,3 - 0,6 J/l, our initial goal was to reduce imposed WOB to this level. This was achieved in simulations for shallow breathing. It seems possible to improve the Demand Flow System and reduce imposed WOB even more. These new data will be presented at the conference.

ACKNOWLEDGEMENT: The work has been supported by grant MSM 6840770012.

REFERENCES:

[1]*Cereda M, Foti G, Marcora B, Gili M, Giacomini M, Sparacino ME, Pesenti A: Pressure support ventilation in patients with acute lung injury. Crit Care Med 2000, 28:1269-1275.*
[2]*Putensen C, Mutz NJ, Putensen-Himmer G, Zinserling J: Spontaneous breathing during ventilatory support improves ventilation-perfusion distributions in patients with acute respiratory distress syndrome. Am J Respir Crit Care Med 1999, 159:1241-1248.*
[3]*Putensen C, Muders T, Varelmann D, Wrigge H: The impact of spontaneous breathing during mechanical ventilation. Curr Opin Crit Care 2006, 12:13-18.*
[4]*Sydow M, Burchardi H, Ephraim E, Zielmann S, Crozier TA: Longterm effects of two different ventilatory modes on oxygenation in acute lung injury. Comparison of airway pressure release ventilation and volume-controlled inverse ratio ventilation. Am J Respir Crit Care Med 1994, 149:1550-1556.*

ROULEAUX AND PULSATILE LIGHT TRANSMISSION SIGNALS

M.P. McEwen[1, 2] and K.J. Reynolds[1]

[1]*School of Informatics and Engineering, Flinders University, Adelaide, Australia*
[2]*Flinders Biomedical Engineering, Flinders Medical Centre, Adelaide, Australia*

INTRODUCTION: In a pilot study the effect of rouleaux formation on the transmission of light through tissue was investigated.

METHODS: The transmission of light through appendages of animals with blood that forms rouleaux (human fingers) and through appendages of animals with blood that forms negligible rouleaux (sheep ears) was measured under normal conditions and during periods of blood flow occlusion.

RESULTS: When blood flow was occluded, the transmission of light through sheep ears gradually altered in accordance with the changing colour of blood as haemoglobin deoxygenated. Whereas during blood flow occlusion in human fingers, the transmission of light showed a decaying increase as well as gradually altering in response to the deoxygenation of haemoglobin. Pulsatile light transmission signals measured under normal (non-occluded) conditions exhibited large variations from humans to sheep.

DISCUSSION & CONCLUSIONS: The differences measured in light transmission during blood flow occlusion in humans and sheep may indicate the formation of rouleaux in humans. Whilst the differences found in pulsatile signals may indicate that pulsatile light transmission signals through tissue may be affected by the formation of rouleaux.

REFERENCES:

[1]*K. J. Reynolds, J. T. Moyle, L. B. Gale, M. K. Sykes, and C. E. Hahn, In vitro performance test system for pulse oximeters, Med Biol Eng Comput 30, 629-635, 1992.*

[2]*I. Fine, B. Fikhte, and L. D. Shvartsman, RBC-aggregation-assisted light transmission through blood and occlusion oximetry, Proc. SPIE 4162, 130-139, 2000.*

[3]*L.-G. Lindberg, P. Sveider, and P. A. Oberg, Optical properties of blood in motion, Proc. SPIE 1649, 116-122, 1992.*

[4]*H. Schmid-Schonbein, E. Volger, and H. J. Klose, Microrheology and light transmission of blood. II. The photometric quantification of red cell aggregate formation and dispersion in flow, Pflugers Arch 333, 140-155, 1972.*

[5]*H. Schmid-Schonbein, K. A. Kline, L. Heinich, E. Volger, and T. Fischer, Microrheology and light transmission of blood. III. The velocity of red cell aggregate formation, Pflugers Arch 354, 299-317, 1975.*

[6]*W. Zijlstra, A. Buursma, and O. van_Assendelft, Visible and near infrared absorption spectra of human and animal haemoglobin (VSP, Leiden, The Netherlands, 2000).*

[7]*R. R. Anderson, and J. A. Parrish, The Optics of Human Skin, J Invest Dermatol 77, 13-19, 1981.*

[8]*S. Takatani, and M. D. Graham, Theoretical analysis of diffuse reflectance from a two-layer tissue model, IEEE Trans Biomed Eng 26, 656-664, 1979.*

REHABILITATION ENGINEERING POSTERS

PREVENTION OF FALL FOR THE ELDERLY

M. Saito[1], Z. Ruijia[2], Y. Ohta[3], C. Takano[4], C. Sugimoto[5], R. Ezoe[6], K. Sasaki[7], H. Hosaka[8], T. Ifukube[9], S. Ino[10] and K. Yamashita[11]

[1,2,3,4]*Ochanomizu University, Graduate School*
[5,6,7,8]*The University of Tokyo, Graduate School of Frontier Sciences*
[9,10]*The University of Tokyo, RCAST*
[11]*Tokyo Health Care University*

INTRODUCTION: In order to prevent falling, biomechanical function of the stance and gait have been assessed for the elderly. Usually, these functions have been examined under a limited environment specially designed for the kinetic/kinematics measurement, such as a gait laboratory or a gym with flat floor by using various specific biomechanical devices such as a force plate or a treadmill[1] Therefore, the gait/posture data acquired from these lab-based measurements do not necessarily reflect the elderly's motor function correctly. In the present study, we proposed new wireless shoes for foot pressure measurement, which could be used for assessment of stance/gait function of the elderly under daily living situations.

METHODS: The shoe device developed consists of an inner sole mounted with seven pressure sensors, an originally fabricated microcomputer for wireless communication, and a power source. Figure 1 shows the position of each sensor mounted on the shoe insole and the foot bone anatomy. Considering bone anatomy, gait kinetics, as well as foot distortion such as flat foot, each sensor position was determined in order to correctly measure the centre of pressure (CoP) during gait.
To assess the performance of the developed shoe device, a comparison experiment was conducted with healthy subject (female, 23 years) by using two kinds of devices: the shoe device and a commercial force plate for gait analysis. The subject walked wearing the developed shoe device for seven-step distance, and was indicated to push the centre of the force plate

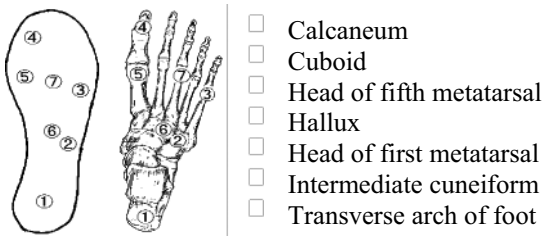

Fiure 1. *Sensor position on the shoe-insole and foot anatomy*

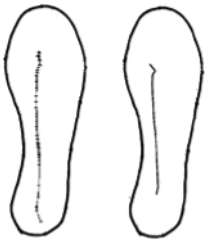

Figure 2. *Tyical examples of CoP trajectory acquired by the devices. (left: force plate, right: shoe device).*

with her foot just at the fourth step. Trajectory of CoP between heel contact and toe-off was calculated and compared between the two devices.

RESULTS: Figure 2 shows typical examples of CoP trajectory acquired by the devices. As shown, the shoe device showed almost same trajectory as the force plate. Through experiments, compared with the force plate, the shoe device developed was found to be able to measure CoP trajectory as the force plate does, even with less sensors.

DISCUSSION & CONCLUSIONS: In the present study, a wireless monitoring shoe device was proposed for ambulatory posture/gait analysis, and was fabricated by using seven pressure sensors mounted on a shoe insole. By using the device, usual gait of the elderly under daily living condition could be analysed and his/her risk factor of fall would be assessed quantitatively, which would contribute increase in QoL for the elderly and thus, decrease in medical costs.

REFERENCES:

[1]*Hessert MJ, et al., Foot pressure distribution during walking in young and old adults, (2005) BMC Geriatr, 19: 5-8.*

OTHER POSTERS

DEVELOPMENT OF A SEMI-AUTOMATED SOLID TARGETRY IRRADIATION SYSTEM FOR AN 18MEV PROTON CYCLOTRON

S. Chan, D. Cryer, R.I. Price and RAPID Group

Department of Medical Technology and Physics, Sir Charles Gairdner Hospital, Perth, Australia

INTRODUCTION: The medical cyclotron facility at Sir Charles Gairdner Hospital produces radiopharmaceuticals using both liquid and gas targets. The short-lived ^{18}F [$T_{1/2}$ = 110 m] is produce daily for PET imaging. The desire to produce longer lived isotopes such as ^{124}I [$T_{1/2}$ = 4.18 d] and ^{64}Cu [$T_{1/2}$ = 12.85 h] has prompted the construct of a compact solid target system. This system complies with the engineering specification of the IBA cyclotron (Cyclone 18/9), and provides sufficient cooling to the target materials.

METHODS: The initial design was inspired by a commercial solid targetry system [1] and existing IBA liquid and gas targets. The aluminium target body, water jet and attachment of the pneumatic rams were machined "in-house". The restricted space at the exit port of the cyclotron requires the solid target system be attached to a 30cm beam line.

The target disk is 25mm in diameter with a thickness of 2mm. The graphite collimator restricts the beam to a maximum diameter of 10mm, thus improving the homogeneity of the beam irradiating the target. To accommodate different target areas the graphite collimator is interchangeable. A reduced collimator size ensures the beam remains perpendicular to the target surface, assisting with the alignment of the non-focused beam. The target rear surface is cooled with a water jet and the front surface by He gas flow. A havar window separates the He-filled space from the vacuum of the beam line. The target and collimator are cooled by chilled water in a closed system that circulates via a heat exchanger. The temperature is maintained at 18°C with a supply flow rate to the cooling jet of 14L/min.

A Siemens programmable logic controller (PLC) is used to activate the various valves for the correct operation. The target is secured in the guiding rail using a pneumatic piston. To prepare for an irradiation, the pneumatic rams seal the cooling mechanisms on both sides of the target. The water cooling circuit is active once the target disk is secured and the cooling jet is in place. The water supply to targetry system is bypassed pre and post irradiation. To unload the target water is purged from the system using compressed air. The pneumatic rams release the target from the cooling mechanisms, and the disk falls into a transport container.

RESULTS: To validate the system and to determine the maximum current achievable, a platinum disk with 2 thermocouples, one mounted at the centre and the other at the 10mm radius, was irradiated. Since the melting point of the target material is much higher than the o-rings, our concern is the integrity of the o-rings at different target currents. At target current of 30μA the temperature near the o-ring seals was approximately 80°C. This is 30°C below the operating limit, but further investigation is required to confirm the temperature at the centre. Thus a target current of no more than 15μA is used for all irradiations.

Irradiation of Mo and TeO_2 target have produced test quantities of ^{96}Tc and ^{124}I respectively [2,3]. These test productions have demonstrated the viability of the solid targetry system.

DISCUSSION & CONCLUSIONS: We have successfully developed a solid targetry system to be used with an IBA 18MeV medical cyclotron. Future development is in progress to remotely extract the irradiated disc from the bunker and to optimise the water cooling for higher beam currents. Concurrent developments include investigations into the preparation of target materials on disk substrate, the sublimation of the target material from the irradiated disc and the development of a positron detector.

REFERENCES:

[1]*Elex Commerce (2002) COSTIS operating Manual, Belgrade Yugoslavia.*
[2]*RA. Fox, (2001) Australas Phys Eng Sci Med, 24:153-159.*
[3]*SM. Qaim (2003) Appl Radiat & Isot, 58:59-78.*

THE WESTERN AUSTRALIAN INHERITED RETINAL DISEASE DNA DATABANK

J. De Roach, E. Chelva, S. Laurin, T. Lamey and R.I. Price

Department of Medical Technology and Physics, Sir Charles Gairdner Hospital, Australia

INTRODUCTION: The Department of Medical Technology & Physics at Sir Charles Gairdner Hospital provides the Western Australian state service for carrying out visual electrophysiological testing of patients. These patients are referred by ophthalmologists for a wide range of presenting diagnoses, and many of them suffer from diseases of the retina which are the result of mutations in one or more of up to 160 different genes. Consequently the department comes into contact with a significant proportion of all of the sufferers of Inherited Retinal Disease (IRD) in Western Australia at least once in their lifetime. An IRD register for the state of Western Australia was therefore established in this department, in 1984. At its inception, and for many years following, the register contained information regarding the clinical status of each subject, their family history, and the results of electrophysiological tests carried out in the department. During the past five years this register has been expanded to include the collection and storage of DNA in the form of blood, Buccal swabs and saliva samples from affected individuals and from appropriate family members. This presentation summarises the current status of this valuable asset.

METHODS & DISCUSSION: The Western Australian IRD Register currently contains information relating to 1340 subjects affected with an IRD or their family members. This number represents an increase of 89 subjects in the past 12 months. Visual electrophysiology has been carried out on many subjects, using an LKC UTAS-E3000 system, and since May 2001 detailed results from these tests have been automatically electronically extracted and stored in tables in the ACCESS database which constitutes the IRD Register. Psychophysical test results and information from the department's Patient Management System are also automatically sent to this database. As a result the register currently contains detailed results of 341 electroretinograms, 309 electro-oculograms, 281 pattern electroretinograms and 309 series of psycho-physical tests, representing increases in these numbers in the last 12 months of 66, 53, 47 and 42 respectively. Collection of DNA began in late 2002, and since that time 368 blood samples and 97 Buccal swabs have been obtained from consenting individuals, resulting in storage of DNA from 465 sufferers of an IRD or their family members. Subjects are currently under selection for having DNA analysis carried out from among those subjects who belong to families showing evidence of the particular IRDs X-linked Retinitis Pigmentosa (RP), Dominant RP, Retinoschisis, Choroideraemia and Stargardt's disease.

CONCLUSION: An Inherited Retinal Disease DNA databank has been established for the state of Western Australia. In addition to DNA extracted from blood or Buccal swabs, this databank also contains demographic and clinical data and the detailed results of electrophysiological tests.

ACKNOWLEDGEMENTS: This project is made possible only by the generous funding from the Western Australian Retinitis Pigmentosa Foundation.

COMPARISON OF GAS FLOW IN THE RESPIRATORY SYSTEM WITH OR WITHOUT TGI CATHETER - VISUAL EXPERIMENT

V. Kopelent and K. Roubik

Faculty of Biomedical Engineering, Czech Technical University, Czech Republic

INTRODUCTION: Mathematical modelling of the respiratory system is very useful, but due to complexity of the respiratory system some simplifications have to be used during the design of the model. Big advantage of the mathematical modelling is its price, on the other hand the design process takes a lot of time. The other advantage is that the outputs of the model are not sensitive on the environmental conditions.

Mechanical experiments can be designed in shorter time. They are very sensitive on its setting and its price is also higher than mathematical modelling. The advantage of the experiments is that the results are more exact, when the settings of the experiment are correct. There exist a lot of types of experiments, but they differ in consequent evaluation. The method used in this work is based on the Mochizuki's work [1]. The disadvantage of this method is that there is not possible to do consequent computer analysis as in case of PIV.

METHODS: The whole experiment of the gas flow in the lung structure is made in water, because of water used as transport medium simplifies the visualisation; the velocities in the lung structures are lower than in the air. It is due to the kinematics viscosity of the water, which is lower than the air. To keep the same conditions for the water as for the air, the Reynolds number and the Womersley number were used. To make pulsatile flow visible, it was necessary to use some kind of dye. The blue ink was used in this case. It has a very small molecular diffusion coefficient in the water, the diffusion is negligible.

The dichotomy model of the first four generations of the lung structure was made from glass. The dimensions and degrees of the glass model follow Weibel's work [2]. The arrangement of the experimental setting is consisted of the mechanism generating oscillations. The output of the mechanical oscillator is connected with stilling box, where the whirls are

suppressed. These whirls could affect whole simulation. The stilling box was connected with the model, which was situated in the water reservoir. The digital movie camera was situated above the reservoir perpendicularly to the model. Four types of the experiments which were made: 1) glass tube, 2) glass model of the lung structure, 3) glass tube with Tracheal gas insufflation (TGI) catheter simulation, 4) glass model of the lung structure with TGI catheter simulation.

RESULTS: The simulations of the gas flow in the lung structure showed; that the bifurcation helps to the gas transport to get deeper into the lung structure. The situation without bifurcations was simulated by replacing of the model of the respiratory system by a straight tube with similar length as length trough the glass model of the respiratory system. The dyed water did not reach the end of the tube. When TGI catheter with a flow representing 24% of inspiratory flow was applied the dyed water reached the tube end. It shows that the TGI is a good support technique. Results in the graphical form will be presented at the conference.

DISCUSSION & CONCLUSIONS: The first visual representation of the gas flow in the model of the lung structure with the TGI flow has been presented. It showed that the TGI is a very good support technique of the artificial lung ventilation, which reduces anatomical dead space. The disadvantage of this visualisation method is that the outputs of the simulation cannot be exactly evaluated similarly as PIV method, but this method can be very useful in the testing of new types of the TGI catheters.

ACKNOWLEDGEMENT: The work has been supported by grant MSM 6840770012.

REFERENCES:

[1]*Mochizuki S: Convective mass transport during ventilation in a model of branching airways of human lungs, Proceeding of PSFVIP-4, Charmonix, France 2003.*
[2]*Weibel E. R.: Morphometry of the human lung, Academic press, New York, 1963.*

AN EVACUATION DRILL SYSTEM USING VIRTUAL REALITY TECHNOLOGY FOR CHILDREN WITH MENTAL RETARDATION

M. Tanaka[1], Y. Ohta[2], K. Matsumiya[3], K. Masamune[4], T. Dohi[5], A. Iimura[6], M. Matsuse[7] and Y. Kobayashi[8]

[1,2]*Ochanomizu University Graduate School*
[3,4,5]*Tokyo University*
[6]*Kamakura Women's University*
[7]*School for Special Needs Education attached Yokohama National University*
[8]*Yokohama National University*

INTRODUCTION: Security at school has been an important issue all over the world. For example, typical security program conducted regularly at schools in Japan is an evacuation drill for fire or earthquake evacuation. However, these drills are not necessarily effective for school children with disabilities, particularly with mental retardation (MR), because the programs are designed for normal children. Our goal is to develop an evacuation drill system by using virtual reality (VR) technologies for school children with MR and to verify its effectiveness through trainings.

METHODS: The three dimensional model of the schoolhouse of a school for the handicapped in the city of Yokohama was created by a modelling software, and a user can walk around in the virtual space by him/herself in order to recognize the escape route. The model data were developed as follows. (1) Surface model of the schoolhouse including the schoolyard was created by using a modelling software (3ds max7, Autodesk, Inc.). (2) Expressions of disasters in the virtual space, such as earthquake, flame, smoke, and sound, were added by using a VR software (Omega Space 3.0, Solidray Co. Ltd., Japan).

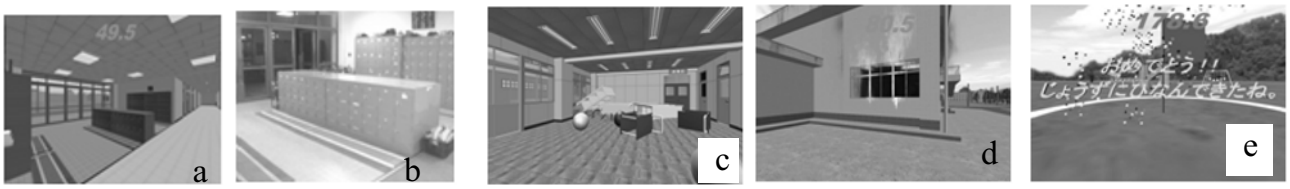

a: entrance of the school, b: photograph of the entrance, c: earthquake, d: fire, e: evacuation completed

Figure 1. *Various Scenes in the VR Evacuation Drill System.*

Twenty one schoolchildren with MR (13-18 years old) participated the VR training. The participants were divided into two groups, VR training group (twelve children) and VR non-training group (nine children), and the effect of the VR training was verified. To quantitate the VR effect, two kinds of the test (a quiz on earthquake and a card test) were conducted before and after VR training. One week later, they had a physical evacuation drill (not a VR one) in the schoolhouse, and their behaviours during evacuation were monitored.

RESULTS: Fig. 2 shows the results of the earthquake quiz and the card test. As shown, the VR training increased percentage of questions answered correctly. Behavior monitoring during the evacuation drill showed that the VR training

group members acted more promptly and calmly, even attended by no teacher, compared to the VR non-training groups. In addition, the questionnaire conducted just after the evacuation drill showed that participants in the VR training group scared less (less panicked) compared with those in the VR non-training group, which means VR training might reduce psychological stress under the sudden change in situation.

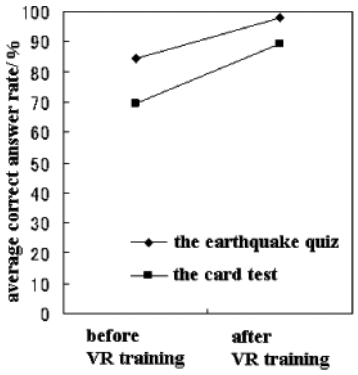

Figure 2. *Increase in the percentage of questions answered correctly due to the VR training.*

DISCUSSION & CONCLUSIONS: The VR system proposed here could be available anytime and anyplace in school. Through experiments, it was suggested that the children with MR improved their understandings on the natural disasters as well as evacuation procedures.

REFERENCE:

Padgett LS, Strickland D, Coles CD, (2006) Journal of Pediatric Psychology, 31(1):65-70.
Tarnanas I, Manos GC, (2001) Studies in health technology and informatics, 81:495-501.

MEASUREMENT OF SKIN RUBOR BY USING BIOELECTRIC IMPEDANCE METHOD: DETECTION OF INITIAL PRESSURE ULCER

T. Uchiyama[1], S. Ishigame[2], Y. Ohta[3] and J. Niitsuma[4]

[1,2,3]*Graduate school of Humanities and Sciences, Ochonomizu University*
[4]*National Rehabilitation Center for Persons with Disabilities*

INTRODUCTION: Pressure ulcer is a serious problem to the people with motor dysfunction. Clinical studies have shown that the earlier detection and treatment of the ulcer could lead to the sooner healing. In this study, Bioelectrical Impedance Analysis (BIA) method was tested to have the possibility to detect the initial pressure ulcer.

METHODS: Fig. 1 shows the schematic diagram of the BIA measurement system used in this study. As shown, impedance value was measured by using a digital lock-in amplifier (LI5640, NF corp., Japan) with the two-electrode method. Two healthy females participated in the experiments. The skin rubor, i.e. the model of the initial pressure ulcer, was developed on the subjects' forearm by causing temporal vasodilatation: it was experimentally developed by dermal inflammation reaction due to ethanol application to the skin. Then, by using a lock-in amplifier with the frequency range of 0.1 Hz-10 kHz, BIA was conducted for the skin rubor as well as the intact skin. Human skin could be electrically modelled, based on the parameters of electric parts: two resistors and a capacitor. By fitting the measured impedance data to this model, changes in the skin impedance value due to vasodilatation were evaluated.

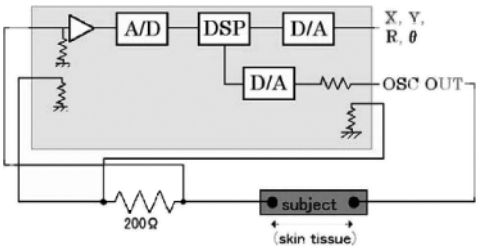

Figure 1. *Schematic diagram of the measurement system. A digital lock-in amplifier was used with the two-electrode method.*

RESULTS: Fig. 2 shows a typical Cole-Cole plot acquired from the skin with inflammation due to ethanol application. As shown, the plotted data could be fitted with circular curves (broken lines), and the tissue resistance value decreases as the frequency increases. In addition, it was found that impedance values of skin rubor decreased compared with those of intact skin. This would be attributed to increase in tissue fluid as well as blood vessel space due to erythema. The decrease was found to be remarkable especially around low frequencies, and the decrease rate was 17.1%. (The decrease rate was evaluated, based on the tissue resistance value at 0 Hz, which was extrapolated by the fitted circular curve.)

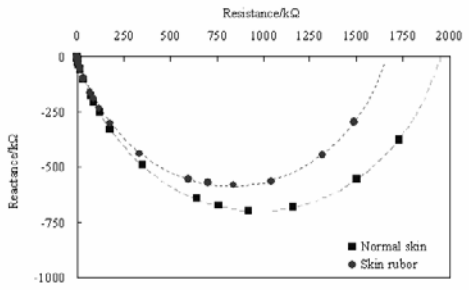

Figure 2. *Typical Cole-Cole plot from rubor and intact skin.*

DISCUSSION & CONCLUSIONS: Aiming to detect the initial pressure ulcer, human skins with and without vasodilatation was assessed by BIA method. The skin rubor model was developed on the subjects' left forearm by using EPT procedure (ethanol application to the skin) and impedance values of the intact skin, as well as the skin rubor, were measured by a lock-in amplifier with the frequency range of 0.1 Hz-10 kHz. As a result, the interstitial resistance value of the skin rubor was found to decrease to 83% of the normal skin. Skin rubor would be distinguished from normal skin, based on the bioelectric impedance value. The method proposed in the present study would be installed in the various clinical environments with the attractive features of the simplicity and reliability of the BIA method.

REFERENCES:

Sverre Grimnes and Orjan Grottem Martinsen, (2000) Bioimpedance and Bioelectricity Basics. Academic press.